AN EVALUATION OF INSTRUMENTAL TOOLS TO SCREEN FOR THE PRESENCE OF BROMINATED FLAME RETARDANTS

By

Antonella Guzzonato

A thesis submitted to the University of Birmingham for the degree of

DOCTOR OF PHILOSOPHY

School of Geography, Earth and Environmental Sciences

University of Birmingham

January 2018

Abstract

In this study a number of analytical techniques for the screening, quantification and identification of brominated flame retardants in consumers' products, electric and electronic waste and indoor dust is explored. The presented work can be conceptually divided in two parts:

- The first explores, evaluates and pushes the limits of solid sampling techniques i.e. X-Ray Fluorescence (XRF) and Laser Ablation Inductively Coupled Plasma Mass Spectrometry (LA-ICP-MS) as a tool for the total elemental quantification of Bromine (Br) and its use as a metric for Brominated Flame Retardants (BFRs) content in consumers' goods and waste. The XRF method proved to be accurate to 94% (relative to LA-ICP-MS results) in an operation range spanning from 0.0011% to 12% w/w Br, the developed correction for thin samples and the matrix matched calibration made the technique reliable for the quantification of Br in polymers. Rare Earths Elements (REEs) concentrations obtained with LA-ICP-MS were used to evaluate the origin of contaminants in Food Contact Articles (FCAs) and toys: the largest source of BFR-contamination in toys and FCAs was identified to be octa-BDE from small WEEE.

- The second part explores the suitability of solid sampling techniques (that do not require sample preparation) and simplified liquid sampling techniques (that require sample preparation in the form of solvent assisted extraction) for the compound specific, semi quantitative evaluation of BFRs in plastic material and indoor dust. Direct Insertion Probe- High Resolution Mass Spectrometry (DIP-HRMS) and Direct Analysis in Real Time-High Resolution Accurate Mass (DART-HRAM) showed sufficient linearity over the calibration range and mass

determination accurate enough to unequivocally identify BDE209 in polymeric matrices. A compound specific quantification method for BDE209 was successfully validated using DIP-HRMS. Gas Chromatography coupled to ICP-MS (GC-ICP-MS) analysis performed with ad-hoc developed hardware provided reliable data for the semi-quantitative evaluation of indoor dust BFRs profile. Room use was found to be related to PBDE signature: rooms that had a substantially different use from offices showed a different PBDE concentration pattern in their dust.

Dedication

A mamma e papà: per arrivare qui ho camminato su una strada battuta da venti piú forti di me,

ma il vostro amore e la vostra grazia hanno fatto cosí che ogni ostacolo non mi fosse mai piú

grave di un sassolino.

Hans, you are the scientist I hope to become one day. Thank you for your shoulder when my

head was too heavy and your head when mine was lost. For your caring insistence, for the

poppy-seed ice-cream and for reading each and every word beyond this page.

Acknowledgements

ABBREVIATIONS

ABS Acrylonitrile butadiene-styrene

BDE-209 Decabromodiphenyl ether

BFRs Brominated flame retardants

Br Bromine

DART Direct Analysis in Real Time

DIP Direct insertion Probe

EC European Commission

EE Electronic Engineering laboratories

EU European Union

FCA Food Contact Article

GC Gas chromatography

GC-ICP-MS Gas Chromatography inductively coupled mass spectrometry

GC-MS Gas chromatography-mass spectrometry

HR/AM High-resolution accurate mass

HR-ms-MS High resolution magnetic sector mass spectrometry

LA-ICP-MS Laser ablation inductively coupled mass spectrometry

MR Meeting rooms

M/Z Mass to charge ratio

NIST National Institute of Standards and Technology

O Offices

PBDEs Polybrominated diphenyl ethers

PCA Principal component analysis

PE Polyethylene

POPs Persistent organic pollutants

PP Polypropylene

PUF Polyurethane foam

SD Standard deviation

SRM Standard reference material

UNEP United Nations Environment Programme

XRF X-ray Fluorescence

List of publications

GUZZONATO, A., MEHLMANN, H., KRUMWIEDE, D. & HARRAD, S. 2016a. A novel method for quantification of decabromodiphenyl ether in plastics without sample preparation using direct insertion probe–magnetic sector high resolution mass spectrometry. *Analytical Methods,* 8**,** 5487-5494.

GUZZONATO, A., MEHLMANN, H., SCHLUETER, H.J. 2017a. *Heated Transfer Line*. US patent application US 20170184552.

GUZZONATO, A., PUYPE, F. & HARRAD, S. J. 2016b. Improving the accuracy of hand-held X-ray fluorescence spectrometers as a tool for monitoring brominated flame retardants in waste polymers. *Chemosphere,* 159**,** 89-95.

GUZZONATO, A., PUYPE, F. & HARRAD, S. J. 2017b. Evidence of bad recycling practices: BFRs in children's toys and food-contact articles. *Environ Sci Process Impacts,* 19**,** 956-963.

1 Introduction

1.1   Background

Throughout modern history, flame retardants (FRs) have been added to a variety of materials including wood, polymers, fibres and foams to prevent fires (Birnbaum, 2004.). There are different types of organic FRs, mainly based on phosphorus, nitrogen and bromine which are often used in conjunction with inorganic FRs (e.g. antimony trioxide, aluminium trihydroxide, magnesium hydroxide, or red phosphorus.). Brominated flame retardants (BFRs) have been one of the most widely used class of FRs over recent decades in two main forms: reactive, that are made to react with the polymer they are added to (e.g. TBBP-A) and additive, that are mixed in during the final stages of polymer manufacture, after polymerisation has occurred (e.g. PBDEs). The latter type has raised the most environmental concern as they are more easily released into the environment as being additive they are not chemically bound to the polymer matrix (Alaee, 2003). All three of the main PBDE commercial mixtures – the Penta-, Octa- and Deca-BDE formulations - have been listed under the Stockholm Convention on persistent organic pollutants (POPs)(2009, Convention, 2009). A chemical is listed as a POP because of its high persistence in the environment, bioaccumulation in the food chain, potential for long-range atmospheric transport (LRAT) and evidence of adverse effects ranging from acute to chronic toxicity (BFIP, 2011, ESWI, 2011). In particular PBDEs are toxic to humans (to different extents,

1

depending on their degree of bromination and steric configuration (Darnerud, 2003) because of their endocrine disrupting (ATSDR, 2017) and neurobehavioural developmental effects (McDonald, 2002). Additionally, when PBDEs are subject to thermal stress (as happens when contaminated waste is disposed of by incineration) they can be converted into the highly toxic PBDDs (polybrominated dibenzodioxins) and PBDFs (polybrominated dibenzofurans) (Weber and Kuch, 2003). Because of their substantial release to the environment, and subsequent environmental transport (de Wit et al., 2006, Hale et al., 2008), PBDEs have been detected in a large number of studies of consumer goods, air, dust, animal tissues, water and soil etc.(Watanabe and Sakai, 2003);(Hale et al., 2002a, Hites, 2004).

1.1.1 How BFRs function as flame retardants

For combustion to take place, two reactants are necessary: a reductant (fuel) and an oxidant (usually oxygen). If the fuel contains hydrocarbons, the combustion products will be mainly CO_2 and H_2O, and the quicker the products are removed from the flame, the more the reaction will approximate completion. This reaction is thermodynamically favoured as it reduces the enthalpy of the reactants, releasing energy (heat). When heated, BFRs react with hydrocarbons volatilised by the fire, with two-fold effect: fuel is subtracted from the reaction, and water is added to the products. The reason for using halogenated FRs is that halogens can catalyse radical reactions, where the initial BFR molecule regenerates itself, reducing the quantity of BFR required in the polymer. To further decrease the amount of FRs necessary to provide flame retardancy, antimony oxides are added in a 1:3 ratio with PBDEs. The antimony oxides act as a co-synergist entering the radical cycle at the propagation step: the antimony trioxide reacts

with HBr to form antimony trihalide, an inert gas that prevents oxygen from reaching the reductant and recondenses on the surface of the object promoting the formation of char, a passivating layer that inhibits further volatilisation and burning of flammable material (Troitzsch, 1990).

Initiation: $RBr \rightarrow R^{\cdot} + Br^{\cdot}$

Propagation: $Br^{\cdot} + RH \rightarrow R^{\cdot} + HBr$

$HBr + OH^{\cdot} \rightarrow H_2O + Br^{\cdot}$

$HBr + H^{\cdot} \rightarrow H_2 + Br^{\cdot}$
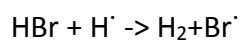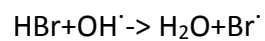
1.1.2 Physicochemical properties of PBDEs

PBDEs are aromatic chemicals that contain bromine in varying mass fractions. With two aromatic rings and a central oxygen atom, these compounds can accommodate 10 Br atoms in 209 different combinations called congeners (Figure 1-1).
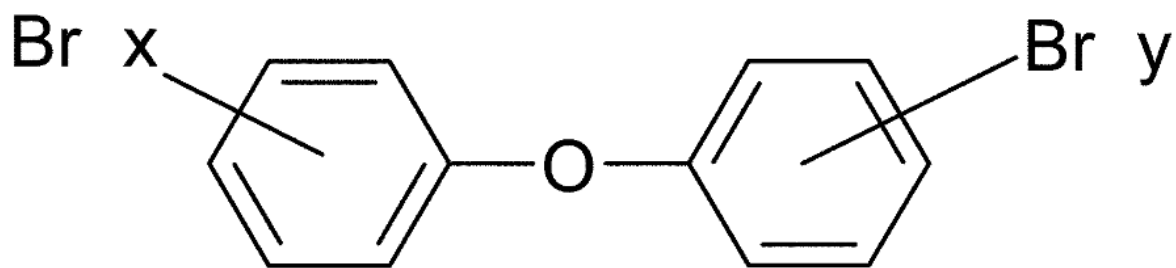
Figure 1-1 Chemical structure of PBDEs

PBDEs are commercially available as three main mixtures, the names of which are dictated by the congener class that is present in the highest proportion: PentaBDE (commercially sold as DE-71 by Great Lakes Chemical Corp., Indiana, or Bromkal 70-5DE by Chemische Fabrik Kalk, Koeln, Germany) with a total production volume of 91,000-105,000 tonnes; OctaBDE (commercially sold mainly as Bromkal 79-8DE by Chemische Fabrik Kalk, Koeln, Germany) with a total production volume of 102,700-118,500 tonnes; and Deca-BDE (commercially sold as Saytex 102E by Albemarle Corp., Louisiana) with a total production volume of 1,100,000-1,250,000 tonnes ((UNEP)-Chemicals., 2010). A summary of the congener distribution of these commercial formulations is provided in Table 1-1(La Guardia et al., 2006b).

1.1.3 Uses and applications

For the listed PBDE mixtures to have a flame retardant effect they were added at between 3 and 30% w/w (Commision, 1994) depending on the specific fire regulation jurisdiction in which the items were manufactured/sold, the polymer compatibility with the FR mixture, and the likelihood of the treated item to reach high operating temperatures (e.g. electronic appliances

have on average higher intentionally added loadings than textiles) (Commision, 2003) Penta-

BDE has been used mainly in polyurethane foam (PUF, in Europe, 95-99 % of production) and to

a minor extent in electrical and electronic appliances.

Table 1-1 Congener composition of the main commercially available PBDE formulations (%w/w). – stands for not analyzed or not detected
[a] Concentrattion span found in commercial mixtures

Congener #	Name	Penta-BDE (% w/w) [a]	Octa-BDE [a]	Deca-BDE (% w/w) [a]
BDE-28	2,4,4'-tri-BDE	0.11	-	-
BDE-47	2,2', 4,4'-tetra-BDE	33-37	-	-
BDE-66	2,3', 4,4'-tetra-BDE	1.02-0.22	-	-
BDE-85	2,2', 3', 4,4' –penta-BDE	3.18-1.6	-	-
BDE-99	2,2', 4,4', 5 –penta-BDE	42.5-35	-	-
BDE-100	2,2', 4,4', 6 –penta-BDE	10.9-6.8	-	-
BDE-138	2,2', 3,4,4', 5'-hexa-BDE	0.24-0.41	-	-
BDE-153	2,2', 4,4', 5,5'-hexa-BDE	3.75- 3.9	-	-
BDE-154	2,2', 4,4', 5,6'-hexa-BDE	3.00 -2.5	0.04-1.07	-
BDE-183	2,2', 3,4,4', 5', 6-hepta-BDE	-	12.6-42	
BDE-207	2,2', 3,3', 4,4' 5,6,6'-nona-BDE	-	11.2-11.5	4.1
BDE-209	Deca-BDE	-	1.31-49.6	91.6

It has been produced in the US, the EU, China, Japan and Israel before being phased out in all

these countries except China in the mid-2000s. In PUF, Penta-BDE was added at concentrations

between 3 and 5% w/w, with the amount usually inversely dependent to the foam pore size

((UNEP)-Chemicals., 2006). Mass flow analysis for Penta-BDE, estimates that in the EU the cycle

starts mainly in the automotive upholstery sector, ending in 94% waste with 6% emitted via

volatile and particulate emissions during use. Solid waste can then take different routes, the

more common being landfill (ca. 48%) and incineration (43%) with the remainder recycled

(9%).((UNEP)-Chemicals., 2010). The main application of Octa-BDE has been in acrylonitrile

butadiene styrene (ABS) casings of electric and electronic appliances (in Europe 95%, ca. 70%

for the rest of the world), mainly cathode ray tube televisions (CRT TV), computers and

copying/printing equipment. Octa-BDE is added to ABS in concentrations spanning between 12

and 18% w/w ((UNEP)-Chemicals., 2010). Considering that that globally more than 70% of Octa-

BDE was used in ABS and that on an average it constituted $1/7^{th}$ of the polymer's weight, the

material flow for the first cycle of treated ABS would have exceeded half a million tonnes. It can

be inferred that the number of second and third generation Octa-BDE-contaminated items

(from recycled plastics) have multiplied since their first addition. The material flow analysis of

Octa-BDE treated waste estimates that every year about 30% goes to landfill, an equal amount

is incinerated, 20% is converted into energy, 18% is recycled and less than half a percent is

reused "as is" (Commision, 2003). About 70% of Deca-BDE produced globally has been used as a

polymer additive (mainly in HIPS and vinylic-olefin polymers) for the production of electrical

and electronic equipment with the remaining 30% used in fibres ((UNEP)-Chemicals., 2010).

Although the characteristic loading can span from 5 to 30% in HIPS, the EU risk assessment

reports an average loading of 10-15% in styrenic polymers. Moreover, Deca-BDE is compatible

with latex, making it suitable for textile coating (Commision, 2002).

Although phased out in 2008, by the European court of justice (Justice, 2008), Deca-BDE was only very recently listed under the UNEP Stockholm Convention on POPs. Deca-BDE's later listing than the Penta- and Octa-BDE formulations is due to evidence that PBDEs with a lower bromination level (such as tetraBDE and pentaBDE) tend to bioaccumulate more and have higher toxicity than higher brominated congeners (such as decaBDE); notwithstanding this, toxicological studies on rats and mice showed a correlation between ingestion of DecaBDE and carcinogenic growths in glands, liver and the pancreas (Mörck et al., 2003), (Tseng et al., 2008). This could be explained with the possibility that lower brominated PBDEs could be generated by radical decomposition of higher brominated PBDEs either in the environment (through UV and combustion) or in living organisms (through metabolic pathways).

1.1.4 PBDEs in Waste

Considering the average turnover time for PBDE-loaded articles (e.g. Penta-BDE in the automotive industry, Octa-BDE in Electric and Electronic Equipment (EEE) and Deca-BDE in textiles), it is to be expected that the flow of contaminated material will grow in the near future ((UNEP)-Chemicals., 2017, UNEP-Chemicals., 2010). The UNEP Stockholm Convention on POPs, listed Best Available Techniques (BAT) and Best Environmental Practices (BEP) in order to reduce and contain the detrimental effect of BFRs on the environment.

The REACH legislation addresses this issue with policies that limit the concentration of Octa-BDE and Penta-BDE in materials (raw material or finished articles) introduced on the EU market (at the time of this study, the concentration limit for Octa-BDE, Penta-BDE or other banned mixtures is 0.1% w/w). The RoHS recast Directive 2011/65/EU limits values for polybrominated

biphenyls (PBBs) and PBDEs at a maximum of 0.1 wt% in homogeneous material and focuses on

waste-related criteria acknowledging poor waste management as the root cause of

contamination in new items. The RoHS directive forces manufacturers to control the presence

of RoHS relevant substances in their EEE components from the upstream perspective i.e. at the

design and the procurement stage. Despite this, such chemicals are now being found as

unintentional contaminants in a wide range of goods that do not require flame retardancy, via

accidental incorporation −during recycling− into items like kitchen utensils and food packaging,

(Samsonek and Puype, 2013a) videotapes, (Hirai and Sakai, 2007) children's toys and household

products (Chen et al., 2009), (Chen et al., 2010),(Convention, 2009). To minimise such

inadvertent contamination, BFR treated plastics should be separated during waste sorting and

dismantling from BFR-free plastics, as prescribed in the Stockholm Convention's BAT and BEP.

Currently, many waste plastics thought to contain Br are stockpiled, re-used in plastics that do

not require a particular mechanical strength, or incinerated (Zhang et al., 2016). These

procedures result in two undesirable scenarios: (a) waste plastics containing high percentages

of BFRs are recycled by mixing with new ("virgin") polymers, thus increasing the quantity of

new items contaminated with BFRs and impeding their elimination from the waste stream; and

(b) thermal degradation of PBDEs into highly toxic halogenated dibenzo-p-dioxins and

dibenzofurans (Sakai et al., 2001). European Standards (International Electrotechnical

Commission (IEC)) give guidance on WEEE sampling, sample preparation methods and specific

measurement methods. Generally, they describe 2 approaches: total elemental screening and

compound specific quantification; the latter typically requires GC-MS analysis (combined with

laborious sample preparation procedures i.e. sub-sample grinding, cryo-grinding, solvent

extraction, extract filtration, selective precipitation for oligomer removal, and chromatographic

purification). Alternatively, as described in the test methods IEC 62321, if characterisation of

individual brominated compounds is not required, the total elemental bromine content can be

measured using Energy Dispersive X-Ray Fluorescence (ED-XRF) technology incorporated into

hand-held instruments as an "analytical procedure to determine the presence or absence of

substances or compounds in the representative part of a product" (International

Electrotechnical Commission (IEC)). The European Directive 2002/95/EC stipulates that at least

50% of collected WEEE must be recovered, reused or recycled (according to the concentration

and nature of present contaminants), although the complexity and cost of traditional

compound-specific analysis are not justified by the value of the analysed items. Rapid Br

screening by XRF to provide pass/fail evaluation of legislative compliance is therefore an

attractive option (Babayemi et al., 2015), (Tien et al., 2013, Commision, 2006). The EU has

opted for a cautious approach to this issue, investigating first the impact that such provisional

limits - if enforced by EU regulations - would have on waste management practice within its

jurisdiction.

There are five possible options for recycling WEEE ((UNEP)-Chemicals., 2010): a) mechanical: by

means of rebonding, regrinding, and remoulding; b) chemical: via hydrolysis, glycolysis, and

solvolysis (Schlummer et al., 2006); c) thermo-chemical: via pyrolysis or gasification; d) closed

loop product clustering (Peeters et al., 2013); and e) incineration (Schlummer et al., 2007).

Knowing what class of BFRs and in what amount they are present in WEEE is important not only

to limit the exposure of workers in the EEE and the WEEE business, but also to make the

recycling processes more profitable and reduce their environmental impact. When recycled

polymers from WEEE contain impurities, their mechanical properties and market value are lessened. Although there are a vast variety of polymers, only a limited number of high-value engineering plastics, i.e., ABS, HIPS, blends of poly-phenyloxide and polystyrene (PPO/PS), and blends of ABS and polycarbonate (ABS/PC) are actually used for EEE production (Schlummer et al., 2007).

1.1.5 PBDEs in Toys and Food Contact Articles (FCA)

The above mentioned legislative actions do not address the presence of BFRs in existing items however, and the presence of restricted BFRs in plastic materials reaching the waste stream is now a serious concern. For example, the presence of restricted BFRs in new plastic items at levels not commensurate with flame retardancy suggests that recycling of FR-treated polymers leads to contamination of new goods. (Stringer et al., 2000), (Chen et al., 2009, Kajiwara et al., 2011). A 2015 study (DiGangi et al., 2017) found significant amounts of PBDEs in 9 of 21 (43%) inspected children's toys. In another study, concentrations of Br were measured in plastic children's toys and food-contact articles, as such items are not required to meet fire safety regulations and are of relevance for human exposure (Ionas et al., 2014). A polymeric food-contact article is described as any polymeric item intended to come into contact with food. Regulations for food-contact articles fall under the European Commission Regulation 10/2011 (Baiguini et al., 2011), (Regulation, 2014) which only establishes limits for evaluated constituents migrating into food or well-defined food-simulating solutions. As for the actual BFR concentration limits in polymers, the guidance prescribes the use of food-grade plastic, to avoid the risk of BFR contaminated plastic coming from recycled materials. For toys such a regulation

is still not in place, and therefore sourcing of materials is not restricted to "new/virgin" polymers (Commission, 2009). Evidence of restricted BFRs as unintended trace contaminants in new plastic items such as children's toys and food-contact articles has been documented in recent years, (Ionas et al., 2016) suggesting that the recycling of FR-treated polymers indeed leads to the contamination of new goods. Studies in this area remain preliminary in nature, with quantification of unintended trace contaminants in new plastic items not yet carried out on a large-scale, nor has much progress been made with identifying the specific origins of such unintended trace contaminants. Moreover, the need to verify compliance with low POP concentration limits for BFRs in materials requires a rapid, inexpensive and reliable in situ method that provides a viable alternative to conventional methods based on gas or liquid chromatography interfaced with mass spectrometry. Waste items are initially differentiated in operational categories when entering the waste stream (e.g. large cooling equipment (fridges/freezers), small WEEE, large WEEE, CRT monitors, and flat screen televisions) (Martinho et al., 2012). The items in these categories contain certain inorganic substances which are characteristic of their destination of use. The practice of mixing recycled plastic in FCAs is illegal in Europe; however, as an exemption, re-use of polyethylene terephthalate (PET) is assumed to be safe as the PET cycle is a closed-loop recycling process. This process is described in detail elsewhere ((EC), 2008, Hopewell et al., 2009) but in brief it consists of a waste management practice where a certain component (e.g. PET) is meant to be recycled indefinitely through the same waste pathway (e.g. water-bottle waste stream) as long as it can be guaranteed that no other waste stream (e.g. WEEE) is flowing into the closed loop. This is a case where waste-tracking information is used to allow certain materials to be sourced for the production of food-

contact articles. This concept is in line with the EU's 7th Environmental Action Plan: "Closing the loop" (Commission, 2015) that suggests circular economy strategies to create non-toxic material cycles that facilitate recycling and improve the uptake of secondary raw materials.

1.1.6 PBDEs in indoor dust

Dust has proven to be a source of PBDEs to human exposure (Allen et al., 2008a) acting both as a store and transport medium (Wilford et al., 2005). There are increasing concerns towards the effects of this exposure on babies due to body burden and behaviour (Jones-Otazo et al., 2005) and recent studies (Rauert and Harrad, 2015, Rauert et al., 2016) investigating how PBDEs end up in indoor dust found that abrasion and direct contact between the appliance and the dust are the principal transfer pathways. Some studies investigate spatial and temporal variability of BFRs concentration, reporting for example how the dust sampled over a long time span (ca. every month for eight months) (Allen et al., 2008a) does not vary significantly in the same room (mainly because the furniture was not changed), but different rooms in the same house can have completely different PBDE compositions in their dust; or the correlation between PBDE concentrations in house dust and in the blood of the inhabitants (Karlsson et al., 2007). In these studies it is suggested that: a) there is a strong correlation between a certain room and the PBDE 'signature' in that room's dust; and b) there is a correlation between PBDE body burdens and concentrations in dust. a) is usually attributed to the larger furniture that stays usually unchanged in a room and to the particular use the inhabitants will make of that room (e.g. as an office space with a higher presence of electric and electronic equipment or as a nursery with a higher presence of fabrics, upholstery etc...). A research gap regarding PBDE source

identification can be attributed to the fact that all investigated environments were already furnished and populated at the time of first sampling. This precludes the possibility of knowing whether a certain PBDE composition in a room is due to the building materials (carpeting, wallpaper, insulating foam, plastic tubing, wiring…) or to the furniture and equipment that was installed later on in that environment.

1.1.7 Overview of destructive analytical methods for the analysis of PBDEs in WEEE: current challenges

The International Standard IEC 62321 Ed.1 (International Electro technical Commission 2008) suggests gas chromatography- mass spectrometry (GC-MS) using electron impact ionisation (EI) as the technique of choice for confirmatory analysis of the BFR content of electro technical products. According to a report from the Danish Environmental Protection Agency (Nilsson et al., 2009) due to the technically demanding plastic extraction process, the costs of this analysis become prohibitive especially when applied to a high volume of samples. These traditional techniques can have a number of drawbacks aside from being time consuming and expensive. Soxhlet or pressurised liquid extraction of plastics often dissolves a substantial fraction of the matrix (polymer) together with the target compound, rendering the ensuing extract purification laborious and often leading to highly variable analyte recoveries. Furthermore, PBDEs are present across a wide range of bromination level, from the lower brominated tri-BDEs and tetra-BDEs with a low boiling point to the most brominated (deca-BDE) with a very high boiling point. This makes it practically difficult to use the same GC-MS system set-up to analyse all PDBE congeners simultaneously in a single GC run: ideally two different GC columns are used,

causing several analytical delays (run the samples on one system set-up first, then switch columns and run them again on the second set-up).

Although other types of detectors are reported in the literature (Covaci et al., 2003b, Covaci et al., 2007b, Riess et al., 2000), (Riess et al., 2000) like electron capture detector (ECD), UV detector or flame ionisation detector (FID), the chromatograms obtained with these can be difficult to interpret and uninformative due to overlapping retention times (Vetter et al., 2009). Some attempts have been made in the past to eliminate the time consuming solvent extraction and clean up steps – proposing e.g. pyrolysis of pulverised plastic coupled directly with gas chromatography and mass spectroscopic detection (py-GC/MS) (Luda et al., 2007, Luda et al., 2002, Abdallah, 2010).

A relatively newer technique proposed by Vazquez et al. (Vázquez et al., 2008) consists of ICP-MS analysis of acid-microwave digested plastics. This kind of approach can give very accurate and reproducible results for total Br content because it does not involve solvent extraction and clean up (for which the recovery can vary greatly). However, as it mineralizes the whole sample so that the Br should in theory stay quantitatively in the injected digestate, the losses in volatile analytes with this technique are not negligible. A test to measure these volatile losses has been developed (Wegner, 2010) that directs the vapours escaping from the digestion vessels in the microwave interfaced to an ICP source and detects the Br concentration in them. Losses of volatile Br compounds can be as high as 13%, not counting other possible losses that might occur during the preparation (e.g. pouring HNO_3 on the plastics generates immediately an exothermic reaction, opening the vessels after the digestion, etc…). Another option to prepare

the samples for ICP-MS analysis is to dissolve the plastics in organic solvents and apply

membrane desolvation to the extracts (Sung and Lim, 2000). A down side of this technique is

that it still requires a sample preparation step that uses expensive hardware (closed vessel

microwave) and solvents. Moreover, it does not provide compound specific information about

the congeners embedded in the plastic.

For all these destructive analytical techniques the analysis time is too long to be practicably

used in recycling plants, and the kind of hardware, consumables, installation requirements and

know-how needed is not always readily available in such locations.

1.1.8 Overview of direct sampling techniques for the analysis of PBDEs in WEEE: current limitations

"Direct sampling" implies the advantage of analysing the sample as it is, thereby eliminating the

sample preparation step. Some of the following techniques are non-destructive only in

principle, as in some cases a smaller piece of the sample has to be excised, but in general they

are meant to provide in-situ results for a high sample throughput.

1.1.8.1 Sink and float method

This is a rudimentary sorting technique based on the principle that Br-containing polymers have

higher specific weights. Changes in specific weight of polymers are measurable with this

method starting from a minimum BFR content of 3% (Schlummer and Mäurer, 2006). The

"detection limits" of this technique can be improved by changing the density of the aqueous

solvents using different salts, and with an accurate separation process a rough differentiation

between polymers (PP, PE, ABS, HIPS, PPO) is possible (Schlummer, 2011). Although not very sensitive and subject to interferences due to the presence of organophosphorus FRs, this method is worth mentioning because of its vast use in developing countries, motivated by the low operating and hardware costs and the possibility of sorting high-volume batches at once (Sindiku et al., 2011).

1.1.8.2 Sliding spark (SS) spectroscopy

The working principle of this optical emission spectroscopy (OES) technique relies on a train of high current sliding sparks to vaporise and atomise small amounts of plastic materials. The atoms are in an excited state that causes them to emit in characteristics lines of the spectrum. To use this system as a surrogate metric for BFRs, the intensity of Br emission lines are associated to the total Br concentration (Seidel et al., 1993). Although the declared (Haarman and Gasser, 2016) lowest detection limit for Br with this technology is 0.1% w/w, it is not considered reliable for quantification and it is only used in a pass/fail mode with a Br concentration threshold set at 1%. The technique is only able to sample the surface material when it is in contact with the spark source, and thus the result cannot be representative of the bulk if the plastic has had a coating treatment. The hardware consists of an affordable hand held device that weighs around 4 kg. Sampling/processing time is a couple of seconds, and measures are usually performed in triplicate.

SS is sometimes coupled to near infrared (NIR) detectors in order to recognise the type of polymer the sample is made of, for better sorting and recycling.

1.1.8.3 Vibrational Spectroscopy Techniques

IR and NIR have been used with varied success for qualitative analysis in heavily BFR loaded

plastics. In polymers, attenuated total reflectance proved to be more successful as it reduces

the matrix effects by sampling a thin layer of plastic. As mentioned above, NIR can also be used

to identify the polymer itself, although its effectiveness is inversely related to how dark the

sample is.

A more accurate technique is Raman spectroscopy, which investigates the low-frequency C-Br

vibrations. It does not require contact with the sample (Sommer and Rich, 2001) and can also

be used to identify the polymer type (Allen et al., 1999).

Raman bench top instruments have proven able to differentiate between different PBDEs in

plastic samples (HIPS, ABS, PC) but they have not been used for PBDE quantification so far

(KIKUCHI et al., 2004). However, some authors have indicated that development of an internal

reference (Zheng et al., 2001) or computational analysis of the results (O'Grady et al., 2001)

might lead to a linear correlation between concentration and response.

The efficacy of different portable Raman instruments has been investigated with results

showing that it is possible to find distinctive BFR peaks, relative to C-Br vibration at 200 to 240

cm^{-1} in the spectrum with no overlapping between the polymer-related vibrations (Baird et al.,

2010).

1.1.8.4 X-Ray Transmission (XRT)

This technique is based on the property of the sample matrix to transmit X-Rays with different attenuation coefficients according to the amount of analytes contained within. The resulting spectrum of this technique is due to absorbance of the non-transmitted photoelectrons. XRT does not need contact with the sample, it can separate at a rate of 1 ton per hour BFR from non-BFR containing plastics and is thus a valid technique for high throughput sorting-recycling plants, but still provides a rough estimate able to produce a Br-reduced WEEE rather than a Br-free fraction (Adamec, 2017). Additionally the high hardware costs render this option not viable for small and medium recycling plants.

1.1.8.5 X-Ray Fluorescence (XRF)

There are two kinds of XRF spectrometry: energy dispersive (ED), which uses the particle nature of light to discriminate the elements according to the energy of the transition experienced by the analyte's inner electrons; and wavelength dispersive, which uses the wave nature of light to discriminate the elements according to differences in wavelength produced by their fluorescence. The latter is a higher end technique, not commonly used for this kind of analysis. This overview will focus on ED-XRF – to date the method of choice to screen restricted substances (IEC, 2008).

Hand-held XRF is a fast, non-destructive in situ applicable technique that can give accurate and repeatable data at relatively low cost and minimal use of consumables (Kalnicky and Singhvi, 2001).

Table 1-2 Summary of current limitations of XRF and LA-ICP-MS analysis for the quantification of BFRs in polymers and improvement strategies using the combined XRF, LA-ICP-MS and TD-GC-MS instrumentation in this study.

Technique	Limitation	Proposed solution/measures applied
XRF	Standard reference material is only available in pellets and only at very low Br concentrations	Design new reference material in the shape of flat disks of varying thicknesses and with a wide range of Br concentration
	Very thin plastics can give errors:	
	-negative: because the absorption of radiation is dependent on the sample thickness, the sample is too thin as polymeric matrixes are virtually transparent to XRF. No absorbance of secondary emissions is performed by the material itself.	develop a thickness calibration to provide a correction equation to account for the influence of polymer thickness on measured Br concentration
	-positive: because Br fluorescence might originate from components located beneath the plastic housing (*e.g.* circuit boards)	samples and standards measured disassembled from the item and a lead-lined auto-sampler stand used to avoid contamination from beneath the sample
	Br might not come from BFRs due to the presence of inorganic Br	Br measurements compared with a BFR specific identification method (*i.e.* TD-GC-MS)
	Spectral interferences (other elements with similar fluorescence energy, overlapping Br emission lines)	Ratio between the two main X-ray fluorescence lines for Br ($K\alpha 1$ and $K\beta 1$) used to normalise the most intense line.
	Analysis of plastics with high levels of BFRs display substantial negative error due to self-absorption	Low *and* high concentration level reference materials used for calibration

Technique	Limitation	Proposed solution/measures applied
LA-ICP-MS	Solid standards that ablate in the same way of the samples for calibration are needed	Use a set of calibration materials based on ABS containing commonly used additives and fillers
	Difficulty to use internal standards	External calibration performed with 9 calibration materials
	Sample inhomogeneity might generate unrepresentative Br concentration data	Macroscopic homogeneity of reference material assessed with XRF; microscopic homogeneity assessed with synchrotron radiation μ-XRF

As concentrations of Br in BFR-containing WEEE are high (percentage levels), the low sensitivity of these instruments (ppm levels), is not problematic for this application. However, XRF is considered reliable only for pre-screening or screening (International Electrotechnical Commission (IEC)) (IEC, 2008) because of its technical limitations, summarised in Table 1-2 (UNEP-Chemicals., 2010), (IEC, 2008). Moreover, XRF is only able to quantify total elemental Br. Any analytical procedure that uses XRF for BFR quantification will always work on the assumption that all the detected Br originates from organic compounds: a reasonable assumption considering Br salts are rarely found in polymers. Furthermore, XRF is still susceptible to source misclassification i.e. the incorrect assumption that all Br content is due to a specific (usually regulated) BFR, e.g. HBCDD, when some or all of the detected Br arises from the presence of another BFR.

1.1.8.6 LA-ICP-MS

ICP-MS is conventionally used with liquid samples, therefore the analysis of polymers should be preceded by acid digestion (with losses in volatile analytes) or dissolution in organic solvent (with maintenance problems arising after a short time in the plasma interface of the ICP-MS due to carbon deposition). For these reasons a solid sampling technique is desirable. Laser ablation, although promising, still needs optimisation for use on polymers as it is a strongly matrix-dependent technique (Kosler, 2008). The ablation quality can vary greatly from one kind of polymer to the other, which is why the calibration has to be matrix-matched with the samples.

The laser transfers a desired amount of sample into the gas phase with what is assumed to be a stoichiometric representation of the sample, and sends the plume to a mass detector (ICP-MS) (Russo et al., 2002). A more detailed explanation of this technique can be found in chapter 2

1.1.8.7 Glow Discharge-magnetic sector MS

For a long time, the analysis of non-conducting materials with solid sampling techniques was restricted to laser ablation. With the technical evolution of glow discharge (GD) in the past twenty years, the requirement for conducting samples can be overcome allowing GD mass spectrometry to be performed on plastic using a conducting mask on the sample surface as a secondary cathode (Donohue and Harrison, 1975) or a radio frequency-glow discharge (rf-GD) ion source (Pisonero et al., 2004). The external calibration can be performed with solid standards as with laser ablation sampling. Moreover, quantitation without standards is also possible using an IBR (Ion Beam Ratio) approach. The working principle is similar to that used

with XRF: the instruments measures "all" the elements present in the sample, and normalises them on the assumption that the sum of all their concentrations will be 100%. This technique has proved less matrix dependent (reducing the need for matrix matched standards with high homogeneity requirements), more robust (the GD source is inherently stable) and easier to calibrate than LA-ICP-MS (Hoffmann et al., 2005). The sensitivity and quantification capabilities of the GD-ms-MS techniques on conductive samples are far superior to LA-ICP-MS, but there is still no record in the academic literature of a comparison of these two techniques for analysis on plastic samples. For the purposes of this application GD-ms-MS is not a viable technique due to prohibitive hardware costs.

1.1.8.8 Direct Analysis in Real Time (DART)

This is a solid sampling technique able – if coupled with a suitable detector- to give compound specific results in the same way as a GC-MS-MS would (Jana et al., 2008). The working principle is similar to APCI: neutral metastable species are formed by electrical discharge (cold plasma) in a gas (helium or nitrogen). Following reaction with components of the atmosphere such as water and oxygen molecules, reactive ionic species are produced. The collision energy can be 'tuned' to have a softer ionisation by changing the gas used to produce the cold plasma (e.g. He is more energetic than N_2, having a higher first ionisation energy), the voltage of the grid producing the discharge, and the temperature of the beam ionising the surface of the material. More details on this technique can be found in chapter 4, section 2. There are several mechanisms by which PBDEs can undergo fragmentation, but the main one is through radical reaction.

1.1.8.9 *Direct Ionisation Probe*

This is a solid sampling technique able to give compound specific results by extracting the accurate masses relative to each compound from the total ion current of a sample. It does not involve chromatographic separation. The sample is accurately weighed and placed in an aluminium crucible. The crucible is inserted in the probe and guided into the ionisation chamber. The temperature of the probe (and of the crucible) will be ramped at a suitable rate and the resulting vapours ionised via EI and analysed with a suitable mass spectrometer. More details on this technique can be found in chapter 3, section 2.

1.2   Aim of this study

Processing of waste electrical and electronic equipment (WEEE) presents a potential risk to human and environmental health, in part due to the high BFR content of a substantial proportion of such items. There is a variety of laboratory-based techniques to analyse PBDEs recommended by UNEP guidance for recycling and inventory ((UNEP)-Chemicals., 2017), using high end equipment and technical know-how that is often unavailable in most locations where waste is sorted. To be able to stock safely, sort and redirect this waste material, it is crucial to develop a rapid and inexpensive method that will not only provide basic screening information, but real-time quantitative metrics for PBDEs in items and consumer products with minimal to no sample preparation required.

Given the above described need for suitable analytical techniques for the analysis of PBDEs in waste material, the overriding hypothesis of this study is that one or more techniques can be found that are capable of providing a low cost, rapid throughput, and user-friendly metric of PBDE concentrations in polymeric articles and in particular whether these exceed limit values. The word "metric" implies that these techniques are able to quantify an observable (e.g. the total Br concentration) that is linearly correlated to the actual PBDEs concentration, providing still an acceptably accurate evaluation (no false negatives) on whether or not a sample exceeds the LPCLs. To test this hypothesis, the aims of the current study are to:

- Understand to what extent field based instruments and/or simpler, cheaper laboratory-based techniques can be used to screen products and waste materials containing high levels of BFRs by evaluating the efficacy of hand-held XRF as a "screening-level" metric of the BFR content of various polymeric matrices.

- Develop a hand-held XRF fit-for-purpose technique for accurate quantification of Br in WEEE plastics as an alternative BFR metric that maintains linearity over a wide dynamic range as the plastic casings for electrical and electronic equipment might contain BFRs from 0 to 30% w/w. To do so, solid reference materials must be designed and developed, the geometry and chemical composition of which are key to a good matrix-matched calibration and error correction. Results will need to be cross validated with a more accurate, more sensitive technique such as LA-ICP-MS.

- Investigate *in-situ* unintended trace contaminants in individual samples by quantifying Br and Sb and validating results against laser ablation-inductively coupled plasma-mass spectrometry.

24

Furthermore, we test the hypothesis that poor recycling practices have led to the presence of restricted BFRs as unintentional contaminants in articles containing recycled polymers. This was achieved by:

- Adding to the currently sparse database on the presence of BFRs as unintended trace contaminants in polymeric consumer goods by investigating the extent to which food-contact articles and toys currently present on the market contain BFRs as such items are not required to meet fire safety regulations and are of relevance for human exposure.

- Generating compound-specific data on solid polymers with TD-GC-MS in order to:
  a) evaluate to what extent the detection in a given sample of both Br and Sb provides a simple indicator of whether the Br detected arises from the presence of PBDEs, as Sb_2O_3 is widely used as a co-additive with PBDEs added to increase flame retardancy but is not used in conjunction with other regulated BFRs; b) Evaluate the suitability of X-ray fluorescence Br measurements as a surrogate indicator of the presence of BFRs in polymers by validating against thermal desorption-GC-MS. This assumption is verified if a Br-positive sample is also a BFR-positive sample; c) Roughly evaluate the qualitative distribution of different BFRs amongst samples, using compound specific results (TD-GC-MS) combined with total elemental results (XRF and LA-ICP-MS).

- Measuring WEEE related elements and use their concentrations in relationship with the Br content and the polymeric matrix to identify the source of contamination in the waste stream.

- Developing and validating a method that reliably quantifies BDE-209 with Direct Insertion Probe (DIP) in combination with magnetic sector high resolution mass

spectrometry (HRMS) with neither sample preparation nor chromatographic separation needed.

- Evaluating the feasibility for using Direct Analysis in Real Time coupled with HRAMS to quantify compound specific PBDEs without sample preparation or sample weighing.

Moreover, this study also aims to:

- Evaluate the efficacy of ICP-MS coupled with GC as a "screening-level" metric of the BFR content of indoor dust.

- Evaluate how the use of electric and electronic office appliances can impact PBDE concentrations and patterns in different work environments and after different periods of occupancy.

- Compare the PBDE signature in the dust before and after occupation (temporal variability, to test the hypothesis that furniture and equipment placed in a room are able to change its initial (when the room was empty and unoccupied) PBDE signature.

- Study the relationships between PBDE signature and room characteristics (e.g. size, number of chairs, number of electric and electronic appliances, etc).

Figure 1-2 gives a graphical summary of how the different parts of the project correlate with each other.
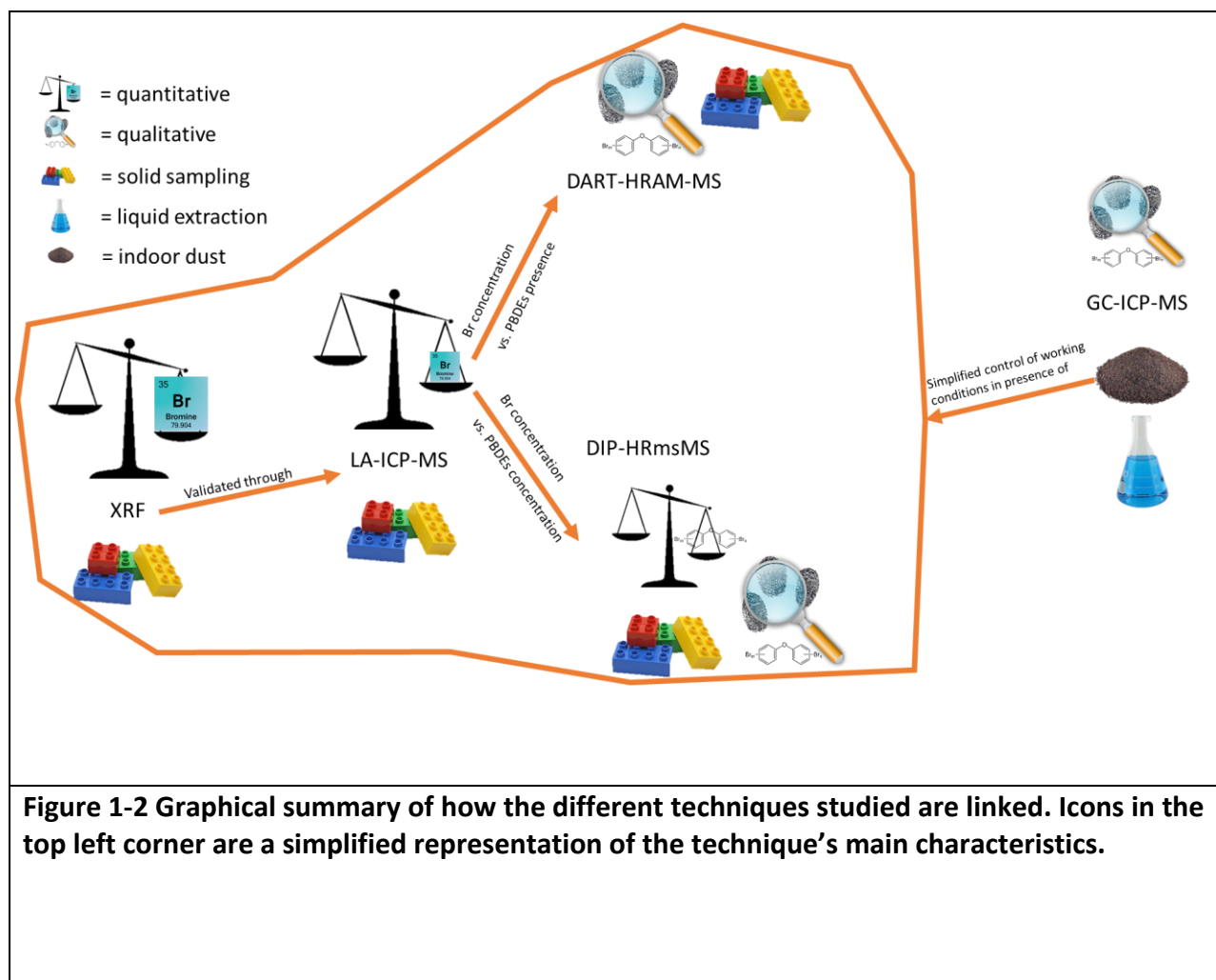
Figure 1-2 Graphical summary of how the different techniques studied are linked. Icons in the top left corner are a simplified representation of the technique's main characteristics.

2 Development and evaluation of XRF and LA-ICP-MS methods for the quantification of Br

Monitum

This chapter contains some material taken verbatim from the following articles:

GUZZONATO, A., PUYPE, F. & HARRAD, S. J. 2016b. Improving the accuracy of hand-held X-ray fluorescence spectrometers as a tool for monitoring brominated flame retardants in waste polymers. *Chemosphere,* 159**,** 89-95.

GUZZONATO, A., PUYPE, F. & HARRAD, S. J. 2017b. Evidence of bad recycling practices: BFRs in children's toys and food-contact articles. *Environ Sci Process Impacts,* 19**,** 956-963.

2.1   Synopsis

This chapter describes the development and validation (by comparison to a more accurate technique) of a novel, robust and reliable procedure that uses hand-held XRF for bromine quantification in polymers as an alternative BFR metric. To do so, an *ad hoc* calibration was developed with XRF and applied to the measurement of real samples. The resulting values were then cross-validated with LA-ICP-MS which was also calibrated with bespoke standards, to ensure that the calibration matches with the matrix. Finally, to check the accuracy of hand-held XRF as a surrogate BFR metric, TD-GC-MS was applied to the samples to ascertain that the measured Br is attributable to the presence of BFR molecules. In keeping with the focus of this

study on easy, fast techniques, TD was used because solid samples like polymers can be directly measured by thermal desorption GC-MS and the sample preparation is practically solvent-free. Thermal desorption GC-MS has been proven to be an effective tool for identification of polymer additives (e.g. antioxidants, UV-stabilisers, initiators, plasticizers, etc.) as well as for the detection of BFRs (Bart, 2001). Making this method practically applicable was the priority of this study, therefore the calibration covers a wide dynamic range for Br concentrations, as the plastic casings for electrical and electronic equipment might contain BFRs from 0 to 30 weight% ((UNEP)-Chemicals., 2010).

2.2   Introduction

2.2.1 Matrix dependence

Matrix dependence for XRF and LA-ICP-MS can be associated – amongst other causes – with the optical response of the matter when hit by emitted light. A major difference between X-ray and laser beams resides in the wavelength (WL or classes of WL) associated with the beam of light. XRF provides information on the elemental composition of the sample, but not much on chemical properties because the X-ray photon wavelength is much shorter than the laser radiation and hence more energetic than chemical binding energies. Therefore, matrix dependence for XRF depends on the atomic weight of the elements in the sample matrix. Metals, which are heavier, lead to a relatively shallow penetration depth, whereas in plastics, which primarily consist of carbon and hydrogen, light-matter interaction penetrates deeper.

Photons produced by a laser are at a lower energy, thus the beam-matter coupling depends on the molecular scaffold of the matrix.
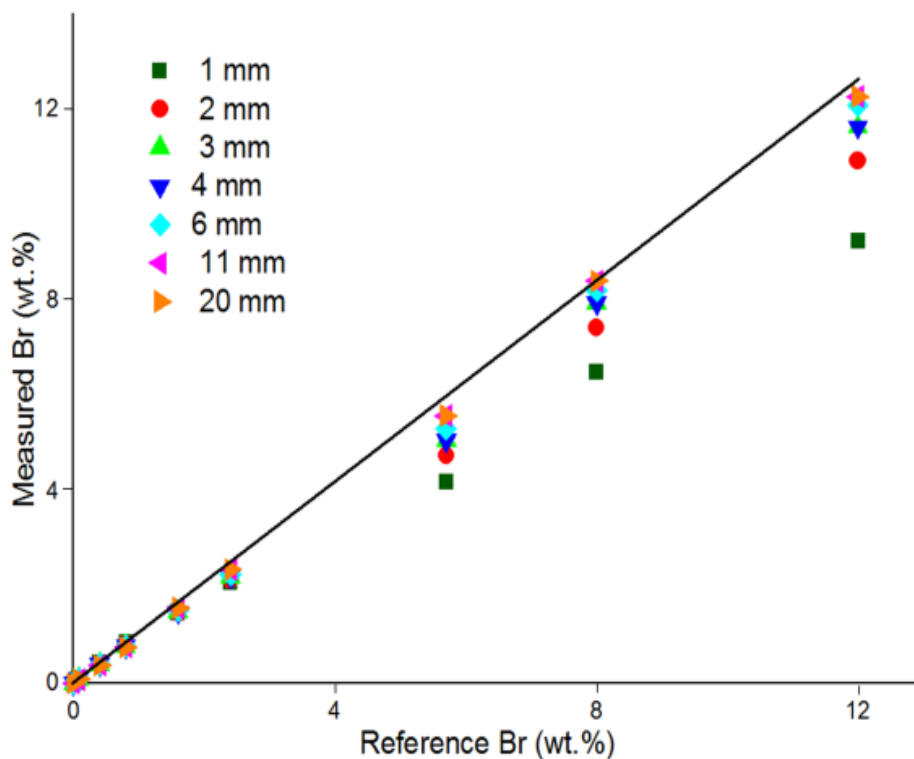
Figure 2-1 Effect of thickness on the measured concentration by XRF. All the RMs were measured at different thicknesses, the measured concentration deviates more from the reference for thinner samples.

For XRF, this matrix dependence results in a negative non-linear deviation in signal intensity for samples with equal concentrations of Br but different thicknesses. Figure 2-1 shows a plot of the measured Br intensity vs. the reference concentration of the SRM designed *ad hoc* for this study: each reference material - produced in a number of different thicknesses - was measured with an XRF device. When a plastic sample is too thin (a condition defined as "intermediate thickness"), the intensity of fluorescence becomes dependent on both concentration and

thickness, introducing a negative error equating to underestimation of Br concentrations. When the sample is thicker (condition defined as "infinite thickness") the measurement occurs under ideal conditions, meaning that the X-rays penetrate the material without escaping via the other side.

For LA-ICP-MS, one effect of the light-matter interaction can be a high fluctuation in the mass of analyte delivered to the ICP-MS (Kosler, 2008). Matrix effect also influences the accuracy of LA-ICP-MS when used for quantification.

The concentration of fillers and additives in the polymeric matrix can influence the average dissociation energy of the molecular clusters that are ablated. If fillers and additives are present in high concentrations, the bonds between polymer chains can be weaker; this will result in a higher amount of ablated material and hence a higher apparent concentration. To account for this, the reference materials used in this study were made of the same polymer as the samples and loaded with the most commonly used inorganic fillers.

Other matrix effects are: the volatility-driven inter-element fractionation that results in fluctuations of relative sensitivities for different elements, elements re-depositing on the melt rims of the ablation pit causing a different relative distribution (Mans et al., 2009), passivation of the layers to be ablated, or large size distribution of particles causing different transport efficiencies (Koch et al., 2002). These effects were addressed by using low fluences (of the laser intensity) in order to minimise the formation of melt rims around the pits and reducing the amount of ablated material. In addition, we perform a scanning ablation, which produces a more constant particle size distribution, with a resultant lower time-dependence on the signal intensity and an overall 2 to 5-fold better precision than static laser ablation (Kosler, 2008).

Moreover, it was not proved that the gain in accuracy observed with static ablation, is solely dependent on the static sampling but could also be the result of particle filtering and ICP sampling position. (Guillong and Günther, 2002, Serafetinides et al., 2001) showed how mass-load effects can be mitigated by reducing the amount of material going into the Ar plasma source; we achieved this by using low fluences, thereby ablating less material, reducing the melt at the ablation site and producing a narrower size distribution of particles centred towards smaller values. Also, the use of fluences in the range of 0.35-0.55 J/cm^2 resulted in less variable ablation rates between different non-halogenated polymers (Serafetinides et al., 2001); this is very important to mitigate any differences (due to changes in the polymer blend, or inorganic fillers of additives) between the polymers used for calibration (RMs) and the unknown samples.

2.3   Experimental

2.3.1   XRF

A Thermo Scientific Niton XL3T Goldd Plus handheld device was used, equipped with a geometrically optimised large drift silicon detector and a 50 keV x-ray tube. The analysis was performed with a molybdenum filter, the emission fluorescence line chosen for quantification of Br was Kα1 (11.92 keV) and the relatively less intense Kβ1 was used for qualitative evaluation of the spectra (13.29 keV) (see Table 2-1 for details).

X-ray fluorescence spectrometry is a widely used analytical technique because it requires no sample preparation and can have sensitivity down to the low ppm levels.

Table 2-1 Optimised experimental conditions for XRF

Energy Dispersive XRF	*Thermo Scientific Niton XL3T Goldd Plus*
Detector	large drift silicon detector
X-Ray tube	50 keV
Filter	Molybdenum
Spectral line (used for quantification)	Kα1 (11.92 keV)
Sampling spot	0.8 cm (0.3 cm for small samples)
Measurement time	120 s
Replications	4
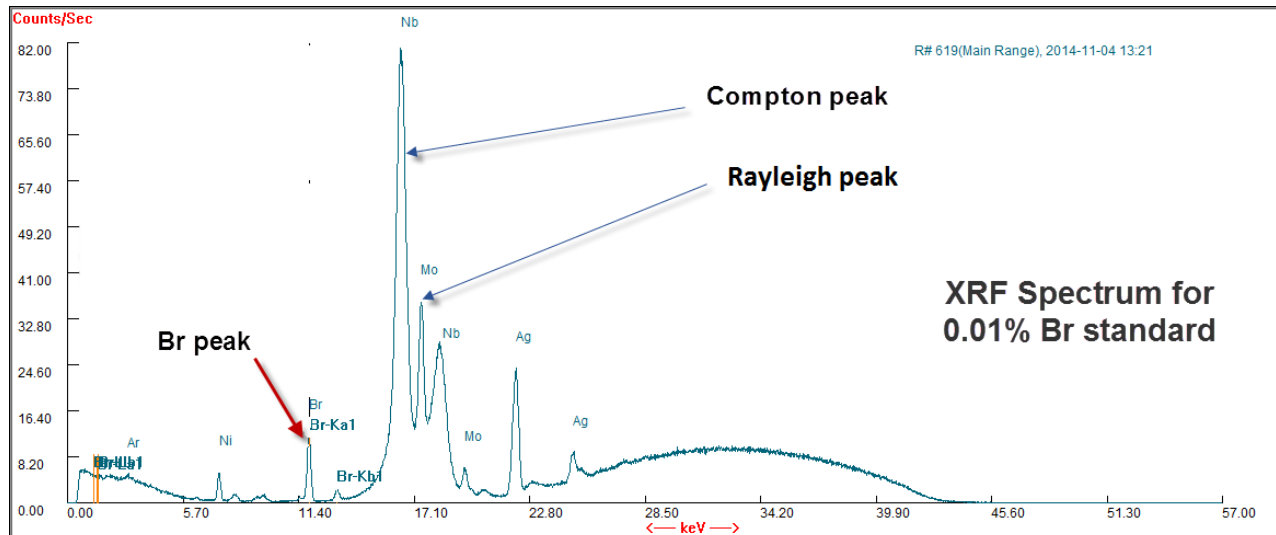
Figure 2-2 Fluorescence spectrum for a polymeric solid reference material containing 0.01% of Br

There are two types of XRF:

-Wavelength dispersive

-Energy dispersive

ED-XRF devices are smaller than WD-XRF spectrometers and can perform simultaneous analysis of all the elements in a sample. For this reason ED-XRF was chosen in this study to develop a solid sampling analytical method for in-situ quantification of elemental Br in WEEE. Therefore, this short overview focuses on ED-XRF.

When an electron is strongly accelerated or it transitions from an outer atomic orbital to an inner orbital, X-rays can be emitted. In XRF, X-rays are produced via both of these mechanisms:

- In the X-ray tube, target atoms are hit by head-on collision with high energy electrons. The kinetic energy of the electron will be converted into X-ray energy
- in the sample's atoms when the X-ray produced in the tube causes the ejection of an inner orbital's electron (K,L or M shells) and subsequently the transition of an outer shell electron into the inner shell vacancy. The energy difference between shells is converted to x-ray emission

The energy of the second type of X-ray is characteristic for a particular element. According to Moseley's law, this characteristic energy is proportional to the square of the atomic number. For this reason, EDXRF is not suitable for low atomic number elements (H, He, Li, Be, O), as the emitted energy would be too low to be detected accurately.

Two kinds of scattering can occur when X-ray interacts with matter:

-elastic scattering (Rayleigh): the incident photon is scattered and escapes with the same initial energy

-inelastic scattering (Compton): the incident photon replaces an outer shell electron which is in turn ejected with a different energy than the incident photon.

The intensity of the last type of scattering is inversely proportional to the average atomic number of the sample material, and in turn to the mass attenuation coefficient (MAC): the MAC is a measure of how much of the intensity of an X-ray passing through matter is absorbed. Plastic for example has a very intense Compton scattering when it contains little to no mass of heavy elements (e.g., Br) as can be observed in this spectrum (Figure 2-2). Due to the inverse proportionality of the Compton scattering vs. the MAC, Compton normalisation can be applied and has an effect which is close to internal standardisation. It works by measuring the ratio of the analytical line intensities and the intensity of a Compton peak, which is proportional to 1/(mass attenuation coefficient of the matrix). The MAC is proportional to the atomic weight of the irradiated matter. For samples with low atomic weight, the portion of X-ray that is scattered, hence not absorbed and measured as characteristic wavelength WL is going to be higher. Therefore the amount of scattered radiation does not constitute a problem for samples with high atomic weights like metal ores or rocks, but for the polymeric samples analysed in this study (the composition of which is mainly ^{12}C, ^{1}H and in some cases ^{14}N), it is at the base of a series of matrix effects that cause the instrument response towards a certain element (e.g. Br) to be not linear over the working concentration range. Especially when analysing organic matrices, for which the absorption from the matrix can have a steep change even with small additions of heavy elements (such as Br), performing a Compton correction can reduce significantly the matrix effect. Instead of building a calibration line with the reference concentration against the raw analyte intensity, this is achieved by calibrating the instrument

using a ratio of the analyte intensity (heavier atom) to the intensity of the Compton peak. In the case of Br in polymers, the Compton scattering and the analyte intensity have an inverse proportionality with each other: when the matrix contains less heavy atoms, its Compton scatter will increase and the analyte (heavy atoms) intensity will decrease. This means that the function describing how the measured intensity (analyte signal) changes with the actual concentration of the analyte has two variables which are interdependent: the analyte concentration and the mass absorption coefficient. When performing a Compton correction, the calibration curve is built plotting the ratio between analyte peaks intensity and Compton peaks and vs. the reference concentration of Br. As these two intensities depend on the MAC with opposite proportionality, using their ratio to perform the calibration will account for the dependency from the MAC.

Thickness error: consider a 'slice' as a very thin layer of material with thickness Δx and a certain concentration C_{Br} of X-ray-absorbing atoms, in this case Br. Out of six incoming photons (represented as arrows) in Figure 2-4, two are absorbed (arrows touching the black dots). This constitutes absorption of the beam of photons at the rate of 1/3 per slice. If another slice of thickness Δx and C_{Br} would be glued to the first one, this double slice would absorb 1/3 of the remaining photons per second. This increase in absorption is exponential and reaches a plateau when enough slices have been added, i.e. when the material reaches the condition of critical (or infinite) thickness. This is a condition for which the photon absorption is virtually independent from the thickness of the material, but only upon its concentration of X-Ray absorbing atoms: this (x) (defined as the depth giving 99% of the maximum obtainable intensity expressed in cm) is estimated as [1]:
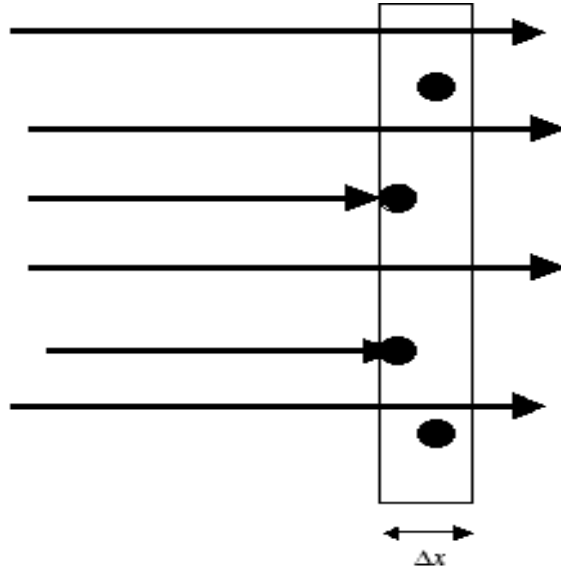
Figure 2-3 Representation of light attenuation in a thin slice of material. Dark dots are light-absorbing particles, arrows represent photons. Δx is the thickness of the slice.

$$X \ [cm] = 4.61/(\mu \ [cm^2/g] \cdot \rho \ [g/cm^3]) \cdot \sin\psi^2 \qquad [1]$$

where ψ is the angle that the emerging radiation takes with the incident radiation, ρ is the sample density and μ is the MAC of the sample at the working WL. Critical thickness is a function of the average atomic weight of the sample, which defines the ρ and the MAC. For metals, this condition of critical thickness is fulfilled at very small thicknesses (e.g. for lead it is only 75 μm), but for lighter matrix elements this thickness can increase up to about 20 mm. Previously, the fulfilment of this condition was necessary to obtain a quantitative measurement, this work suggests instead a new approach to quantitatively measure Br in samples that are thinner than the infinite thickness.

37

2.3.1.1 Estimating the critical thickness
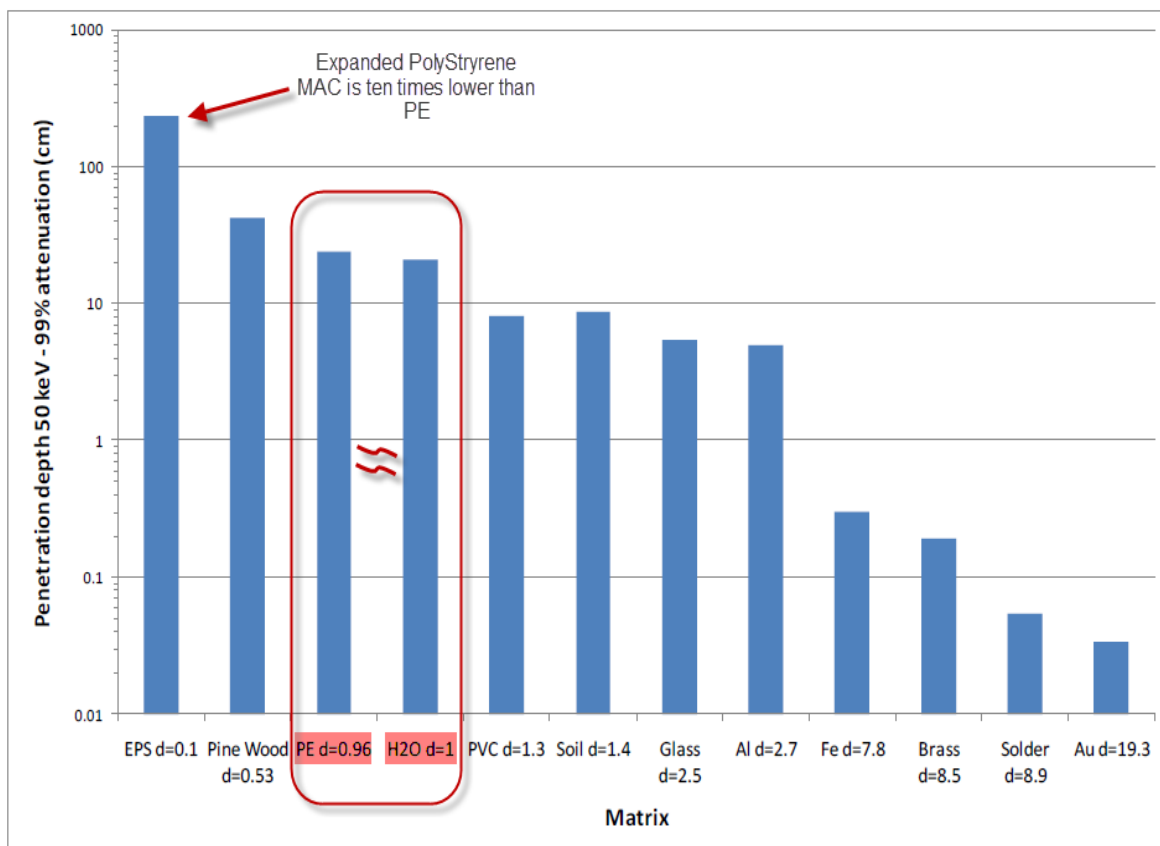
Figure 2-4 Penetration depth of X-Rays in common matrices. MAC stands for Mass Attenuation Coefficient, and it is a measure of how transparent a material is to X-Rays

A feasibility study was conducted before designing and producing solid reference materials for this application. The aim of this exploratory experiment was to understand how the critical thickness of a sample of virgin polymer is influenced when heavier atoms (such as Br) are added to the matrix. This information would then be used to design the standards in the most representative thicknesses for this particular matrix.

Since the solid reference material requires a laborious and expensive procedure to be prepared and moulded correctly, this initial test was performed to also understand the range of thicknesses the solid samples should be produced for the actual matrix matched calibration.

The testing strategy was thus:

- a liquid that has a similar MAC to virgin plastic able to dissolve a Br containing compound was chosen: the best choice for this was water: as shown in the graph (Figure 2-4) because it has a reasonably similar MAC to PE and it can dissolve Br salts

- 9 calibration solutions with water and varying concentrations of KBr from 9 calibration standards were prepared with water and KBr containing from 0.01% to 17% w/w Br.

- Each of the 9 solutions was then transferred in seven XRF sampling cups (Figure 2-4). Each of the seven cups was filled at increasing volumes of each concentration spanning from 1 to 18 mm of thickness.

- The XRF user method was modified to acquire the ratio of Br intensity and the Compton peak intensity for each of the 63 cups in triplicates and their results averaged.

Results were plotted against sample thickness and evaluated (Figure 2-6). Each series of symbols is a different calibration solution (they were all normalised to 1 for infinite thickness in order to compare them). In a scenario where the measurements are not affected by matrix effects, the Br/Compton intensity ratio would be one (horizontal line), meaning that the Br intensity and the Compton scattering increase with the same function when the Br reference concentration increases. For low thicknesses the variation in intensity for the same concentration is greater.

Figure 2-5 Example of XRF sampling cups
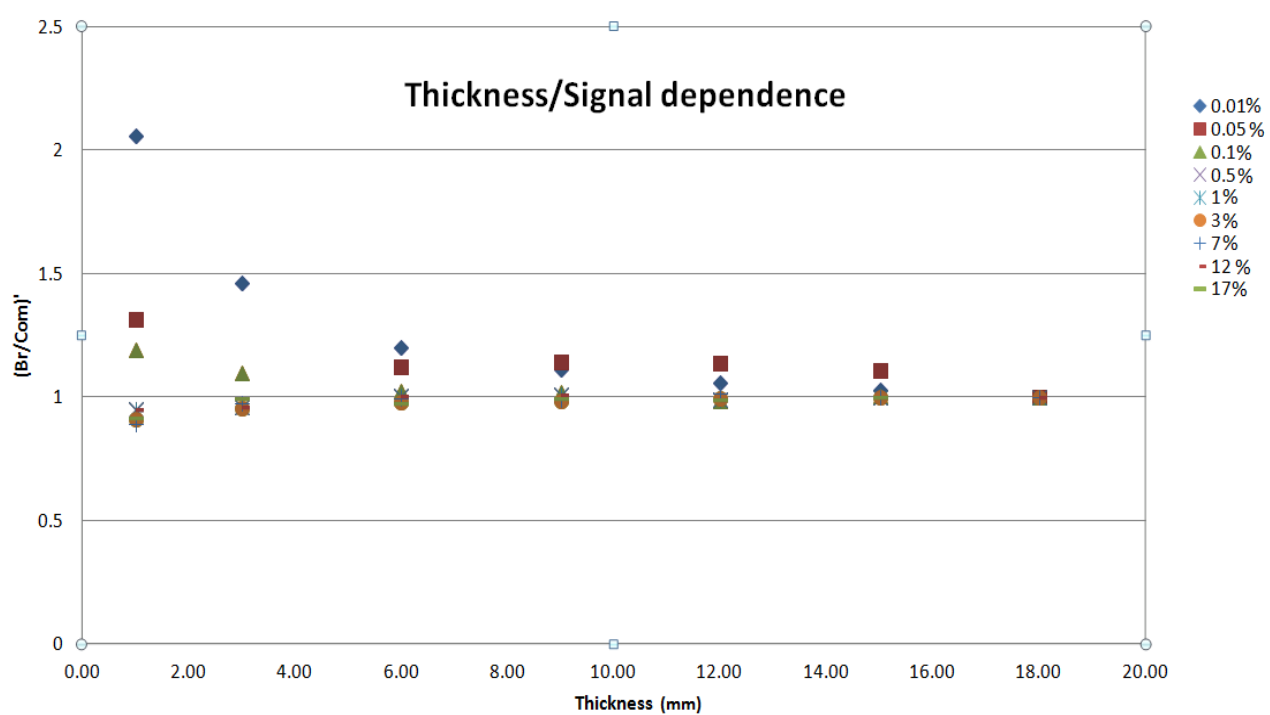
Figure 2-6 Compton-normalized Br signal vs. sample thickness.

This explains why in the literature (Gallen et al., 2014) there are positive Br results when the results of the destructive (more accurate) test is instead negative: thin samples can give such erroneous results (especially at low-to-very low concentration of Br) if corrected for the Compton effect, because the matrix is not absorbing emergent secondary and tertiary emissions, which will instead all go to the detector as Compton scattering. Figure 2-7 shows that the error will be larger for plastic layers thinner than 6 mm and samples with Br concentrations lower than 0.5%. Most of the EEE appliances that have plastic casings fall in the 0-6 mm thickness range, often in the 1-3 mm range: hence a special calibration for this application is required. Expanding the plot in the thickness region of interest it is visible how for more concentrated samples the critical thickness is reached faster: this is because more

Figure 2-7 Effect of Compton scattering over the most common thicknesses for EEE casings

concentrated samples have a higher MAC. Each concentration gives a signal to thickness dependence that is described by a certain function. The results of this preliminary test are:

- For a virgin material with a similar MAC to plastic that is loaded with Br atoms the MAC varies quickly with the concentration of the added Br within a normal concentration range for this application (0.01-17%). Thus a matrix matched calibration is necessary for quantitative analysis of Br in plastics.
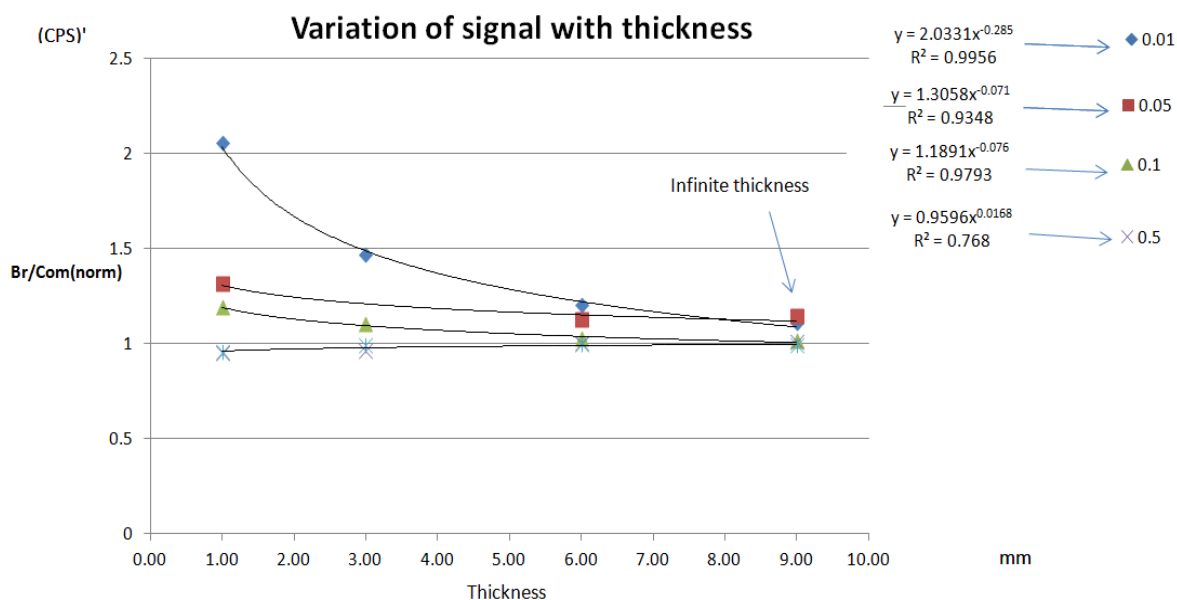
- The largest deviation from the reference Br concentration is observed for thicknesses that are typical of the samples in this application. Thus the solid reference materials developed need to be produced in layers covering a span between 0 and 20 mm, but with a finer distribution between 1 and 6 mm.

The aim of this study is to find a fitting function that describes the experimental data and implement this function in the instrument firmware so that this correction becomes automated for quantifying Br in plastic.

2.3.1.2   Development of a calibration

XRF spectrometry is able to quantify elements in many applications using the calibration equations set on the instrument during production and testing. This kind of calibration, called "calibration of fundamental parameters" is intended to work with well defined, broad applications, in which all constituents of a sample can be measured. Typical applications are: analysis of alloys and analysis of processed ores and minerals. It is based on the following parameters:

- Mass attenuation coefficients, or "cross-sections"

- Fluorescent x-ray energies

- Absorption edge energies

- Fluorescent yields

- Jump ratios

- Relative line yields

- Coster-Kronig transition yields (L-shell)

- Form-factor and S-matrix (for coherent/ incoherent scatter)

In order to optimise the XRF for Br quantification in a light matrix such as plastic, a matrix matched calibration is needed. Empirical calibration is labour intensive and requires a good set of calibration samples. However, it is always more accurate than the Factory Parameter calibration (FP).

Effectively, an empirical functional relationship is determined:

Concentration = Function (X-ray Intensity)

The function to be found must account for geometry, thickness and secondary Compton scattering. The calibration has to be designed in a way that it also corrects for:

- Compton scattering: that can be higher for polymeric matrices like the ones analyzed in this study

- Penetration of x-rays greater than dimensions of source-sample-detector system: assumption of infinite sample thickness fails (Vanhoof et al., 2013).

- Sherman's geometry (Markowicz and Van Grieken, 1993) assumptions are fulfilled –

  specifically, regarding the attenuation of signal with increasing distance of the sample

  surface from the detector: the length of the optical path between the outgoing x-ray

  source and the surface emitting fluorescence has an optimum for which the instrument

  is calibrated; if the analyzed surface is not flat the distance between surface and

  detector will deviate from the ideal conditions (Beckhoff et al., 2007).

2.3.1.3   Design of Solid Standards for LA-ICP-MS and XRF Calibration

The first step of this study was to design and verify ABS reference materials (RMs) that fulfill the

requirements of XRF and LAICP-MS analysis containing realistic elemental compositions. In the

literature it is shown how, even with optimal ablation conditions, quantification can be difficult

due to the lack of appropriate calibration standards (Stehrer et al., 2010). To account for the

strict matrix dependence of these two techniques the RMs must:

- be made of the same plastic as samples;

- cover a wide calibration range from very low to very high concentrations of BFRs, to

  account for plastic that contains both unintentionally (e.g. those present in plastic that

  while not directly flame retarded, contains recycled material that was) and intentionally

  added BFRs;

- be homogeneous: in order to exclude intensity fluctuations due to local concentration

  changes during the laser ablation (Mans et al., 2009);

- contain also BFR co-synergist and other elements commonly used as additives in the

    plastics under test (e.g. Sb_2O_3, $CaCO_3$, TiO_2) (Jakab et al., 2003),(Mark, 2013).

- have a similar sample mass absorption coefficient for X-rays and be representative of

    the different ablation behaviour due to the presence of inorganic fillers in polymers as

    described by Todoli and Mermet (Todolí and Mermet, 1998); and

- have a flat surface: XRF works under the assumption of Sherman's geometry, when the

    surface of the sample is not flat these assumptions may fail (Mans et al., 2007). The

    standards were produced according to these specifications by Fachhochschule Muenster

    Labor für Instrumentelle Analytik. The method used to produce and test the standards is

    described in detail elsewhere (Mans et al., 2009) but a brief summary is provided here.

Br (in the form of commonly used flame retardant Deca-BDE) and Sb (in the form of Sb_2O_3)

were added to an acrylonitrile-butadiene-styrene terpolymer melt with the aid of an

extruder (Figure 2-8). A set of nine different reference materials where BDE-209 was added

in 9 different concentrations, were produced in the form of pellets containing different

mass fractions of both Br and Sb. The pellets were used to produce solid cylindrical discs

(pucks) with a diameter of 40 mm at five different thicknesses (Figure 2-9).

Figure 2-8 Laboratory extruder used to produce ABS solid reference material

Figure 2-9 Discs of BDE209-loaded ABS. 5 pucks of different thicknesses were produced for each of the 9 concentration levels

A 20 mm thick disc was produced for measurements at infinite thickness (i.e. measurements that are not influenced by the small thickness of the sample) for each of the 9 RMs. The thicknesses of the remaining four discs were chosen to yield the highest number of possible permutations between them. In this way, by stacking discs with different thicknesses, it was possible to obtain the highest number of different thicknesses from their combination inside each of the calibration levels. To do so the group theory was applied to decide the thickness at which the four discs had to be produced: the thickness of each individual disc is given by 2^n mm, $0 > n > 3$. Therefore the first disc's thickness is $2^0 = 1$ mm, the second disc's thickness is $2^1 = 2$ mm, and so on, giving for each of the 9 reference material four discs 1, 2, 4, 8 mm thick. Mass fractions of Br and Sb in the produced materials were determined by Fachhochschule Muenster Labor fur Instrumentelle Analytik using Neutron - Activation - Analysis (NAA). The uncertainty of NAA is about 7% wt. Br (Table 2-2). To assess macroscopic homogeneity, a wavelength dispersive X-ray spectrometer was used with RSD below 2% wt. for Br. To assess microscopic homogeneity a synchrotron radiation μ-XRF (SR μ-XRF) was used (Figure 2-10). The spot size of the exciting beam was 200 μm, the RSD for Br was 0.7%.

Homogeneity was also tested with LA-ICP-MS, using the same spot size repeated 20 times over area of ca. 3 cm^2; the RSD for these Br measurements was 8.8%. Br was added in the form of BDE-209, which, being an organic molecule allowed better homogenisation into the polymer. Ti and Sb dispersed as oxides do not dissolve in polymeric matrices, thereby resulting in poor homogeneity.

Table 2-2 Composition of Reference Materials. Results obtained with NAA. Each RM was produced in discs of 1, 2, 4, 8 and 20 mm of thickness.

	Mass fraction			
RM#	Br		Sb	
	wt.%	±%	wt.%	±%
1	12.0	0.84	0.08	0.06
2	8.0	0.56	3.1	0.22
3	5.7	0.40	0.76	0.05
4	2.4	0.17	1.2	0.08
5	1.6	0.11	1.8	0.13
6	0	0	2.5	0.18
7	0.4	0.03	0.	0
8	0.08	0.01	3.9	0.27
9	0.8	0.06	0.3	0.02
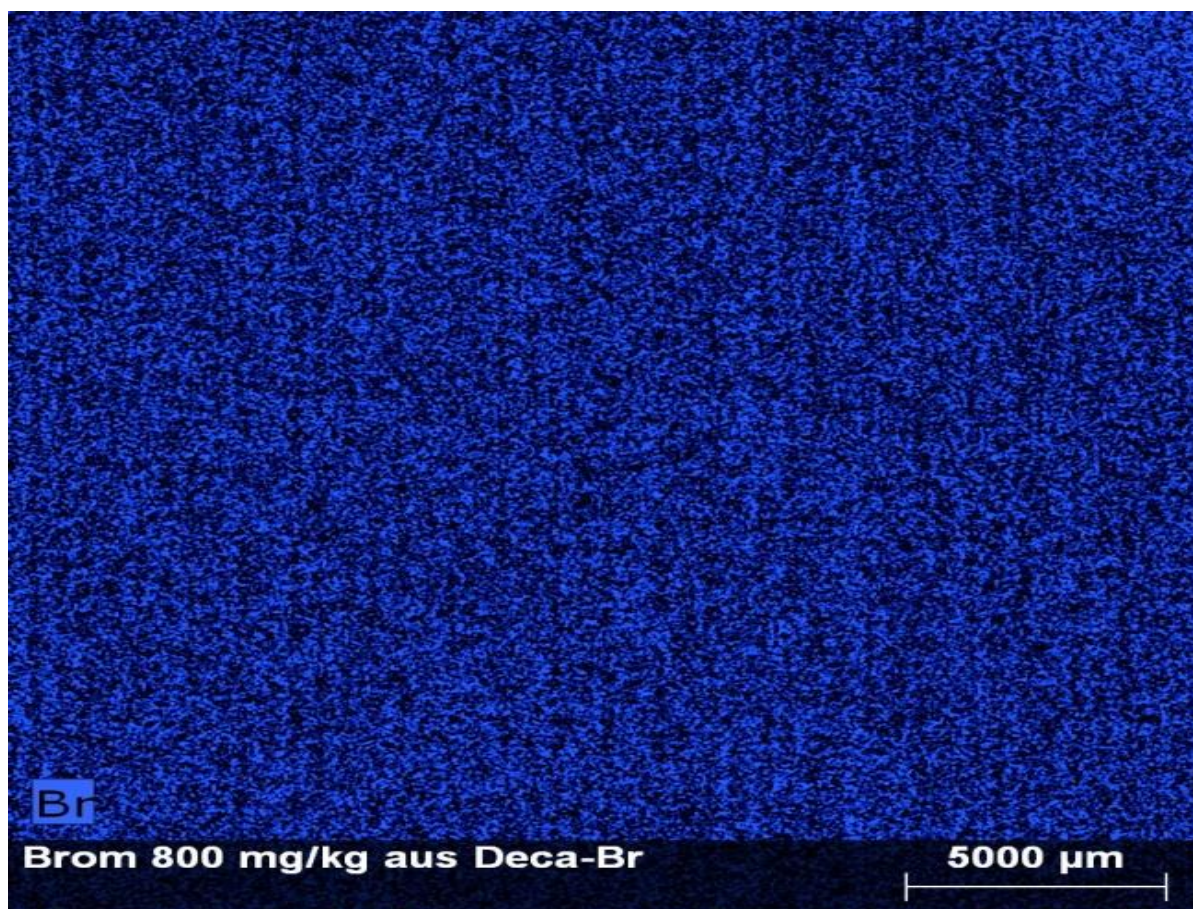
Figure 2-10 Microscopic homogeneity analysed with synchrotron radiation μ-XRF (SR μ-XRF)

2.3.1.4   Development of an ad-hoc thickness correction for ABS with XRF

This calibration approach comprised measuring the Br intensities non-corrected for thickness

for each concentration level of the solid reference materials at different thicknesses. These

concentration values were plotted against thickness (Figure 2-11). The obtained "thickness

calibration curve" showed similarities with the exponential Attenuation Law for photons in

matter (Lambert Law of Absorption). Therefore, a generic negative exponential function [2] was chosen as the starting point for our model.

$$I = cI_0 \cdot (a - e^{-b \cdot D})$$ [2]

Where I = signal (corrected for Compton scattering); I_0 =signal for infinite thickness; D = thickness in mm; a is a parameter regulating the offset with respect to the y axis; b is a function of the material in terms of mass absorption: defined as the linear absorption coefficient. The inverse of b, is what has been defined as "infinite thickness", to which corresponds the concentration value found on the plateau of the exponential function (the assumption that b remains constant when the Br concentration changes is an approximation); and c is the parameter that regulates the slope of the unsaturated region of the function. To fit this equation to the empirical results, these parameters were varied recursively until the squared deviation was minimised (using Excel's 'Solver' algorithm) keeping the constraint that the product between a and c is 1. The value of b was found to be 0.26 mm^{-1}, hence the calculated "infinite thickness" (1/b) was 3.85 mm which, i.e. when D=3.85 mm Figure 2-11 the function starts to saturate, so 1/b is the value that D has to assume in order to fulfil the "infinite thickness" condition (equation [1]); the value of c was 0.56 and the value of a was 1.78 (these numbers are unit-less as they are factors in the equation [3]). Once the parameters for this equation were calculated, it was solved for I$_0$ in order to adjust the uncorrected signal I to the sample thickness [3]. The parameters found for this equation are valid only for the region under study, i.e. the function was solved only to fit the empirical results shown in Figure 2-11.

$$I_0 = I/[c \cdot (a - e^{-b \cdot D})] \qquad [3]$$
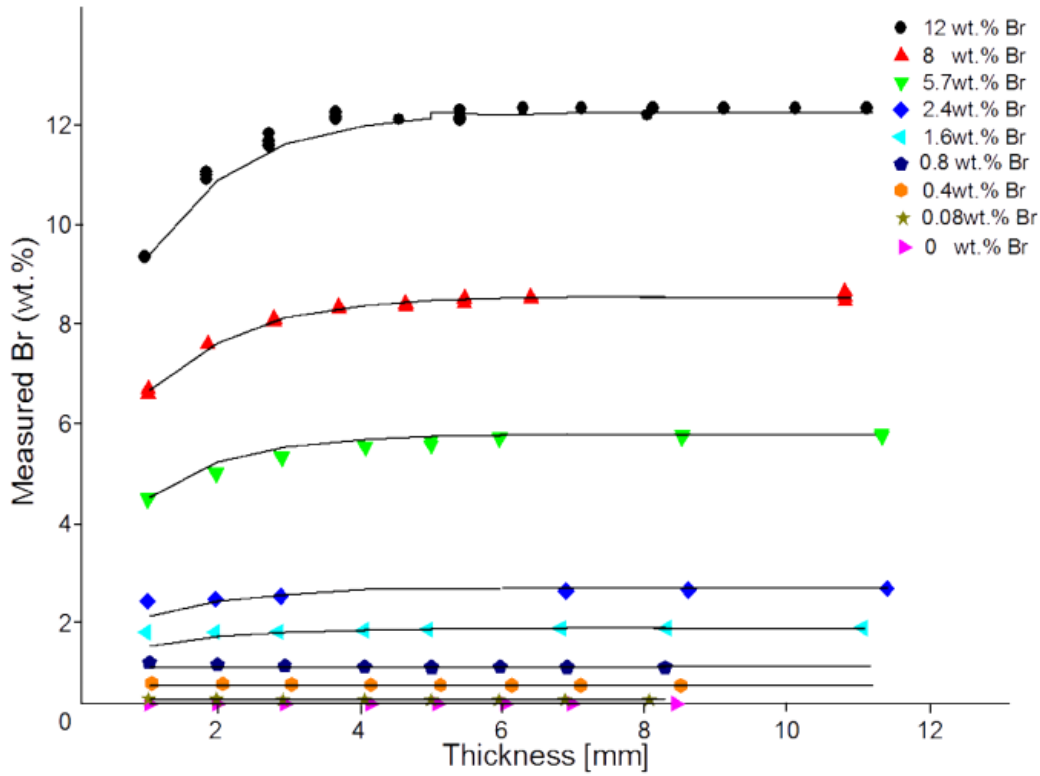
Figure 2-11 Measured Br concentration by XRF against thickness for different concentration levels of the RMs. Proposed model (equation [2]) for the fitting function (black line). Br intensity was obtained by measuring Compton corrected Br intensity in all SRMs.

Hence, for given values of signal intensity and thickness of the sample, the equation returns the value of intensity corresponding to the "infinite thickness". The accuracy of this method was evaluated by comparing the corrected values obtained from the thickness calibration and the reference values, according to the formula [4]:

$$Accuracy\ (\%) = (Reference - (Measured - Reference)/Reference) \cdot 100 \qquad [4]$$

Average accuracy without thickness correction for thin layers (1-3 mm) was 82.8%, while after the thickness correction the accuracy is improved to 93.9%. This value is satisfactory considering that a value of 89% on one single-controlled standard was obtained in a recent study (single measurement) (İzgi and Kayar, 2015). We next evaluated the method uncertainty (precision) as the standard deviation between four replicates. For RMs this value is independent on the homogeneity of the material (because both macro and micro homogeneity were tested for these RMs). Differences between measured RMs and their reference concentrations were always within the measurement uncertainty (Figure 2-12). XRF accuracy was measured comparing the reference value to the corrected values of Br (wt.%) measured at the infinite thickness. Error bars for the measured concentrations are the SD between the 3 replicates done for each measure at infinite thickness; error bars for the reference concentration are uncertainty of the NAA used to validate the RMs. Linearity for LA-ICP-MS was assessed splitting the SRMs into two concentration groups – high and low- and for both calibrations the R^2 was > 0.99 in the ranges 0 to 0.8 wt. % Br and 1.6 to 12 wt.% (see section 2.3.2.1). Inter- and intra-day accuracy were not assessed in this study. Concentrations reported without correction show negative errors for RM 1-3 and positive errors for RM 4-9: this effect is a direct result of Compton scattering: the Compton scatter intensity increases with the decreasing of the average atomic number of the scattering material, when the Br (Z=80) amount relative to the C in the matrix (Z=12) decreases under a certain threshold the MAC of the material decreased, and the Compton scattering has a more prominent effect. As an effect of varying MAC, it is well accounted for in the thickness correction. The LOD -calculated as three

times the SD of the blank response (Br-free RM) divided by the slope of the calibration curve, according to (Guideline, 2005)- was 0.0011%, LOQ was 0.0036%.
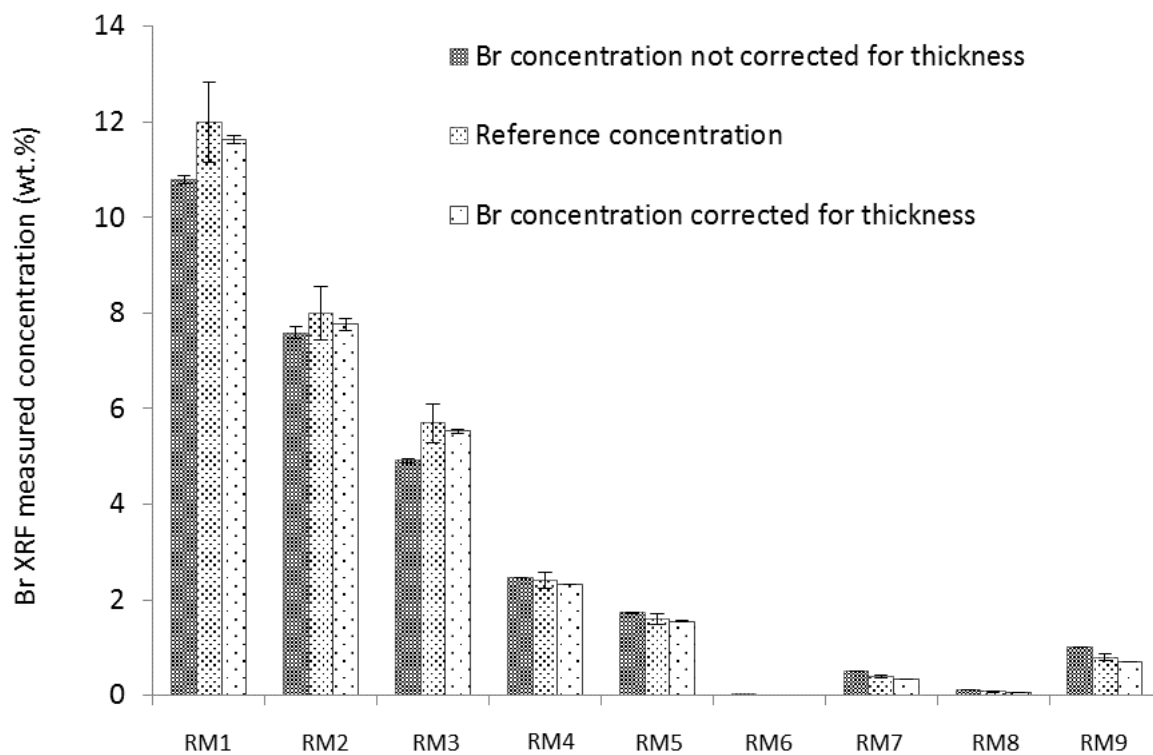

Figure 2-12 XRF measurements of solid reference material

2.3.2 LA-ICP-MS

Laser ablation-inductively coupled plasma-mass spectrometry LA-ICP-MS was conducted using a Teledyne CETAC Technologies Analyte™ G2 nanosecond excimer laser (ArF) hyphenated to a Thermo Scientific iCAP-Q single quadrupole ICP-MS. This short wavelength laser has considerable advantages in enriching the amount of on-surface absorbed light relative to in-depth transmitted light (Guillong et al., 2003), (Gonzalez et al., 2002). A digital microscope (Keyence, Digitales Mikroskop VHS-600DSO) and a depth profiling tool (Mitutoyo SJ-410) were used for ablation crater evaluation. Thermo Scientific Qtegra ISDS software was used for LA-ICP-MS data acquisition and evaluation, while Chromium software was used to control the Analyte G2 LA. Background correction was achieved by selecting a 5 s region of interest (0-5 s) from the transient signal (laser off) and subtracting its mean intensity ('gas background') from the mean intensity of ^{79}Br in the selected 12 s (laser on) region of interest (16-28 s): mean count rates are used instead of time integrated signals as the background and the region of interest for ^{79}Br have different acquisition times (Longerich, 1996). The uncertainty of each measurement (expressed as relative standard deviation - RSD) was calculated as the SD between each sweep over the selected region of interest divided by the mean count rate in that region and multiplied by 100. A 20 s measurement of sample ablation required approximately 520 sweeps. Ten points per spectral peak were acquired with the most intense of those selected for quantification. Measurement precision was calculated as the SD between two replicate line scans on different positions on the sample (but within the 8 mm diameter sampling area similar to XRF). For both these values the heterogeneity of the samples might give a contribution (Danyushevsky et al., 2011) which will vary with the element analysed

(Stehrer et al., 2010). Although cryogenic milling of the samples has been proven to reduce this influence on the RSD (Stehrer et al., 2010), it was not used in this study as doing so would defeat the purpose of an inexpensive technique with no sample preparation. The LOD for this technique was calculated as three times the SD of the blank response (Br-free RM) divided by the slope of the calibration curve, according to (Guideline, 2005). A polyatomic plasma-based interference for ^{79}Br is given by $^{40}Ar^{38}Ar^{1}H$, $^{40}Ar^{39}Ar$ and for ^{81}Br by $^{40}Ar^{40}Ar^{1}H$. To remove these interferences the collision reaction cell of the ICP-MS was pressurised with a mixture of 7 v/v% H_2/He as collision gas in order to perform kinetic energy discrimination on the unwanted polyatomic interferences. Br was quantified based upon ^{79}Br signal intensity with ^{81}Br measured to evaluate deviations from the ^{79}Br to ^{81}Br isotopic ratio. It can be assumed that oxides and polymer samples lose an electron at different depths into the ICP, giving a different ionisation yield. As this study focuses on Br determination as a surrogate metric for BFRs, we chose to optimise the sampling depth especially for Br (present as an organic species) (tuned parameters are listed in Table 2-3).

2.3.2.1 Optimised LA-ICP-MS method for styrenic polymers - method development and matrix matched calibration

An initial attempt was made to place all the RMs, and samples in the ablation cell. Unfortunately, the background produced by the higher Br concentration level RMs and samples was too high to obtain useful information out of the lower concentration level samples. Due to this, a calibration was first performed on the four low concentration-level RMs (0%, 0.08%, 0.4% and 0.8% Br), giving the calibration curve in Figure 2-13. The equation fitting this curve

was used to convert into concentrations, the count rates of ^{79}Br in the low concentration

samples placed in the cell together with this set of low concentration RMs. The same procedure

was followed for the high concentration RMs (1.6%, 2.4%, 5.7%, 8.0% and 12.0% Br) placed in

the cell together with high concentration samples. For the low Br concentration batch the

obtained R2 was 0.9990, while for the high Br concentration batch, R2 was 0.9986 (Figure 2-14).

Table 2-3 Optimised experimental conditions for LA-ICP-MS

|	
Laser parameters	*Teledyne CETAC Technologies Analyte™ G2*
Excimer ArF	193 nm, ns pulse length
Laser repetition rate	300 Hz
Spot Size on the sample	150 um circle, 1 mm line
Fluence	0.45 J cm^{-2}
Linear speed	50 um s^{-1}
He flow sampling cup	0.7 L min^{-1}
He flow ablation cell	0.7 L min^{-1}
ICP-MS parameters	*Thermo Scientific iCAP-Q ICP-MS*
Plasma power	1550 W
Auxiliary flow	0.78 L min^{-1}
Collision gas	4.5 mL min^{-1}
Ar flow	0.95 L min^{-1}
Isotope measured (dwell time)	^{79}Br (0.01s), ^{81}Br (0.01s)
Measuring mode Kinetic Energy Discrimination voltage	2.5V
Analysis mode	Transient signal
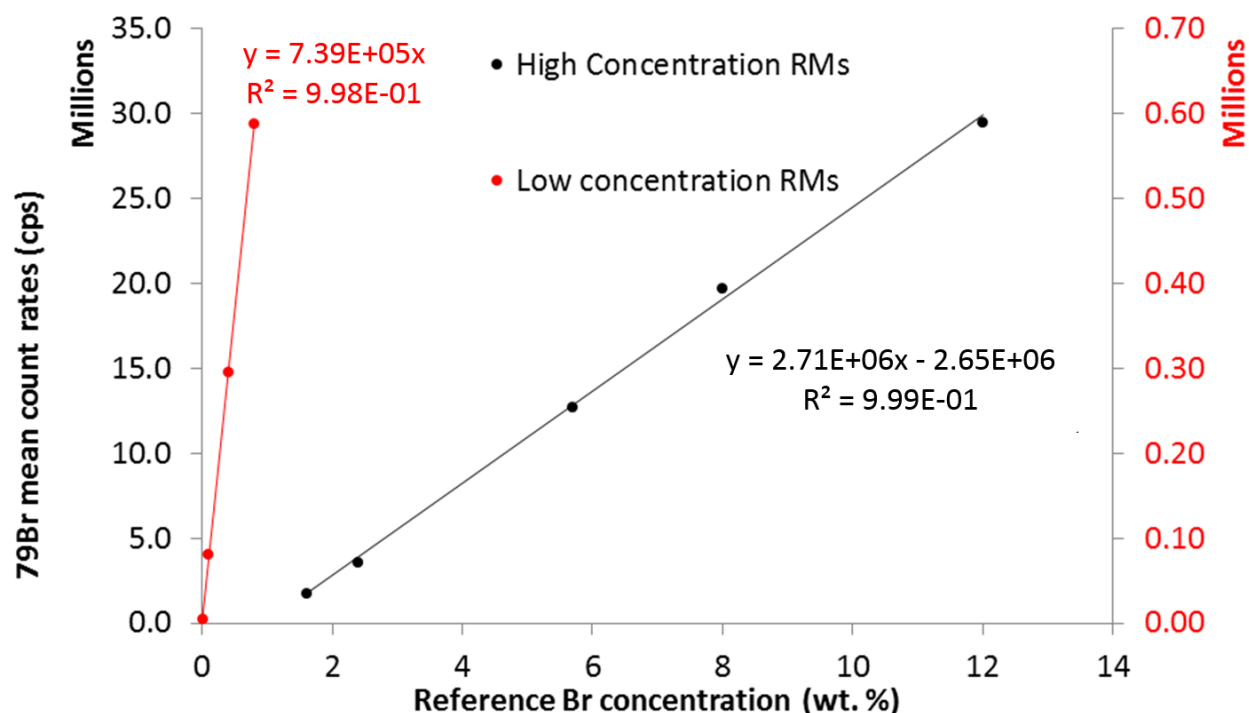
Figure 2-13 Calibration line on the low concentration range (0.08-0.8 wt.% Br) red markers and axis in red font and on the high concentration range (1.6-12 wt.% Br) black markers and axis in black font, performed using LA-ICP-MS. Due to high gas background and consequent background over-correction, the equation used for the high concentration batch does not intercept the origin.

The average accuracy obtained for the reference materials (calculated as per equation (3)) was

93.3%, with lowest values of 78.8% and 79.2% obtained for the two RMs that have a

concentration of Sb equal or exceeding that of Br (SD for these measurements performed in

triplicates are shown in Figure 2-12 as error bars). This suggests a negative influence of Sb on

the measured concentration of Br. It has been shown (Evans and Giglio, 1993) that the matrix

effect depends on the concentration of the matrix-element and not on the matrix-element to

analyte-element ratio, so this loss of accuracy is more likely ascribable to a particle effect. For

each RM the difference between the measured value and the reference was within the

measurement uncertainty (Figure 2-14). The LOD for ^{79}Br was 0.0004% while the LOQ was 0.0012%.
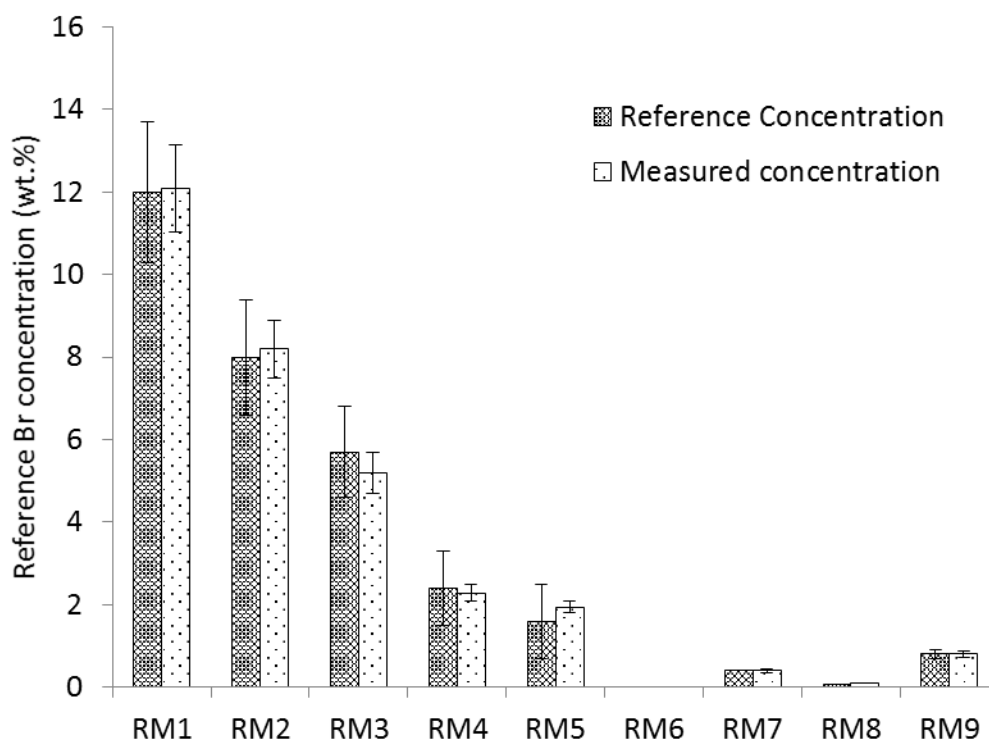

Figure 2-14 Comparison for each RM between the measured value (LA-ICP-MS) and the reference. Error bars for the RMs values is the RSD of the LA-ICP-MS used to measure the Br concentration in the RMs by Fachhochshule Muenster Labor fur Instrumentelle Analytik n; error bars for the measured concentration is the RSD of the individual ablations.

Two tuning procedures have to be performed and the choice of the tuning standards must reflect what has to be tuned at each point. Tuning of torch position, sampling depth, RF power, gas flows, potential applied to the second extraction lenses of the ICP-MS was undertaken with NIST-612 (glass). The preference for a matrix matched tuning standard is overcome for the ICP-MS tuning, by homogeneity and ease of ablation requirements that only the NIST-612 standard

provides compared with plastic reference materials. This is a tolerable compromise because when tuning the plasma source, the laser parameters remain unchanged and what is tuned at this stage is the ionisation efficiency and ion transportation through the ICP source.

The ablated mass quantity and composition are influenced by certain laser beam properties. There are different parameters that need to be tuned manually like laser intensity, ablation geometry and size, repetition rate, linear speed, helium flow in the ablation cell and in the sampling cup, optical focus, etc... For each parameter a series of ablations are performed for a range of values. For the first coarse tuning the measured intensity of the ICP-MS transient signal is evaluated "on-the-fly": the value producing the highest intensity was chosen as the optimum for that parameter. The optimized parameters and their optimization ranges can be found here in Table 2-4.

**Table 2-4 LA-ICP-MS parameters operating ranges and optimisation increment**

	Test range	Optimisation increment
Laser repetition rate	10-300Hz	10 Hz
Spot Size on the sample	30-150 um circle	10um
Fluence	0.4-4 J/cm^2	0.5 J/cm^2
Linear speed	10-50 $um·s^{-1}$	10 $um·s^{-1}$
He flow sampling cup	0.3-0.7 $L·min^{-1}$	0.1 $L·min^{-1}$
He flow ablation cell	0.3-0.7 $L·min^{-1}$	0.1 $L·min^{-1}$

Using high fluences causes the laser-material interaction to be non-linear (Guillong et al., 2003) because of the high coherence and the multi-photon interactions, which become more

probable with increased number of photons per unit area (Diwakar et al., 2013). Moreover, higher fluences causes the development of melt, swollen polymer and high temperatures that in turn cause the aromatic compounds (of which the polymer is partially made of) to start unpredictable radical reactions with the ablated material in the cell. A 0.45 J cm^{-2} fluence showed to have a number of advantages as observed with an optical microscope and a depth profiling tool. These include:

- charring of the polymer is very mild

- higher depth and lateral resolution is achieved, crater shape appeared regular and close to the size set in the ablation patterns (diameter of 150 µm), resulting in less variable mass removal.

- the initial hump in the transient signal due to the first burst of higher energy resulting from the laser shutter opening, creating larger particles (Kosler, 2008) is eliminated (Figure 2-15)

A relatively high 300 Hz repetition rate was used. It has been shown in the literature (Diwakar et al., 2013) that - up to a point - high repetition rates can increase the sensitivity (with a non-linear function) increasing the number density of particles and the total number of particles but if the repetition rates are too high the pulse energy is not maintained. This effect is likely to exert greater impact when higher energies are used than with such low radiant exposure. Moreover, we compare here in Figure 2-16 the ^{79}Br LA-ICP-MS signal intensity for a reference material (to exclude signal heterogeneity due to analyte distribution) at different repetition rates; the signal appears to be higher and with a lower RSD for the 300 Hz ablation.
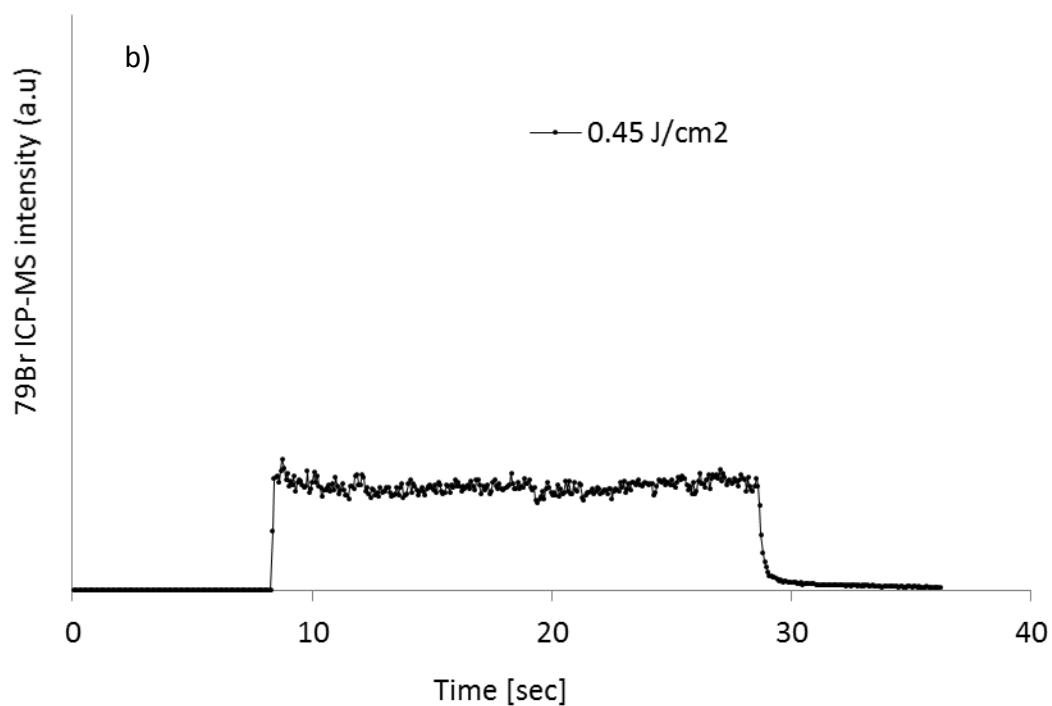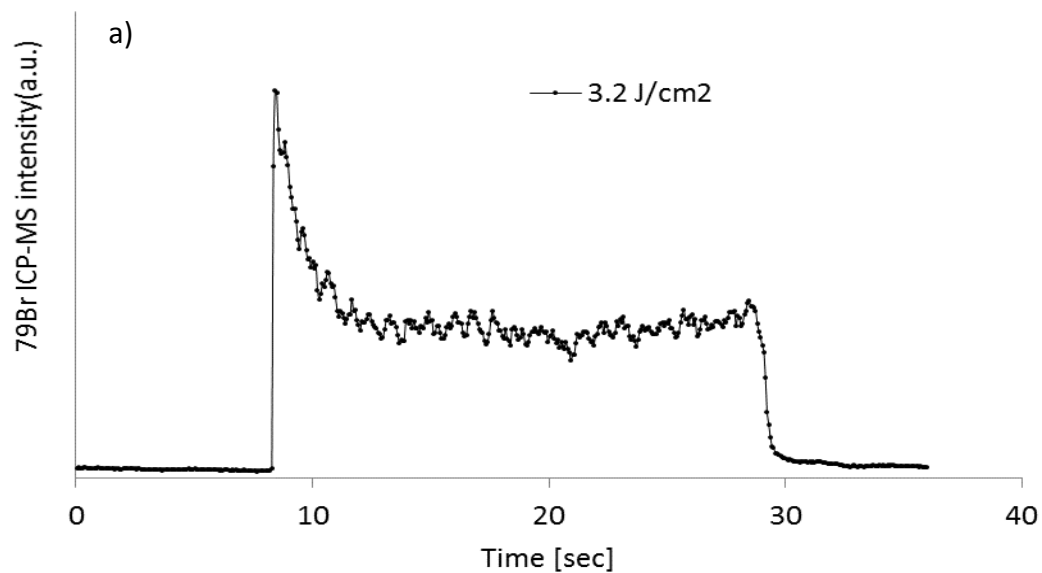
Figure 2-15 a) Effect of high fluence (3.2 J/cm^2) on the ICP-MS signal fluctuations using an ABS reference material (0.8 wt.% Br).
b) Effect of low fluence (0.45 J/cm^2) on the ICP-MS signal fluctuations using an ABS reference material (0.8 wt.% Br).
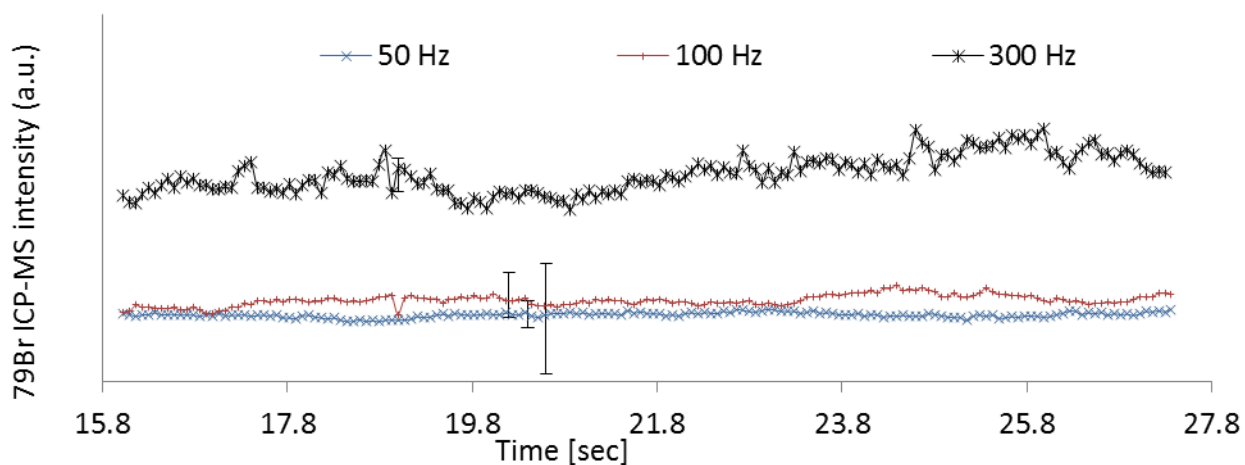
Figure 2-16 Effect of increasing repetition rate on LA-ICP-MS signal intensity (normalised) for RM loaded with 0.8 wt.% Br in a line scan at 50 μm·s⁻¹. Spot size was 150 μm, laser energy was 0.45 J/cm2. Error bars are the RSDs on the time signal (normalised).
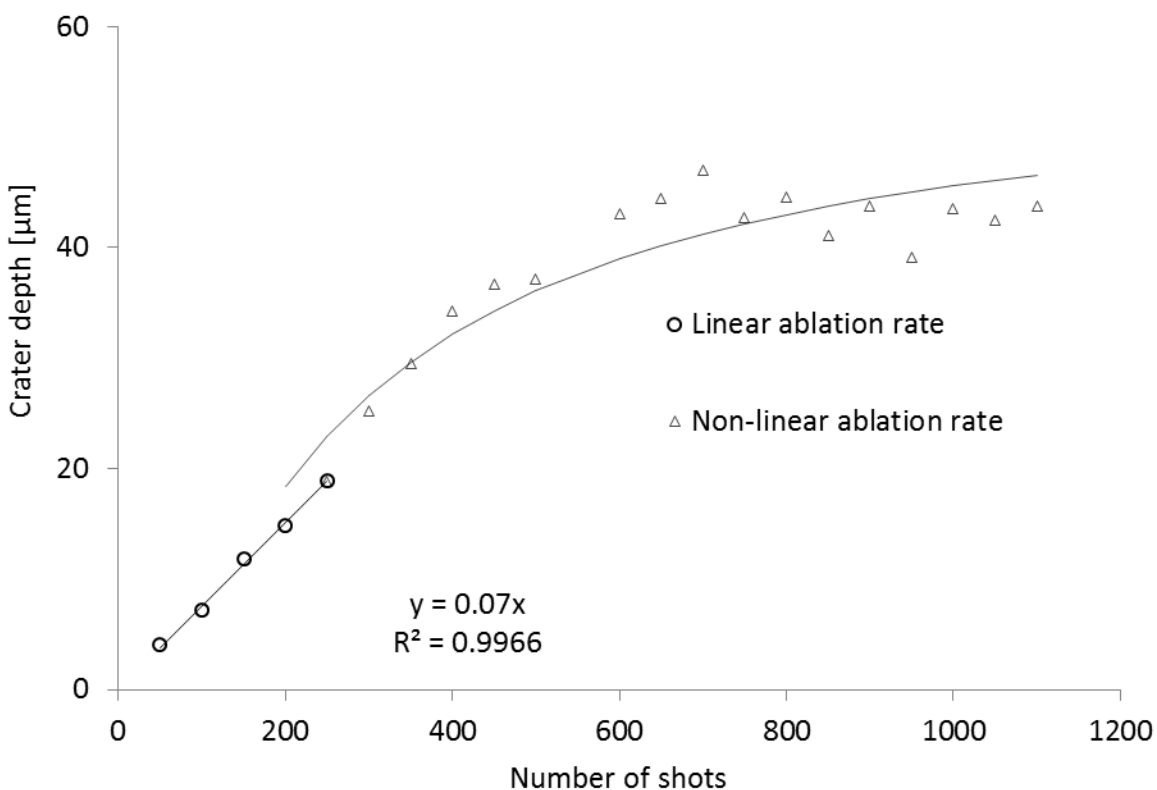
Figure 2-17 Number of shots vs. crater depth with LA-ICP-MS. The circles are the values of shots for which the crater depth increases linearly. The linear equation shown in the graphs was used to extrapolate the ablation rate.

The ablation rate was studied performing 20 different ablation spots at increasing shot number (from 50 to 1100), with the results plotted here as Figure 2-17. In the 50-400 shots range, the ablation depth follows a linear function, while between 450-1100 shots it is saturated following a negative exponential function. The calculated ablation rate is 0.07 μm/ shot. In the study by (Diwakar et al., 2013), it is shown how higher repetition rates can improve the fractionation indices on line scans ablations. The formation of rims on the crater (that tends to increase with the repetition rate was reduced by the low fluence and the scan speed (50 μm·s^{-1}).

2.3.2.2   Carbon correction

The efficacy of C as an internal standard for LA-IP-MS was evaluated. Assuming that the amount of C in the polymers is usually constant (e.g. for ABS is around 92% (Todolí and Mermet, 1998)), thus - given that the abundance of ^{13}C is 1% - the concentration of ^{13}C will be of the same order of magnitude as that of Br, making it a representative IS. The total carbon was measured with LA-ICP-MS as IS and with CEA to obtain a reference value against which correct the Br signal of LA-ICP-MS. This method assumes that fluctuations in the signal intensity of C (the concentration of which is known via CEA) will be of similar magnitude to those for Br.

2.3.2.3   REE quantification

A glass-based solid reference material NIST 612 and solid reference material NIST 610 containing Y, La, Ce, Pr, Nd, Sm, Gd, Tb, and Dy at concentrations respectively spanning

approximately one order of magnitude were used for a two-point calibration. The same data acquisition method used for Br was used for REEs.

2.3.2.4   Attenuated total reflection-Fourier transform infrared spectroscopy

For identification of the main polymer matrix, a Shimadzu IRPrestige FTIR spectrophotometer (Kyoto, Japan) equipped with a single reflectance diamond attenuated total reflection crystal was used. All spectra were compared with commercial libraries e.g. RoHS; ATR-Polymer2; IRs Polymer2; T-Polymer2 combined with in-house libraries requiring a minimum match of 90% or higher.

2.3.2.5   CEA Analysis

Quantification of total carbon to correct for the matrix effect in LA-ICP-MS was done through weight percent determination with Combustion Elemental Analysis (CEA) using a Thermo Scientific Flash HT Elemental Analyzer. A small amount of sample (350 mg) was weighted, inserted in a tin crucible and placed in an autosampler to be combusted in a reactor and quantified with a thermal conductivity detector (TCD). A calibration curve plot was built using the same RMs used for XRF and LA-ICP-MS. RMs and samples were analyzed in triplicates and their results averaged. The SD between replicates was multiplied by the slope to obtain the analytical error.

2.3.2.6   TD-GC-MS and Py-GC-MS

The following measurements were performed by Franky Puype and his team at the Institute for Testing and Certification (T. Bati 299, 76421 Zlin, Czech Republic).

For the identification of BFRs, a thermal desorption unit (Multi-Shot Pyrolyser EGA/PY-3030D, Frontier Laboratories LTD., Koriyama, Japan) equipped with a 48-position auto-sampler (Auto-Shot Sampler AS-1020E, Frontier Laboratories LTD., Koriyama, Japan) was interfaced with a GC-MS (GC-MS QP2010 Plus, Shimadzu, Kyoto, Japan). Several BFRs like higher brominated PBDEs are heat sensitive and may debrominate at elevated temperatures; therefore a short residence time is favoured on the separation column (Ultra ALLOY-PBDE; 0.25 mm inner diameter x 15 m; 0.05 μm film of dimethyl polysiloxane, Frontier Laboratories LTD., Koriyama, Japan).

All samples were analysed in duplicate with further QA/QC provided by conducting multiple blank measurements to check for analyte carryover between samples. Method accuracy was assessed by analysis of a certified reference material (ERM-EC591, a polypropylene (PP) sample containing decabromobiphenyl, along with Penta-, Octa- and Deca-BDE at realistic concentration levels (200-700 mg kg^{-1})). From the analytical point of view this method is limited to BFR identification, and is not recommended for BFR quantification as polymers have a very diverse hardness. The variation in polymeric sample matrices results in variable extraction efficiencies for each BFR, making calibration for quantitative measurement of BFRs in different polymer matrices very difficult. Moreover, in recycled polymer fractions, debrominated, oxidised and hydrolysed substances appear and in some cases degradation products indicate the presence of originally added BFRs; e.g. tribromobisphenol A indicates the presence of TBBPA. Hence, this method works mainly as a screening method for common BFRs and their degradation products. Target analytes are: brominated biphenyl (PBBs), PBDEs, hexabromocyclododecane (HBCDD), tetrabromobisphenol A (TBBPA), tetrabromobisphenol A bis(2,3-dibromopropyl ether) (TBBPA-DBPE), bromophenols, 1,2-Bis(2,4,6-

tribromphenoxy)ethane (BTBPE), tetrabromobisphenol A bismethylether (TBBPA-BME), HBB, and other substances which can be identified in full scan mode (up to 1090 m/z) by electron impact ionization (70 eV) as this method uses the combination of full scan and single ion monitoring in one run. The method is capable of identifying BFRs down to a bromine level of 10 mg kg^{-1} (ppm).

The optimal thermal desorption settings, having the lowest debromination yield for BDE-209, were: initial temperature 150 °C, ramp rate 80 °C min^{-1} to 350 °C and held for 2 min. Due to the risk of thermal debromination of PBDEs, an optimal GC interface temperature has been found at 300 °C with a high and safe yield for BDE-209 and the lowest formation of thermal debromination products (heptaBDEs, octaBDEs, and nonaBDEs). At higher temperatures than 310 °C, thermal degradation of BDE-209 occurs with loss of sensitivity as a consequence.

Pyrolysis and thermal desorption GC-MS methods use the same hardware. After analysis, the sample cup is removed from the furnace by a pressurised shot system and caught in a sample cup-recovery container. The thermal desorption sequence is programmed so that firstly a blank sample cup without any sample or toluene extract is injected and measured in order to evaluate the background of the whole sample path and to screen potential carryover effects from a previous measured sample (sample path and carryover check). As a next step, a sample cup spiked with toluene and quartz wool plugs (without sample) is measured in order to see if there is any contamination from the toluene/quartz wool plug (reference blank measurement) and is then compared with two following measurements of a sample extract/or solid sample (generally performed in duplicate). This 4-position cycle including four measurements is

repeated as many times as there are samples. The decision of repeating the measurements twice (instead of 3 times) is due to the fact that these analysis are merely done to confirm the presence of Br in the samples is due to BFRs and subsequently to use their relative content to obtain a semi-quantitative result when combined with total elemental Br quantification. The demonstrated hardware configuration and application has proven its effectiveness and stability in the past and is described elsewhere in more detail (Hosaka et al., 2005, Puype et al., 2015, Samsonek and Puype, 2013b).

Pyrolysis-GC-MS was used as an additional instrumental method that enables a reproducible characterization of (co-)polymers either as a major component or as a trace contaminant. This method detects monomers and significantly abundant pyrolysis degradation products to get a full composition overview of the polymer matrix. The hardware configuration is the same as used for the thermal desorption GC-MS experiment – i.e. the pyrolyser is programmed at a temperature of 650 ˚C, injecting up to 10 mg of the isolated sample. All peaks from the pyrograms were identified by using the NIST 05 library (National Institute for Standards and Technology, USA). Similar to the thermal desorption GC-MS method, all measurements were repeated twice and compared to blank measurements to check the cleanliness of the system and to avoid potential carryover issues.

2.3.2.7 Principal Component Analysis (PCA)

The choice of WEEE-related elements monitored was made by selecting the chemicals that are used in association with BFRs (i.e. Sb_2O_3, used as a co-synergist in the radical reaction between PBDEs and O_2 as well as $CaCO_3$, used mainly as a moulding agent (Pritchard, 2012);(Jakab et al.,

2003) for which a linear correlation with PBDEs is to be expected). REEs were also chosen because of their use in electric components and their otherwise extremely low natural concentrations. Descriptive statistics were applied to study the intra-sample variance between concentrations of Br and REEs between and within different polymeric matrices to highlight influential components responsible for the difference between REEs concentrations in different polymer types. Identification of the polymer matrix was achieved by combining attenuated total reflectance Fourier-transformed infrared spectroscopy and pyrolysis-GC-MS.

2.3.3 Sampling

We applied the aforementioned methods to samples of EEE, toys, and FCAs in the guise of two case studies, specifically:

Case study #1: 28 samples of various items of EEE were collected from different locations (Table 2-5), with a preference for styrenic polymers such as acrylonitrile butadiene styrene (ABS) and high impact polystyrene (HIPS) as they cover the vast majority of the polymers used for these appliances (Stockholm Convention, 2015).

Case study #2: In this study we selected samples that are likely relevant to human exposure. 26 polymeric samples were obtained (more than 1 sub-sample was taken from some items) from 16 toys, FCAs and one item of WEEE (this was included in the sample list to compare concentration levels and REEs presence between different applications). The toys and FCA were purchased on the European market: Italy, Czech Republic and Germany; however they were made in China and Turkey.

All samples of FCAs and toy materials were not part of an electric or electronic device (no RoHS

restriction) and therefore should not contain BFRs to meet fire safety regulations

Table 2-5 Sample list. LOD is 0.0004 weight % for LA-ICP-MS and 0.0011 weight% for XRF.

Sample number	Item	Part	Polymer	Production year	Provenance	Colour	Thickness (mm)	^{79}Br measured concentration with LA-ICP-MS (%)	SD on the individual LA-ICP-MS intensity over one ablation (%)	Br measured concentration with XRF (%)	2σ on the individual XRF intensity (%)
1	Mouse	Lower case	ABS	-	China	Grey	2.47	<LOD	-	<LOD	-
2	Mouse	Upper cover	ABS	-	China	White	1.34	<LOD	-	<LOD	-
3	Headphones	Volume regulator	ABS	-	China	Black	1.49	<LOD	-	<LOD	-
4	Headphones	Speaker	ABS	-	China	Black	1.11	0.051	0.007	0.013	<0.001
5	Headphones	Arch	ABS	-	China	Grey	1.24	<LOD	-	<LOD	-
6	Pump	Case	ABS	-	-	Black	1.18	<LOD	-	0.004	<0.001
7	Laptop	Bottom case	HIPS	Sept '07	China	Black	2.29	<LOD	-	<LOD	-
8	Cellphone	Back case	PC	May '03	China	Black	0.71	<LOD	-	<LOD	-
9	Cellphone	Inside plastic	ABS	May '04	China	Black	0.76	<LOD	-	<LOD	-
10	Adaptor	Case	PS	-	China	Black	1.48	0.302	0.032	0.178	0.007
11	Pc transformer	Case	ABS	-	China	Black	1.88	1.722	0.274	0.814	<0.001
12	First aid box	Case	ABS	-	Germany	Black	1.27	<LOD	-	<LOD	-
13	TV CRT	Back case	HIPS	1995-1996	Japan	Black	2.09	10.494	0.609	11.294	0.203
14	TV CRT	Back case	HIPS	1995-1996	China	Black	2.50	8.071	0.822	8.052	0.238
15	TV CRT	Back case	HIPS	1995-1996	China	Black	2.07	8.831	0.671	9.318	0.207
16	TV CRT	Back case	HIPS	1995-1996	Thailand	Black	2.47	9.939	0.596	9.548	<0.001

17	TV CRT	Back case	HIPS	1995-1996	Malaysia	Black	2.06	9.01	0.550	9.635	0.180
18	TV casing powder	Homogenised casing	HIPS	-	-	Black	1.45	10.054	0.643	10.090	0.225
19	TV casing powder	Homogenised casing	HIPS	-	-	Black	1.76	9.396	1.005	8.929	0.156
20	HDMI socket	Cover	ABS	-	-	Beige	0.69	16.811	1.227	16.820	0.157
21	Modem	Bottom cover	ABS	oct '05	China	Grey	1.83	8.395	0.672	7.793	<0.001
22	Modem	Upper cover	ABS	oct '05	China	Beige	2.20	8.680	0.521	7.407	0.091
23	DSL splitter	Cover	ABS	jul '05	China	White	1.48	<LOD	-	<LOD	-
24	Adapter	Cover	PP	-	Hungary	Black	2.49	0.826	0.177	0.620	<0.001
25	Power supply	Cover	PC	-	Italy	Black	1.29	4.36	0.209	4.826	0.001
26	Power adapter	Cover	HIPS	-	Germany	Black	1.93	0.062	0.012	0.011	0.001
27	Scart socket	Cover	HIPS	-	-	Black	1.00	7.005	0.806	6.426	0.007
28	TV LCD	Back case	ABS	dec '12	China	Blac	1.68	0.136	0.029	0.031	0.010

2.3.3.1   Sample preparation and extraction

For hand-held XRF, samples were wiped with ethanol, their thickness measured with a digital caliper and then cut into pieces of at least 8 mm diameter. For LA-ICP-MS, samples analysed previously by hand-held XRF were grouped into two analytical batches based on Br concentration: low (<LOD - 0.8 weight%) and high (1.6 – 12 weight%) concentration and placed into the ablation cell. The samples were divided into two batches in order to minimize background generated by evaporation of low boiling BFRs in the polymers.

For thermal desorption GC-MS measurements, the samples were cut into smaller ca. 2 mm cubes and 0.2 g of sample was dissolved/leached in 1 mL of toluene (GC/ECD-grade residue analysis, Chromservis s.r.o., Prague, Czech Republic). For the extraction of BFRs, toluene was chosen as this solvent enables high extraction yields for all targeted BFRs. The applied thermal desorption method including the sample preparation method is described in detail elsewhere ((Hosaka et al., 2005), (Puype et al., 2015)), but a brief summary is provided here. All extracts were kept with regular shaking for 5 days at room temperature in darkness in order to minimise photodegradation of the higher brominated PBDEs in the extract (Niu et al., 2006). Following extraction, 80 μL aliquots of the toluene extracts of the polymer samples were spiked into metallic 80 μL sample cups coated with fused silica (< 1 μm thickness) and evaporated until dry at room temperature. The advantage of this sampling method is that a very thin film of oligomers and non-volatile target analytes remains in the sample cup, giving significantly cleaner chromatograms than direct liquid sample injections or thermal desorption of the

polymer sample itself. Via free fall injection, the cup quickly enters the heated furnace of the thermal desorption unit, which is heated sequentially using a temperature program starting at 150 °C and heated at 80 °C min^{-1} to 315 °C and held for 2 minutes, heated up till 315 °C with a heating rate of 80 °C min^{-1} and kept for 2 minutes. The sample cup is removed after measurement by a pressure shot and captured into a receiver outside the instrument, followed by a rinsing sequence of the sample path with He as carrier gas.

2.4   Discussion

2.4.1 Case study #1

29 WEEE samples analysed with XRF to quantify total Br and compared with LA-ICP-MS results.

2.4.1.1   XRF vs. LA-ICP-MS

The Br data measured by XRF and LA-ICP-MS displays excellent accordance (inset of Figure 2-18) and the XRF thickness correction accounted for up to 46% increase in measured Br. The evident differences in Br data between these techniques are within analytical uncertainty (RSD of each measurement for LA-ICP-MS, 2σ error for XRF; error bars in Figure 2-18) for most of the samples. Moreover, hand-held XRF is shown to deliver quantitative determination of Br in WEEE. Table 2 5 Reports XRF and LA-ICP-MS results and relative analytical errors for the complete sample list.
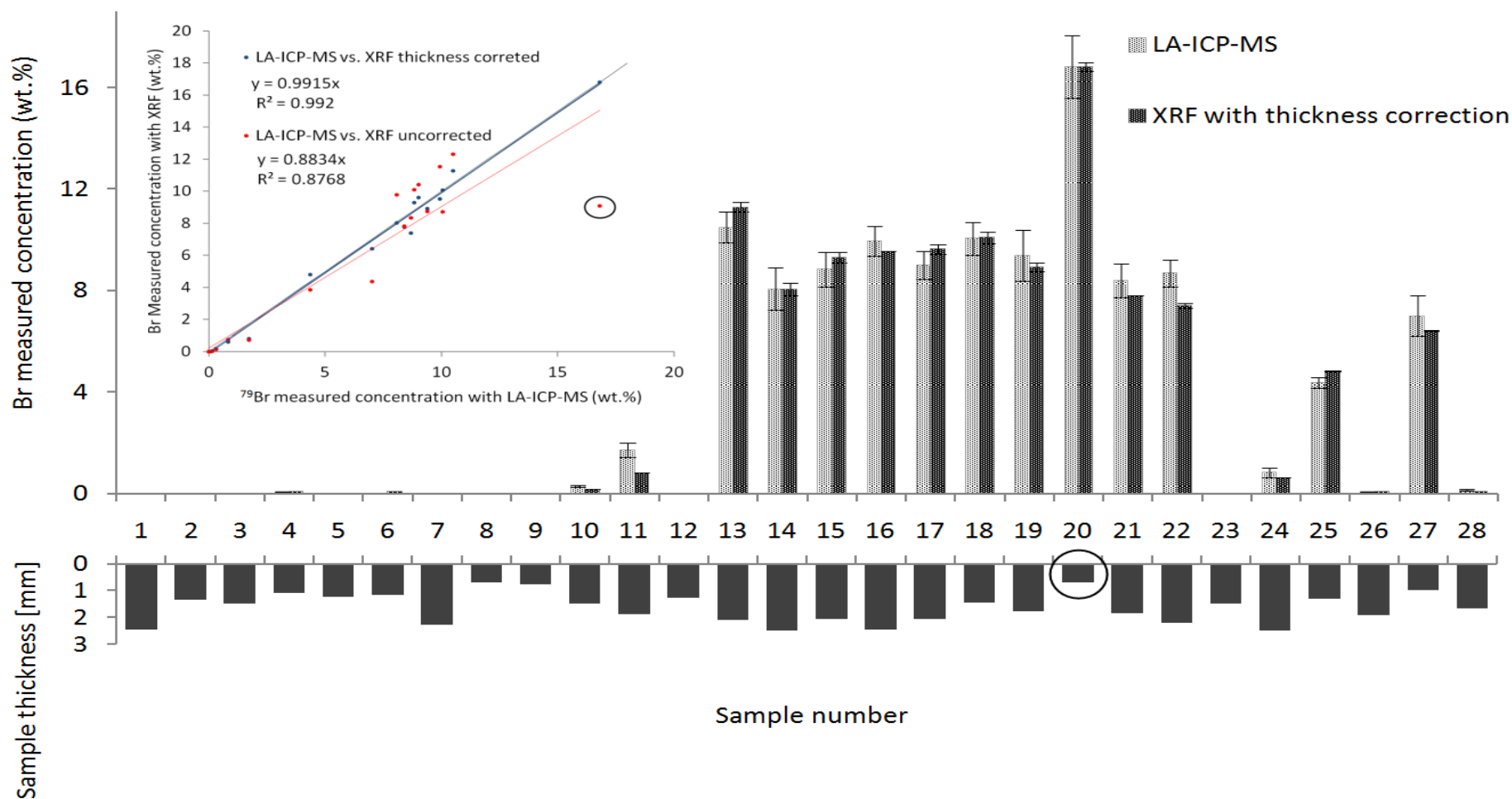
73

Figure 2-18 Comparison between LA-ICP-MS measured values and thickness corrected XRF measured values. On the bottom the corresponding thickness for each sample indicated as black bars under each sample number. Inset plot: correlation between LA-ICP-MS results and XRF. The thickness corrected results (blue dots) show a better correlation (R^2=0.9926 for 28 samples) compared to the correlation ((R^2=0.8788 for 28 samples) of the non-corrected XRF results (red dots). The circled red dot (in the inset) shows a bigger deviation from the LA-ICP-MS results: this is in fact a very thin sample (0.69 mm) circled thickness bar, hence when the thickness correction is not applied the negative error is substantially bigger.

2.4.1.2   TD-GC-MS

A key problem with elemental analysis of Br in polymers using XRF and LA-ICP-MS is that the Br

might be present in both organic (BFR) and inorganic form (Br salts contained in the inorganic

polymer's filler). As a consequence, this produces a potential positive error on the organic Br

quantification in XRF and LA-ICP-MS analysis of polymers. To investigate the occurrence of such

positive errors in this study, thermal desorption GC-MS analyses were performed to determine

BFRs. The BFRs most frequently detected in the WEEE samples tested in this study are BDE-209

and TBBPA (Table 2-6). Generally, samples might contain one or two different BFRs, however, in

some cases several different BFRs are present. This suggests the use of recycled WEEE fractions

in these samples, and highlights the potential for source misclassification whereby a Br signal

may be incorrectly attributed in its entirety to a single specific regulated BFR. Our data also

confirm that the majority of the WEEE samples studied contained BFRs.

Table 2-6 Thermal desorption GC-MS results for BFR identification in 28 WEEE samples

[1] N.D. means no BFRs were detected in the samples by the applied method.

Sample No.	Identified BFRs
1	N.D. [1]
2	N.D.
3	N.D.
4	TBBPA
5	N.D.
6	N.D.
7	N.D.

8	*N.D.*
9	*N.D.*
10	TBBPA, penta-BDE, deca-BDE, HBB
11	TBBPA, deca-BDE, HBB
12	TBBPA, deca-BDE
13	TBBPA, deca-BDE
14	deca-BDE
15	deca-BDE
16	deca-BDE, HBB
17	TBBPA, deca-BDE, HBB, TBBPA-BME
18	TBBPA, penta-BDE, deca-BDE
19	DBDPE,deca-BDE, HBB, TBBPA-BME
20	TBBPA, deca-BDE
21	deca-BDE, tribromophenol
22	deca-BDE, tribromophenol
23	deca-BDE
24	TBBPA, deca-BDE, HBB
25	TBBPA, tribromophenol, BTBPE
26	Octa-BDE
27	Octa-BDE
28	TBBPA, penta-BDE, deca-BDE

2.4.2 Case study #2

In this study we selected samples that are likely relevant to human exposure. 26 polymeric samples were obtained (more than 1 sub-sample was taken from some items) from 16 toys, FCAs and one item of WEEE (this was included in the sample list to compare concentration levels and REEs presence between different applications). The toys and FCA were purchased on the European market: Italy, Czech Republic and Germany; however they were made in China and Turkey.

2.4.2.1   XRF vs. LA-ICP-MS

For LA-ICP-MS the LOD was 0.0001% of Br and 0.001% of Sb. The average accuracy was 93.3%, with the lowest value of 79%.

For XRF the LOD was 0.001% of Br and 0.0005% of Sb. The average accuracy, calculated comparing the XRF equivalent concentration values and the reference values was 93.9%. A comparison between Br and Sb concentrations obtained via X-ray fluorescence with those measured using laser ablation inductively coupled plasma-mass spectrometry is reported in Figure 2 18 and Figure 2 19. In summary, Br concentrations detected with X-ray fluorescence showed a strong linear association (R^2 = 0.9802 for Br and R^2 =0.9768 for Sb) with concentrations detected with laser ablation-inductively coupled plasma-mass spectrometry, validating our X-ray fluorescence method for quantitative analysis of Br and Sb in polymers. To give an estimation of the BFR concentration equivalent to the detected Br, assuming conservatively that the detected Br has originated from a widely used BFR with the lowest mass

fraction of Br (i.e. triBDE, $\Box$Br= 0.59), Br concentrations above 0.059% w/w would correspond to 0.1% w/w of BFR (1,000 mg /kg), the maximum allowed limit in homogenous materials. Of the 26 samples analysed with X-ray fluorescence, 11 of them (61%) exceeded the estimated low POP concentration limit and 7 more samples exceeded the detection limit of this technique (>0.001% w/w). A quarter of all our samples with detectable concentrations of Br were food-contact articles (Table 2 7 reports Sb and Br concentrations for the complete sample list). With the exception of one sample (a blue miniature car launcher from a Dutch distributor), Sb was detected in all samples in which Br was detected.
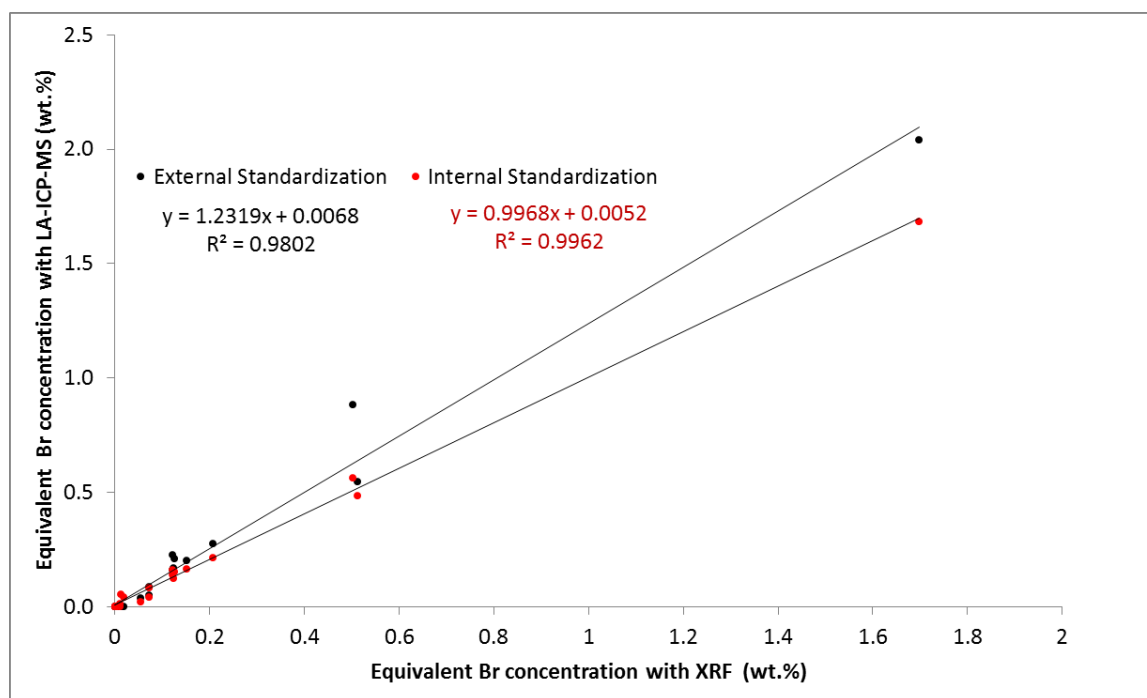

Figure 2-19 Comparison of Br concentration values obtained with XRF and with LA-ICP-MS (^{79}Br). Red markers represent data corrected with IS, black markers represent data not corrected with IS
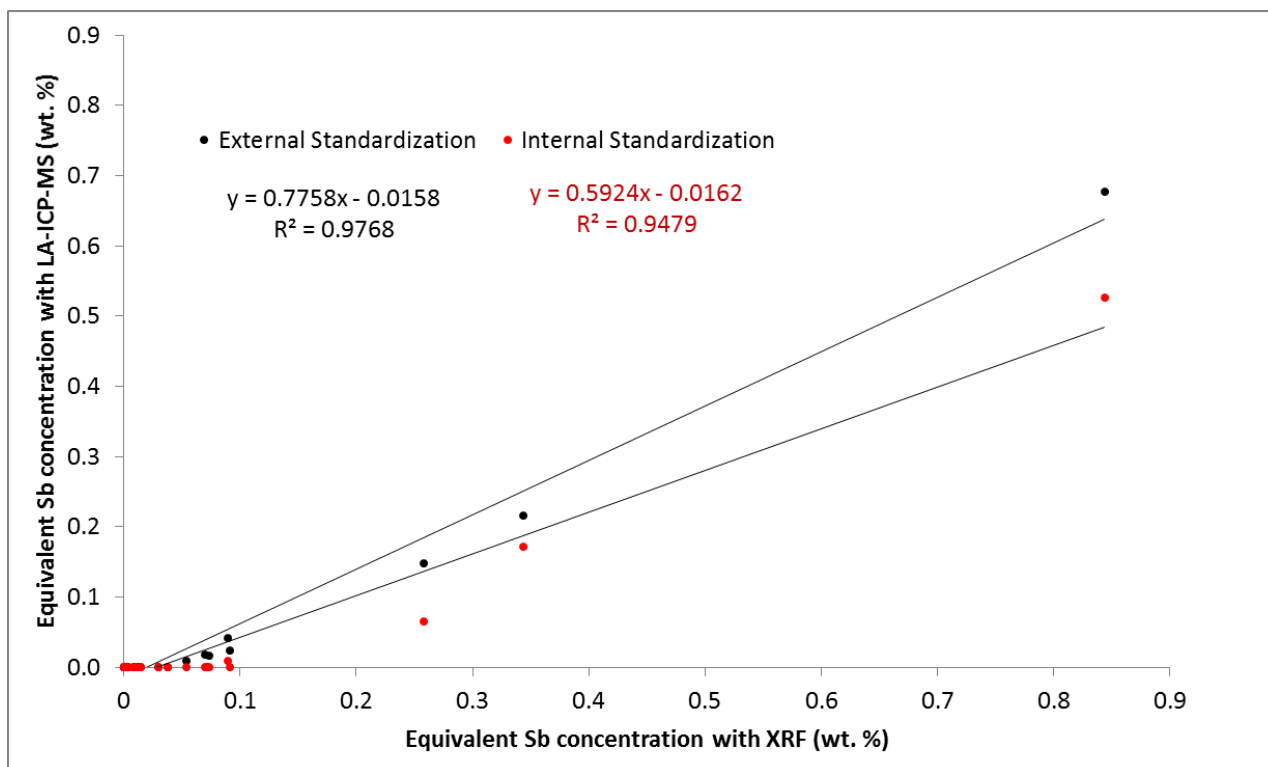
Figure 2-20 Comparison of Sb concentration values obtained with XRF and with LA-ICP-MS (^{121}Sb). Red markers represent data corrected with IS, black markers represent data not corrected with IS

Concentrations of Br spanned between 0.0004 and 1.7% w/w (this calibration is to be repeated every time the plasma is switched off), indicating that BFRs were unintentionally mixed (and their original concentration diluted) via recycling, because if they were intentionally added with the purpose of flame retardancy, they would be present at higher concentrations (10–30% w/w) (Gallen et al., 2014).

2.4.2.2   Carbon correction

For Br measurements, little improvement in the R^2 is observed for the IS corrected values (R^2=0.9987) with respect to the external calibration results (R^2=0.9985), for the measurements of the real samples instead, when compared to the XRF data, the average relative residual was

11.1% for the uncorrected results and 6.2% for the Carbon corrected, as it can be noticed in

Figure 2-19 this brings the slope between XRF and LA-ICP-MS closer to 1.

Table 2-7 Br and Sb concentrations in toy and FCA samples obtained with XRF. The analytical error is calculated as a function of SD between triplicate measurements of the same sample in different spots. Linearity range between 0.001% and 1.6% for Br and between 0.0005% and 0.76% for Sb.

	Place of Manufacture	Place of Purchase	Br%	+/- Br%	Sb%	+/- Sb%
Shield toy	China	Czech Republic	0.013	0.002	0.011	0.005
Sword toy	China	Czech Republic	0.011	0.007	0.013	0.008
Olympics medal toy	China	Czech Republic	0.010	0.004	0.008	0.006
Rubik's cube - Czech Republic	China	Czech Republic	0.018	0.007	0.014	0.005
Rubik's cube - German	China	Germany	0.071	0.002	0.029	0.006
Black Gun toy	China	Germany	0.501	0.022	0.258	0.015
Star Wars cereal bowl	China	Germany	<LOD	0.003	<LOD	0.004
thermal cup	China	Germany	<LOD	0.008	<LOD	0.004
small gun toy	China	Italy	<LOD	0.000	<LOD	0.005
binocular toy	China	Italy	<LOD	0.001	<LOD	0.005
target man toy	China	Italy	0.002	0.001	<LOD	0.005
spring gun toy	China	Italy	0.072	0.001	0.038	0.004
spring gun red toy	China	Italy	<LOD	0.001	<LOD	0.006
black spring car	China	Germany	0.208	0.000	0.089	0.010
black spring car	China	Germany	0.124	0.001	0.054	0.008
blue car launcher	China	Germany	0.054	0.001	<LOD	0.008
grey car launcher	China	Germany	1.697	0.002	0.844	0.005
grey miniature car	China	Germany	0.121	0.000	0.091	0.006
black miniature car	China	Germany	0.151	0.000	0.070	0.003
thermal cup	China	Czech Republic	0.002	0.000	0.004	0.007
thermal cup	China	Czech Republic	<LOD	0.003	<LOD	0.004
thermal cup	China	Czech Republic	0.122	0.000	0.072	0.006
thermal cup	China	Czech Republic	<LOD	0.003	<LOD	0.004
thermal cup	Turkey	Czech Republic	0.125	0.009	0.074	0.008
thermal cup	Turkey	Czech Republic	<LOD	0.000	<LOD	0.005
thermal cup	Turkey	Czech Republic	<LOD	0.000	<LOD	0.004
Radio back panel	China	Czech Republic	0.512	0.000	0.344	0.005

For Sb the use of an IS improves the calibration curve (R^2=0.9517 vs. R^2=0.9946) but not the correlation with the XRF results: this is likely due to the difference in micro-homogeneity (due to different polarities) between Sb_2O_3 and BDE-209, which affects the LA-ICP-MS reproducibility (having a micrometric sampling area) but not XRF (0.8 cm sampling area), this is also observable in Figure 2-20 where the slope between XRF and LA-ICP-MS results is worse after the IS correction.

2.4.2.3   Compound specific evaluation with TD-GC-MS

Thermal desorption-GC-MS is a technique that is mainly intended for qualitative evaluation of the compound specific BFR composition of samples. Nonetheless, combining the fully quantitative total elemental information for Br concentration and the inter-sample relative concentration of the detected BFRs, it was possible to obtain compound specific semi-quantitative data, the operating ranges of this method are reported in Table 2-8. For the semi-quantitative evaluation of the relative concentrations of BFRs in the samples, a one-point calibration was performed using a previously characterised sample (PBDE-treated plastic TV casing sample) (Table 2-9). The obtained response factor for each target BFR was used to convert the GC peak intensity into a concentration value. The relative concentration of the single compounds in each sample was normalized against the total concentration of Br to give a representative compound specific concentration profile of each sample. The analytical error was calculated as the SD between two replicate runs for each sample.

Table 2-8 TD-GC-MS method operating ranges

Compound	Method operating range (mg/kg)
PBDEs (tri- to decaBDE)	1-10000
TBBPA	70-7000
DBDPE	20-10000
BTDPE	90-10000

Compound specific evaluation on those samples containing Br > 0.059% w/w is reported in Table 2-10. With the exception of the single WEEE sample, for which only BDE-209 was observed, for all the other 11 samples (toys and food contact articles) containing >0.059% w/w Br, PBDEs and TBBP-A were detected together. The most abundant BFR in the majority of cases (73%) was BDE-209 at concentrations ranging from about 200 to about 10,000 mg/kg. TBBP-A followed in a range from about 200 to 8,000 mg /kg; while BTBPE and DBDPE were detected at trace levels only and not quantified. Although the European Commission moved recently to restrict the use of decaBDE, a low POP concentration limit for this substance has yet to be promulgated. Should a 1,000 mg /kg low POP concentration limit be applied to decaBDE – as it is for the other restricted BDEs – then 45% of the analyzed samples would exceed this limit. No samples exceeded the limits for Penta- and Octa-BDE.

Table 2-9 Composition report of the Inter laboratory TV casing sample used for TD-GC-MS calibration.

The Inter laboratory TV casing sample was a composite of 50 cathode ray tube (CRT) back casings (high impact polystyrene) that had been melted and remoulded to form a material for interlaboratory tests. The data in this table was part of a recent study (Rauert and Harrad, 2015) and obtained analysing four replicates of the TV casing using methods reported previously (Takigami et al., 2008)

Results of TV casing composites (InterLab Sample Waste TV backplate)			
Compounds	*n*	Mean Conc.	%RSD
PBDEs		(μg/g)	
2,4,4'-TrBDE (#28)	*4*	0.024	10
2,2',4,4'-TeBDE (#47)	*4*	1.3	15
2,2',4,4',5-PeBDE (#99)	*4*	3.2	27
2,2',4,4',6-PeBDE (#100)	*4*	1.1	39
2,2',4,4',5,5'-HxBDE (#153)	*4*	520	26
2,2',4,4',5,6'-HxBDE (#154)	*4*	59	22
2,2',3,4,4',5',6-HpBDE (#183)	*4*	3700	21
2,2',3,3',4,4',5,6'-OBDE(#196)	*2*	930	--
2,2',3,3',4,4',6,6'-OBDE(#197)	*2*	2100	--
2,2',3,3',4,4',5,5',6-NoBDE(#206)	*2*	3000	--
2,2',3,3',4,4',5,6,6'-NoBDE(#207)	*2*	1950	--
DeBDE (#209)	*4*	90000	19
TrBDEs	*4*	0.059	7
TeBDEs	*4*	1.4	14
PeBDEs	*4*	5.8	26
HxBDEs	*4*	620	24
HpBDEs	*4*	3700	21
OBDEs	*4*	3000	25
NoBDEs	*4*	4800	19
Other BFRs		(μg/g)	
TBBPA	*3*	6800	11
2,4,6-Tribromophenol (TBP)	*3*	5	44
HBCD	*2*	13	--
n: number of analysis			
--: not calculated			

Table 2-10 Compound specific semi quantitative report of Br-positive samples obtained with TD-GC-MS. The relative concentration of each BFR in each sample was normalized by the total elemental Br measured with XRF. The analytical error is calculated as the SD between duplicate measurements with TD-GC-MS.

Sample	decaBDE (ppm)	+/-	TBBPA (ppm)	+/-	heptaBDE (ppm)	+/-
Rubik's cube	330	<10	390	<10	<1	-
Toy gun	4350	220	660	220	<1	-
Spring car	1300	70	770	70	<1	-
Spring car	940	100	280	90	20	<10
Car launcher	9230	1140	7750	1140	<1	-
Miniature car	290	<10	930	<10	<1	-
Miniature car	1280	50	210	50	20	<10
Spring gun	210	<10	510	<10	<1	-
Thermal Cup	780	90	440	90	<1	-
Thermal Cup	780	20	470	20	<1	-
Radio back panel	5120	120	<70	-	<1	-

2.4.2.4 PCA analysis of the relationship between concentrations of REEs and appliance class

We tested the hypothesis that if circuit boards and other electronic parts (con\taining REEs and BFRs in high concentrations) are mixed together with polymers, thus leading to contaminated recycled material, then REEs and Br concentrations in items containing such recyclates should vary together. To do so, we conducted principal component analysis of our data on concentrations of individual REEs and Br in our samples. A general evaluation of the principal components was performed analysing a data table in which the concentrations of Br, Sb, Ca, Ti, Y, La, Ce, Pr, Nd, Sm, Gd, Tb, and Dy were expressed in the same unit for all samples. The first principal component accounted for 68% of the variance where REEs had the highest score in the first component and Br had the highest score in the orthogonal component (Shaw, 2009). Assuming that grouping of REEs is due to their use in different application categories, we grouped the samples by polymer type: polyolefin (PE and PP), styrenic (PS and HIPS) and copolymer (ABS, PC/ABS) before conducting between-group principal component analysis and within-group principal component analysis (data on polymer type were obtained with attenuated total reflection-Fourier transform infrared spectroscopy and pyrolysis GC-MS Table 2-11). In between-group principal component analysis (Boulesteix, 2005) data are projected onto the principal components of the group means and this usually leads to a better group separation than in conventional principal component analysis. In within-group principal component analysis, the average within each group is subtracted before the eigenanalysis: this has the effect of de-trending a group.

Table 2-11 Overview of ATR-FTIR and pyrolysis GC-MS data on polymer composition

Sample	Main polymer[a]	Most abundant polymer impurities[b]				
		PS/HIPS/ABS/ SAN	PC	PMMA	PA6	PET/PBT
Rubik's cube	HIPS	+	+	+	+	+
Toy gun	HIPS	+	+	+	+	+
Spring car	HIPS	+	+	+	n.d.	+
Spring car	HIPS	+	+	+	n.d.	+
Car launcher	HIPS	+	+	n.d.	n.d.	+
Miniature car	PS	+	+	+	n.d.	+
Miniature car	PS	+	+	+	n.d.	+
Spring gun	HIPS	+	+	+	n.d.	+
Thermal Cup	ABS	+	+	+	n.d.	+
Thermal Cup	ABS	+	+	+	n.d.	+
Radio cover	ABS	+	+	+	n.d.	+

[a]Data obtained by FTIR

[b] Data obtained by pyrolysis GC-MS; the symbol ``+`` means that polymer's specific precursors were detected in the pyrogram while ``n.d``. means not detected. The polymer precursors in the pyrogram are styrene (PS/HIPS/ABS/SAN); bisphenol A (PC); methylmethacrylate (PMMA); caprolactam (PA6) and benzoic acid (PET/PBT).

After grouping, the variance substantially increased between groups (89.3%) and decreased

within groups (60%), showing that the polymer type is a valid grouping strategy; when the

samples are grouped by polymer, the first component is responsible for ca. 30% more variation

in the data. In other terms, the data vary within the same polymer-type to a lesser extent than

within all samples; hence the polymer type is responsible for a trend in the data. Figure 2-21

shows a biplot of the first two principal components in a matrix of heptaBDE, TBBPA, Br, Sb, and

decaBDE concentrations for samples of different polymeric matrices. This graphical

representation of PCA is called a biplot because it allows row effects (in this case concentration-

related variables) and column effects (in this case polymeric matrix-related variables) to be
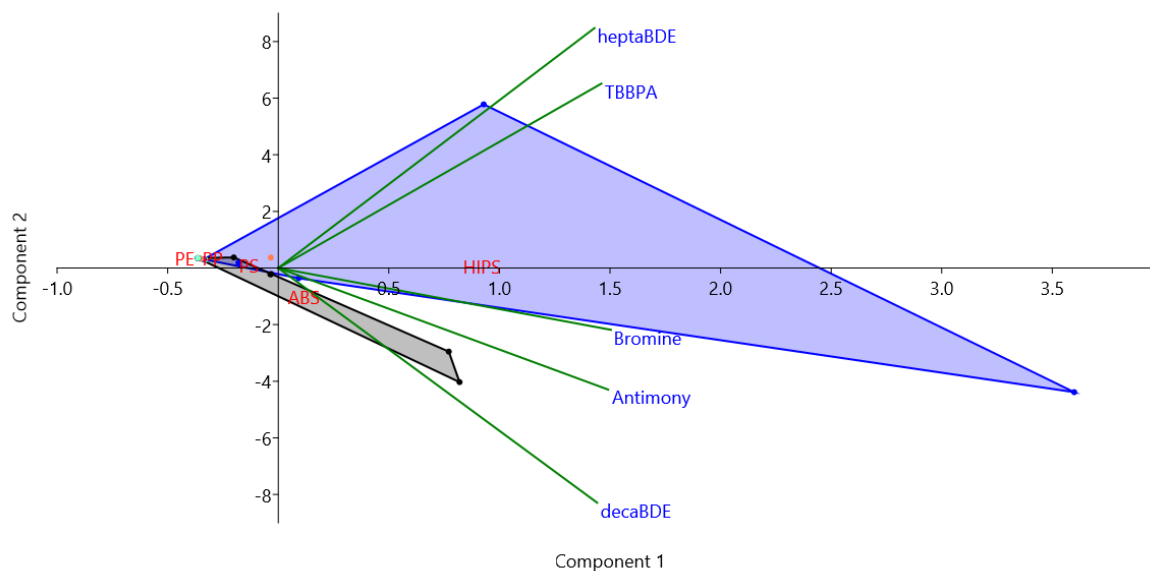

Figure 2-21 PCA of polymer type and BFR class shown in a biplot of the first two principal components. The angles between vectors shows that concentrations of PBDEs, bromine and antimony are all positively correlated with each other. Inspection of the "group" vectors (here represented as dots), shows these to fall into 3 main clusters (corresponding to the type of polymer of each sample). HIPS samples have the largest positive variations with respect to bromine and TBBPA. ABS samples have smaller but positive variations related to antimony, bromine and decaBDE. PP and PE have no noticeable deviations with respect to any of the plotted variables. This is because the concentrations of the above compounds are lowest in the PP/PE group of samples.

plotted jointly so that factorial axes are represented relative to individual (sample-wise) locations. This type of plot is meaningful when the two chosen components explain the large majority of the variance for the matrix of samples and variables to be represented. In this example this is a valid assumption as 99% of the variance is explained by the first two components (Br and TBBPA). The green lines are called eigenvectors, and their length is defined by an eigenvalue. The eigenvalue is the standardised variance i.e. the standard deviation of a certain variable: the longer a vector, the wider the range of values that variable assumes over the sample population. As a rule of thumb, positive and negative correlations between variables can be estimated by the cosine of the angle between their eigenvectors. A more detailed explanation of the theory behind the graphic display of matrices can be found elsewhere (Gabriel, 1971). The results showed that Br has the highest load in the first component (75%) and TBBPA in the second component (76%). When considering only the ABS based samples, BDE-209 has the highest loading in the first component (Figure 2-21). From Figure 2-22it is possible to observe how for ABS (group c), Br, Sb and REEs are inter-correlated quantitative dependent variables. Br, Sb and REE vectors form a very small angle with each other showing a strong positive correlation, and are almost orthogonal to Ca (no correlation); for HIPS/PS (group b) the Br and Sb vectors have very similar eigenvalues, meaning these variables have a similar influence on the data variance, but REEs loadings are close to zero; for PE/PP (group a) the opposite behaviour is observable, most REEs have similar loadings onto the two main components, (which causes them to point in the same direction) and similar eigenvalues (which gives their vectors similar lengths), whereas Br and Sb vectors are instead close to zero, indicating a small influence on the data variation (Martinho et al., 2012)

88

conducted a study on more than 3000 plastic samples arranging the polymer distribution by appliance class. The following observations are based on their findings: ABS is mainly used for central processing units and small copying equipment, and therefore the interdependence of REE and Br concentrations is explainable with the incorporation of printed circuit boards that contain the central processing units of computers (with high REE and BFR content) into the recyclate material. The main use of HIPS/PS is in housing for large cooling appliances and TVs. For these larger appliances it is reasonable to assume that separation of the cover from the electric and electronic components is more widely achieved given the dimensions of the parts and the fact that the plastic/circuitry ratio is higher than for small appliances.
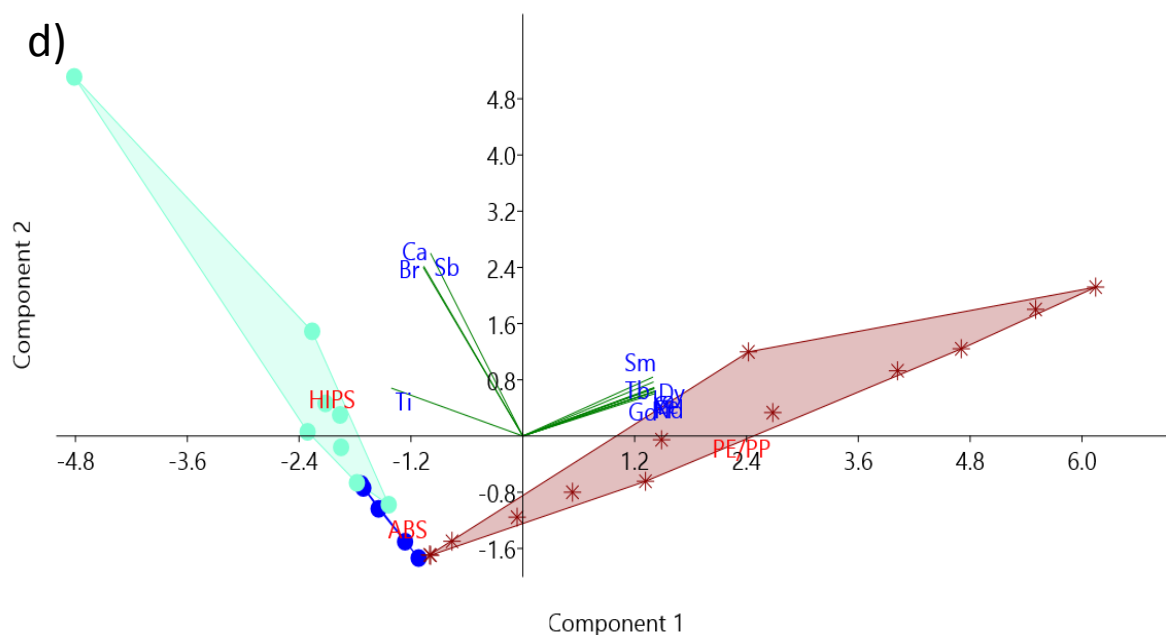

a)

b)

c
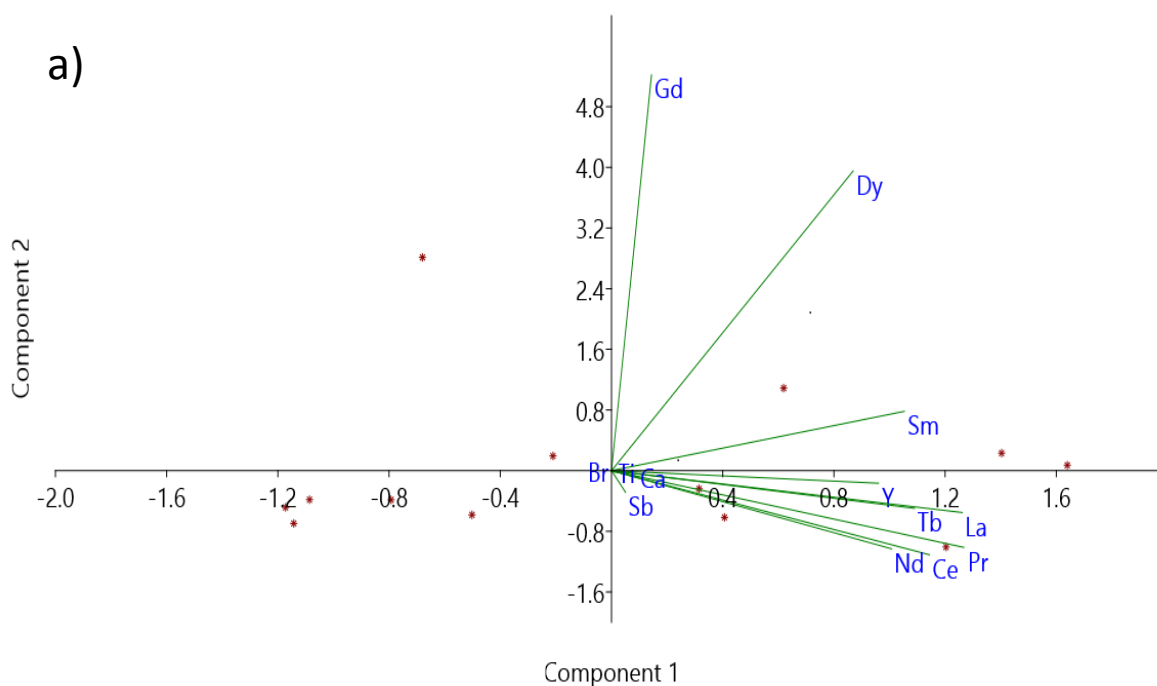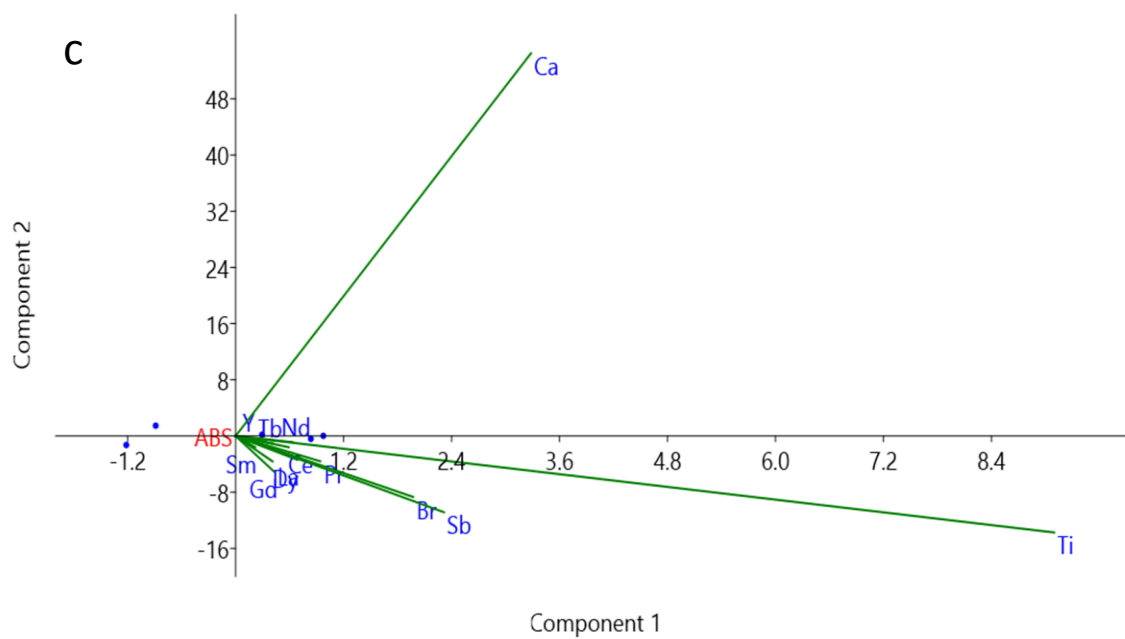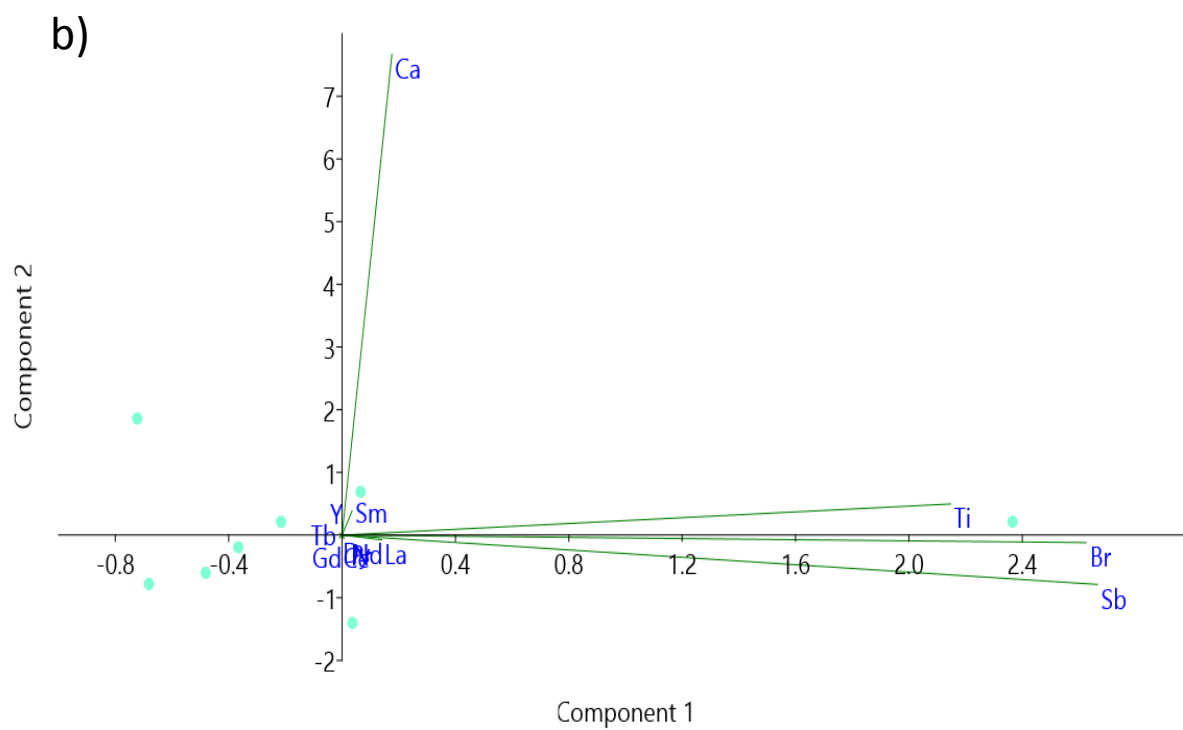
Figure 2-22 Principal Component Analysis for REEs, Br, Sb and inert fillers (Ca and Ti). d) bi-plot of the two main components for the complete group of samples, the filled coloured regions are correlation polygons joining sample groups (grouping is by polymer type). a) bi-plot for olefin polymers, b) bi-plot for styrenic polymers, c) bi-plot for acrylic co-polymers.

For these reasons Br and REE concentrations are not the main factors in the data variation within this polymer group. Finally, in the ((UNEP)-Chemicals., 2017) it is reported that BFRs have only a minor use in polyolefins and usually in fibres, not in hard plastic items (such as those analysed in this study), which explains the low Br and Sb concentrations found for this class of polymers. It was also observed that Ca was in all cases not following the distribution of the other vectors, which is probably because Ca is also added after recycling -when recycled polymers are added to new polymers-in the form of $CaCO_3$ as an inert filler to facilitate moulding of new large parts; therefore the cause of its increased concentration is not

interdependent with REE concentrations as it happens during a separate process. We thus normalized our data by Ca and analyzed the loadings of each analyte for the first component. For (a) PE/PP the major loading is on Y (used as a catalyst in ethane polymerisation) and Nb (used for the production of magnets employed in mobile phones, microphones, loud speakers and headphones), fitting well with the main application of this polymer which is small WEEE. For (b) the major loading is on Ce (used in flat-screen TVs and self-cleaning ovens) and on Gd (used for cathode ray tube screens), consistent with the main use of HIPS/PS in large appliances and TV sets (Martinho et al., 2012). The main loading for ABS was on Gd which is also used for data storage discs and central processing units, for which ABS is widely used as a casing material. The clustering over polymer type can be explained as follows: different polymers are used for different purposes (depending on the required cost, mechanical resistance, flexibility, etc.), therefore showing different BFR types and loadings and will be differently sorted during the recycling rounds. In conclusion, goods that are made of the same polymer type tend to have similar BFR profiles because of their similar manufacturing, use and recycling processes.

2.4.3 Method validation

For LA-ICP-MS the average precision for all samples given by the RSD between two line scan replicates was 5.9%; for XRF it was 1.5%. The average RSD of 79Br counts on each line scan was of 10.7% (although better results have been observed in specific measurements) a reasonably good value compared with RSD of 15% obtained for Br in line scans on polymers in a recent study (Izgi et al., 2005), compared to prior literature on line scans on polymers (Stehrer et al., 2010), or to raster scans of styrenic polymers (Austin et al., 2010). Also a higher RSD calculated on the measurement points of a line scan with respect to the RSD calculated between two line

scan repetitions, corroborate the hypothesis of micro-homogeneity of the samples having a greater influence on the time signal fluctuations. As expected, the LOD for LA-ICP-MS was almost a factor of 3 better than XRF (LOD for LA-ICP-MS was 0.0004% and 0.0011 % for XRF) and overall satisfactory for LA-ICP-MS considering the matrix and the high ionization potential of Br. In a recent study (İzgi and Kayar, 2015) the LOD for LA-ICP-MS determination of 79Br was calculated as 0.0612% in plastic. The accuracy of both techniques (XRF and LA-ICP-MS) is comparable (respectively 93.9% and 93.3%) while high accordance between the data produced by both techniques shows that the XRF thickness correction developed here is a reliable improvement compared to the use of this tool in the literature (Gallen et al., 2014) for Br screening on polymers (no false positives were detected by XRF) in a concentration range between 0.08 an 12% Br.

2.5 Conclusions

2.5.1 Case study #1

Empirical corrections and tuning for hand-held XRF and LA-ICP-MS provided more accurate and precise Br data for WEEE plastics compared with uncorrected data and compared with the most recent literature on Br analysis in polymers using LA-ICP-MS and XRF (İzgi and Kayar, 2015). Therefore, automating these analytical techniques would greatly benefit Br analysis. Key findings from this research are:

-        Br quantification by hand-held XRF can be improved substantially by the use of a matrix matched thickness correction.

-       The matrix matched calibrations presented here resulted in strong correlation between Br data obtained for the same samples using hand-held XRF and LA-ICP-MS. For hand-held XRF, this suggests it constitutes an accurate, rapid, inexpensive technique for the on-site quantification of Br in WEEE plastics.

-       TD-GC-MS analysis confirmed that the majority of the bromine measured in the samples is organic (i.e. BFRs). In many samples only one or two BFRs were detected, however in some cases a mixture of 3 or 4 BFRs were found. The presence of several BFRs in one sample may indicate the presence of a WEEE recycled fraction, and highlights the potential for source misclassification whereby a Br signal may be incorrectly attributed in its entirety to a single specific regulated BFR. The BFRs most frequently detected in the WEEE samples tested in this study are BDE-209 and TBBPA (Table 2-6). Our data also confirm that the majority of the old monitor casings samples contained BFRs and that other, more recently produced appliances show a higher number of Br-free polymers.

Considering how the resulting Br concentrations will be used, an easy to operate, accurate, affordable, fast method for quantifying BFR concentrations with a reasonably low LOD may provide an appropriate solution for WEEE sorting and recycling plants as well as control laboratories. LODs for both techniques were far below the lowest of the low POP concentration limits (LPCLs) in Annex IV of the POP Regulation for BFRs in plastics (EC No 850/2004); therefore these techniques are capable of addressing current legislation but are also future proofed for any future reductions in the maximum concentration levels.

Given the advantages of speed and relatively low cost of hand-held XRF, it holds much promise as the method of choice for large-scale monitoring of compliance with legislative limits on BFR concentrations in WEEE. However, although the current limits such as EU directive 2011/65/EU are specified in terms of the concentration of the BFRs, XRF can only measure elemental Br. This presents a practical problem, as for example the limit for PBDEs is 0.1%, then if the XRF reports 0.075% in weight of Br, this equates to 0.09% BDE-209, but 0.106% Penta-BDE. In other words, the limit is exceeded if the Br is due to Penta-BDE but not if it results from the presence of Deca-BDE. A possible practical "work around" is to specify the limit in terms of Br, but making a conservative assumption that it originates from the presence of a widely used BFR with the lowest proportion of Br, such as Penta-BDE. While doing so will result in some marginal false exceedances of the limit, it will facilitate the widespread use of hand-held XRF to monitor compliance with limit values. Given the enormous mass of WEEE and waste soft furnishings that contain BFRs, the implementation of such an accurate yet rapid and relatively inexpensive monitoring technique is essential, as large-scale application of traditional GC-MS and LC-MS methods appear uneconomic.

2.5.2 Case study #2

This study uses XRF to measure concentrations of Br and Sb in toys and FCAs as an inexpensive, rapid, in situ metric of unintentional BFR contamination. LA-ICP-MS measurements on the same samples validates the use of XRF in this application for accurate Br and Sb quantification in polymers. Our results show that – in contravention of Regulation (EC) No. 202/2014 - FCAs that can be bought on the European market are not being produced exclusively with food-grade

95

polymers, specifically, one third on the FCAs in this study tested positive for Br. BFRs were more frequently found in children's toys with concentrations in some samples exceeding low POP concentration limits (LPCLs) applied for WEEE, almost half of the analyzed toys in this study. Children's toys do not fall under European Commission directives relating to BFRs or REACH unless they have electric or electronic components, in which case they fall under the WEEE directive. Considering the extent of contact and the vulnerability to toxic chemicals of their users, this class of consumer goods should undergo the same strict regulation as FCAs, banning the use of uncontrolled recycled material at the material sourcing stage, and we believe this study- together with other recent ones on this issue -by measuring the extent of contamination of these items and adding to the library of UTCs in toys and FCAs, helps form an argument for it.

Although other matrix effects might influence the accuracy of element concentration; using matrix-matched, homogenous reference materials and observing similar ablation behaviour between references and samples allows us to make the assumption that, when other matrix effects arise, they are likely to have similar influences on both calibration standards and samples.

PCA analysis displayed potential to be a valid tool to provide insights into the recycling pathways and sources from the observation of their end result (recycled plastics).

 The results also provided information on the main issues causing poor sorting practices i.e. laborious sorting of small EEE and separation of covers from CPUs in small appliances. The identification of the critical points along the waste cycle is the first step for establishing good recycling practices.

2.6   Future developments

In order to reduce the total BFR content (and thereby cost) while maintaining the same flame retardant effect an inorganic flame retardant, Sb_2O_3, is usually added in a 1:3 ratio with PBDEs and PBBs, the two most common restricted classes of BFRs found in polymeric materials. Fluctuations between different samples were noticed in the Sb/Br ratio: this leads to the hypothesis that this value could be used when performing in-situ XRF analysis to identify the specific presence of PBDEs as opposed to other BFRs on which LPCLs do not apply, such as TBBPA. It should be noted that the same 1:3 ratio could be observed when HBCDD- which is instead covered by the LPCLs- is present, but- as this BFR rarely exceeds the LPCLs in WEEE- it is unlikely that it would hamper the identification of PBDEs with this method. Should this method be implemented in a regulatory guidance in the future, inter- and intra-day accuracy should be assessed.

Because Sb is used as a co-synergist only with BFRs that are restricted at low concentration levels, if Br is found without Sb, the sample is likely to contain a different – non restricted - type of BFR (e.g. TBBPA). This correlation is true when used to identify the presence of PBDEs when Sb is also detected, but is not applicable to exclude the presence of TBBPA. This is because most plastics contain a recycled fraction in them, meaning that PBDEs found together with Sb might come from one recycled fraction and TBBPA from another recycled fraction in the same sample. This study shows potential in measuring the deviation from the mass ratio between Br and Sb (3:1) as a metric for the relative amounts of PBDEs and TBBPA. A study that focuses on the correlation of this ratio with the presence/absence of PBDEs (and PBBs) in polymers has the

potential of providing compound-specific insight using only very simple, inexpensive trace

elemental (inorganic) analysis (XRF), therefore it could be useful in the future to measure Sb:Br

in articles for which Br suggests LPCLs-exceeding amounts of BFRs.

3 Compound specific BFR quantification with DIP-MS-HRMS

Monitum

This chapter contains some material taken verbatim from the following article:

GUZZONATO, A., MEHLMANN, H., KRUMWIEDE, D. & HARRAD, S. 2016a. A novel method for
quantification of decabromodiphenyl ether in plastics without sample preparation using
direct insertion probe–magnetic sector high resolution mass spectrometry. *Analytical
Methods,* 8**,** 5487-5494.

3.1   Introduction

Screening is preferred for in situ evaluations as it is usually performed via solid sampling

techniques like hand-held X-ray fluorescence spectroscopy (XRF) although this can only quantify

Br as a proxy for the total BFR content, thereby running the risk of false positives. More

conventional techniques are recommended for high-accuracy determination of BFRs like PBDEs.

Specifically, RoHS requires GC-MS analysis to determine the BFR content in styrenic polymers

(preceded by different sample preparation steps: sub-sample grinding, cryo-grinding, solvent

extraction, extract filtration, selective precipitation for oligomer removal, and chromatographic

purification). However, these traditional techniques can have a number of drawbacks aside

from being time consuming and expensive. Soxhlet or pressurised liquid extraction of plastics

often dissolves a substantial fraction of the matrix (polymer) together with the target

compound, rendering the ensuing extract purification laborious and often leading to highly

variable analyte recoveries. Furthermore, PBDEs are present across a wide range of

bromination level, from the lower brominated tri-BDEs and tetra-BDEs with a low boiling point to the most brominated (deca-BDE) with a very high boiling point. This makes it practically difficult to use the same GC-MS system set-up to analyse all PDBE homologues simultaneously in a single GC run: ideally two different GC columns are used, causing several analytical delays (run the samples on one system set-up first, then switch columns and run them again on the second set-up), although a better solution was achieved by Ballesteros-Gómez (Ballesteros-Gómez et al., 2013) using GCxGC to resolve coeluting interferences in the second dimension, thus eliminating the need for two different GC runs. The high boiling point and its enhanced susceptibility to degradation and debromination when exposed at the elevated temperatures of the injector, column, ion source and detector make BDE-209 a challenging analyte (Covaci et al., 2007a, Dirtu et al., 2008, Pöhlein et al., 2005, Hosaka et al., 2005, Llorca-Porcel et al., 2006, Abdallah et al., 2008, Vilaplana et al., 2008, Sánchez-Brunete et al., 2006, Serôdio et al., 2007, Christiansson et al., 2006, Xie et al., 2007).

To face these analytical challenges novel methods for the quantification of BFRs have been developed recently combining GC, LC or GCxGC with a soft ionisation method (APCI) and a high resolution time-of-flight mass spectrometer or for compound-specific screening using direct probe with HR-TOF (Ballesteros-Gómez et al., 2013). One attempt to develop a solid sampling, compound-specific analysis was made by exploring the potential of Direct Analysis in Real Time coupled with Time Of Flight Mass Spectrometry (DART-TOF-MS), (Jana et al., 2008) but results revealed it as constituting only a qualitative method to screen for the presence of BFRs in environmental matrices. Elsewhere in this thesis, the feasibility of using DART as a source for

compound specific quantification of PBDEs is also tested, coupling DART with a high resolution

mass spectrometer (Orbitrap), details about this can be found in the chapter 4.

Against this backdrop, it is evident that a method that combines the convenience of a solid

sampling technique with compound specific quantification is highly desirable.

We present here a simple, sensitive, and rapid method using Direct Insertion Probe (DIP) in

combination with magnetic sector high resolution mass spectrometry (HRMS). This method

characterises target compounds without a chromatographic separation needed, solely via

accurate mass determination combined with a traditional library search. To our knowledge, this

is the first approach for compound-specific direct analysis of BFRs in polymers that does not

require any sample preparation nor a GC or LC inlet. The method is validated via determination

of BDE-209 in ABS solid reference materials (RMs), but accurate mass determination can be

applied to unambiguously identify other PBDE congeners.

3.1   Experimental

3.1.1 Overview

This method involves the use of matrix matched RMs for the compound specific quantification

of BFRs in polymers. ABS was used as polymeric matrix as it is one of the most common

polymers used in electrical and electronic equipment (EEE) and toys. Our target BFR was BDE-

209 as it displays a small temperature difference between evaporation and thermal

degradation, as a proof of concept for the DIP method that samples the analytes via thermal

desorption. Calibration of the method was carried out using RMs at 5 different concentrations of BDE-209.

RMs loaded with different concentrations of BDE-209 were produced by Fachhochshule Muenster Labor fur Instrumentelle Analytik. The method used to produce and test the RMs is described in detail elsewhere (Mans et al., 2009), but in summary, Br (in the form of deca-BDE) and Sb (in the form of Sb_2O_3) were added to an ABS terpolymer melt with the aid of an extruder. Sb_2O_3 is generally used as a synergist FR in combination with BFRs (Pitts, 1972). A set of five different reference materials was produced in the form of pellets containing different mass fractions of both Br and Sb plus typical fillers commonly used in ABS (see Table 2-2) in order to best simulate the matrix of the samples. Mass fractions of Br in the produced materials were determined (by Fachhochshule Muenster Labor fur Instrumentelle Analytik) via Neutron-Activation-Analysis (NAA). The uncertainty of NAA is about 7% (for exact values see Table 2-2). To assess macroscopic homogeneity a wavelength dispersive X-ray spectrometer was used with RSD below 2% for Br. To assess microscopic homogeneity a synchrotron radiation m-XRF (SR m-XRF) was used. The spot size of the exciting beam was 200 μm, the RSD for Br was 0.7%.

3.1.2 Sampling

No sample preparation was required. A very small amount (ca. 0.045 mg) was scraped from the pellets of the RMs with a scalpel(this sampling is representative enough for the RMs for which micro- and macro-homogeneity were tested but it may need multiple sampling for "real" samples) , accurately weighed with a precision scale (±0.0005 mg) and inserted in the

aluminium crucibles for the DIP. The influence of the scale error on such a small sample is

±1.1%.

3.1.3 Instrumentation

The Thermo Scientific™ DFS™ magnetic sector high resolution mass spectrometer (HRMS) was

used for DIP-HRMS analysis. The probe temperature program is software controlled. The

Thermo Scientific™ ISQ™ QD Single Quadrupole GC-MS System was used for the comparison of

mass spectra obtained with the most common GC-MS technique (and relative sample

preparation) (Hacaloglu, 2012).

3.2   Results and discussion

3.2.1   Mass spectrometric determination

As no GC column is used, the only time difference in vaporisation is dictated by the compound's

vapour pressure. The RMs we used to test this method were loaded with BDE-209, although

due to the process of their production (melted and extruded several times to ensure

homogeneity), some thermal decomposition is likely to have produced a small amount of

decomposition products inside the polymer (Figure 3-1). Thermo Scientific™ Mass Frontier

Software was used to simulate all the potential BDE-209 fragments and hence identify target

ions. For this method we chose the molecular ion of BDE-209 (m/z 959) and one of its main

breakdown products octaBDEs (m/z 799). Isotopic patterns and exact masses corresponding to

these two ions were simulated using the Thermo Scientific™ Xcalibur™ Software. The exact

$$\Delta m_m = \frac{(m_m - m_c)}{m_c} \times 10^6 \hspace{4cm} (1)$$

masses were used to calculate the mass measurement error (ppm) following the expression (1):

where m_m is the measured accurate mass and m_c is the exact mass. The deviation of the

measured masses from the exact masses was for all isotopologues of BDE-209 (averaged over

20 scans) less than 1 ppm using a dedicated pre-calibrated method based on the reference

material perfluorokerosene (PFK) which uses all the exact masses contained in the PFK mixture

to perform a polynomial correction of the measured accurate masses (see Figure 3-2 and Table

3-3).
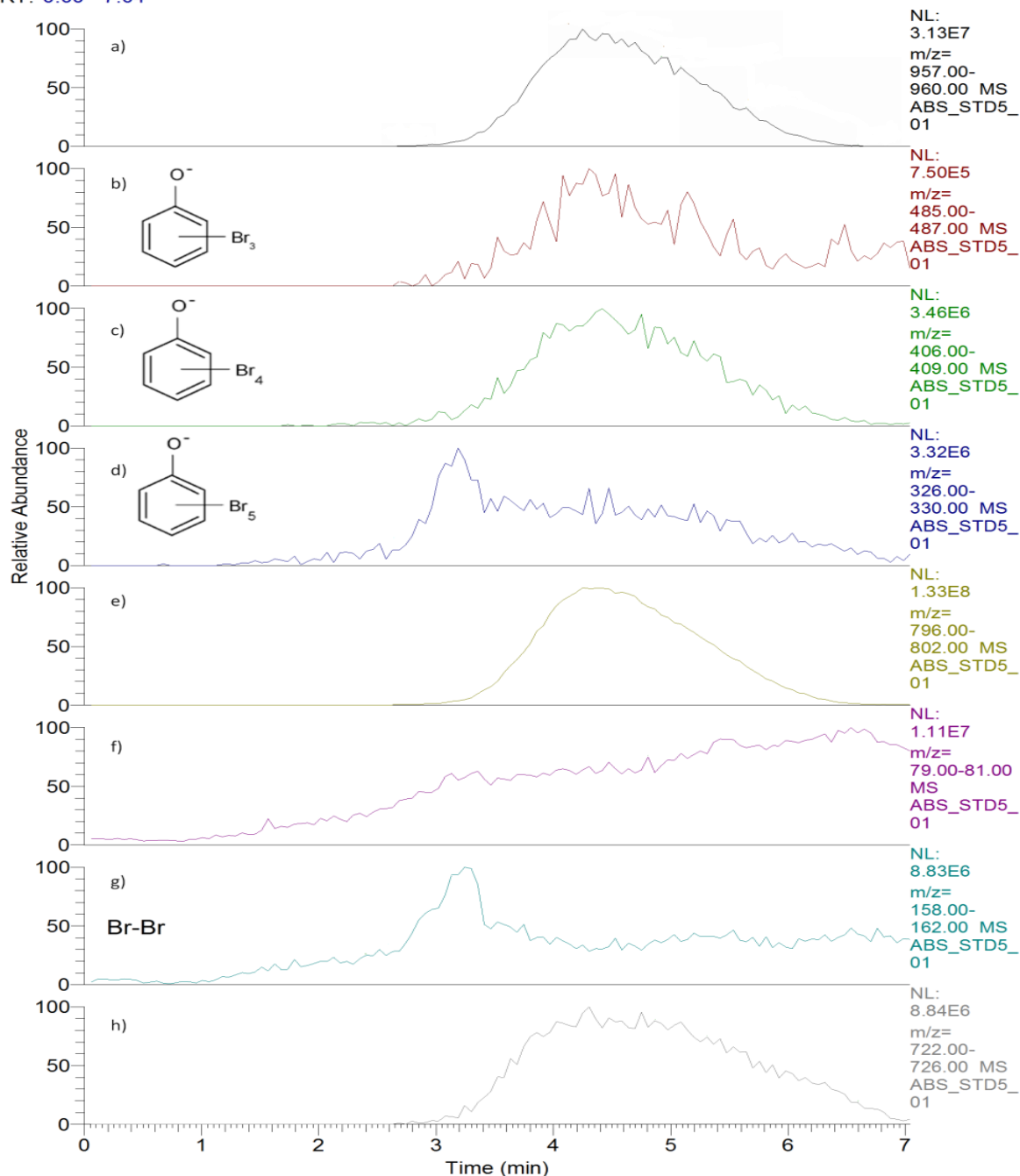
Figure 3-1 Time signal obtained with DIP-HRMS (selected over the entire time signal for a) m/z 957-960; b) m/z 485-487; c)m/z 406-409; d) m/z 326-330; e) 796-802; f) m/z 79-81; g) m/z 158-162; h) m/z 722-726. It can be seen that the formation of the penta brominated ions (d)) corresponds to a simultaneous release of Br₂ molecules (g)).
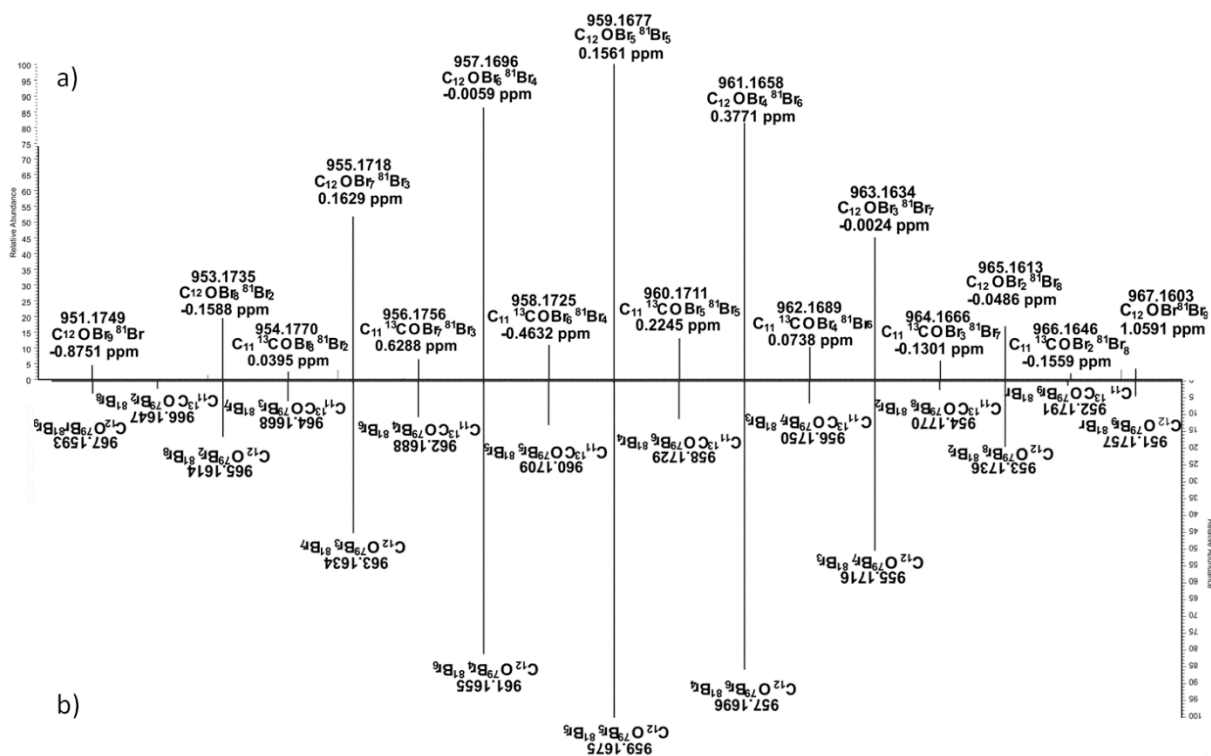
Figure 3-2 Comparison of a) accurate masses measured over 20 scans for BDE-209 (reported in Table 3-1), and b) their calculated exact value of the mass.

3.2.2 Method development: study of inlet and EI source parameters

The optimised conditions for BDE-209 were obtained959 by varying one parameter at a time, performing a measurement and observing the influence of this variation on sensitivity, reproducibility and degree of fragmentation of the parent ion. After a preliminary evaluation, the two most relevant parameters turned out to be: the temperature programme of the heated probe (i.e. ramp speed) and the ionisation strength (electron energy of the electrons emitted by the ionising filament in the EI source).

The temperature ramp speed was optimised by keeping the source's electron energy constant at a "standard" value of 71 eV (most commonly used when a GC is attached to this HRMS instrument), analysing the same RM (containing 1% w/w of BDE-209) in triplicate for each temperature gradient (in steps of 20 ˚C/min). Results were evaluated by measuring the intensity of the fragmentation product, of the molecular ion and the sum of both. The value of 75 ˚C/min maximised the total signal intensity over the decomposition (799 m/z over 959 m/z intensity ratio) and was chosen as the optimal value. The electron energy was then optimised by keeping the temperature ramp speed at the optimised constant value of 50 ˚C/min and analyzing in triplicate the same RM (containing 1% w/w of BDE-209) for each electron energy value (in steps of 5 eV). The optimised electron energy value was 46 eV.

Initial temperature, duration of the initial temperature step and final temperature were chosen on account of the physicochemical properties of the polymer and the BFR dissolved therein, so that the complete time signal would have a defined region where no Br- containing molecules are being volatilised at the beginning of the run and that all Br-containing molecules reach a defined minimum at the end of the run. Faster DIP temperature ramps increase the thermal breakdown while higher electron energies were found to increase the ion fragmentation but both tend to be proportional to the overall signal intensity, therefore a compromise between these two effects was found in the values reported in Table 3-2.

To set the desired resolution of 20,000 FWHM, PFK was monitored on mass 792.9499 m/z and the entrance and exit slits were closed recursively until the desired resolution was reached, these parameters were stored in the measurement conditions and the instrument response was regularly checked using the same reference gas.

Table 3-1 Mass Table of measured isotopes

m/z	Relative intensity	Delta (ppm)	Composition
951.1749	4.34	**-0.88**	$C_{12} O Br_9 [81]Br$
953.1735	19.34	**-0.16**	$C_{12} O Br_8 [81]Br_2$
954.1772	2.5	**0.24**	$C_{11} [13]C O Br_8 [81]Br_2$
955.1718	51.57	**0.16**	$C_{12} O Br_7 [81]Br_3$
956.1756	6.25	**-0.41**	$C_{12} [13]C Br_5 [81]Br_5$
957.1696	86.22	**-0.01**	$C_{12} O Br_6 [81]Br_4$
958.1725	10.78	**-0.46**	$C_{11} [13]C O Br_6 [81]Br_4$
959.1677	100	**0.16**	$C_{12} O Br_5 [81]Br_5$
960.1711	12.92	**0.22**	$C_{11} [13]C O Br_5 [81]Br_5$
961.1658	81.39	**0.38**	$C_{12} O Br_4 [81]Br_6$
962.1689	10.16	**0.07**	$C_{11} [13]C O Br_4 [81]Br_6$
963.1634	45	**0.00**	$C_{12} O Br_3 [81]Br_7$
964.1666	5.79	**-0.13**	$C_{11} [13]C O Br_3 [81]Br_7$
965.1613	16.71	**-0.05**	$C_{12} O Br_2 [81]Br_8$
964.1646	1.76	**-0.16**	$C_{11} [13]C O Br_2 [81]Br_8$
967.1596	3.52	**0.33**	$C_{12} O Br [81]Br_9$

Table 3-2 DIP-MS conditions

Ion Source temperature	260 ˚C
Source mode	EI Positive
DIP temperature programme	40 (0.5˚C/min)-75-400 (2 min)
Scan mode	Magnetic scan
Mass range	30-1000 m/z
Resolution FWHM	20000
Electron energy	46 eV
Emission current	1 mA
Acceleration voltage	4800 V

3.2.3 Verification of the DIP-HRMS method

Octa-BDE and deca-BDE were measured and their ratio evaluated to test the reproducibility of the fragmentation. Although selected ion mode analysis can provide better sensitivity and transient signals that are easier to interpret, we decided to acquire in the complete mass range (m/z 30–1000) for BDE-209 for three reasons: (a) when BDE-209 is present in consumer goods, whether it is added intentionally or not, its concentration is usually orders of magnitude higher than the detection limits of the DFS magnetic sector GC-HRMS; moreover the regulatory limits set a relatively high concentration threshold of 0.1% in homogeneous material; (b) for quantitative purposes it is very important to include in the calculation every fragment (including molecular Br) deriving from the parent ions present in the samples. This approach allowed us to

understand whether it was reasonable to assume that – granted a very stable fragmentation yield – the total Br would have been linearly proportional to any of the main fragments produced (octa-BDE and nona-BDE); and (c) such a wide mass range – covering the vast majority of commonly used BFRs – delivers the flexibility to identify and quantify different compounds simultaneously.

The calibration curve (Figure 3-3) was determined by analysing each of the five solid RMs (0%, 0.1%, 0.5%, 1%, 2% w/w of BDE-209) in triplicate. Intensities were considered selecting the 3 most intense m/z values from the isotopic pattern and averaging the intensities of the time signals corresponding to those 3 masses. Scans from the tails of the transient signal were excluded when their relative intensity was less than 5% of the most intense scan (this corresponds to ca. 40 scans for each "peak").

The signal intensity of BDE-209 (average intensity for m/z 959, 957, 961, which are the 3 main isotopologues of $C_{12} O Br_{10}$) was plotted against the reference value of the RMs. In the same way, the signal intensity of the -2Br fragment (average intensity for m/z 799, 797, 801) was plotted against the reference value. The correlation factor R^2 was >0.999 for both BDE-209 and its octabrominated breakdown product, showing linearity over the selected range. The calibration curve for BDE-209 was obtained by averaging the signal intensity of the three most abundant isotopologues of BDE-209, m/z 959, 957, 961 for each calibration level (Figure 3-2 a)). The calibration curve for the main fragmentation product of BDE-209 – which is octaBDE – was obtained by averaging the signal intensity of the three most abundant isotopologues of octaBDE, m/z 799, 797, 801 for each calibration level (Figure 3-2 b)). The LOD was defined as in the ICH1 Guidance (Q2, R1: validation of analytical procedures) as 2 σ: where σ is the standard

deviation of the response on the triplicate measurement of blank samples (RM BDE-209) and S

is the slope of the calibration curve. The noise – defined as the intensity of the signal given by

the target mass on a blank measurement – was below 1/3 of the instrument detection limits.

This result was foreseeable, considering that each sample, and the crucible containing it, was

removed from the probe before inserting a new sealed crucible containing a different sample,

therefore no physical residues of the previous sample could be left on the one following (unlike

a traditional GC analysis, where polymeric residues might build up in the injector liner and in

the column and create a memory effect). The calculated LOD with this method was 0.112 mg

kg^{-1}, and the LOQ was 1.12 mg kg^{-1} for BDE-209, slightly lower than a similar study performed

with Direct Exposure Probe (DEP) (Jung et al., 2009), and with the advantage of no sample

preparation needed.
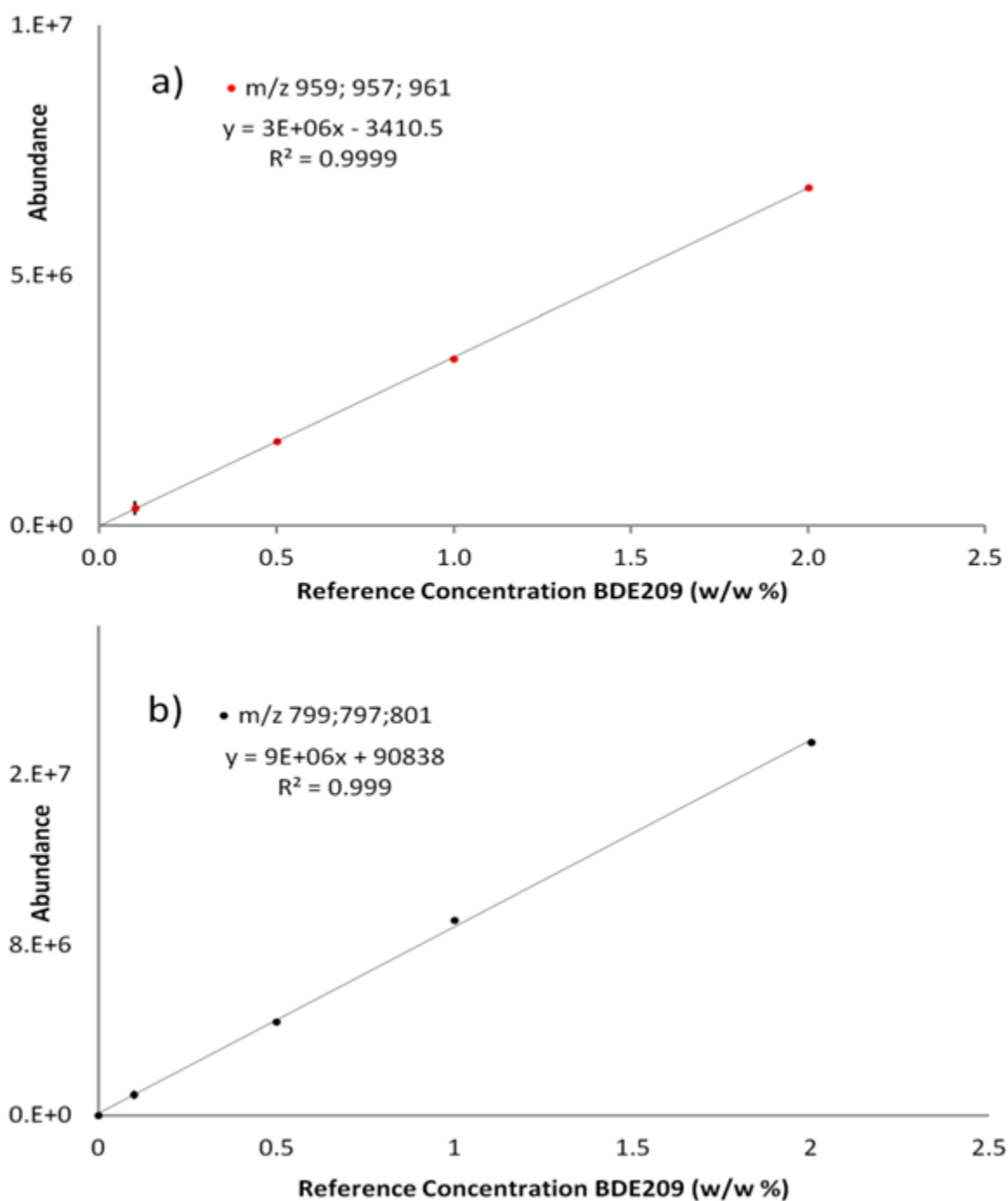
Figure 3-3 Calibration curves and linearity for the analysis of (a) [BDE-209]+, (b) [BDE-209-Br2]+ obtained by DIP. Error bars are the SD between triplicate measurements of each RM, and only visible for the lowest concentration in plot a).

The precision was evaluated by calculating the RSD between triplicate measurements of the most concentrated RMs; the percent variation was 0.47% and no increasing trend was observed. Intraday stability was evaluated by performing control runs of RM3 at the beginning, in the middle and at the end of each day of analysis. Over 3 days the intraday RSD of the signal intensity for BDE-209 averaged at 1.96%, while interday RSD was 0.51%. The method was applied to 21 real polymeric samples (children's toys and food contact articles, Table 3-3) for which the BDE-209 concentration was measured. BDE-209 data and total elemental Br measured with an X-ray fluorescence spectrometer were plotted to evaluate if a correlation existed between the two metrics. BDE-209 was detected in a concentration ranging from 8.8 mg kg^{-1} to 4327 mg kg^{-1}. Considering that these data refer to real samples, containing a suite of different BFRs, each potentially contributing to the total elemental Br concentration; the correlation (R^2 =0.86) between our BDE-209 concentration measurements and those for total Br is striking. Moreover, our measurements of BDE-209 – which is likely to be a fraction of the total BFR content – never exceeded those of total detected Br (Figure 3-4).

Table 3-3 Comparison of DIP-MS-HRMS measurements of concentrations of BDE-209 and those of Br recorded with X Ray Fluorescence (concentrations expressed as the average of triplicate measurements).			
Sample	Description	BDE-209 (w/w%)	Br (w/w%)
1	Coffee cup lid	0.047	0.122±0.0002
2	Coffee cup lid	0.015	0.125±0.009
3	Miniature Car	<LOD	0.121±0.0001
4	Miniature Car Frame	0.038	0.151±0.0003

5	Rubik's cube	0.010	0.071±0.0.002
6	Rubik's cube	<LOD	0.018±0.007
7	Spring Car	0.107	0.208±0.0001
8	Spring Car	0.032	0.124±0.001
9	Spring Car Base	<LOD	0.054±0.001
10	Thermal coffee mug	<LOD	0.002±0.0001
11	Thermal coffee mug	0.001	<LOD
12	Toy Binocular	<LOD	<LOD
13	Toy Bowl	<LOD	<LOD
14	Toy Coin	<LOD	<LOD
15	Toy Gun	0.433	0.501±0.022
16	Toy Gun	<LOD	<LOD
17	Toy Shield	<LOD	0.013±0.002
18	Toy Spring Gun	<LOD	0.072±0.001
19	Toy Spring Gun	<LOD	<LOD
20	Toy Sword	<LOD	0.011±0.007
21	Toy Target	<LOD	0.002±0.001
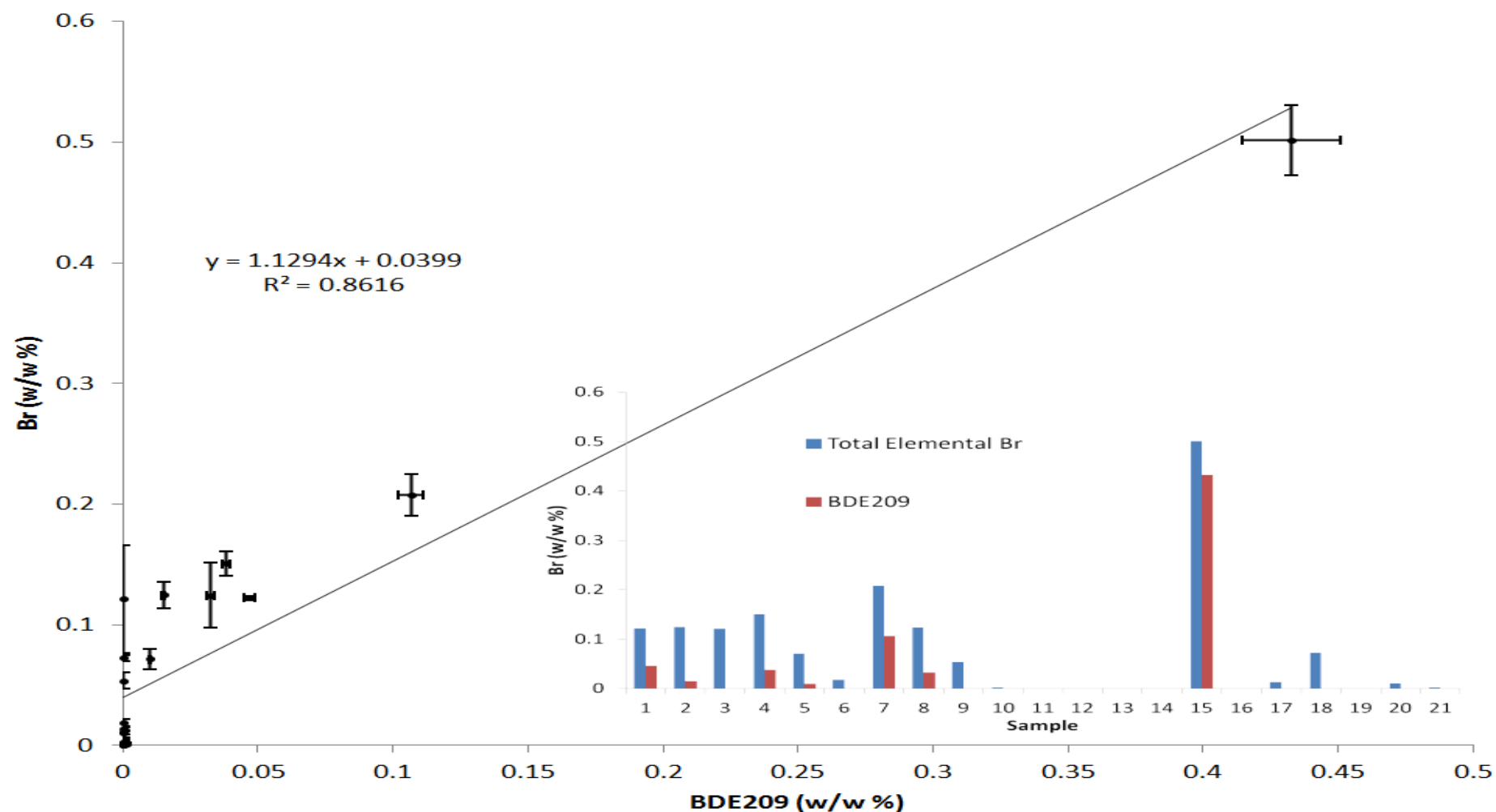
Figure 3-4 Correlation between BDE-209 measured with DIP-MS-HRMS and total elemental Br measured with X-Ray Fluorescence. Considering that these data refer to real samples, and thus contain a suite of different BFRs each contributing to the total elemental Br concentration, the proportionality between the BDE-209 concentration and that of Br is clear. In addition, the inset plot shows that on no occasion does the detected BDE-209 (which is likely to be a fraction of the total BFR content) exceed the total detected Br. Error bars for X-Ray Fluorescence results are equal to 4 SD, for DIP-MS-HRMS to the relative measurement accuracy.

3.2.4 Reproducibility of the fragmentation ratios

The ionisation behaviour was tested for reproducibility by selecting m/z 799 and m/z 959 from the time signal and measuring the intensity for these masses over the selected time interval. DIP offers a specific advantage with respect to GC-MS analysis: as there is no column or injector between the sample introduction system and the ionisation volume, it is possible to differentiate between breakdown products (caused by thermal degradation) and ionisation fragments (produced by the EI process). This is easily done by comparing the time signals for the molecular ion and for its possible moieties as shown in Figure 3-3 (a) and (e) which show the overlap in intensities of the time signal respectively for the decabrominated ion and the octabrominated ion, meaning that the latter was formed simultaneously in the source, as a fragment of the former. Following this approach it can be concluded that as the pentabromophenate ion (d) was detected at the same time as molecular bromine (g), the debromination happened in the ion source and not as a thermal process in the sample; moreover, time signals (d) and (g) are both detected before the deca- and octa brominated fragments meaning that their parent ion was already present in the reference material before its insertion in the source.

The ratio between the molecular ion and its main fragmentation product was – for all measured concentrations – 3.1 ± 0.04 (see Table 3-4), showing it to be independent of the sample concentration and suggesting very reproducible fractionation behaviour. This is important as it allows subtraction of the contribution made by the BDE-209-2Br fragment to the signal for m/z 799, thereby facilitating quantification of any octa-BDEs present.

116

A comparison between the mass spectrum of the sample RM obtained using our DIP-HRMS

method and that obtained via GC-MS following traditional sample preparation methods and

liquid sampling in Figure 3-5 shows that the ratio between m/z 799 and m/z 959 is almost two

times higher for the traditional GC-MS technique. The thermal decomposition leading to

generation of the M-2Br ion is reduced in the DIP method because the sample is introduced in a

chamber under vacuum (instead of under pressure as it would be in a GC injector) therefore

lower temperatures are required to reach sufficient vapour pressure.

Table 3-4 Fragmentation ratio between the two main BDE-209 ions.

Reference BDE-209 w/w%	Ratio m/z 799 and m/z 959	SD of the m/z ratio
0.1	3.002	0.04
0.5	3.079	0.04
1	3.051	0.04
2	3.002	0.04
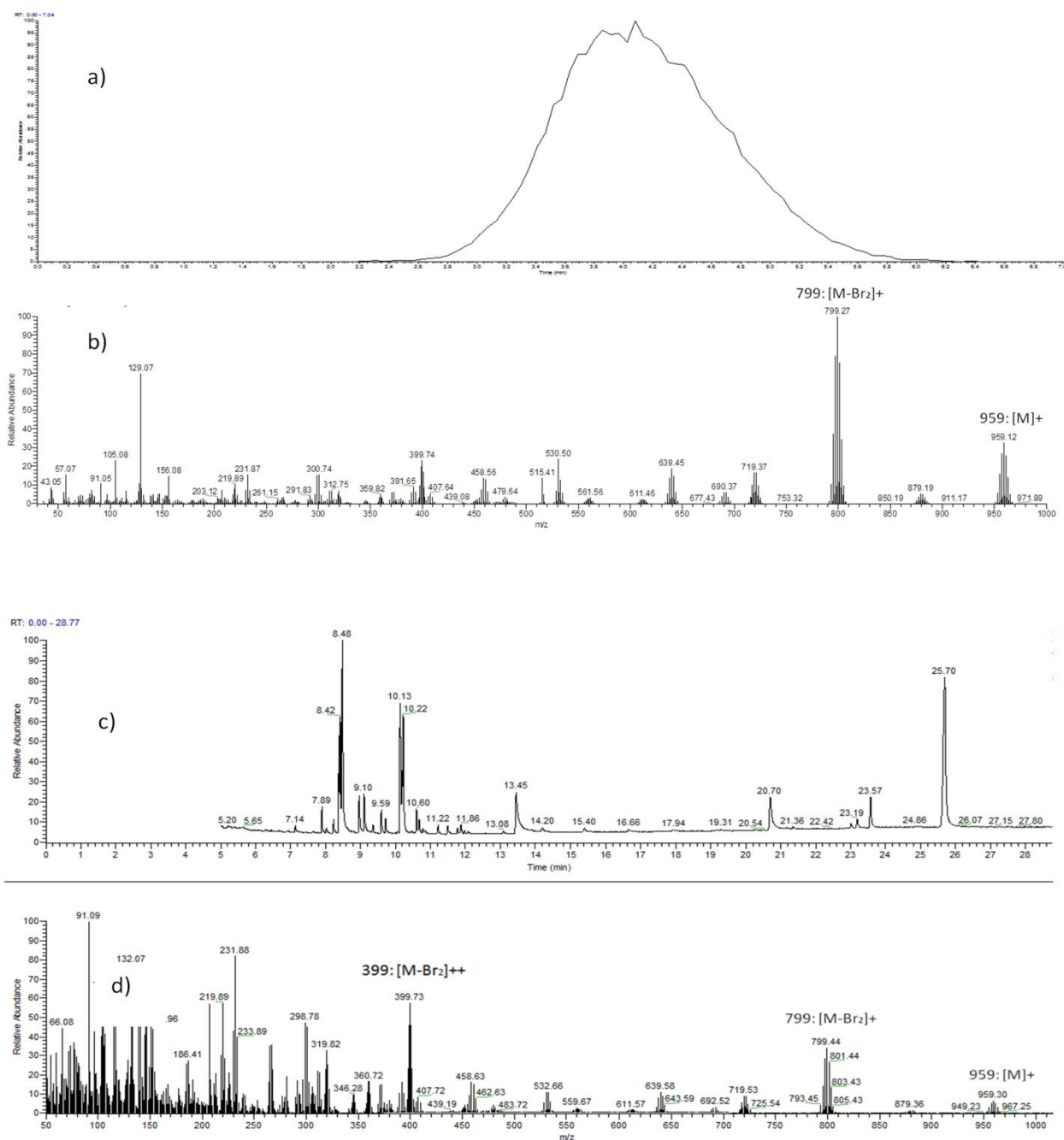
Figure 3-5 TIC for the same RM (ABS with 0.5% BDE209) obtained with a) DIP-HRMS, c) GC-MS. Mass spectra obtained with b) DIP-HRMS (selected over the entire time signal for m/z 799; 959), and d) GC-MS (selected over the chromatographic peak RT:25.70, corresponding to BDE-209)

3.3 Semi-quantitative study on tri- to deca-BDEs and deca-BB using multi-component standards

In the ERM certificate one of the laboratories used a solid sampling technique, ion-attachment mass spectrometry (IA-MS). In the IA-MS, sample (almost 1 mg) without pre-treatment is introduced and heated directly, and then the evaporated BFRs are determined by mass spectrometry.

The 5 point matrix-matched calibration performed in the study illustrated above was possible because ad-hoc RMs with the same base polymer (ABS) and different concentrations of BDE-209 were created allowing for a calibration procedure that correlates the signal intensity of each RM measured in the same sample size versus its reference concentration. The downside of this approach is that multiple RMs for each polymer type will have to be created at different calibration levels in order to build matrix- matched calibration curves for the most common polymers and BFRs. At the time of this study such an array of RMs is not available, but two types of European Reference Materials produced by the Institute for Reference Materials and Measurements exist. These are polyethylene (PE) and polypropylene (PP) based reference materials (respectively ERM-EC590 and ERM-EC591) loaded with known (to a level of confidence of about 95%) concentrations of polybrominated diphenyl ethers (PBDEs) and decabrominated biphenyl; Table 3 5 shows the certified values for tri- to decaBDE in polymeric matrices, while Table 3 6 shows the nominal concentrations of commercial mixes added to the Solid Reference Material used in this study.

Table 3-5 Certified concentrations of tri to deca-BDE in polymeric solid reference material ERM-EC590 and ERM-EC591

	ERM-EC590 [g/kg]	ERM-EC591 [g/kg]
Br	2.13 ± 0.09	2.08 ± 0.07
2,4,4'-TriBDE (BDE-28)		0.0025 ± 0.0006
2,2',4,4'-TetraBDE (BDE-47)	0.23 ± 0.04	0.245 ± 0.023
2,2',3,4,4'-PentaBDE (BDE-99)	0.30 ± 0.06	0.32 ± 0.04
2,2',4,4',6-PentaBDE (BDE-100)	0.063 ± 0.016	0.066 ± 0.007
2,2',4,4',5,5'-HexaBDE (BDE-153)	0.047 ± 0.012	0.044 ± 0.010
2,2',4,4',5,6'-HexaBDE (BDE-154)	0.026 ± 0.007	0.026 ± 0.006
2,2',3,4,4',5,6'-HeptaBDE (BDE-183)	0.132 ± 0.012	0.087 ± 0.008
2,2',3,3',4,4',6,6'-OctaBDE + 2,2',3, 4,4',5,6,6'-OctaBDE (BDE-197+204)	0.076 ± 0.015	0.052 ± 0.009
DecaBDE (BDE-209)	0.65 ± 0.010	0.78 ± 0.09

In addition to these, a multi component ABS based inter-laboratory standard (ILS) was available, for which the certified composition is reported in Table 2-9. These RMs have the advantage of being loaded with a suite of different BFRs, and – with the exception of HIPS (which could be assimilated to ABS for its physical properties) – cover the most used polymers for production of EEE, toys and FCA (Wäger et al., 2010). The disadvantage is that they are only present in one concentration for each plastic type. For this reason an attempt to build an alternative calibration curve, based on the absolute amount of BFR introduced instead of its concentration in the plastic was carried out. Traditionally, the calibration curve span should be created based on the parameter that is likely to vary in the unknown samples and the instrument response this variation causes; for example different plastic samples are likely to have different concentrations (i.e. the ratio between the amount of dissolved analyte - BFRs in this case- and the polymer, which acts as the solvent) of BFRs in them, to measure this

concentration it is necessary to compare the instrument response given by a known amount of

BFRs in plastic (standard material) to the instrument response in the sample. The calibration

plot must account for the variations in the ratio between analyte and matrix (the weight of the

sample being kept the same).

Table 3-6 Nominal concentration of commercial mixes added to PP and PE to prepare ERM-EC590 and ERM-EC591

	ERM-EC590	ERM-EC591
Matrix	Polyethylene	Polypropylene
Additives	none	Ca-stearate, Irgafos 1638, Irganox 1010
technical Penta-BDE	0.7 g/kg	0.7 g/kg
technical Octa-BDE	0.25 g/kg	0.20 g/kg
technical Deca-BDE	0.7 g/kg	0.7 g/kg
Sb_2O_3	0.8 g/kg	0.8 g/kg

Instead, it is hypothesised that the calibration line can be built by varying the total weight of

the standard, but keeping the ratio of PBDE:polymer the same. In theory this calibration would

only be useful in an experiment where the "unknown" in the sample is not the PBDE

concentration, but the total weight of the sample. Nonetheless the hypothesis is that this

calibration can be used for this particular technique assuming that the vapour pressure

lowering is only colligative to the polymer (i.e. concentration-dependent and not compound-

dependent) for non-volatile solutes (i.e. when non-volatile substances are mixed in the

polymer) where the solute presence in the gas phase is negligible. This means that the more

non-volatile solute is added to the polymer, the less volatile the polymer will be. In case of

plastic samples containing PBDEs, where the solute is volatile, the vapour pressure is given by a

combination of the vapour pressures of both the polymer and the PBDEs and therefore the PBDEs' presence in the gas phase is non-negligible. This means that if a BFR that is more volatile (higher vapour pressure) than the polymer is added, the obtained mixture (polymer plus BFR) will evaporate more than the pure polymer. The hypothesis is that the proposed calibration, although in principle not wholly correct, can be used for practical purposes as the sampling technique - thermal desorption- relies on the vapour pressure above the solution (melted polymer plus BFRs) which is bound to change because of a) changes in the concentration of BFRs in the sample b) changes in polymer weight (which given the relatively low concentrations of BFRs can be considered as changes in sample weight). If during calibration a) is kept constant and known, the changes in b) can be used to simulate the instrument response for changes in a) and build a calibration curve; after this, when measuring the actual samples, b) will be kept known and constant (weight of the sample) so that a) can be calculated. This principle is only applicable because the absolute amount of polymer does not change significantly the fugacity of the PBDEs in the polymer-plus-PBDEs mixture, due to its relatively low vapour pressure. What follows is a brief report of a calibration approach based on weight increments instead of concentration increments.

3.4 Feasibility study

First of all it is important to investigate whether the previously stated hypothesis is correct – i.e. that in a thermal desorption sampling, changes in concentration of PBDEs in plastic ($w_{PBDE}/w_{Polymer}$) produce a similar instrument response to changes in total amounts of sample

(W_{PBDE}): within a certain concentration range the PBDEs signal is only dependent on the absolute amount of PBDEs in the crucible regardless of its proportion to the polymer they are dispersed in. For it to be true, the response factor (slope of the calibration curve) to the absolute amount of BDE-209 in the sample should be the same for both calibration approaches: i.e. whether the different calibration levels are obtained by varying the total sample weight (the absolute amount of BDE-209 in the crucible increases but its proportion to the matrix stays constant) or by using the same aliquot for each level, but changing the RM to use different concentrations of BDE-209 (the absolute amount of BDE-209 increases and its proportion to the matrix increases as well). To test this, 5 ABS-based RMs loaded with 5 concentrations of BDE-209 were loaded in the sampling probe keeping the sample size constant (but not the concentration). This provided a "traditional" calibration curve. Subsequently increasing sample sizes of ERM-EC590, ERM-EC591 and ILS were then loaded and analysed. For both set-ups the absolute amount of BDE-209 present in the sampling crucible was calculated. The signal intensity for BDE-209 was then normalised in order to compare the slopes obtained with the two different calibration approaches. Results are plotted together in Figure 3-6.

3.5   Discussion

For ABS-based polymers the calibration curve obtained with concentration increments (RMs loaded with different concentrations of BDE-209) has virtually the same slope as the calibration plot obtained with sample weight increments (ILS). This is supported by the fact that the vapour

123

pressure of BDE-209 is not colligative (dependent on the molar concentration in a polymer), therefore - as long as the same polymer (solvent) is analysed - the absolute weight of BDE-209 (solute) can be used to build a calibration curve based on a thermal desorption process, assuming that the relationship between exposed surface and total mass does not vary dramatically with different amounts of polymer: this is a valid assumption because the crucible used has a much higher capacity than any sample volume, and before volatilization the plastic liquefies coating the crucible's walls and increasing the surface area prone to evaporation. As this holds for BDE-209 notwithstanding its low volatility, we can reasonably assume it will still stand for PBDEs that have lower molecular weight and hence higher volatility. No matter which approach is followed for calibration, the intensity will be correlated with the same response factor to the absolute weight of BDE-209 in the crucible.
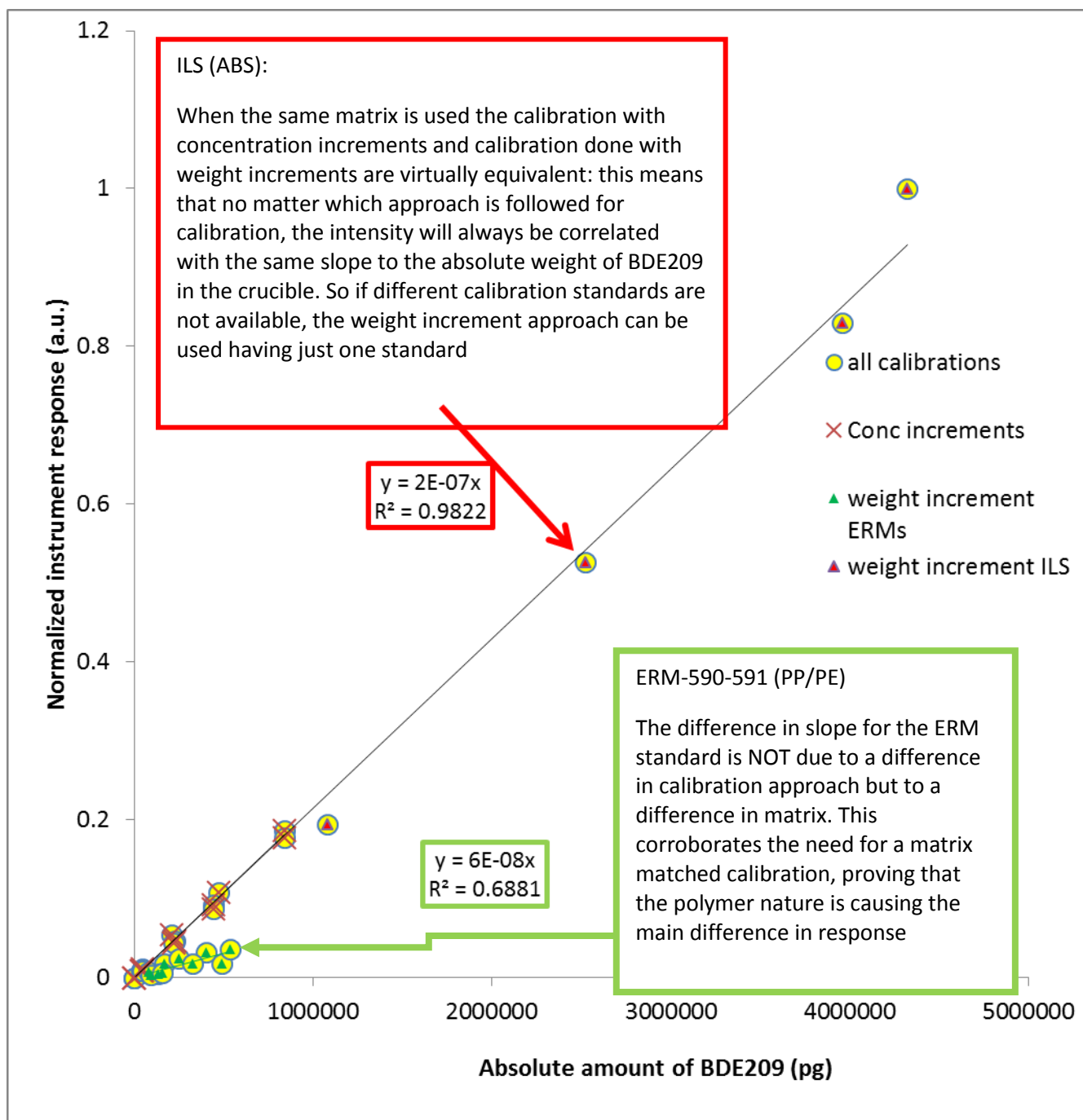
Figure 3-6 Combination of 3 calibrations: 1) standard calibration performed using a set of ABS RMs with increasing concentrations of BDE209 dissolved in them (the sample weight is kept constant) 2) test calibration performed using two reference materials ERM590 and ERM591 made respectively of PP and PE and varying the sample weight (the concentration is virtually the same for both ERM) 3) test calibration performed with one RM (ILS) made of ABS, varying the sample weight (the concentration stays constant as the same material is used in different aliquots)

So if different concentration levels of the same polymer standard are not available, the weight increment approach can be used having just one standard analysed in different sample sizes. For PP/PE the difference in slope for the ERM standard is not due to a difference in calibration approach but to a difference in matrix (solvent). This corroborates the need for a matrix matched calibration, proving that the nature of the polymer is the main cause for differences in response factor. This experiment was carried out keeping the solute (BDE-209) constant but varying the solvent (ABS, PE, PP) and observing that the response factor depends mainly on the nature of the polymer instead of the molar fraction of BDE-209. It is to be expected that keeping the polymer the same, different BFRs will have different evaporation rates due to the specific pressure (or more appropriately fugacity, as these high molecular weight compounds deviate from the behaviour of an ideal gas) of the different BFRs contained in the same sample. To observe this behaviour the following experiment was set up. For each RM (ERM-EC590, ERM-EC591), samples were prepared weighing different aliquots in a range spanning from 100 to 800 µg of RM. The response factor was calculated as the coefficient a in a simple y=ax equation, where y is the raw signal and x is the reference concentration in the SRM. This factor can be expressed as the combination of different effects arising from both the sample introduction method (e.g. active surface vs. concentration, fugacity, boiling point vs. degradation temperature…), and the ionisation source (e.g. first ionisation potential, electron collision cross-sectional area, sample density, molecular weight…). Furthermore, if the coefficient a for the same PBDE but in different polymeric matrices (PE and PP) is compared, the difference between PP and PE, can be ascribed merely to the matrix effect of the polymer on the evaporation of the sample. This difference was, for the four classes of PBDE observed in

126

this experiment, always below 10%, with a slightly higher average for PE (Table 3-7). This fits

with the difference in melting point of PP (130 to 171 °C) and of PE (115–135 °C): as PE is the

lower melting polymer, it will release the dispersed BDEs more easily and with less thermal

decomposition than PP.

Table 3-7 Response factors for tetra-, penta, hexa and decaBDE congener classes in the two ERMs			
	ERM591 (PP)	**ERM590 (PE)**	**RSD%**
tetraBDE	6.4	6.8	4.3
pentaBDE	6.9	6.8	1.0
hexaBDE	42.3	46.2	6.2
decaBDE	2.3	2.3	0.3

3.6 Conclusions

The method reported here represents a rapid, accurate way of performing compound specific

quantification of BDE-209 in polymers that avoids completely the labour intensive, time

consuming preparation of the samples. Because of the conveniently small sample size required

for our analysis (0.045 mg), this virtually non-destructive method is designed to be used on

articles still in use as domestic appliances (therefore allowing application in studies requiring

identification of putative source items in human exposure studies) as well as waste items. With

a linear range covering a concentration span of 19,000 mg kg^{-1} which for new and recycled plastics represents the full range of detected concentrations (a considerable improvement with respect to a recent DEP study (Jung et al., 2009) where the calibration span was from 0.5 to 16 mg kg^{-1}) this technique can be a valid, easier, alternative to existing analytical methods for monitoring RoHS compliance in consumer goods. These articles belong now to a second and third generation of recycling; and thus contain lower concentrations of BFRs (compared to the concentrations of the intentionally added BFRs in older items) as the contaminated polymeric fractions have been mixed with new polymers (Gallen et al., 2014).

This is illustrated by a recent study where a direct injection probe coupled with a HR-TOF-MS was used to screen BFRs in plastics, in which the concentration of FRs in the analysed samples never exceeded 1.6% in WEEE items (Ballesteros-Gómez et al., 2013). Our method is tested here for BDE-209 in ABS as a proof of concept, but given suitable solid RMs, quantification of lower brominated compounds in other polymers and over wider calibration ranges should be feasible. DIP-MS optimised for PBDEs in plastics is able to give results that are as accurate as GC-MS (Ionas et al., 2014) but are at least 50 times faster to achieve. Considering the burgeoning need for quantification of BFRs in waste samples [IEC 62321], we believe our method will be of significant value.

3.7   Future developments

This solid sampling technique has the advantage of being completely solvent-free and hence a "greener" alternative to techniques that involve sample preparation. It would be desirable – in order to make it routinely available – to have a more complete set of solid reference materials that represents 3 of the most widely used FRs (the Penta-BDE, Octa-BDE and Deca-BDE commercial mixtures) in their respectively most commonly used polymers (mainly ABS, PS, and PP/PE). The resources required for production of such suitable reference materials for matrix-matched calibrations with this method would be significantly less than the multitude of sample preparation steps this technique would render redundant.

4 Feasibility study for Rapid Analysis of Brominated Flame Retardants in Polymers with DART-Orbitrap HRAM.

4.1 Synopsis

This chapter reports a feasibility study that explored the capabilities of Direct Analysis in Real Time (DART) system coupled to a Q Exactive™ Focus mass spectrometer to accurately perform compound specific BFRs in polymers without sample preparation. Such a method, suitable for high throughput sampling, capable of unequivocally identifying and quantifying BFRs in solid samples with virtually no waiting time would be highly desirable.

Compound specific analysis of BFRs is achieved under ambient conditions with no chromatographic separation. Linear proportionality is observed between signal intensities and reference concentrations in a Standard Reference Material (SRM).

4.2 Working principle

This technique is able to perform ambient desorption ionisation coupled with a high-resolution accurate-mass (HR/AM) Q Exactive™ Focus mass spectrometer using Orbitrap technology (i.e. an ion-trap mass analyser). The Q Exactive™ Focus achieves a 70,000 FWHM resolving power at m/z 200 and a mass accuracy of <3 ppm by external calibration. The combination of high

resolving power and high mass accuracy is used to compensate for the lack of chromatographic

separation thus allowing direct high-throughput sample analysis.

The DART source has similar working principles to atmospheric pressure chemical ionization

(APCI); a cold plasma (metastable He/N$_2$) reacts with oxygen and water molecules in air,

creating reactive multimolecular ions (labelled as metastables in Figure 4-1) which are directed

towards the solid sample surface (indicated with a red arrow) to ionise the analytes evaporated

from the sample (red dots in Figure 4-1). The ions produced in this manner are analysed in full

scan mode (blue arrow pointing towards MS) following transmission by a heated capillary,

through the Stack-ring ion guide lens (s-lens), filtered by a quadrupole mass filter based on the

selected mass range, and detected in the Orbitrap mass analyser.
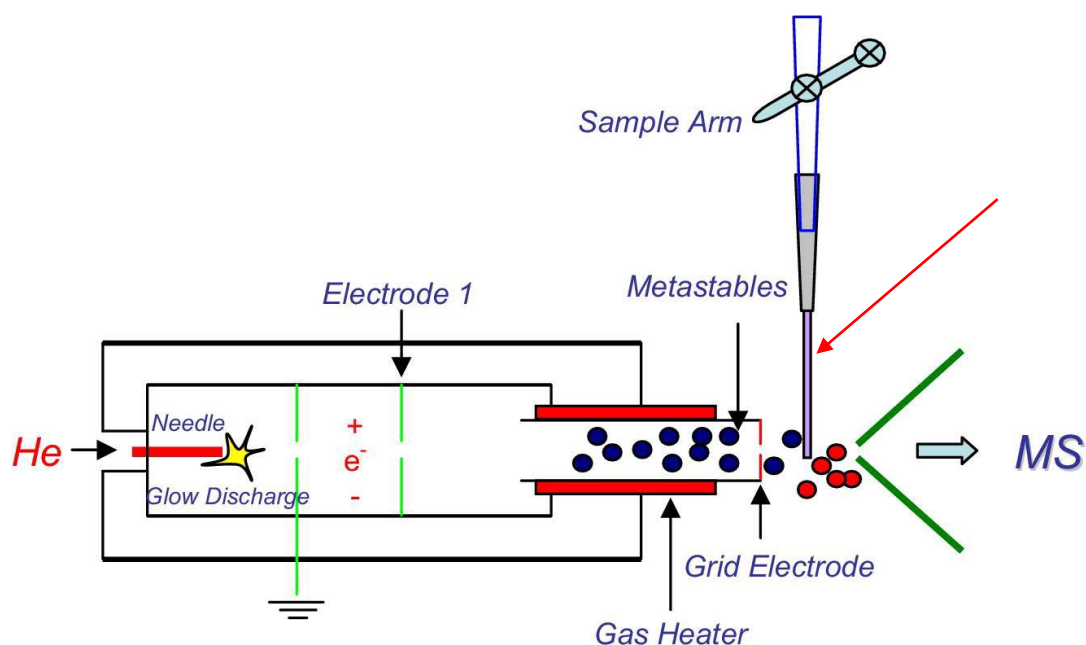
Figure 4-1 Experimental set-up of the DART-Orbitrap apparatus. The red arrow points at

the solid sample.

To obtain higher mass resolution, a longer transient time and a lower scan speed are needed in the Orbitrap. When for example liquid chromatography is coupled to the Orbitrap, the choice of scan speed is limited by the duration of chromatographic peaks. In contrast, as DART produces a continuous flow of analyte to the detector, it is possible to slow down the scan speed and acquire for a longer time to increase the number of microscans or perform averaging via software to acquire high resolution spectra and improve signal-to-noise (S/N) without time-penalty.

4.3   Materials and methods

For optimisation purposes, solid reference materials (SRM) made of acrylonitrile butadiene styrene (ABS) were produced by homogenising different concentrations of decabromodiphenyl ether BDE-209 in the polymeric matrix. In total, nine SRM were created covering a BDE-209 concentration range of 0.1% to 15%.

Samples were ionised using a DART ion source Time (DART, IonSense Inc., Massachusetts) (Cody et al., 2005) and analysed on a Thermo Scientific™ Q Exactive™ Focus mass spectrometer. The DART was operated in negative ion mode at 350 ˚C with nitrogen as the carrier gas. The gap between the inlet and the DART apparatus was 1 cm. Samples were introduced manually by holding the plastic sample between the cold plasma jet and the detector inlet. After a preliminary test, it was observed that using helium as a collision gas (cold plasma) causes stronger fragmentation, because of the high first ionisation potential (24.6 eV) limiting the

possibility of seeing the parent ions of the higher brominated PBDEs. For this reason nitrogen (with a first ionisation potential of 14.5 eV) was used, providing a "softer" fragmentation.

The mass spectrometer was operated in negative ion mode; the full scan mass range was set to 70-1,050 during the preliminary phases of the method optimisation, and then set to 700-1,050 (range where the majority of product ions were formed) to improve selectivity, sensitivity and signal-to-noise (S/N). Spectra were recorded with a resolution setting of 70,000 at m/z 200. Source parameters such as the collision gas, the S-lens RF level (this is the RF amplitude calculated based on the first mass in the scan range) and capillary temperature on the Q Exactive Focus mass spectrometer were optimised for these samples. Fragmentation patterns were simulated using the Mass Frontier 7.0 software and used to identify daughter ions. Evaluation of Total Ion Current and mass spectra was performed using Qual browser in Xcalibur 2.2 SP1.48. Descriptive statistics evaluation was performed using Microsoft Excel 2007. The S-lens RF level, capillary temperature, and auxiliary gas heater temperature were optimised to the respective values of 12, 350 ˚C, and 30 ˚C. The optimal capillary temperature was the same as the optimal DART source temperature, considering evaporation efficiency and thus transmission of the target analyte.

4.4 Optimisation of the DART source (source/front end settings)

4.4.1 Source temperature Profile

Since the vapour pressure of the molecule forming the sample can differ considerably, depending on the polymer type and on the inorganic fillers and additives inside the polymer; it is important to build a temperature profile for each matrix analysed in order to account for matrix effects. This was achieved by placing the sample in front of the DART source and ramping the gas temperature for about 15 seconds for every step on difference positions from 150 ˚C, in steps of 50 ˚C, up to 450 ˚C. These experiments were performed using an ad hoc plastic reference material made of ABS homogenised with 7% wt. of BDE-209. It is possible that in one material the ion abundance of the observed analyte reaches a maximum at a different temperature to another material even though it is the same chemical; this is because different components of the plastic might act to create a matrix effect when desorbed simultaneously with the chemical of interest. For this reason, the same procedure should be repeated with different reference materials to "matrix match" the sample. The total ion current (TIC) and the relative intensity of Br isotopes (Figure 4-2) are used as a measure of – respectively – the total intensity of the signal and the degree of fragmentation, the bottom panel of Figure 4-2 is an ion map over the mass range of Br stable isotopes . The gas temperature increases not only the level of fragmentation (Figure 4-3) but also the intensity of the parent ion (BDE-209) (Figure 4-4, the bottom panel is an ion map of the complete scanned mass range) which did not follow linearly the increase in Br isotopes concentration: this is because certain de-bromination

reactions are favoured towards other depending from the parent ion. After evaluation, the

most suitable gas temperature for this matrix proved to be 350 ˚C.
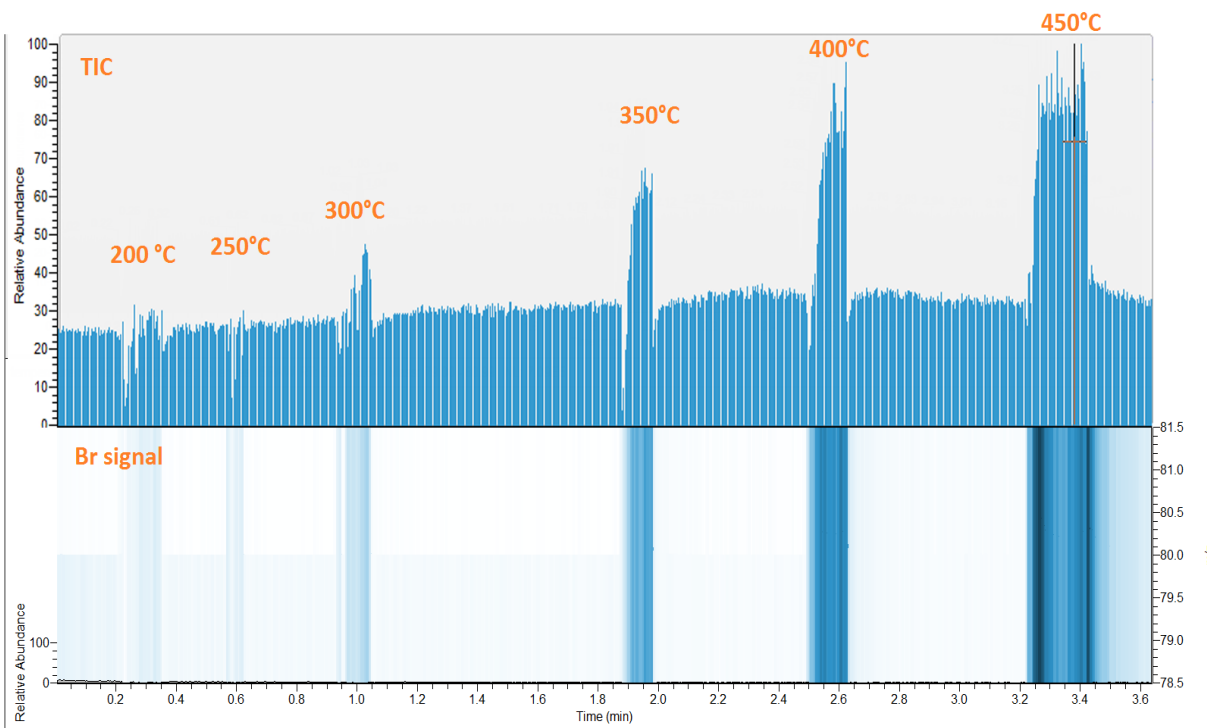
Figure 4-2 Fragmentation degree vs. total signal intensity. Upper window showing the TIC signal acquired during the temperature profile experiment. Lower window shows (with matching time axis) an ion map of the two Br isotopes: it is possible to see an increase in relative abundance corresponding to the increase in the source temperature.
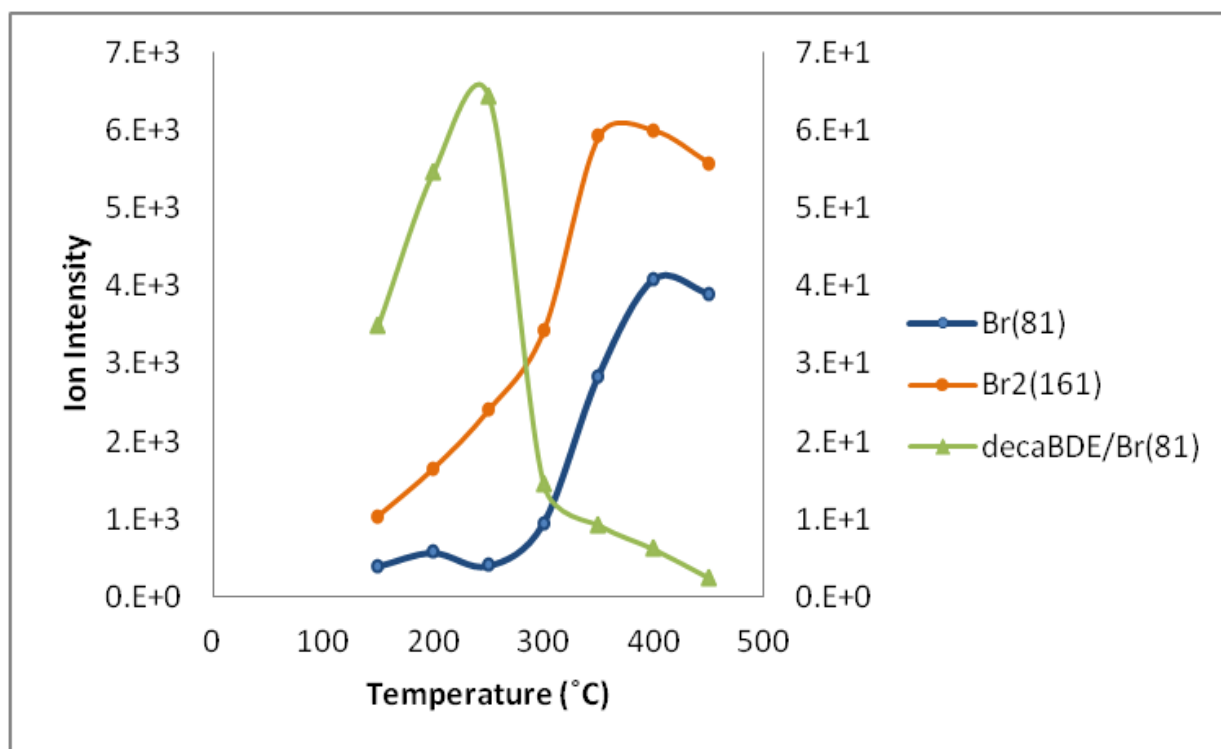
Figure 4-3 Atomic and molecular Br signal intensity with varying gas temperature. Decomposition of decaBDE follows a quasi-exponential behaviour with temperature increase, reaching a plateau after 350˚C. The green trace represents the ratio between decaBDE and atomic Br, showing that the Br (atomic and molecular) are coming from the decomposition of the parent ion.

Decomposition of BDE-209 occurs at a very similar temperature to its boiling point, which causes it to thermally degrade during analysis. For this study, the temperature profile is designed for BDE-209 inside an ABS matrix, to find the best compromise between the amount of analyte released by the heat applied on the surface of the ABS polymer, and possible decomposition to other compounds (which results in a drop of signal intensity of the BDE-209 in favour of lower brominated compounds). To do so, data were acquired at different source (DART) temperatures and the resulting spectra evaluated. BDE-209 signals and atomic Br were identified by observing the isotope pattern of Br and their ratio evaluated as a rough measure

of the degree of decomposition (when the temperature is too high, the BDE-209 signal

decreases and the free Br signal increases). Our results show that at source temperatures below

200 ˚C, BDE-209 is not observed (because not enough analyte is evaporated), while above 350

˚C, thermal decomposition of the compound of interest is experienced. The optimum was found

to be at 350˚C.
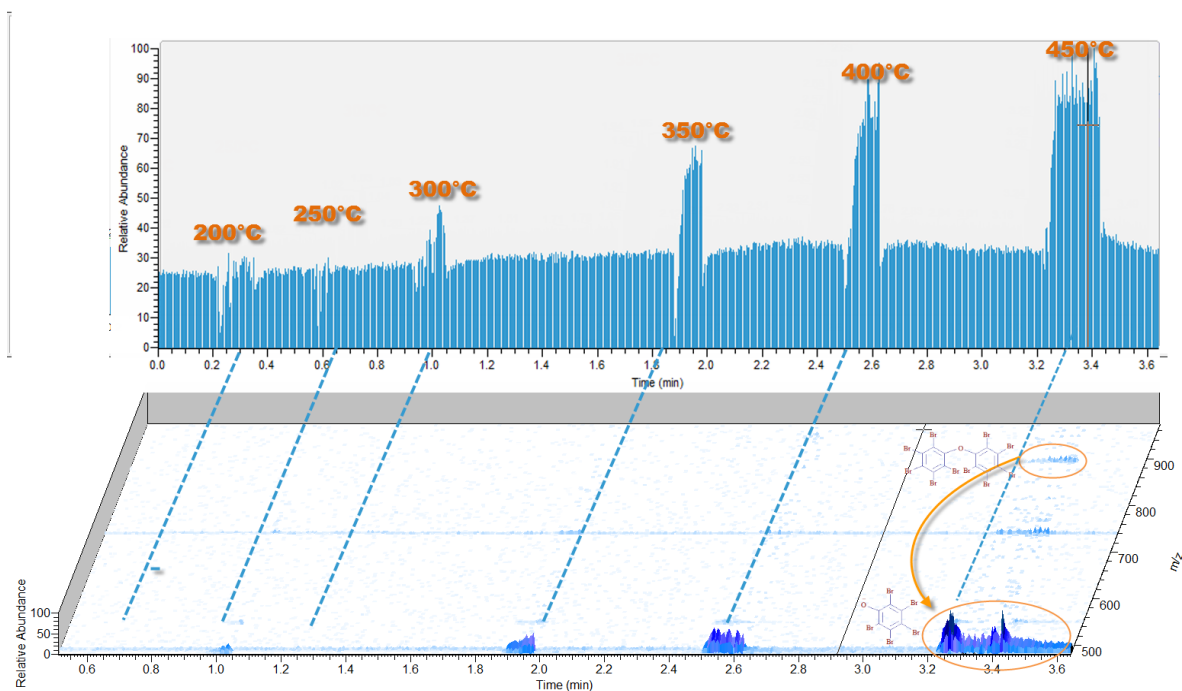
Figure 4-4 Fragmentation pattern vs. gas temperature. Ion map of the temperature profile experiment. Fragmentation of the parent ion (m/z 959.1676) into pentabromo phenate, characterised by producing the fragmentation pattern for APCI and calculating the de-protonated accurate mass of the daughter ion (m/z/ 486.58306)

4.4.2 Optimisation of ion transmission

The S-Lenses RF level has an impact on the mass of the transmitted ions, higher values (80-100) are used for biological molecules (in the order of thousands amu) and lower values are better for smaller molecules. The capillary temperature does not only influence the fragmentation degree, but also the kinetic energy of the ions passing through it, therefore capillary temperature and the S-lens value for this inlet system tend to be interdependent.

The optimisation was carried out as follows:

- One pellet of the high-concentration solid reference materials (7% BDE-209) was held with a pair of tweezers

- The software FreeStyle was set to acquire online the signal coming from the MS

- The s-lens RF level and the capillary temperature were varied one at a time over their complete setting span, in steps of 10% of the total span

- For each setting and each value a spectrum was collected

- The optimal settings were selected judging on total intensity of the fragmentation ion and ratio between the highest and the second highest m/z ion intensity.

Starting with the assumption that a lower capillary temperature is the best choice to be able to monitor higher brominated BDEs, the S-lens value was tuned to obtain maximum ion transmission. Looking at the transmission efficiency for different S-lens values it is shown that

for lower S-lens values (Figure 4-5), the transmission for the higher masses (parent BDE-209)

appears to be better than for the most intense fragmentation ion (pentabromophenate).

Setting the S-lens at a higher value (Figure 4-6), results in the transmission of the fragmentation

ion being better than that of the parent ion. This is opposite to the usual effect of the S-lens.

The reason for this might be a dependence on the low capillary temperature. With these

settings it was possible to identify BDE-209 as a parent ion unambiguously with the use of

isotopic pattern recognition and accurate mass determination (Figure 4-7 and Figure 4-8).

Upon evaluation of the mass spectra the following observations can be made:

- The fragmentation mechanisms with the DART ionisation source are different from EI

  fragmentation but in most cases they fall under the mass frontier predictions for APCI

  sources: consistent with the physical similarities between DART and APCI

- DART produces M-Br and M-2Br in broadly equal abundance

- DART produces a larger variety of ions than EI, with different bromination levels

  appearing more than once with a different number of H or O atoms

- Although one of the molecular cluster-ions (m/z 959.1676) was visible, a more intense

  signal from the M-Br and M-2Br negative ions was used for further evaluation of

  linearity between concentration and response
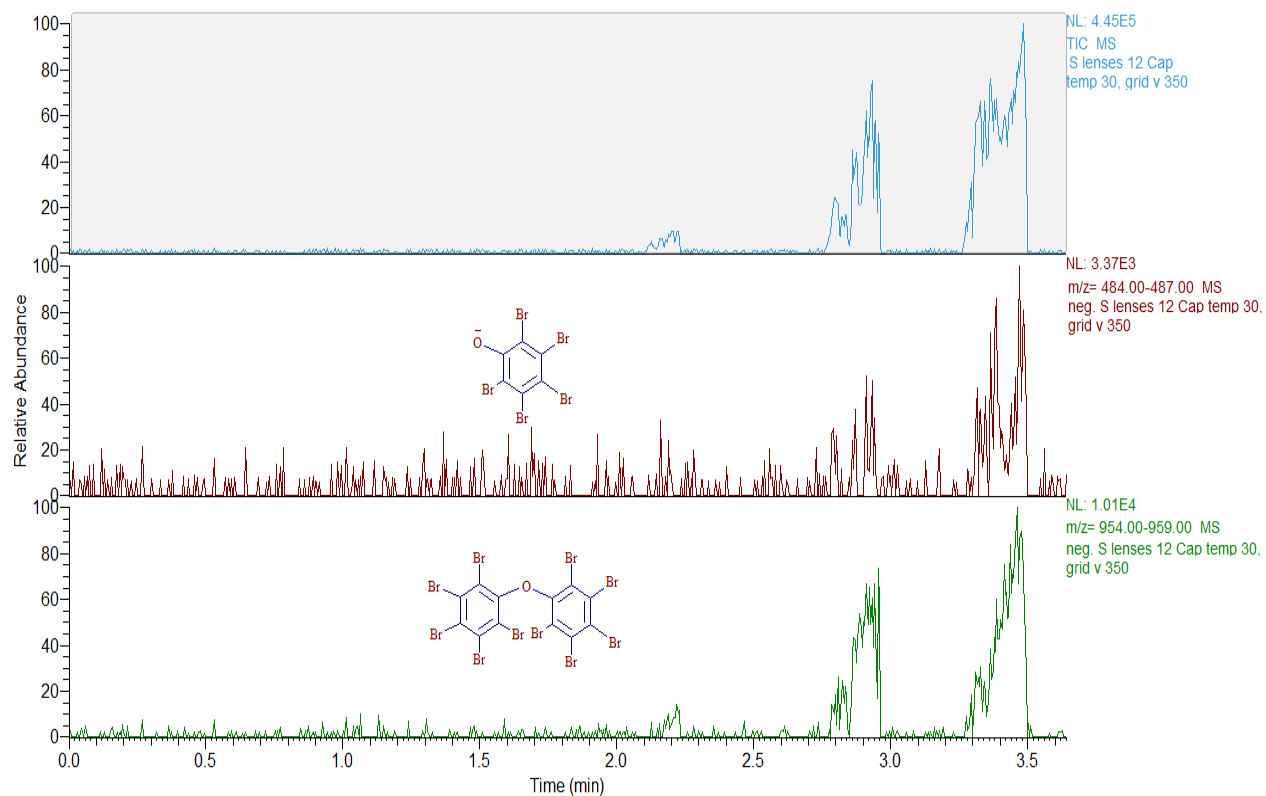
Figure 4-5 S-lens 12. Keeping the capillary temperature the same and varying only the S-lens value to 12, the transmission for the higher masses (parent decaBDE) appears to be better than for the most intense fragmentation ion (pentabromophenate). The background is also lower than for higher S-lens settings.
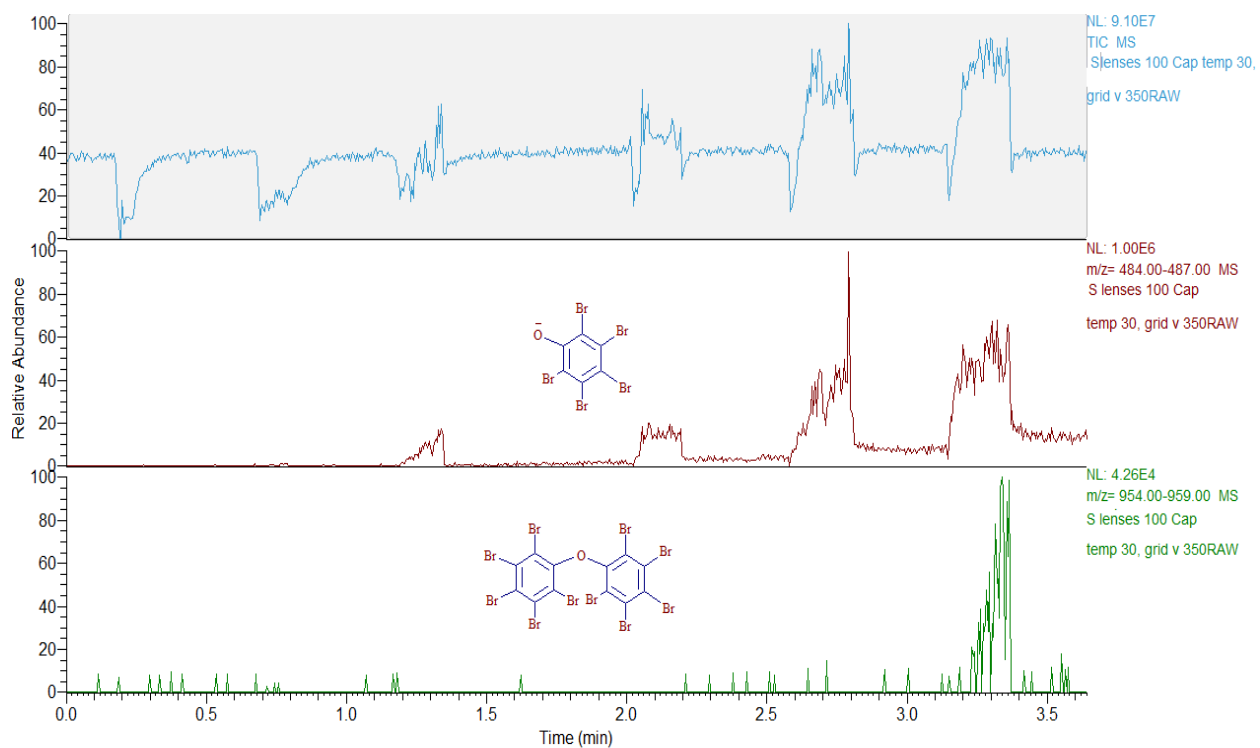
Figure 4-6 S-lens 100. Setting the S-lens at a value of 100 the transmission of the fragmentation ion is better than the parent ion.
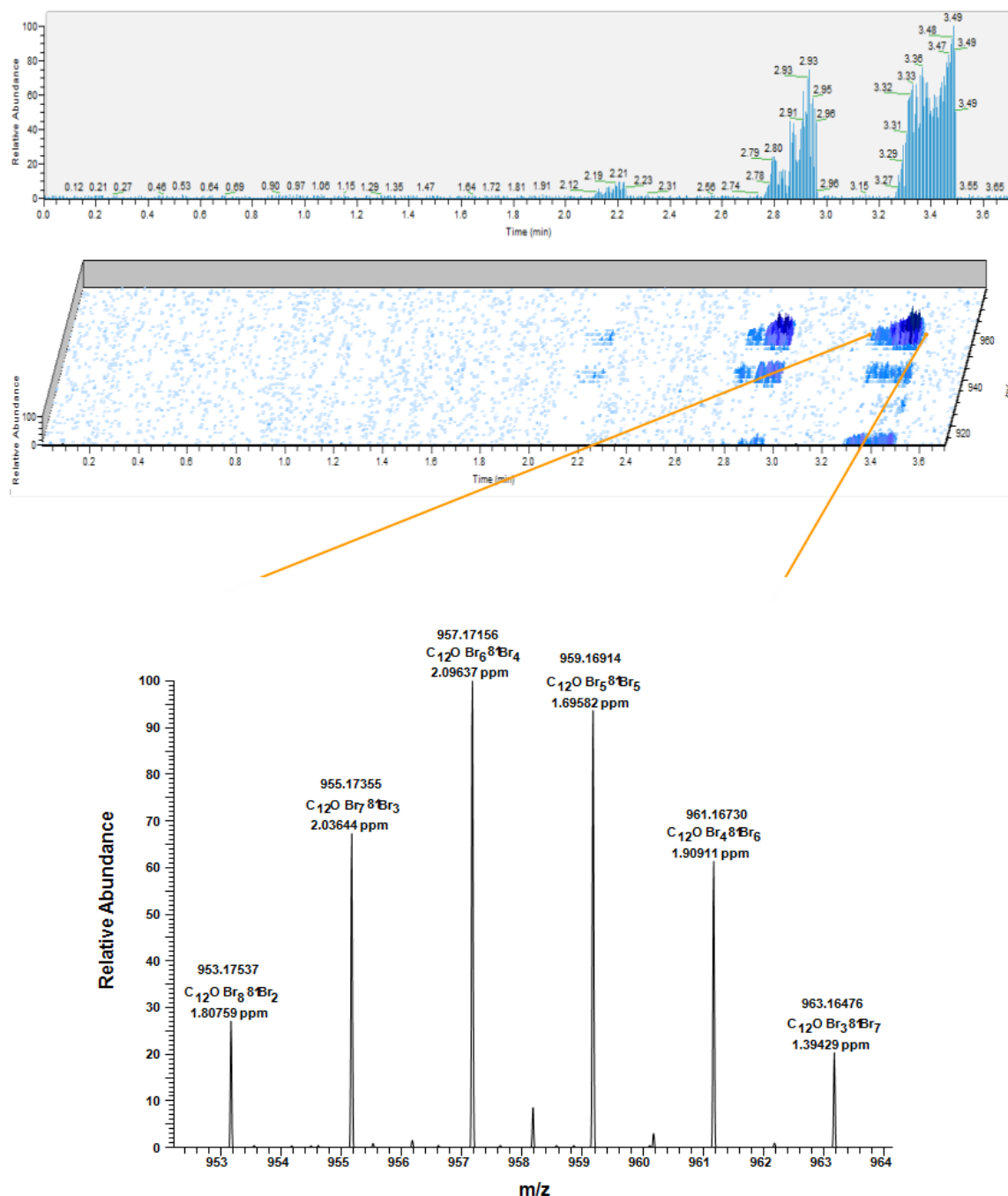
Figure 4-7 Accurate mass determination. From the top: TIC of temperature profile for the SRM built with the final instrument conditions. Ion map showing simultaneous ion signals for each temperature step. Mass spectrum recorded for decaBDE: labels under the molecular formula represent the delta value between the recorded accurate mass and the theoretical mass. A small delta (as observed in this study) is crucial for the accurate mass determination to be effective.
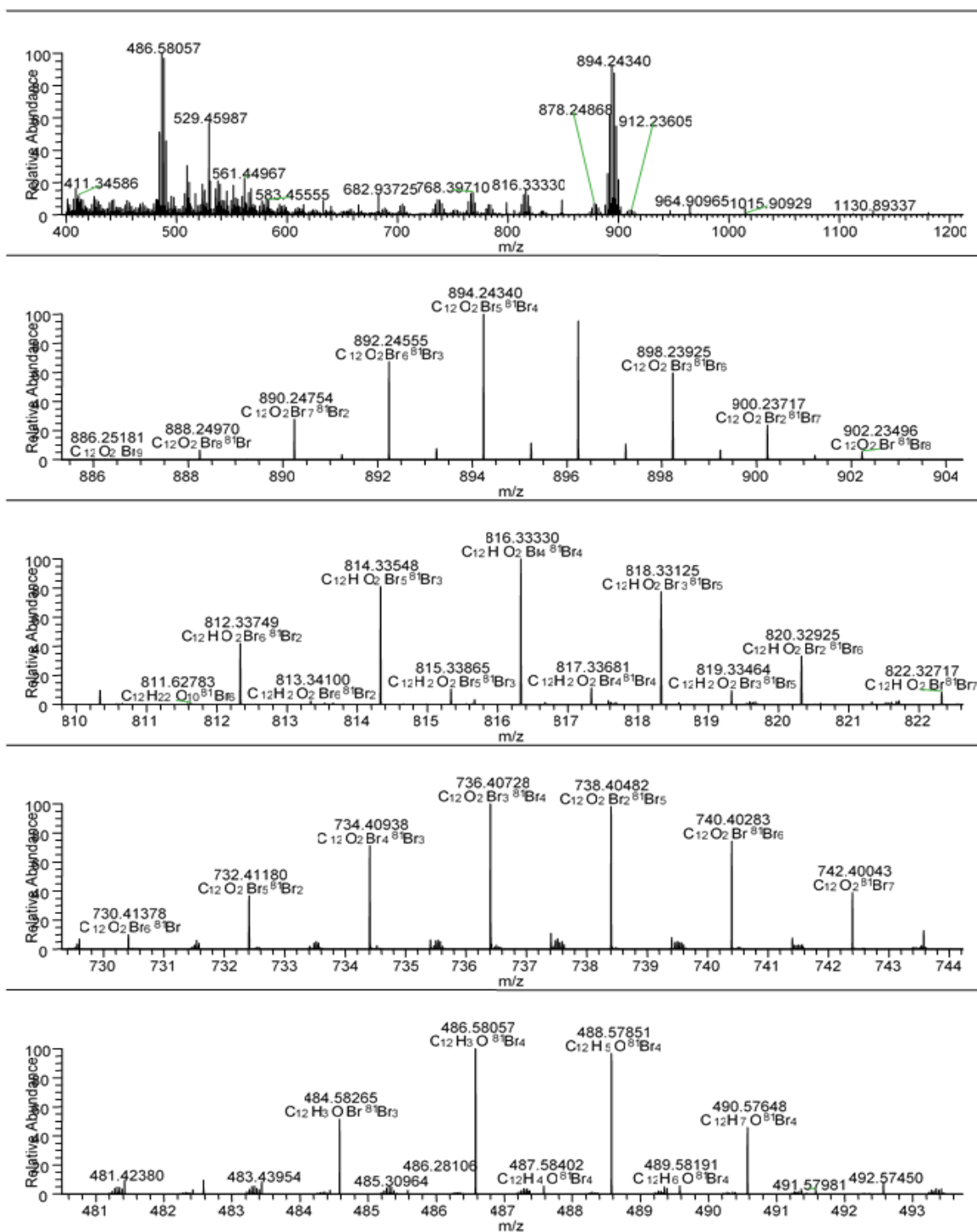
Figure 4-8 In the upper cell: mass spectrum of a reference material (7% BDE-209). In the lower cells: magnified mass spectrum over most intense ions. The elemental composition is simulated using the accurate mass search that associates the element combination of which the theoretical mass is the closest (and never larger than 140 ppm) to the measured mass
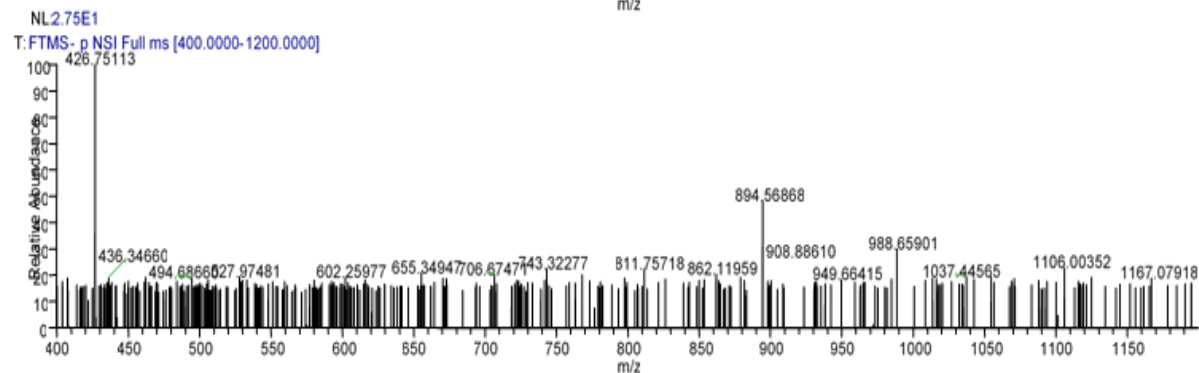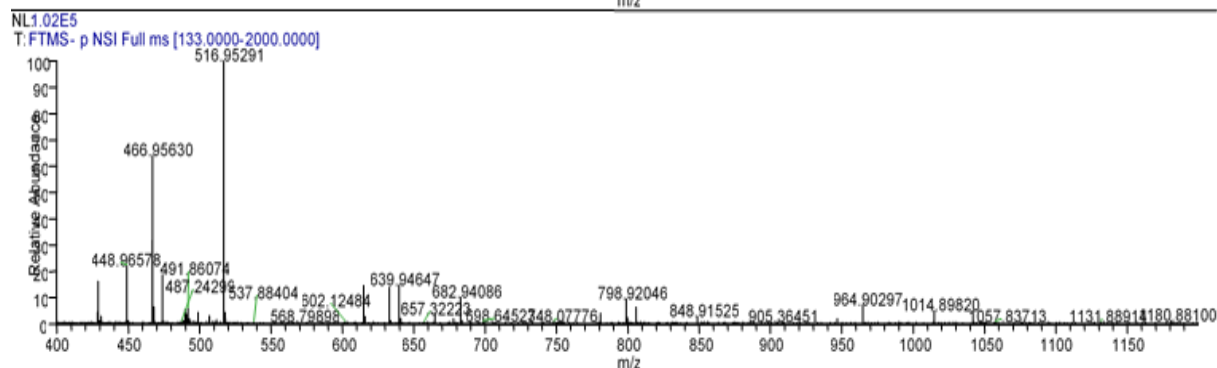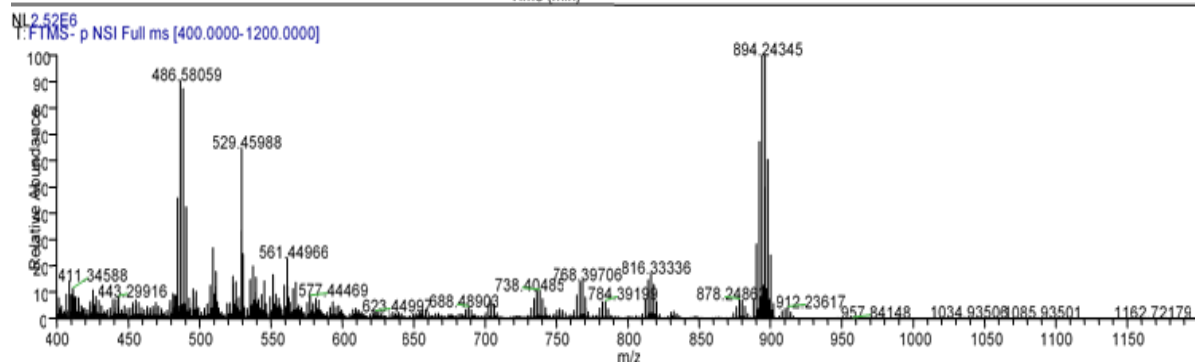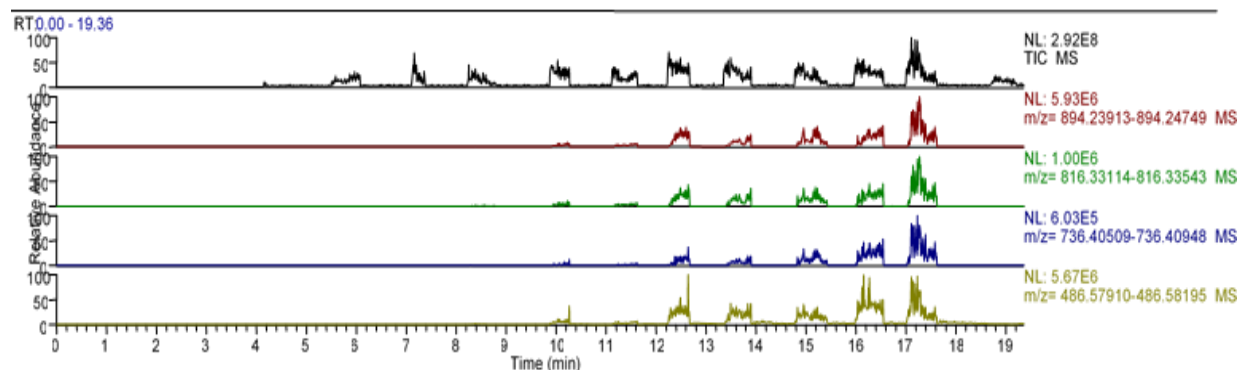
Figure 4-9 From the top cell: 1) time resolved signal for the total ion current (black trace) generated by the 9 SRM (peak 1, 2, 3 and 12 are measurements of a SRM containing 0% decaBDE); [M-Br]- ion current (bordeaux trace), [M-2Br]- ion current (green trace), [M-3Br]- ion current (navy trace), [M-4Br]- ion current (ochre trace); 2) MS spectrum in the m/z interval 400-1200 amu recorded while SRM is in front of the DART source (section 2); 3) MS spectrum in the m/z interval 133-1200 right after removing SRM from the DART source (section 3); 4) MS spectrum in the m/z interval 400-1200 right before placing SRM in front of the DART source (section 1)

- A calibration plot was made with the two most intense product ions (m/z 894.24331 and m/z 816.33330).

- To date, as this technique is still at the experimental stage, there is no automated data processing system to evaluate the DART results. In this study the intensity of the target ion was obtained by acquiring each of the nine solid RMs (0%, 0.1%, 0.5%, 1%, 2%, 3%, 7%, 10%, and 15% w/w of BDE-209) in triplicate (quickly placing and removing the sample in front of the source). Intensities were considered selecting the most intense m/z value and averaging the intensity of the time signals over the ten most intense scans in each section of the acquisition. The acquisition is divided in 3 sections corresponding to 1) the time before placing the sample in front of the source – no analyte –; 2) the time while the sample is in front of the source – analyte signal –; 3) the time after removing the sample from the source – no analyte – in Figure 4-9, top cell this procedure is recorded "on-line" with increases of ion current corresponding to the moment when the sample is placed in front of the source. A better and more efficient data elaboration is likely to benefit the quality of future data, but for the current feasibility study, this was done manually as a proof of concept.

A clear linear proportionality between reference concentration in the solid standards and signal intensity for the [M-Br]+O (m/z 894.24331) ion was visible (Figure 4-10), while for the [M-2Br]+O ion, a polynomial trend line fit the results better, this could mean that different molecules (interferences) have been targeted under this mass filter (Figure 4-11).

4.5   Conclusions

The analyte could be detected in the SRM containing BDE-209 in the lowest concentration available (0.1% w/w) in its [-Br] fragment, with a linear response obtained up to 15% BDE-209.

The plot shows Reference bde209 (% w/w) on the y-axis versus Measure signal (arbitrary units) on the x-axis. Data series labeled m/z 894.24331. Trend line equation: $y = 7\text{E-}06x + 0.0071$, $R^2 = 0.998$.
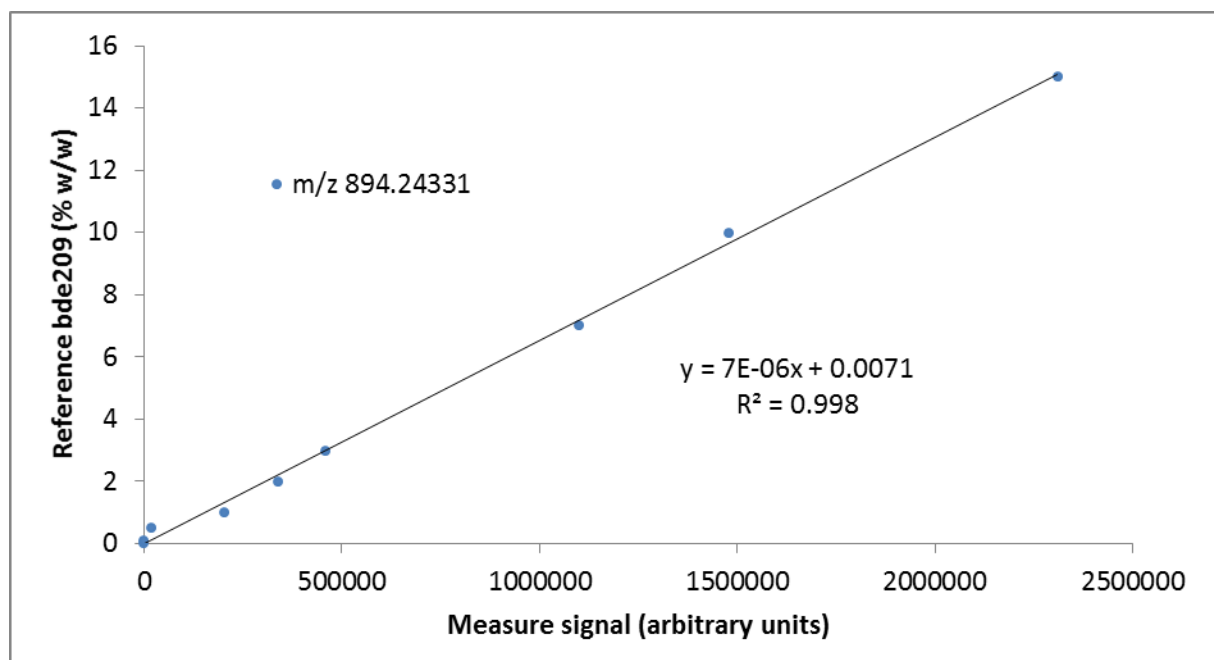
Figure 4-10 Plot of reference material concentration of m/z 894.24331 vs. relative instrument response

146
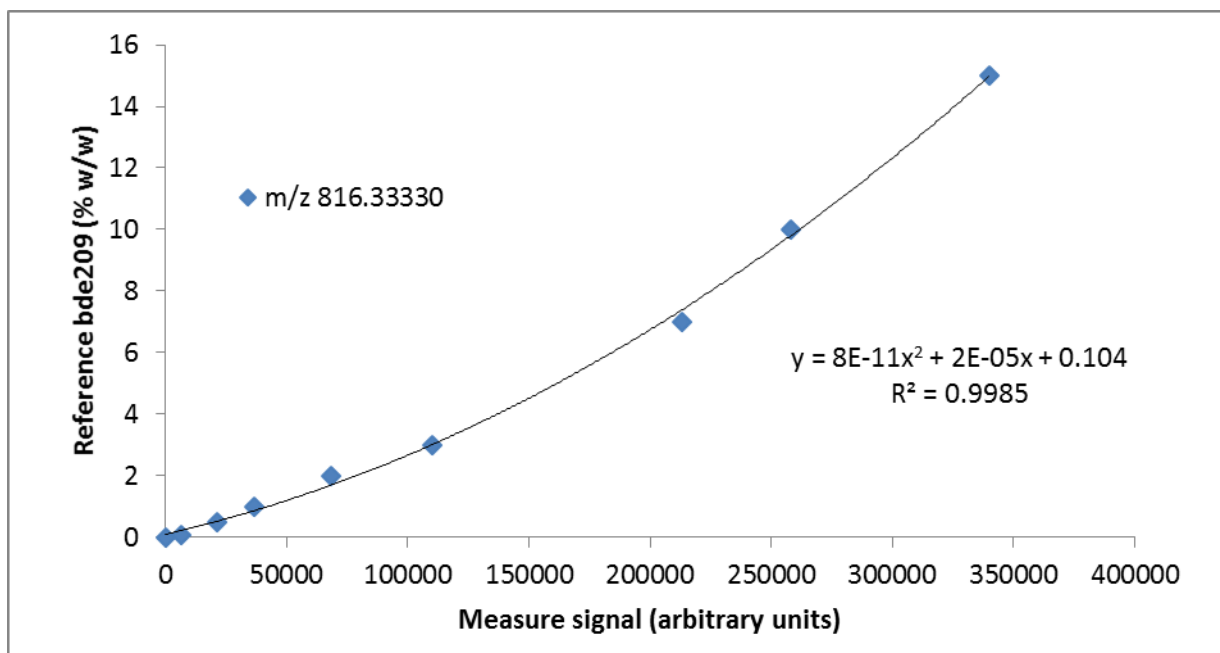
Figure 4-11 Plot of reference material concentration of m/z 816.33330 vs. relative instrument response

Performing a selective ion monitoring study in the future will most certainly improve the quality of the calibration and the sensitivity of the technique. The narrower the mass range in the full/SIM scan the better the S/N. A further development would be to design a targeted SIM method to quantify specific analytes on MS1 (first quadrupole) level or a parallel reaction monitoring (PRM) method to perform a targeted quantification on MS2 (second quadrupole) level.

Both the high mass accuracy and the 70,000 resolution appear to be sufficient for direct high throughput analysis of BFRs/PBDEs meaning it can be performed on a high resolution-accurate mass instrument coupled to a DART source without the need for chromatographic separation and sample preparation. The study of more complex samples or near isobaric analytes will most

likely benefit from the higher resolving power capabilities of other Orbitrap-based instruments. The most critical instrument and source settings are the ones related to evaporation of the analyte (capillary temperature and DART source temperature). S-lens RF level is secondary to optimal ion transmission. It should also be noted that the positioning and timing of the sample in front of the source was done manually: there are many factors that could vary the signal intensity e.g. amount of time the sample is held in front of the source, how close to the source or to the ceramic sampler the sample is, position of the sample and to what extent it is blocking the flow of ionized gases going into the analyzer, etc.… all of these can in the future be mitigated by an auto-sampler designed for this purpose. In addition to compound specific screening of PBDEs it is also feasible – given an appropriate set of standards - to develop methods for the quantification of specific congeners in polymeric matrices.

Achieving this degree of linearity and accuracy without any sample preparation and performing the analysis under ambient conditions, can be considered a promising starting point for the future exploration of this application, but more work is needed to improve reproducibility of sample introduction and standardization.

5 Development of a novel GC-ICP-MS apparatus and of a semi-quantitative method to analyse PBDEs in indoor dust

Monitum

This chapter contains some material taken verbatim from the patent P10830GB00

5.1   Introduction

In the present study, concentrations of PBDEs in indoor dust taken from offices, laboratories and meeting rooms are reported. All samples were collected in a new building, before furniture was installed and before employees populated the rooms. After 3 months of regular use of the rooms, another sampling campaign was carried out.

The objectives of this study are:

- To investigate PBDE contamination of hitherto unstudied occupational microenvironments and add to the research database on indoor dust

- To provide a comparison between PBDE contamination of dust from indoor microenvironments before and after occupation by evaluating the extent to which furniture, equipment and usage contribute to the PBDE concentrations in a microenvironment based on the variation from a "blank" reference point (initial samples from unoccupied rooms).

- To trace the origin of PBDE composition in dust and observe possible correlation with the function/use of a room.

- To evaluate the potential of GC-ICP-MS as a tool for semi-quantitative evaluation of o qualitatively evaluate the extent to which furniture, equipment and usages contribute to the relative PBDEs concentration in a microenvironment based on the variation from a "blank" (initial samples from unoccupied rooms).

A summary of the analytical methods most commonly adopted for the analysis of PBDEs in dust is reported in Table 5-1.

Table 5-1 Overview of methods for the analysis of PBDEs inn dust

Extraction Technique	Extraction solvent	Clean up	Detection
Soxhlet extraction(Gouin et al., 2006)	Acetone (Takigami et al., 2009)	Gel permeation chromatography (GPC) (Harner and Shoeib, 2002)	EI-GC-MS (Fromme et al., 2009)
Microwave-assisted extraction (MAE) (Wurl et al., 2006, de los Contaminantes and Persistentes)	Dichloromethane (Sjödin et al., 2008)	Column adsorption chromatography (Harrad et al., 2004)	GC-ECD (Wilford et al., 2008)
Ultra-sonication (Sjödin et al., 2008) (Johnson, 2008)	Toluene (Hayakawa et al., 2004)	Sulfuric acid treatment (Harrad et al., 2004)	ECNI- GC-MS (Cunha et al., 2010)
Accelerated solvent extraction			

(ASE) (Stapleton et al., 2006)	Petroleum ether (Wilford et al., 2005)		
Supercritical fluid extraction (SFE) (Covaci et al., 2003a)	Hexane/acetone (Harrad et al., 2008b)		
	Diethyl ether (Covaci et al., 2003a)		
	Hexane/dichloromethane mixtures (Harrad et al., 2004)		
	Ether/hexane mixtures Zota, A. R., Rudel, R. A., (Zota et al., 2008)		
	Hexane/diethyl ether (Rudel et al., 2003)		
	Hexane (Harrad et al., 2004, Harrad et al., 2008b)		

5.2   Collection of dust samples

Indoor dust was collected from 23 rooms. These were ten electronic engineer's laboratories, one printing room, four meeting rooms and eight offices.

A map of the planned structure of rooms and furniture was used to choose the sampling areas. The position of each sampling area was drawn on the map as a reference for the following sampling campaign. The sampling area was delimited with masking tape over a 1 m^2 square.

Figure 5-1 Set up for first sampling campaign. Brown squares are made with adhesive tape as a trace for the sampling area

The second sampling campaign was carried out 114 days after the first. Employees moved to the new offices 14-18 days after the first sampling campaign, therefore the dust sampled in the second campaign is representative of ca. 100 days of office "population".

- A Miele C3 PowerLine SGDE1 Cylinder vacuum cleaner was equipped with a cellulose-polyester 20 µm filter mounted on the last section of the vacuum nozzle: this was done to reduce the path area leading to cross contamination and simplify the between-sample cleaning. One metre of carpeted floor was traced –as a guide- with adhesive tape (Figure 5-1) and vacuumed evenly for 2 minutes according to a previously validated method (Muenhor et al., 2010, Muenhor and Harrad, 2012). After collection, samples were stored at -18 ˚C. All filters were weighed and numbered before sample collection and after sample collection, to measure the mass of dust collected (dust loading). This was done in order to be able to express the PBDEs concentrations as ng/m^2 and also to acquire additional information on the dustiness of the room that was later used to evaluate statistical correlations. Basic information was collected about each room (i.e. function of the room, number of monitors, number of people, number of sponge chairs, number of phones, number of laptops/computers, number of printers, number of windows, size of the room) to be used in the multi-component analysis of the data (Table 5-2). The data obtained in this fashion was used to evaluate between-room spatial variability and temporal variability.

Table 5-2 Room characteristics for each of the sampled rooms. EE stands for electronic engineers' rooms, O stands for offices, MR for meeting rooms and P for printer room. The size was classified as 1= small (<13m², 2=medium (<20 m²), 3=large (>20 m²)

	Room	Monitor	People	Sponge chairs	Phones	Laptops/ computers	Printers	Windows	Size
1	EE	2	2	2	2	2	0	2	2
2	EE	2	2	2	2	2	0	1	2
3	EE	2	2	2	2	2	0	2	2
4	EE	2	2	2	2	2	0	1	2
5	EE	1	1	1	1	1	0	0	1
6	EE	3	0	4	3	3	0	1	2
7	EE	1	4	4	4	4	0	1	2
8	MR	0	0	0	0	0	0	1	2
9	EE	2	2	2	2	2	0	1	2
10	EE	1	1	1	1	1	0	0	1
11	EE	2	2	2	2	2	0	1	2
12	O	4	2	3	2	2	0	1	2
13	O	1	1	1	1	1	0	0	1
14	O	5	3	4	3	5	0	1	3
15	MR	0	0	5	0	0	0	2	2
16	O	2	1	6	1	1	1	1	2
17	P	0	0	0	0	0	1	0	1
18	O	4	2	2	2	2	0	0	1
19	O	3	3	3	3	3	0	3	2
20	O	8	4	5	4	6	0	2	2
21	O	4	2	0	2	2	0	1	2
22	MR	1	0	0	1	0	0	0	2
23	MR	0	0	0	1	0	0	1	1

5.3 Extraction of dust samples

The main topic of this research work is the evaluation of fast, easy and affordable analytical methods for the screening/determination of PBDEs. Therefore a simplified extraction method was used in this study. The dust was carefully sieved through a 500 µm mesh sieve. Sub-samples of dust were accurately weighed and placed inside a 5 mL syringe. The syringe was equipped with a 200 µm PTFE pre-filter and a 45 µm PTFE filter. A known amount of hexane was pipetted

into the syringe and the plunger inserted to expel the hexane through the dust into a pre-weighed glass vial. The extract was weighed and placed in a rack. This procedure was carried out over the same day for all samples, four method blanks and different aliquots of SRM2585 and the vials stored at -18 °C. No purification or concentration was performed. The advantage of such a simplified extraction method is that it requires substantially less time than a traditional extraction (on an average it takes about 2 minutes for the extraction of a sample), it uses a fraction of the solvents and consumables and does not employ expensive isotopically labeled internal standards, nor a purification step. On the other hand, this method is suitable only for semi-quantitative screening of the PBDEs concentration in dust. A solid reference material (SRM2585 indoor dust reference material from the U.S. Department of Commerce, National Institute of Standards and Technology (NIST) was used to estimate the method accuracy (recovery) for each quantified congener and the extraction linearity over a range of extracted dust weights. This recovery factor was then applied to obtain the final results. This simplified extraction method relies on the used analytical apparatus to be effective: a GC coupled with an ICP-MS (Guzzonato et al., 2017a).

5.4 Development of an interface system for GC-ICP-MS analysis of PBDEs

This chapter provides a short description on the working principles of GC-ICP-MS, its advantages over traditional GC-MS techniques for the analysis of PBDEs and how suitable hardware was developed to successfully perform these analyses.

Gas chromatography (GC) can efficiently separate volatile (gaseous) species in accordance with their boiling point characteristics and their affinity for a stationary phase component (capillary columns with bonded phases). Species separations are performed on-line in a flow of heated gaseous mobile phase and the species are then transferred to the ICP-MS detector. These analytical systems facilitate rapid and highly sensitive analyses of elemental species and can exhibit detection limit capabilities in the ppt range. Critical components of the GC-ICP-MS system include the temperature control of transfer line between the GC and the ICP-MS and the interface to the ICP torch. The GC and heated transfer line configuration coupled with an ICP source proved to have the highest sensitivity and the lowest instrumental detection limits (compared to traditionally used techniques for this application GC–NCI MS and GC–EI MS–MS) for the determination of PBDEs in water (by means of isotope-dilution mass spectrometry using [81]Br-labelled PBDE spikes) (Gonzalez-Gago et al., 2015). The main reason for the lower detection limits of this technique resides in the way the analytes are detected and quantified. After undergoing chromatographic separation, the compounds are fed into the ICP source. Unlike EI that ionises a molecule breaking it into smaller moieties, the plasma is a high energy ion source that first atomises and then ionises the species producing a high yield of positive monoatomic ions. This aspect of the technique is crucial when it comes to analysing etheroatomic organic molecules because the quantification of the organic compound is effectively performed by quantifying the etheroatom(s) in it. The advantage in doing so is two-fold:

a) Co-eluting organic molecules will not be detected

b) Matrix related substances that would raise the baseline are not detected

c) The high energy source is able to yield orders of magnitude more ions, giving this

technique a higher sensitivity than traditional methods (Gonzalez-Gago et al., 2015)

These first two statements are valid for interfering substances which do not contain the

etheroatom being measured. This assumption- that bromine is found in consumer goods is

almost certainly coming from BFRs- was proven valid in numerous studies (Allen et al., 2008b)

(Guzzonato et al., 2017b). Figure 5-2 shows a schematic diagram of the instrumental set up.
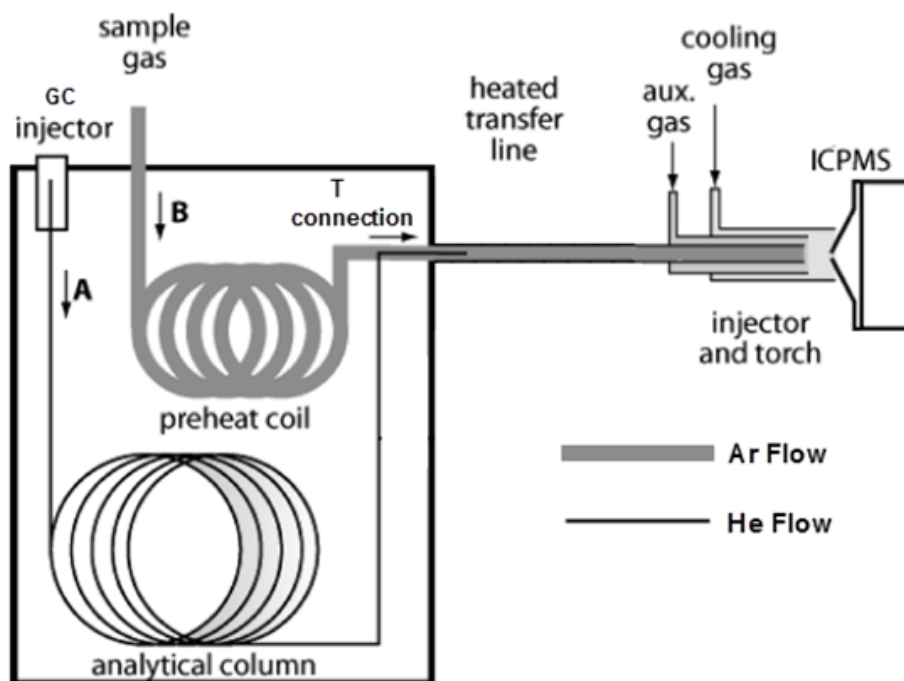
Figure 5-2 Experimental set-up for coupling a GC to an ICP-MS

Typically, the connection between the gas chromatograph and the ion source is a solid, semi-permanent transfer device, adapted to interface with the ion source which can be under vacuum, such as in Electron Impact (EI) mass spectrometry, or at atmospheric pressure, such as in inductively coupled plasma (ICP).

In ICP-MS, the ion source is provided by an inductively coupled plasma that is generated within an ICP torch. The ICP torch is typically made of quartz glass and its position is adjustable in three dimensions for optimization of the plasma conditions. For some applications, mass spectrometers are permanently set up to be used with a gas chromatograph, while in others (such as ICP-MS), connection to a GC instrument may be optional, and used interchangeably with other sample provision systems. Common problems that such bridging devices face and ideally should be overcome include: 1) the heat profile along the transfer line should be homogeneous and constant (Figure 5 3 shows the temperature profile of an older apparatus used for GC interfacing applications and Figure 5 4 shows the temperature profile of the interface developed for this study); 2) the transfer line should be flexible enough to allow three-dimensional movement of the ICP injector in order to perform a tuning procedure in dry-plasma conditions, when the entry end is connected to a gas chromatograph; and 3) there should be no cold spots that can lead to condensation of analytes and peak broadening as a consequence; 4) there should be no hot spots that can cause decomposition of the analysed compounds.
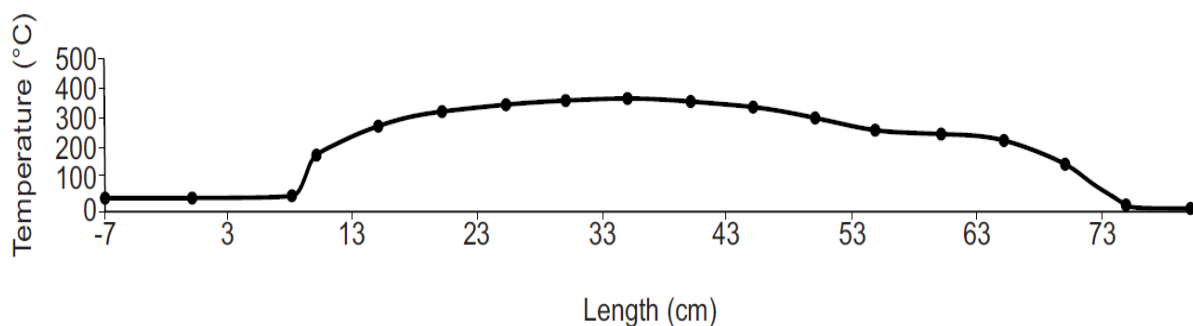
Figure 5-3 Temperature profile measured with a temperature probe inserted in the transfer capillary at different depths of an older apparatus used to interface a GC with an ICP-MS
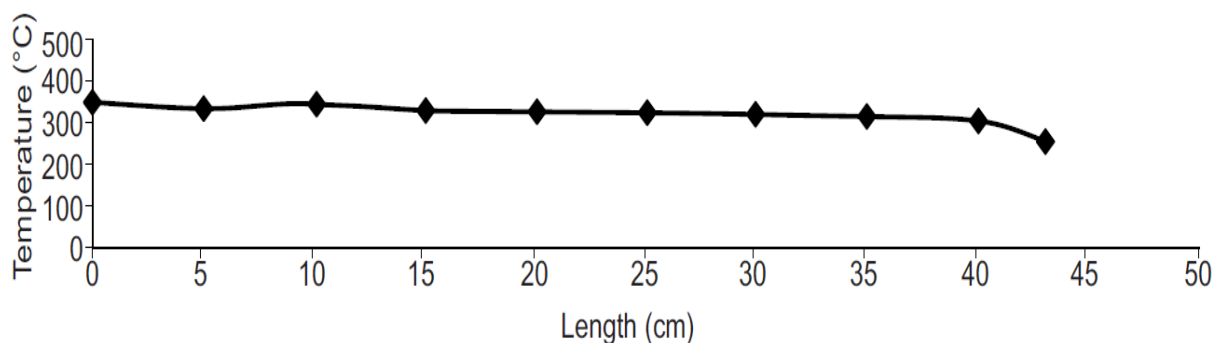
Figure 5-4 Temperature profile measured with a temperature probe inserted in the transfer capillary at different depths of the transfer line developed for this study

 The last two points are particularly relevant in the case of PBDE analyses, as some of these compounds are high boilers with a tendency to decompose very close to their boiling point; for this reason the temperature profile of the transfer line needs to have the smallest possible variation over its length.

The transfer line developed for this study provides an interface that overcomes these and other challenges. The transfer line has an entry end for connecting to the GC column and an exit end for connecting with a spectrometer, and comprises:

a) a flexible transfer capillary for receiving one end section of a GC column

b) a resistive heating arrangement surrounding the transfer capillary;

c) the resistive heating arrangement being able to follow the GC temperature programs or to be kept in constant isotherm;

The homogeneous temperature was achieved in a two-step approach:

a) Reducing the thermal mass of the transfer line so that the heat transfer process would be more controllable and mainly due to radiating heat (and to a lesser extent to conductive and convective heat). The developed transfer line has a specific heat capacity in the range of 100 J/Kg·K (for more details on how this was achieved and measured, please refer to (Guzzonato et al., 2017a))

b) Winding the resistance wire in a pattern that would compensate for the loss of heat from the two unheated ends of the transfer line (Figure 5-5 shows such a winding pattern).

c) These improvements can influence dramatically the quality of the chromatograms obtained, a comparison between the chromatograms obtained with an older transfer line available at the beginning of this study and the one that was developed during the research period is showed in Figure 5-6 and Figure 5-7.
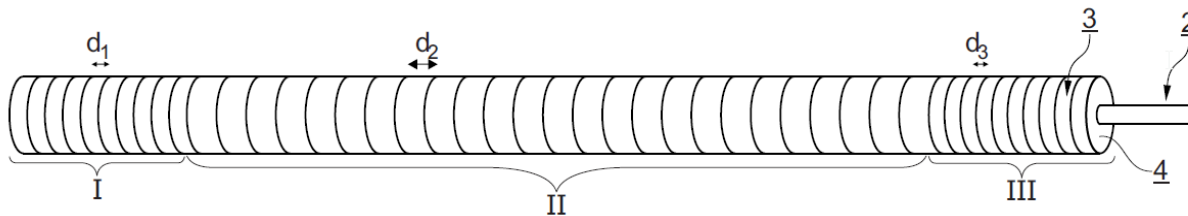
Figure 5-5 Winding pattern of the resistive wire (3) used to create a 'flat' temperature profile over the complete length of the transfer capillary (2). To compensate for the loss of heat at the two ends (region I and III) have resistive wire would at a smaller pitch (d1 and d3) with respect to the region II (d2). A sleeve of insulating material is inserted between the resistive wire and the transfer capillary (4).
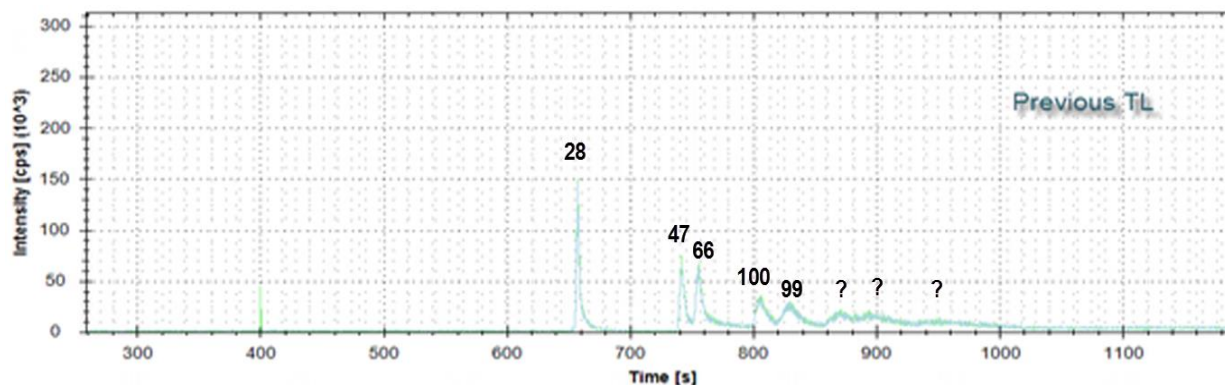
Figure 5-6 Chromatogram of 9-component PBDE standard obtained with previous transferline
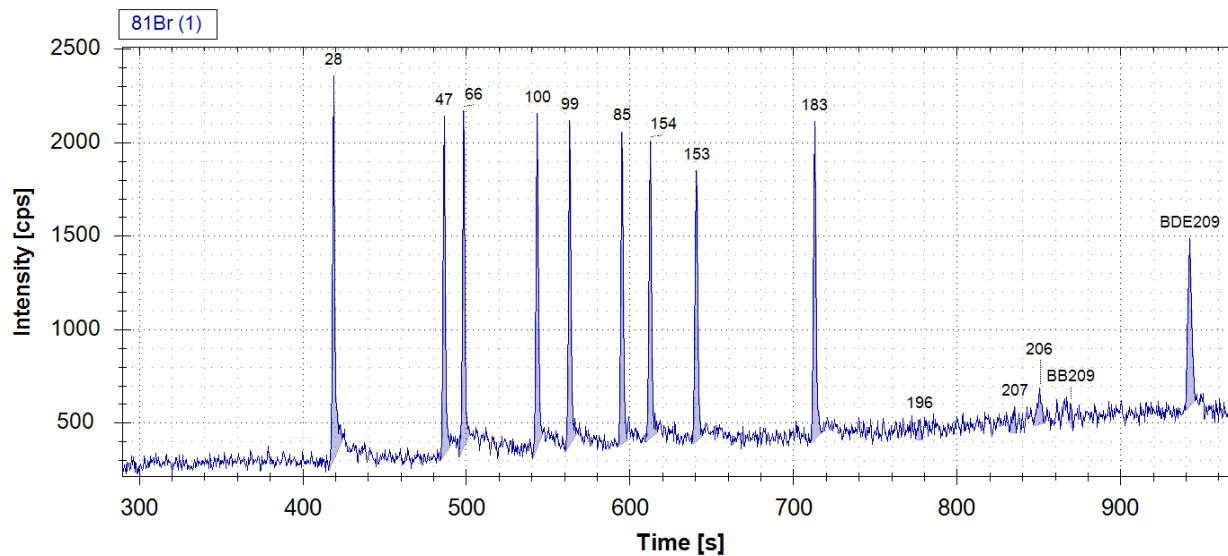
Figure 5-7 Chromatogram of 10-component PBDE standard obtained with newly developed transfer line

 For more information on how the transfer line was developed and tested, a complete report is

available in the patent describing this invention (Guzzonato et al., 2017a).
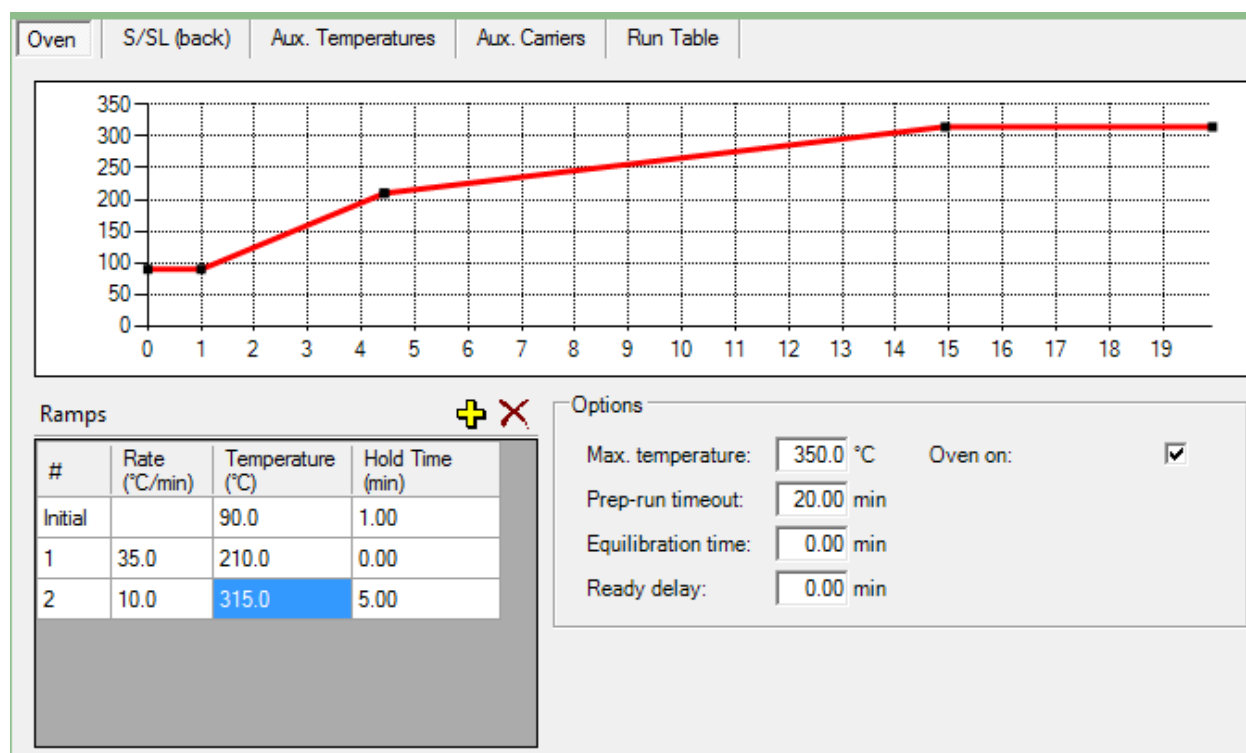
Figure 5-8 Oven program used to separate chromatographically PBDEs in indoor dust with GC-ICP-MS

5.5   GC-ICP-MS analysis of PBDEs

In this study the 46 dust samples collected were investigated for 12 PBDE congeners (BDEs 28, 47, 66, 85, 100, 99, 154, 153, 138, 183, 206 and 209). All analyses were performed on a Thermo Fisher Scientific GC Trace 1310 (using He as a GC carrier gas) coupled to an iCAP Q single quadrupole atmospheric pressure inductively coupled plasma mass spectrometer (using Ar as the plasma gas). The GC was equipped with a PTV (programmed temperature vaporisation) injector where a 'cold on column' liner was installed to reduce BDE-209 degradation. The on

column liner was connected with a deactivated capillary (pre-column) through a zero volume connector to the analytical column. The chosen column was a 15 m, 0.25 mm ID, 0.1 µm film thickness, 5% diphenyl, 95% dimethyl polysiloxane Rtx-1646 (Restek). More details on the GC conditions can be found in Table 5-3. The GC oven program was set to start at a temperature of 90 ˚C kept for 1 minute, then a fast ramp to 210 ˚C (at 35 °C per minute) followed by a slower ramp to 315 °C (at 10 °C per minute) and five minutes in isothermal (Figure 5-8). This system works at atmospheric pressure, therefore higher flow can be used without the risk of disrupting the source's vacuum. Additionally the GC column is connected to the transfer line via a T piece (Figure 5-2); on the bottom arm of the T piece a high flow (ca. 1 L/min) of Ar is fed through and around the GC column and into the ICP injector. The Ar acts as a sheath gas surrounding the GC column and "pushing" the Helium and the organic substances from the column to the plasma. The Ar gas creates a back pressure on the GC column of about 240 kPa, therefore if the set flow produces a lower or equal pressure to the outside of the column, no analyte will be able to exit the column; for this reason during method development particular attention was paid to optimise the flow of the GC carrier. The optimal flow program was to start with a pressure surge of 5 mL/min for one minute and to gradually reduce the flow as the oven temperature increases, bringing it down to 2.6 mL/min and maintaining it till the end of the run (Figure 5-9).

Table 5-3 GC-ICP-MS optimised parameters for PBDEs analysis in dust

Parameter	Setting
GC Column	Rtx-1614 capillary column, 0.25 mm ID, 0.1 μm film thickness, 15m length (Restek)
Injection mode and liner	PTV Splitless with Silicosteel on-column liner and 3m deactivated pre-column (0.52 mm ID)
Injector temperature	Oven track
Injection volume	1 μL
Carrier flow (He)	3 to 4.5 mL/min
Interface temperature	Oven track
Initial temperature	90 ˚C
Initial time	1 min
Ramp rate	35 ˚C min^{-1}; 10 ˚C min^{-1};
Final temperature	315 ˚C
Final time	5 min
Isotopes and dwell times	^{79}Br is 100 ms; ^{81}Br is 80 ms
Transient acquistion time	1200 secs
CCT Entry Lens	-108 V
Angular Deflection	-377 V
Deflection Entry Lens	-35 V
Spray Chamber Temperature	2.7 ˚C
Cool Flow	14 L/min
Sampling Depth	5 mm
Plasma Power	1550 W

Auxilliary Flow	0.8 L/min
Nebulizer Flow	0.93 L/min
Torch Horizontal Position	-0.5 mm
Torch Vertical Position	0.5 mm
Extraction Lens 2	-168 V
CCT Focus Lens	-1.56 V
CCT Bias	-2 V
CCT Exit Lens	-160 V
Focus Lens	18.8 V
D1 Lens	-198.4 V
D2 Lens	-80 V
Quad Entry Lens	-22.4 V
Pole Bias	-1 V
Virtual CCT Mass to Dac Factor	130
Virtual CCT Mass to Dac Offset	-150
Virtual CCT Mass parameter b	0.65
Virtual CCT Mass Maximum Dac Limit Set	4095

The ICP-MS tuning procedure is performed automatically by the instrument control software (Qtegra ISDS). Traditionally – for liquid sampling analysis – an aqueous tune solution with known amounts of a number of elements is sampled; source parameters such as nebulizer flow, cooling gas, auxiliary gas, torch position on the x-y-z axes are recursively varied while the software

detects which values generate the best performances on one or more chosen elements. It is important to perform this tuning procedure on the analyte of interest because –mostly depending on the ionisation energy of that particular element – the ideal source settings can vary considerably. When using the dry plasma configuration (i.e. coupled to a GC where only gas is fed through the source) the above described tuning procedure is not applicable. In this case a Br containing organic solvent (dibromoethane $C_2H_4Br_2$) was chosen and slowly injected in the GC (connected to the ICP-MS) during an isothermal GC program at 135 ˚C in order to create a stable Br signal. The auto tune procedure was set up to find the source values that would maximize the signal over ^{79}Br and ^{81}Br. The ^{81}Br trace was used for the analytical determination and the $^{79}Br/^{81}Br$ isotope ratio was monitored during the chromatogram to check for sudden changes in pressure or temperature leading to decomposition of the PBDEs.
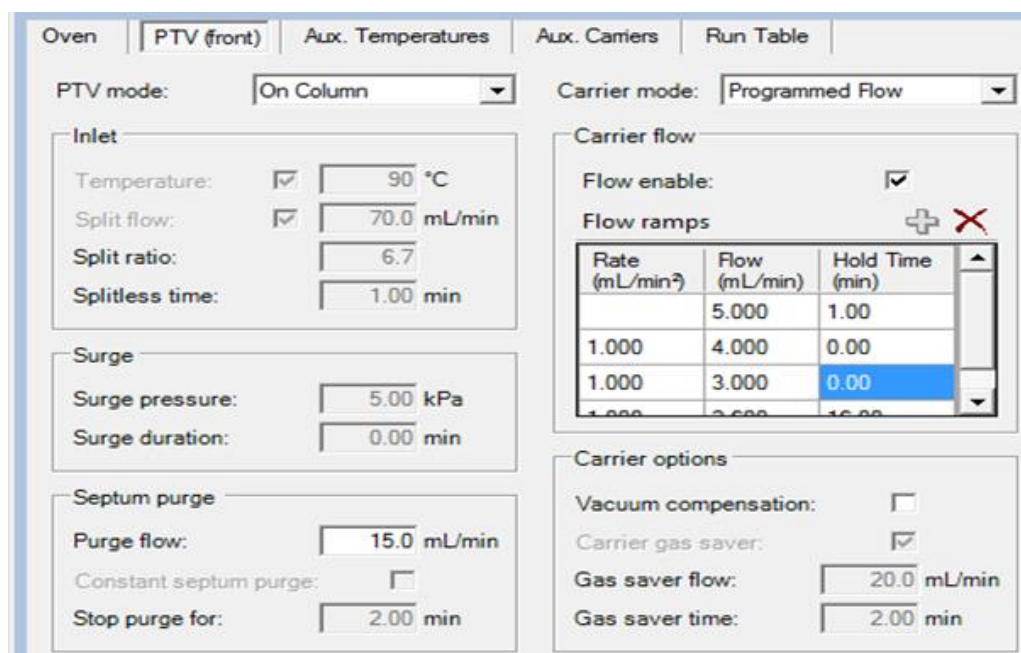
Figure 5-9 Carrier Flow program used in the GC method for PBDEs in dust
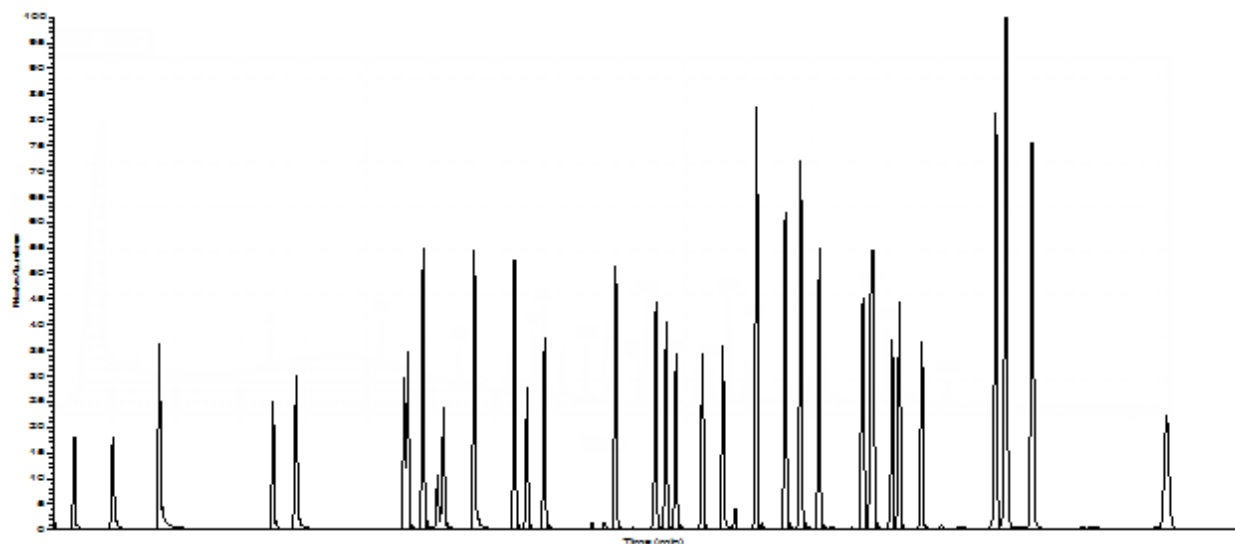
Figure 5-10 Chromatogram of congener mix analysed with GC-ICP-MS

The transient signal produced by this analysis is comparable to a Total Ion Current plot, with the only difference that in this case the peak intensity is produced by ^{81}Br only and not by the different molecular ions. The advantage of having such a result is the certainty (provided isobaric interferences are avoided or accounted for) that every peak is measuring a Br-containing substance. The disadvantage is that there is no molecular mass information related to each peak, meaning that the peak identification must rely solely on retention time.

 In order to assess linearity of the MS response over the concentration range of PBDEs, a 5-point calibration was carried out prior to analysis of the samples sequence using a calibration kit of 5 ampoules. Each calibration solution included the analyzed BDE congeners (BDEs 28, 47, 66, 85, 100, 99, 154, 153, 138, 183, 206 and 209). The chromatograms obtained with these

168

standards were then used to define the correct retention time for each congener analyzed (and

by comparison with later acquired HR-GC-MS data) and use this information to identify the

compounds in the unknown samples (Figure 5-10). The same set of calibration standards and

samples were analyzed in parallel with a Magnetic Sector High Resolution Mass Spectrometer

using EI as Ionization source in order to confirm the identity of the peaks at the recorded

retention times. The detection limits for this technique, estimated as recommended in ICH1

Guidance as three times the standard deviation (SD) of the lowest calibration standard, are

reported in Table 5-4.

Table 5-4 Limits of detection for target PBDEs	
IDL (ppb)	BDE
0.1	BDE 28
1.1	BDE 47
0.8	BDE 100
0.1	BDE 99
0.5	BDE 154
1.1	BDE 153
0.1	BDE 138
0.1	BDE 183
0.3	BDE 206
0.3	BDE 209

Linearity in the extraction yield was checked measuring the concentration of the BDE congeners

in 3 samples obtained by extracting different aliquots of SRM 2585 indoor dust and comparing

the obtained values with the reference concentration (Table 5-5). The correlation coefficient (r) was in all cases >0.9. The standard deviation between recovery values was between 2.0 and 14.6%. The method tends to overestimate BDE28 probably because UV degradation of the higher brominated BDE congeners into BDE 28. The RSD between duplicate measurements was between 0.03% and 0.72%.

Table 5-5 Mean values and standard deviations (ppb in dust) of flame retardants measured in SRM 2585.

	Reference (ppb)	Uncertainty (+/-)	Measured (ppb)	Uncertainty (+/- 2σ)
BDE-28	46.9	4.4	53	6.5
BDE-47	497	46	410	9.1
BDE-66	29.5	6.2	20	2.7
BDE-100	145	11	120	14
BDE-99	892	53	770	15
BDE-85	43.8	1.6	33	3.8
BDE-154	83.5	2	74	11
BDE-153	119	1	95	13
BDE-138	15.2	2	14	1.9
BDE-183	43	3.5	35	3.4
BDE-206	271	42	210	29
BDE-209	2510	190	2300	210

5.6 High resolution MID data acquisition for target compound analysis of PBDEs in dust

The data obtained from the analysis of dust extracts with GC-ICP-MS contain two types of information:

- Retention time (RT) of the compounds
- Selectivity over Br containing substances

With this level of information it should be possible to identify the PBDEs by injecting a standard mixture that contains the compounds of interest and comparing the RT of the standard chromatogram to the RT of the target compounds in the unknown sample. Interfering molecules that do not contain Br and co-elute with one of the congeners will not be seen by the MS that is only "counting" the Br ions. To confirm the identity of the target molecules, and to test the hypothesis that the GC-ICP-MS is able to identify them correctly using only the retention time information, the same standards and samples were also analysed with a GC-HRMS instrument (a Thermo Scientific Dual Focus System) that provides the accurate mass information in addition to the retention time.

In order to identify the compounds with accurate mass determination, a MID method (Multiple Ion Detection) was developed. This method requires the definition of regions of interest (windows) within the total mass span covered by the target compounds. Below is a brief explanation of its working principle.

This instrument uses two focusing elements:

- A magnetic field that is able to separate the molecules according to their momentum (which depends both on mass and velocity of the ion): the magnetic field is kept constant. The calibration of the magnet is performed *una tantum* and its function is stored in the instrument. This function is not linear as it correlates the magnetic field to the kinetic energy (Lorentz force).
- An electric field that compensates accurately the energy dispersion of the magnetic field by the opposite energy dispersion of the electrostatic field: the combination of both fields focuses ions of the same mass into the detector.

During MID analysis the accelerating voltage and therefore the kinetic energy of the ions undergoes scan-inherent mass calibration in every scan, just before the target compounds are monitored. A reference compound containing molecules in the mass range of interest is leaked continuously in the ion source together with the analytes coming out of the GC column during the chromatographic run. Each window is bracketed by two compounds in the reference mixture that have a slightly lower mass than the lighter target compound and slightly higher mass than the heavier target compound. For each defined window the instrument will "park" the magnet at the value that in the magnetic calibration curve corresponds to the smallest mass selected. The electric field will instead "move" (quickly vary the accelerating voltage) between the voltage corresponding to the reference lighter mass and the voltage corresponding to the reference heavier mass: the target masses found in between will be accurately interpolated.
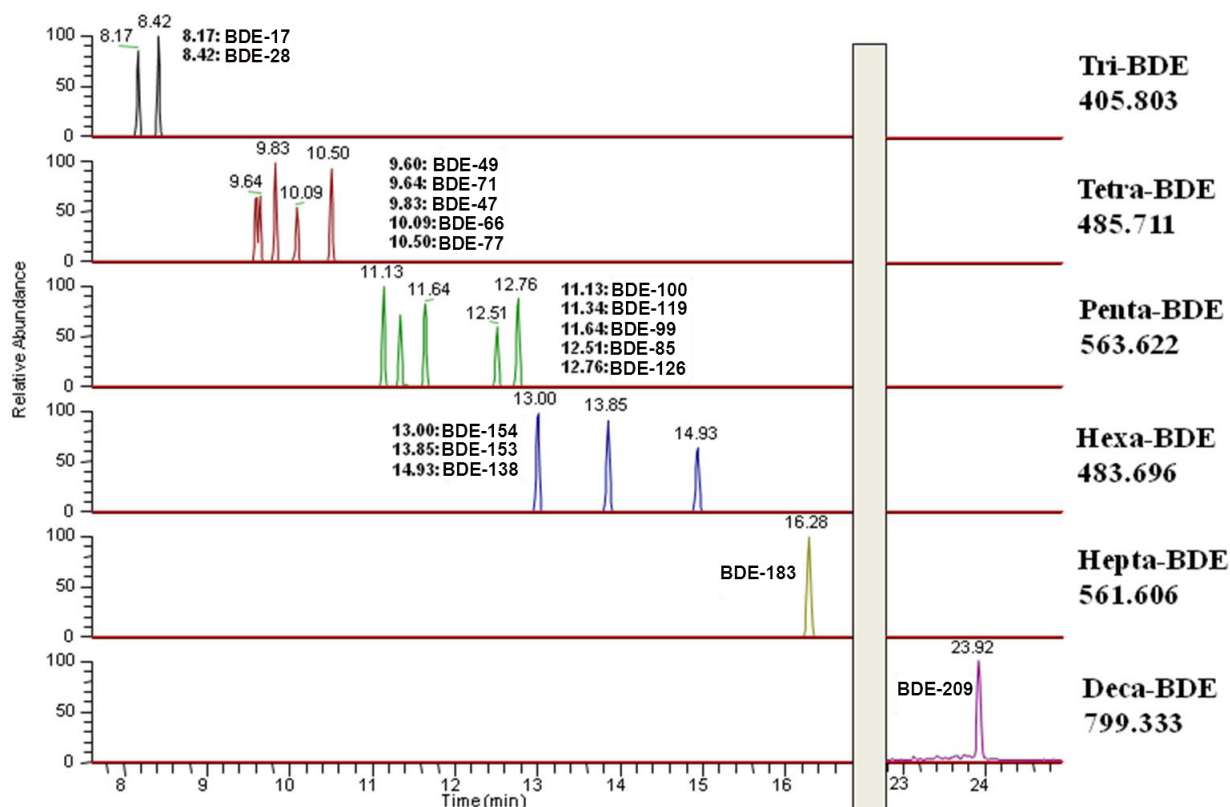
Figure 5-11MID time resolved signal for target congeners

For this method eight windows were defined for eight mass ranges (tri- to decaBDE). Each mass range covers a bromination degree (e.g. the first window spans from m/z 403 to m/z 408, for tri brominated compounds BDE-17 and BDE-28). An example of the obtained MID chromatograms is in Figure 5-11.

	# Br	m		m+2		m+4		m+6		m+8		m+10		m+12		Int. M-2Br
[M]⁺	1	247,984	100	249,982	98											100
	2	325,894	51	327,892	100	329,890	49									100
	3	403,805	34	405,803	100	407,801	97									100
	4			483,713	68	485,711	100	487,709	65							100
	5			561,624	51	563,622	100	565,620	97							85
	6					641,532	76	643,530	100	645,528	73					60
	7					719,443	61	721,441	100	723,439	97					55
	8							799,351	81	801,349	100	803,347	78			50
	9							877,262	68	879,260	100	881,258	97			40
	10									957,171	85	959,168	100	961,166	81	25
	1															0
	2															0
	3															0
[M-2Br]⁺	4	323,879	51	325,877	100	327,875	49									95
	5	401,789	34	403,787	100	405,785	97									100
	6			481,698	68	483,696	100	485,694	65							100
	7			559,608	51	561,606	100	563,604	97							100
	8					639,517	76	641,515	100	643,513	73					100
	9					717,427	61	719,425	100	721,423	97					100
	10							797,336	81	799,333	100	801,331	78			100

Table 5-6 m/z vs.intensity list for PBDEs (relative intensities of M+ versus [M-2Br]⁺). Bold numbers next to accurate masses represent the relative intensity between isotopologues. Red numbers represent the bromination level at which the [M-2Br]⁺ has a relative higher intensity than [M]⁺. The lower group [M-2Br]⁺ refers to the same header at the top of the table.
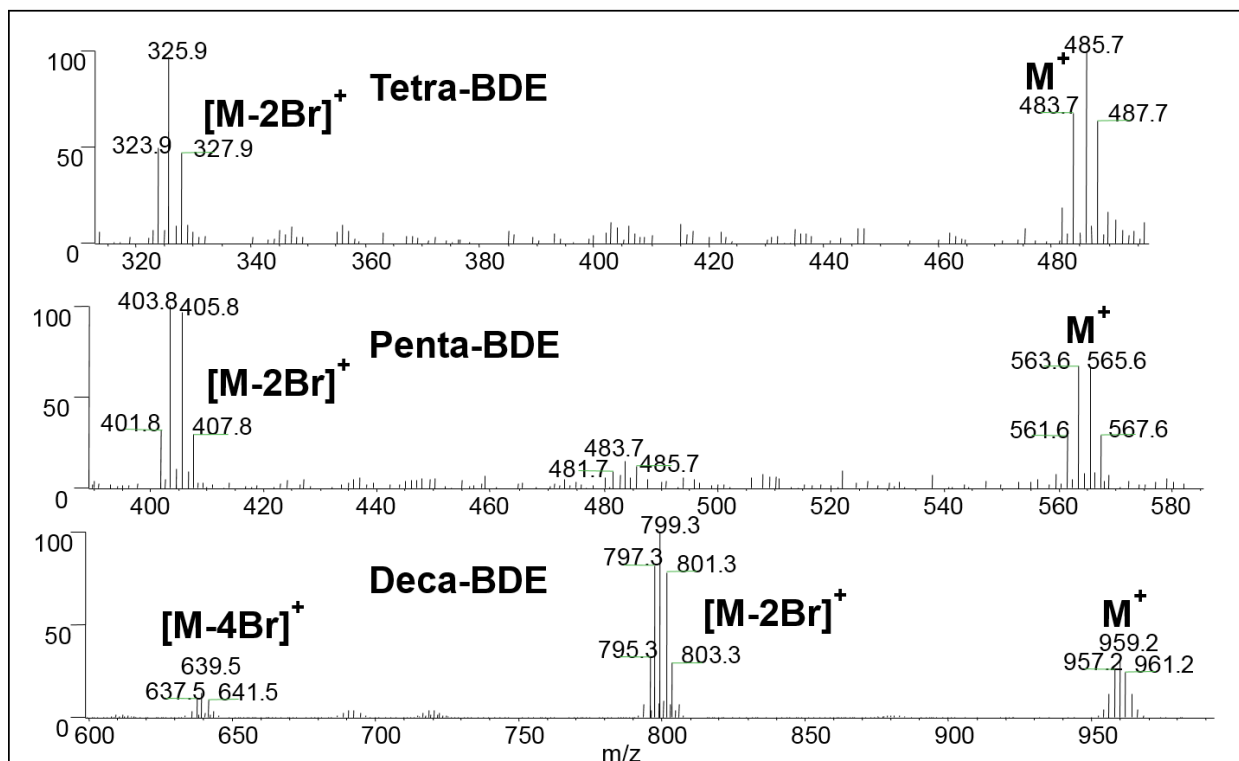
Figure 5-12 Mass spectra of tetra-, penta- and decaBDE M⁺ and [M-2Br]⁺ ions

In Figure 5-11 it is also noticeable that after PentaBDE, heavier compounds are identified through their [M-2Br]⁺ ion, while for PentaBDE and less brominated congeners the precursor ion is chosen. This is because, as Table 5-6 shows, M+ ions are not the most intense for all bromination degrees. Depending on the selected GC method, the transition of the most abundant ion from M⁺ to [M-2Br]⁺ might be shifted to Tetra/Penta- or Hexa/Hepta-BDE (Figure 5-12 and Table 5-6). The same set of PBDE standards used for the GC-ICP-MS analysis was used in this case to identify the compounds with accurate masses. The GC method was kept the same except for the flow speed of the carrier, which was set constant at 1 mL/min (that in the GC-ICP-MS method had to be set at a higher value to contrast the Ar backpressure in the sample gas of the ICP source) and for the ramp speeds of the oven program which was kept of the same

175

shape, but extended over a longer run time, this way the relative retention times were kept

constant (Figure 5-13).
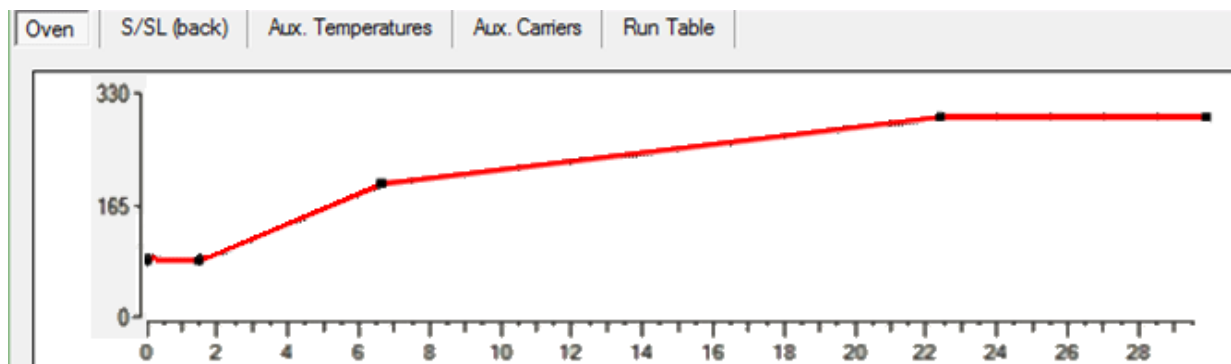
Figure 5-13 Oven program used to separate chromatographically PBDEs in indoor dust with GC-ms-HRMS

 Chromatograms obtained with GC-ICP-MS and obtained with GC-HRMS were compared for

each SRM 2585 extract. Each peak was observed to confirm its identity with accurate mass

determination: masses that differ for more than 30 ppm from the simulated value were

discarded as interference. Figure 5-14 shows an example of a dust extract containing mainly

BDE-209 and nonaBDEs. The upper trace is a TIC signal, the middle trace is the accurate mass

corresponding to the last chromatographic peak (decaBDE), showing the two accurate

isotopologues masses measured for decaBDE and the lower trace is the simulated trace of

decaBDE (containing all the isotopologues generated by the different Br isotope combinations).

It should be noted that when comparing standard mixtures this method proved to be reliable,

but when inserting the expected time window in the peak recognition tool used for transient

signal GC-ICP-MS analysis, it was necessary to manually correct most peaks for most of the real

samples because of matrix effects causing peak shifting over time. This issue could be overcome

by applying a clean-up procedure following the extraction of dust samples.
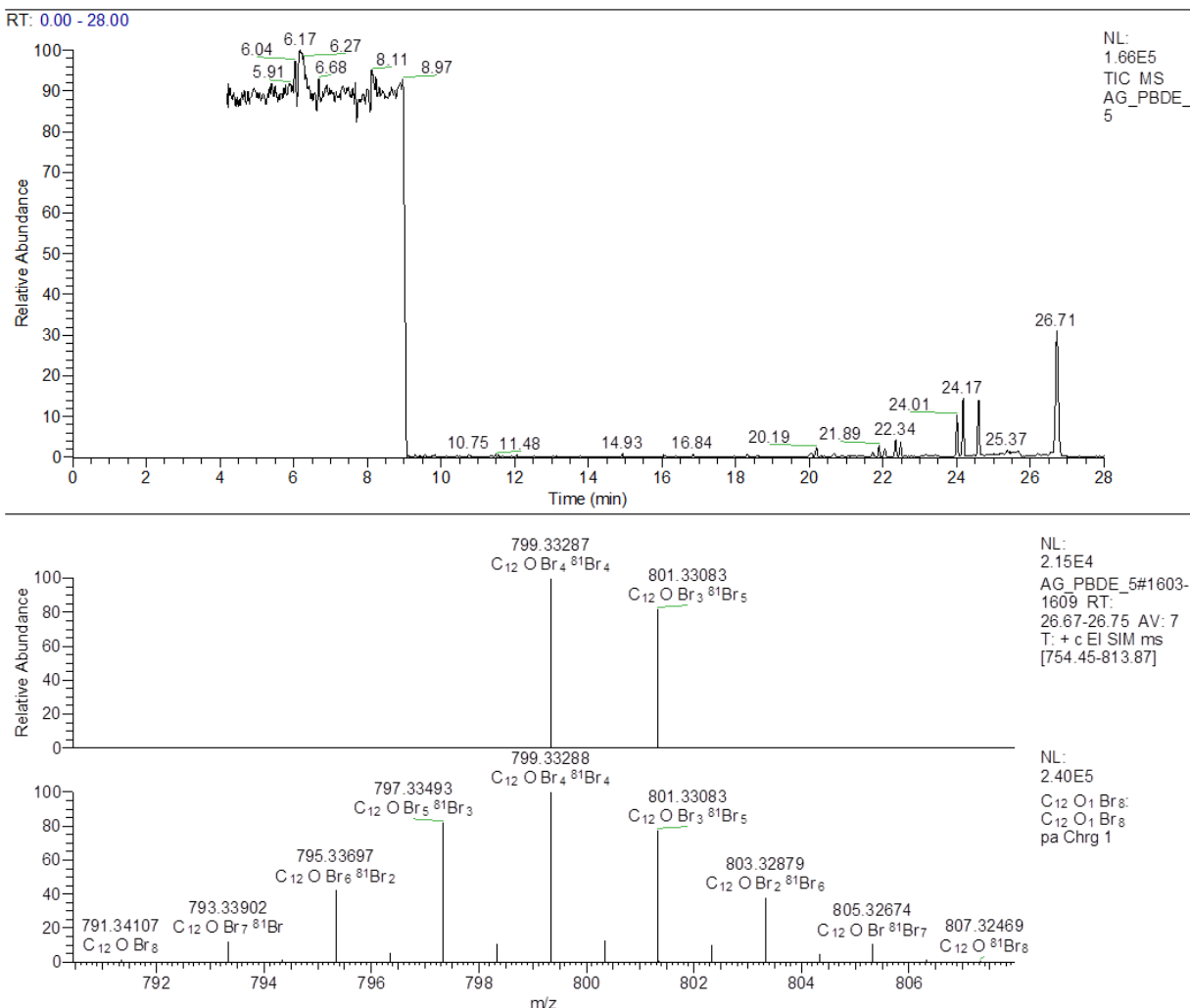
Figure 5-14 Upper trace: TIC of dust extract. Middle trace: measured accurate masses of [M-2Br]+ ion of decaBDE. Lower trace: simulated isotope pattern of decaBDE product ion.

5.7 Data and statistical analysis

The software Qtegra ISDS was used to acquire the time resolved MS signals. Excel was used to export and elaborate raw data from Qtegra. Information collected in the questionnaires for each room and concentration values for the analysed BDE congeners were studied with

multivariate analysis of the principal components (PCA). The software PAST was used to perform PCA and Spearman's rank correlation tests. (Hammer et al., 2001).

5.8   Discussion

5.8.1   Concentration of tri- to hexa-BDEs (Σ12PBDEs) in indoor dust samples from Germany

For this study, two sampling campaigns were carried out in a building of new construction. The first sampling campaign was carried out 2 weeks after the carpeting and the windows were installed.

Table 5-7 and Table 5-8 summarise the concentrations (expressed in ng/g) of the target PBDEs in dust samples taken during the two sampling campaigns. Concentrations of Σ12PBDEs from indoor dust spanned from a minimum of ca. 400 ng/g to a maximum of 90,000 ng/g in the first sampling campaign and from a minimum of ca. 3,200 ng/ to a maximum of ca. 102,000 ng/g in the second. The average concentration of Σ12PBDEs in the dust was ca.13,700 ng/g (median ca. 6,100 ng/g) right after construction and ca. 18,200 ng/g (median 8,600ng/g) after about 100 days of use. While the average concentration increased between first and second campaign, the relative congener composition variation is of particular interest as Figure 5-15 and Figure 5-16 show.
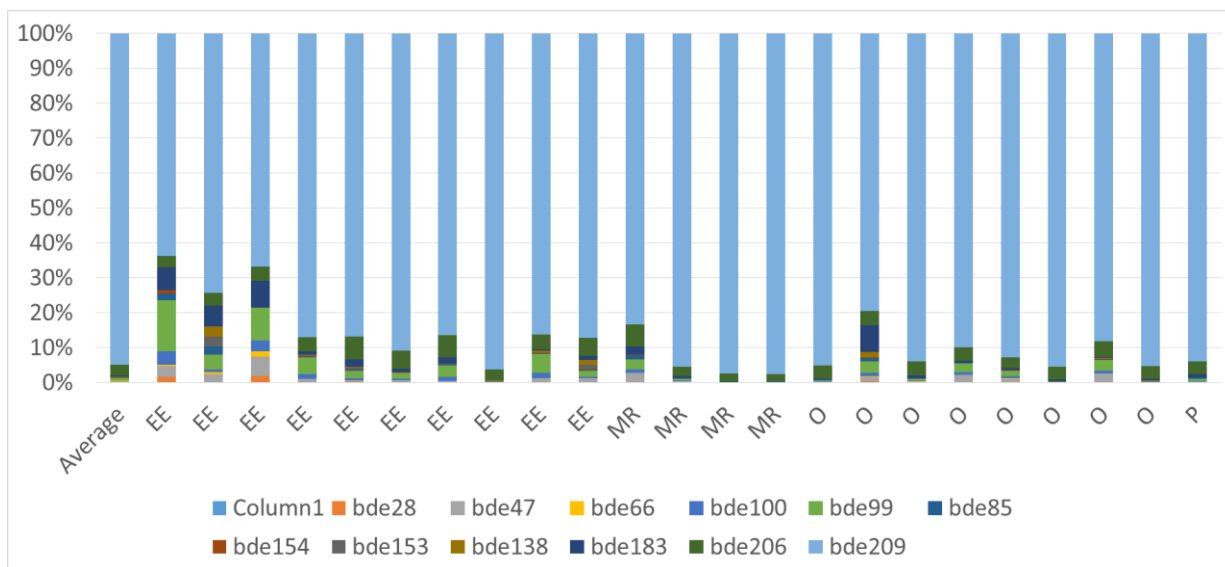
Figure 5-15 Proportional contribution of each BDE congener for dust samples collected in the first sampling campaign. The bar on the far left indicates the average.
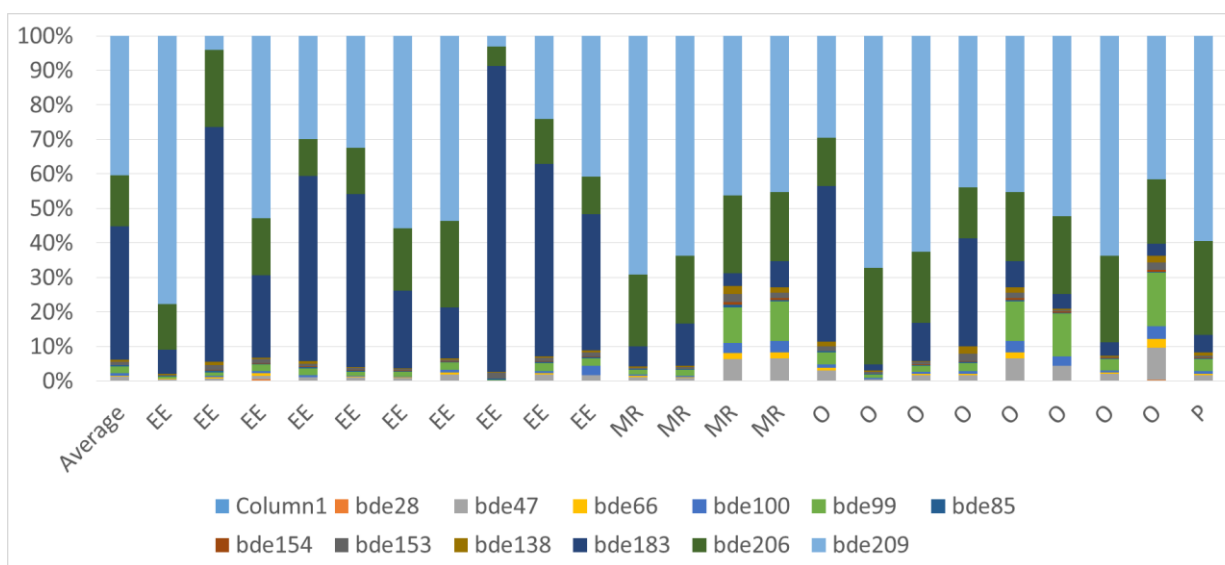
Figure 5-16 Proportional contribution of each BDE congener for dust samples collected in the second sampling campaign. The bar on the far left indicates the average

.

Table 5-7 Concentrations of PBDEs (ng/g) in indoor dust samples from offices and other working environments (first sampling campaign).

BDE	28	47	66	100	99	85	154	153	138	183	206	209	Σ₁₂PBDEs	Dust loading (g/m²)
EEb	10	310	84	110	310	73	10	<DL	<DL	4500	8400	50000	64000	0.12
EE	<DL	120	70	71	200	120	<DL	250	180	13000	4200	770	19000	0.14
EE	47	110	83	63	190	<DL	<DL	<DL	<DL	2500	1700	5500	10000	0.11
EE	10	160	2	85	270	58	12	130	98	7800	1500	4300	15000	0.15
EE	24	210	58	53	290	84	9	140	64	12000	3100	7500	23000	0.14
EE	7	120	32	25	210	50	7	<DL	<DL	3400	2700	8300	15000	0.13
EE	<DL	160	44	74	190	23	9	<DL	<DL	1300	2200	4800	8900	0.12
EE	3	95	26	37	140	350	11	<DL	<DL	91000	5700	3200	100000	0.11
EE	<DL	240	65	81	350	51	9	<DL	72	8000	1900	3500	14000	0.20
EE	<DL	360	1	710	570	60	88	270	160	10000	2800	10000	25000	0.15
Average	10	190	46	130	270	87	15	79	57	15000	3400	9800	29000	0.14
RSD	150	48	66	160	45	110	170	140	120	180	63	150	100	19.00

Median	5	160	51	72	240	59	9	<DL	32	7900	2700	5200	17000	0.14
Minimum	<DL	95	1	25	140	<DL	<DL	<DL	<DL	1300	1500	770	8900	0.11
Maximum	47	360	84	710	570	350	88	270	180	91000	8400	50000	100000	0.20
	<DL	<DL	<DL	<DL	<DL	<DL	<DL	<DL	<DL	<DL	<DL	<DL	<DL	<DL
MRc	<DL	180	50	77	210	19	11	<DL	<DL	960	3400	11000	16000	0.13
MR	<DL	110	29	48	200	33	5	<DL	<DL	1500	2400	7800	12000	0.05
MR	5	200	55	90	330	21	27	<DL	<DL	120	720	1500	3000	0.11
MR	4	360	99	190	650	17	37	<DL	<DL	430	1100	2600	5500	0.10
Average	2	210	58	100	350	22	20	<DL	<DL	750	1900	5800	9200	0.10
RSD	120	51	51	60	59	32	72	<DL	<DL	81	63	79	65	35.00
Median	2	190	52	84	270	20	19	<DL	<DL	700	1800	5200	8800	0.11
Minimum	<DL	110	29	48	200	17	5	<DL	<DL	120	720	1500	3000	0.05
Maximum	5	360	99	190	650	33	37	<DL	<DL	1500	3400	11000	16000	0.13
	<DL	<DL	<DL	<DL	<DL	<DL	<DL	<DL	<DL	<DL	<DL	<DL	<DL	<DL
Od	10	180	49	58	210	23	7	<DL	<DL	2700	850	1800	5900	0.05
O	3	93	26	47	210	40	10	<DL	97	370	5700	14000	20000	0.09
O	<DL	130	35	48	150	22	11	<DL	<DL	910	1700	5200	8200	0.07

O	4	78	21	33	110	22	11	<DL	<DL	1500	720	2100	4700	0.05
O	4	360	99	190	650	17	37	<DL	<DL	430	1100	2600	5500	0.24
O	16	670	4	440	2000	28	52	<DL	<DL	690	3600	8300	16000	0.19
O	15	<DL	<DL	99	460	36	18	<DL	61	540	3600	9100	14000	0.07
O	<DL	390	110	150	650	14	21	<DL	<DL	140	780	1700	4000	0.13
Average	7	240	42	130	550	25	21	<DL	20	920	2300	5600	9800	0.11
RSD	96	93	95	100	110	35	75	<DL	190	92	81	79	62	63.00
Median	4	150	30	79	340	23	15	<DL	<DL	620	1400	3900	7100	0.08
Minimum	<DL	<DL	<DL	33	110	14	<DL	<DL	<DL	140	720	1700	4000	0.05
Maximum	16	670	110	440	2000	40	52	<DL	97	2700	5700	14000	20000	0.24

[a]- denotes not calculated for this congener.

[a]Relative standard deviation of concentrations expressed as ngm^{-2} for BFRs and g m^{-2} for dust loading.

[b]Electronic engineers laboratories

[c]Meeting rooms

[d]Offices

Table 5-8 Concentrations of PBDEs (ng/g) in indoor dust samples from offices and other working environments (second sampling campaign).

BDE	28	47	66	100	99	85	154	153	138	183	206	209	Σ₁₂PBDEs	Dust loading (g/m²)
EE[b]	7.4	13	2.1	16	64	8.6	4.2	<DL	<DL	28	14	280	440	0.15
EE	<DL	11	3	3.7	19	11	<DL	14	14	27	16	340	460	0.11
EE	7.1	20	6	12	35	<DL	<DL	<DL	<DL	29	15	250	380	0.19
EE	5.6	28	4.8	46	160	7.8	5.5	8.4	8.3	31	140	3000	3400	0.07
EE	18	30	8.1	41	160	28	13	22	22	150	490	6500	7500	0.14
EE	14	52	5.1	26	160	13	9.2	<DL	<DL	99	490	8800	9600	0.2
EE	<DL	10	2.8	26	80	7.3	7	<DL	<DL	39	150	2100	2400	0.16
EE	17	13	3.7	18	69	11	4.3	<DL	<DL	37	690	23000	23000	0.05
EE	<DL	56	0.73	66	250	4.3	8.5	<DL	24	23	190	3900	4500	0.08
EE	<DL	67	<DL	22	99	13	4.7	76	76	71	290	4900	5600	0.08
Average	6.8	30	3.6	28	110	10	5.7	12	14	54	250	5200	5800	0.12

RSD	100	70	68	67	64	72	72	200	160	79	95	130	120	43
Median	6.3	24	3.3	24	89	9.6	5.1	<DL	4.1	34	170	3400	3900	0.13
Minimum	<DL	10	<DL	3.7	19	<DL	<DL	<DL	<DL	23	14	250	380	0.05
Maximum	18	67	8.1	66	250	28	13	76	76	150	690	23000	23000	0.2
	<DL	<DL	<DL	<DL	<DL	<DL	<DL	<DL	<DL	<DL	<DL	<DL	<DL	<DL
MR^c	<DL	41	1.8	13	45	15	3	<DL	<DL	38	96	1300	1500	0.13
MR	<DL	41	0.88	11	46	9.6	3.4	<DL	<DL	53	250	8600	9100	0.05
MR	7.2	21	7.9	18	70	12	3	<DL	<DL	43	1800	74000	76000	0.11
MR	4.5	62	17	15	69	8.6	2.1	<DL	<DL	<DL	2100	89000	91000	0.1
Average	2.9	41	6.9	15	57	11	2.9	<DL	<DL	33	1000	43000	44000	0.098
RSD	120	40	110	20	24	26	18	<DL	<DL	69	97	100	100	35
Median	2.3	41	4.9	14	58	11	3	<DL	<DL	40	1000	41000	42000	0.11
Minimum	<DL	21	0.88	11	45	8.6	2.1	<DL	<DL	<DL	96	1300	1500	0.05

Maximum	7.2	62	17	18	70	15	3.4	<DL	<DL	53	2100	89000	91000	0.13
	<DL	<DL	<DL	<DL	<DL	<DL	<DL	<DL	<DL	<DL	<DL	<DL	<DL	<DL
O[d]	4.7	25	16	9.3	40	7.9	3.1	<DL	<DL	48	510	13000	13000	0.05
O	4.5	26	2.2	18	58	18	3.7	<DL	29	140	73	1500	1800	0.09
O	<DL	29	13	14	46	12	2.1	<DL	<DL	81	380	8800	9400	0.07
O	9.2	120	0.69	50	160	3.7	<DL	<DL	<DL	39	230	5500	6200	0.05
O	8.4	60	16	37	98	10	6	<DL	<DL	42	200	6200	6700	0.24
O	5.1	22	0.88	8.6	29	20	1.3	<DL	<DL	130	870	23000	24000	0.19
O	4.2	140	<DL	52	180	13	6.8	6.9	6.8	16	260	5200	5900	0.07
O	<DL	9.7	2.7	5.9	18	6.7	2.5	<DL	<DL	42	280	7300	7700	0.13
Average	4.5	54	6.5	24	78	11	3.2	0.86	4.5	68	350	8800	9400	0.11
RSD	74	93	110	78	78	49	71	280	230	68	70	75	72	63
Median	4.6	27	2.5	16	52	11	2.8	<DL	<DL	45	270	6800	7200	0.08
Minimum	<DL	9.7	<DL	5.9	18	3.7	<DL	<DL	<DL	16	73	1500	1800	0.05

| Maximum | 9.2 | 140 | 16 | 52 | 180 | 20 | 6.8 | 6.9 | 29 | 140 | 870 | 23000 | 24000 | 0.24 |

- denotes not calculated for this congener.

[a]Relative standard deviation of concentrations expressed as ng m^{-2} for BFRs and g m^{-2} for dust loading.

[b]Electronic engineers laboratories

[c]Meeting rooms

[d]Offices

A previous study (Batterman et al., 2010) provided an extensive assessment of the time trends of BFRs in a building of new construction (1st sampling) with 7 sampling campaigns conducted over the following 15 months. However, in contrast to our study, the building sampled by Batterman et al was already furnished and carpeted when the 1st sampling happened. Initial $\sum_{21}$BDE concentrations were at very low levels (e.g. 145 ng/g) and after ca. 100 days they increased by about 5,000 ng/g, which is comparable to the absolute increase measured in this study between the 1st and 2nd campaign. It should be noted that in the study of (Batterman et al., 2010) a stabilisation time of 6-8 months is observed by modelling the concentration trends over time: assuming a similar stabilisation period for the present study it would mean that the second campaign was carried out while concentrations were still increasing (between 1/3rd and 1/2 of the rapid increase part of the modelled trend). It can be then roughly extrapolated for this study that a third sampling campaign carried out after 3 more months would have produced a "stabilised (or steady state) value" for the Σ_{12}PBDEs concentration between 36,000 and 54,000 ng/g. These results are also in the same order of magnitude of a previous study in offices in the UK as summarised in Table 5-9 (Harrad et al., 2008b), but are higher (but still of the same order) than a previous study of three Australian offices that spanned between ca. 600 and 3,000 ng/g (Toms et al., 2009).

A Spearman's rank correlation test showed strongly correlated congener groups that are typically found together in commercial mixtures: a) BDE-47, -100, 154 and -99 (main components of commercial penta mixture) have correlation coefficients between 0.75 and 0.95; while b) BDE-183 and 153 (main components of commercial octa mixture) showed correlation coefficients between 0.77 and 0.8.

Table 5-9 PBDE concentrations (ng/g) measured in a previous study on office dust, 30 samples Harrad et al., 2008b.

	28	47	99	100	153	154	183	209	ΣPBDEs
Average	0.7	15	36	5.6	14	4.4	71	260000	260000
Median	<0.5	10	20	3.4	5	2.8	4.2	8100	8100
Minimum	<0.5	1.2	2.8	<0.5	<0.5	<0.5	<2.0	<3.0	4
Maximum	2.1	58	180	17	110	16	550	2200000	2200000

A paired t-test was performed to evaluate if there is a statistically significant difference between log-transformed concentrations in the dust collected in the first sampling campaign and the second sampling campaign. The t-values for each individual congener are represented in Figure 5-17: BDE-209 shows no significant increase in the median concentration between 1st and 2nd sampling campaign (the null hypothesis being that there is no significant difference between the concentrations measured between 1st and 2nd campaign) after population. This trend is substantially different from a similar study (Batterman et al., 2010) where BDE-209 was the compound that increased the most from the first sampling (new building, not occupied) to successive samplings in the following 15 months where the BDE-209 level reached 48,000ng/g. As the PBDE signature varies significantly with the room type, a paired t- test was also
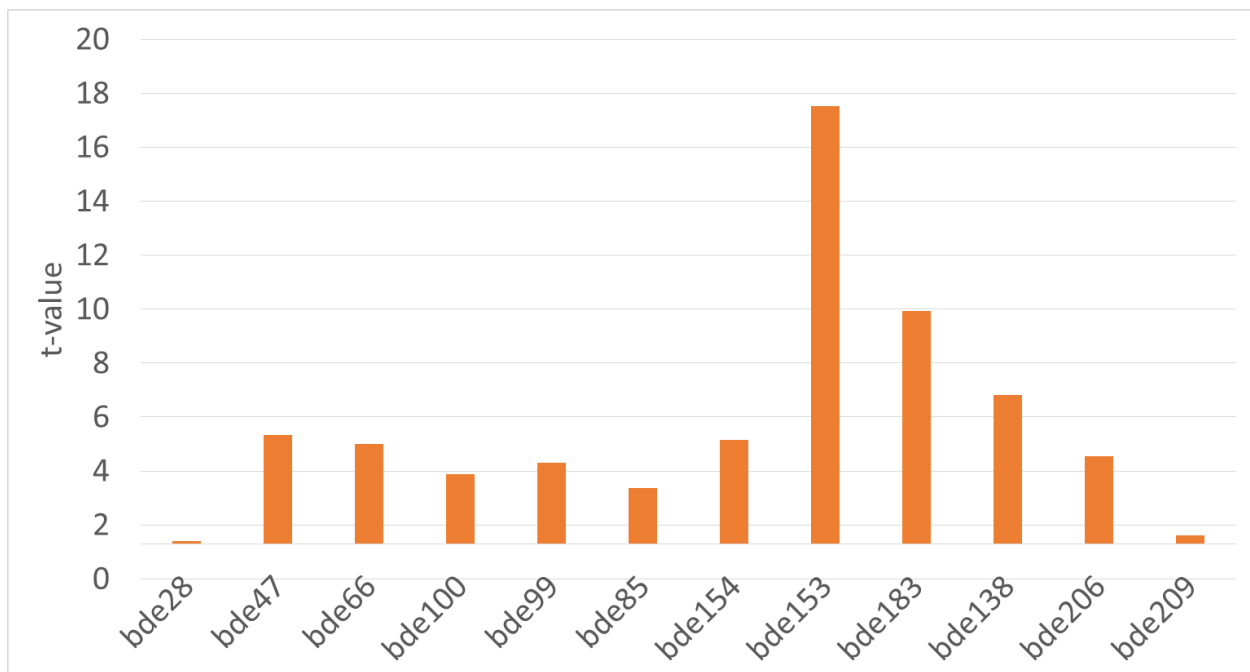
Figure 5-17 Results of paired t-test between 1st and 2nd sampling campaign for log-transformed concentrations of each individual congener. The vertical axis is crossed at the Student value for which the null hypothesis is rejected (1.3)

performed separately for concentrations in EE, MR and O. Typical congeners were chosen to represent the 3 major commercial PBDE mixtures, respectively for EE, MR and O. BDE-47, -99, -100, -154 and -153 were selected to represent penta-mix; BDE-183, -153, -206, -209 were selected to represent octa-mix; BDE-206 and -209 were selected to represent deca-mix. In MR and O ($p<0.05$) a significant change is recorded in penta-mix concentrations, while octa- and deca-mix did not vary in a statistically significant way in these room types.

InEE rooms octa-mix concentrations, together with Penta-mix, which seems to be the predominant contribution to changes in PBDE pattern caused by occupation and use of all the sampled rooms in the building.

5.8.2 Spatial distribution of PBDEs in sampled rooms

In the first sampling campaign, the congener profile is very homogeneous, with a clear prevalence of BDE-209 over all sampled environments, for all sampled rooms the most abundant congener is BDE-209. The presence of mainly BDE-209 can be explained with the construction material recently used to build, carpet, and insulate the rooms.

In the second sampling campaign after new furniture and electronic appliances were installed in the rooms according to their uses, the congener profile became differentiated between different rooms. Particular differences are apparent between the electronic engineering laboratories and the other room types (offices and meeting rooms). Electronic engineers' rooms showed a clear prevalence of octa-mixture congeners, namely the most abundant constituent of a commercial octa-mixture known as DE-71, BDE-183.

It was observed that a certain congener profile seemed to associate with a certain room use, therefore - to better elucidate patterns between the concentration profiles and the sampled environment - a number of matrices displaying different selected variables were built to perform multivariate analysis

5.8.3 Principal component Analysis of PBDEs concentrations in indoor dust

Principal Component Analysis (PCA) is a mathematical method used to perform multivariate statistics. It serves to simplify, structure and visualise large data sets by reducing the number of initial variables to a smaller number that can still meaningfully describe the initial data set.

These new variables are a "summary" of the initial ones and are called principal components. The initial data set is presented as a matrix with n test-objects (in this case, sampled rooms) and p characteristics (variables associated to the samples, in this case PBDEs concentrations, size of the room, etc.). Such matrix swipes a p-dimensional space, after principal axis transformation it will be a q-dimensional space (where q≤p). Mathematically, this is achieved by transferring the characteristics that correlate in more than 2 dimensions into a vector space, described with an orthogonal matrix which is formed from the eigenvectors of the covariance matrix. The correlation matrix is diagonalized to decorrelate the data (the correlations are the entries that do not fall in the diagonal). In this study the visual appraisal of the data structure was done through biplot display, which consists of a vector for each row (of the rank-two matrix) and a vector for each column and the weight of each factor in the linear combination that forms the principal components was represented in a bar chart. This type of visual representation was

chosen for being revealing of variances and correlations of the variables. For more details on how to interpret this kind of plots, please refer to chapter 2.

The first matrix was built taking all individual congener concentrations (expressed in ng/g) of each room, this is done to express the amount of a certain congener in a unit weight of dust: this is a good representation of the dust composition. Data expressed in ng/g can be multiplied by the dust loading (g/m^2) of each room, to obtain the concentration of a congener over the sampled surface (ng/m^2).

The first principal component (PC 1) accounts for 62% of the variance within the dataset including first and second campaigns and its main loading in a positive direction is BDE-209 (ca.99%,); BDE-183 contributes almost exclusively to the second principal component (PC 2) and BDE-209 in a negative direction, meaning that it has an ascending trend in the sampling group (2nd sampling campaign) where the BDE-209 has a descending trend).

The effect the room use has on the variance is negligible in the first sampling campaign. This fits expectations, as rooms were only assigned on paper but not populated with their intended use. Analysing the variation over room type the distribution of variance remains virtually unchanged, i.e. the rooms at this stage can be considered equal.

After the population period, when the difference between room types is much higher (different furniture, appliances and use), it can be observed that the room occupation is almost completely responsible for the variance, showing that after a period of population a differentiation in the PBDEs distribution develops. BDE-183 is the main constituent of the first

PC, and the group of BDE-47, BDE-99 and BDE-100 have the highest load on the second component.

A clear differentiation (clustering) between microenvironments can be observed where Electronic Engineers (EE) rooms display strong variance for BDE-183 which is a marker for octa-mix, while offices and meeting rooms show smaller but still considerable variance for BDE-99 and BDE-47 which are markers for penta-mix.

A matrix containing the individual concentration of congeners for each sampled room and for each of the six most common commercial PBDEs mixtures i.e. DE-71 and Bromkal 70-5DE (penta mixture), DE-79 and Bromkal 79-8DE (octa mixture), Saytex 102E and Bromkal 82-0DE (deca mixture) (data on relative abundance of individual congeners sourced from (La Guardia et al., 2006b)) was built to obtain the biplot in Figure 5-18. PC scores obtained for each sample/commercial formulation are respectively for PC1 and PC2 72% and 24%. PC1 is driven in a positive direction by penta mixtures (orange triangles) and in a negative direction by deca mixtures (light green squares). PC2 is driven in a negative direction by one octa mixture formulation (DE-79, aqua diamond) and in a positive direction by deca mixtures. The EE rooms in this study occupy a region of component space that extends from the middle upper left corner (occupied by deca mixtures) down to the far lower right corner (occupied by the octa mixture DE-79), their positions being most influenced by the relative contributions of octa and deca formulations. O and MR span mainly over PC1, showing that the highest variability in concentration for the dust of these two room types happens over deca- and penta mixtures.
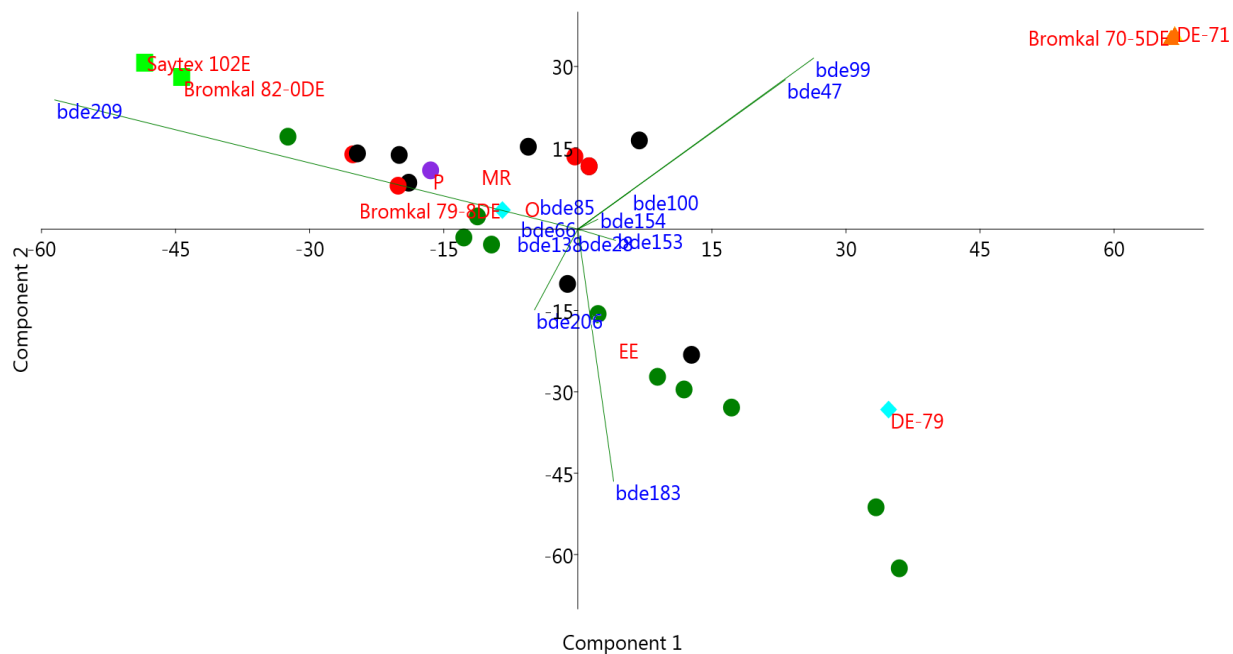
Figure 5-18 Bi-plot of the first 2 principal components of the second sampling campaign. The green dots represent the EE rooms, the red dots the MR, the purple dot is the Printer room and the black dots are the O. Light green squares are the two main commercial deca mixtures, aqua diamonds the two main octa mixtures and orange triangles represent the two main penta mixtures.

Offices and meeting rooms' variance regions overlap for most of the total area. This is in line with the similarity between offices and meeting rooms, that are carpeted, as well as having similar furniture and similar electronic appliances (with the exception of laptops which are carried inside the room occasionally by the meeting attendees). It should also be noted that these two room types tend to cluster because the majority of the electronic equipment and furniture come from the same suppliers. In the first sampling campaign BDE-209 represented the most abundant congener in the sampled rooms;

thus the fact that after population of the room this same congener remains the most stable in concentration across different rooms (uncorrelated to room use) suggests that its main source is the initial building and insulating material and carpeting. This could be considered a baseline signature that is more related to the building itself and the type of building material used and less to the individual room use. For the 1st sampling concentration matrix, it appears that highest concentrations are mainly caused by the Deca-mixture in the building material, which would explain why BDE-209 does not increase significantly after population (as it is coming from the building itself rather than installed appliances and daily use, and thus occupancy of the building does not introduce significant additional sources of BDE-209). A very recent study analysed a range of building materials used in Europe and found that of all PBDEs, BDE-209 is indeed the most abundant (Vojta et al., 2017), reaching concentrations of 600,000 ng/g in a sample of pipe insulation. The kinetics of release from new carpet, upholstery, and furniture is likely to have a higher release rate in the initial period after installation and to plateau after it, as modelled by (Batterman et al., 2010).

The proportions of the different PBDE congeners present in samples can give an indication of their origin: a way to understand to what extent these two congeners come from a commercially used Penta-BDE formulation is to observe the ratio between BDE-47 and BDE-99 and how it varies with respect to the reference values found in commercially available Penta-BDE formulations.

The BDE47:99 ratios in our dust samples are comparable to past literature values Table 5-10, Table 5-11, averaging at 0.65 for all room types during the second campaign. In Figure 5-19 the

proportion of the different congeners compared to commercially available penta and octa mix (La Guardia et al., 2006a) is reported for where a pattern was most notable. In the 1st sampling campaign, all rooms show a clear correspondence with deca-mix proportions (Figure 5-19a); the dust collected in the 2nd sampling campaign in the EE rooms shows a congener pattern that is similar to octa-mix (Figure 5-19b). Meeting rooms (MR) and Offices (O) don't show a recognizable pattern but are both different for the EE rooms and similar to each other (Figure 5-19c): this is in line with the similar use between MR and O as opposed to EE laboratories.

Table 5-10 Summary of BDE-47:BDE-99 ratios measured in dust samples in previous studies

Origin of the study	Ratio BDE-47:BDE-99
UK (Harrad et al., 2008b)	0.73
US (Lagalante et al., 2009)	0.62
Portugal (Cunha et al., 2010)	0.6
Canada (Wilford et al., 2005)	0.59
New Zealand (Harrad et al., 2008b)	0.41
USA (Harrad et al., 2008b)	0.58
Japan (Suzuki et al., 2009)	0.64
Germany (Fromme et al., 2009)	0.69

Table 5-11 BDE-47:BDE-99 ratios measured in dust samples in this study after occupation (2nd sampling campaign).

BDE47:99 Ratio	Room type
0.98	EE
0.64	EE
0.60	EE
0.58	EE
0.74	EE
0.56	EE
0.83	EE
0.85	MR
0.70	EE
0.68	EE
0.64	EE
0.87	O
0.45	O
0.85	O
0.52	MR
0.69	O
0.46	P
0.55	O
0.34	O
0.60	O
0.60	O
0.60	MR
0.55	MR
Tot avg	0.65
EE avg	0.69
O avg	0.62
MR avg	0.63
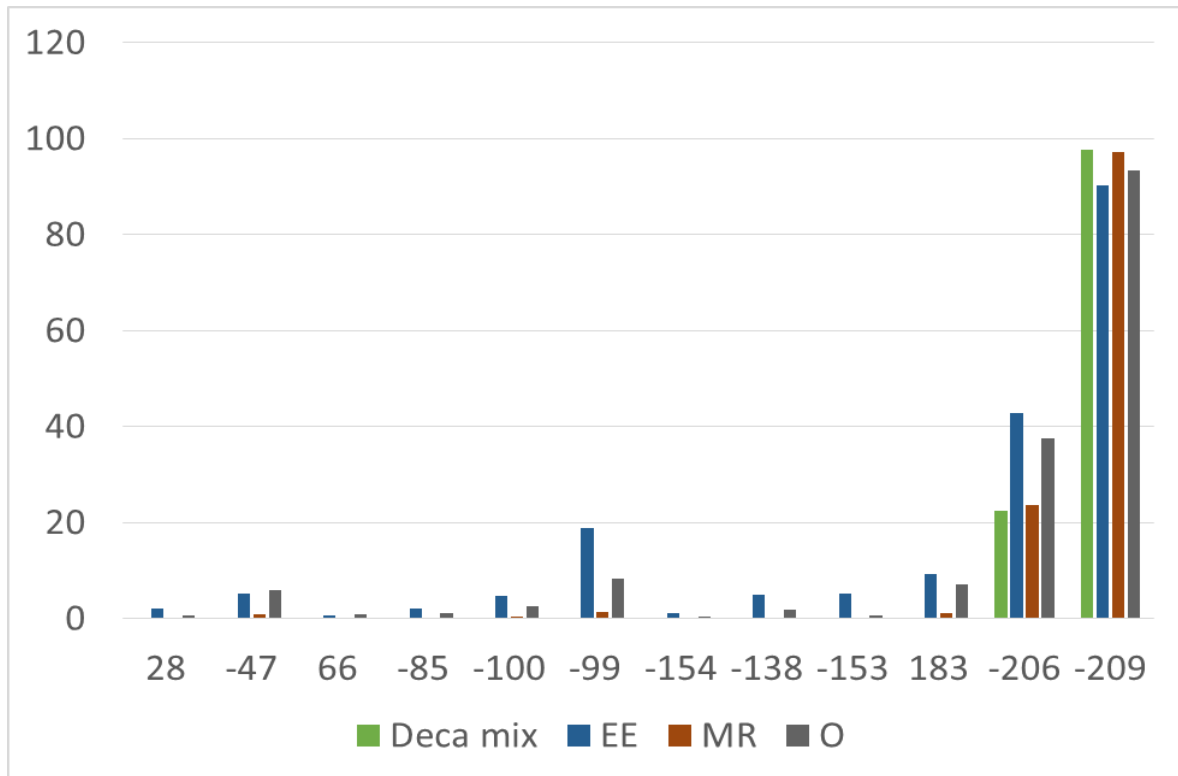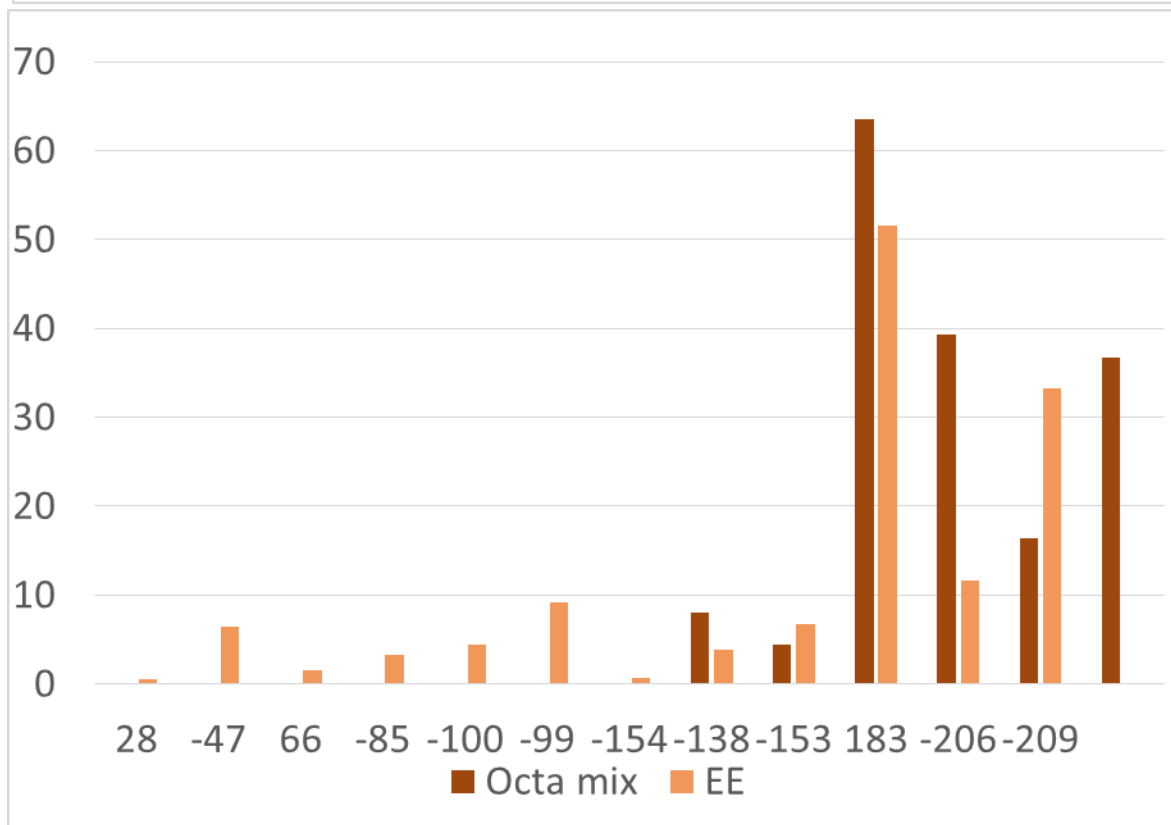
c)
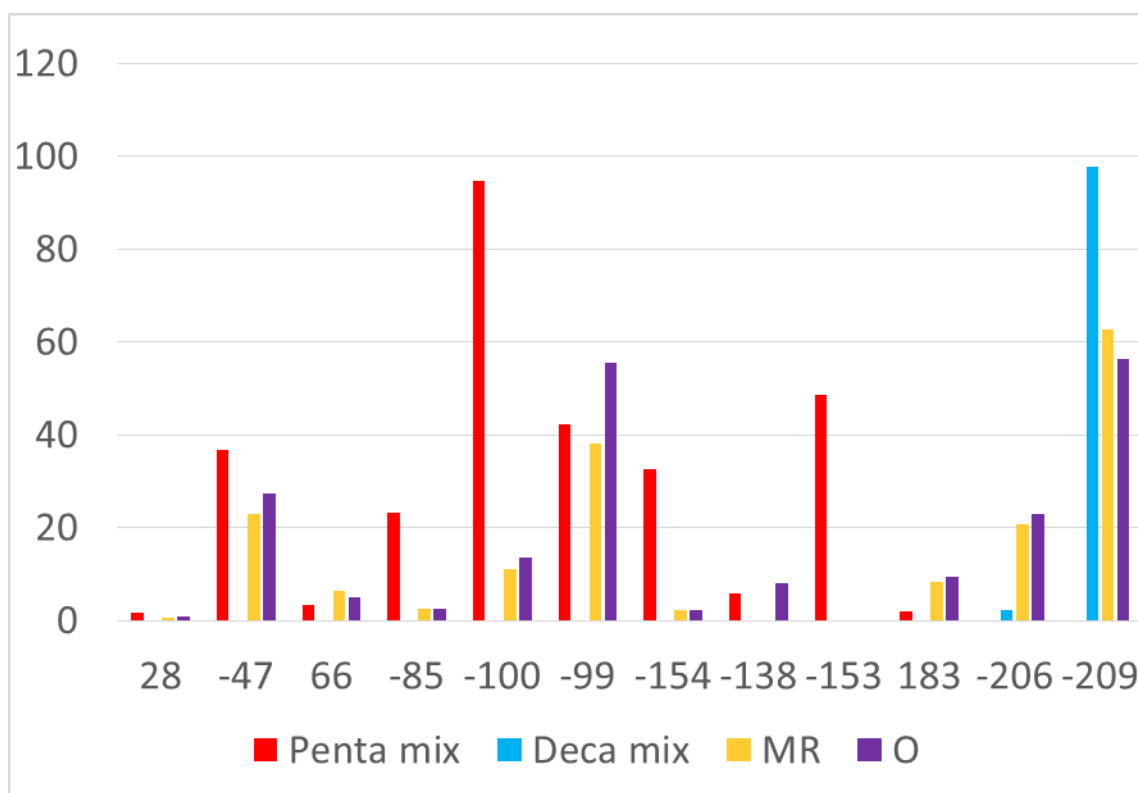
Figure 5-19 Proportion of the different congeners measured in the sampled rooms (during the 2nd campaign) compared to commercially available penta, octa mix and deca mix. Compounds that appeared in proportions below 1% (BDE- 47, 66, 85, 100, 99, 154, 153) were multiplied by 10 for better visibility.

5.8.4 BDE signature vs. room characteristics

In this section the influence of different characteristics of the sampled rooms on the PBDEs concentration is evaluated. Data on each room during the 2nd sampling campaign was collected to form a matrix of n characteristics by p samples containing the room characteristics (number of appliances, chairs, windows, etc…) and the compound specific concentration for tri-deca-BDEs and the principal components of the resulting matrix plotted in a biplot (Figure 5 20) where the characteristics (room characteristics and PBDE concentrations) are represented as vectors labelled at their end points.
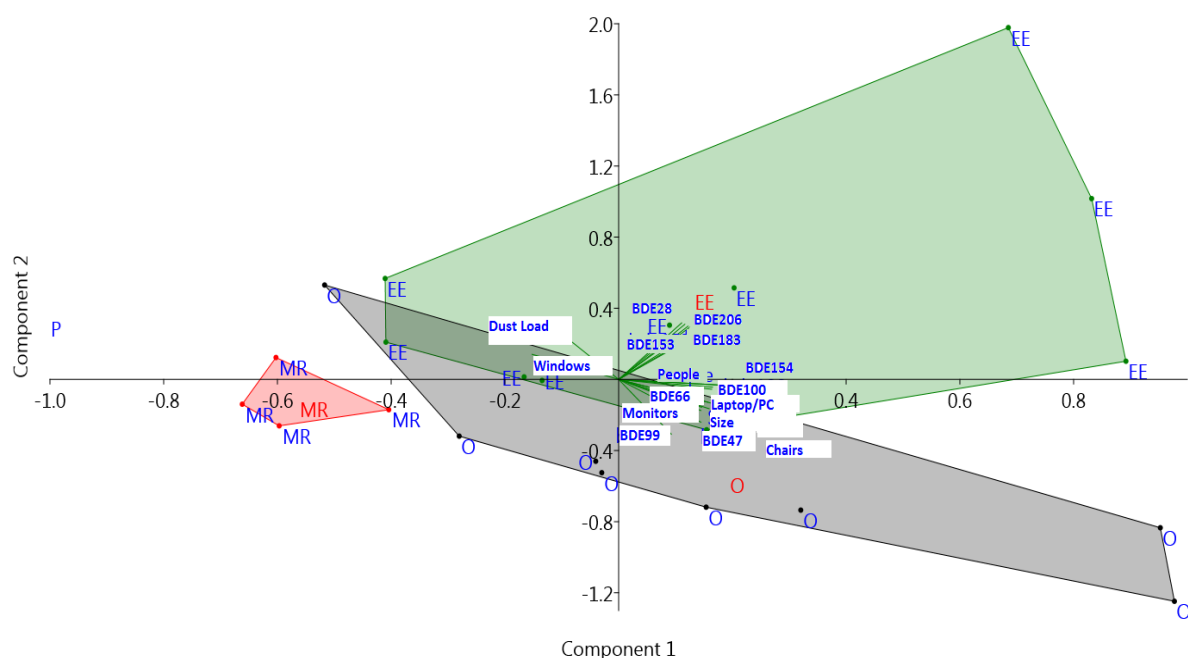
Figure 5-20 PCA of room characteristics, dust load and compound specific concentration of tri-deca-BDEs. Electronic Engineer room=green, Meeting Room=red, Offices=black, Printer Room= purple

To avoid overpopulation of the plot, the vectors indicating the sample number were not represented with a green line but with a coloured dot, the colour representing the room type. Some features of the data that can be seen in this biplot are the following. The standard deviations of BDE-183 (a marker for the octa-mix), BDE-154, and BDE-100 are larger over the quadrant populated by EE rooms, while BDE-100, -47 and -99 positively follow the number of chairs, phones and laptops (more present in offices). The number of windows is the room characteristic with the highest load on the first component and most of the analysed congeners showed a large negative deviation, meaning that concentrations of these congeners tend to decrease when the window number (and the dust loading) increases. This "dilution effect" caused by the amount of dust accumulated in a room, has been documented in past literature

((Batterman et al., 2010), (Harrad et al., 2008a)) with a negative correlation between dust loading and BFR concentration. BDE-47 showed a strong correlation to the number of sponge chairs and monitors which show a positive loading in the first component, while windows and dust have the highest negative loading. Interestingly the second component shows a decreasing pattern in the loadings of congeners that follows the decrease in bromination and similar loadings to the dust load. This can be explained considering the partition kinetics of congeners between air and dust is strongly related to the size of the molecule (and to the charge distribution on the potential energy surface): the smaller the molecule the more likely it is to volatilise in air, the larger the molecule, the more it will remain in the particulate phase (Wilford et al., 2005).

It should be noted that this PCA can only highlight correlations between features that are quantifiable. Little can be said about the main source of contamination in the EE rooms, because it is likely to be related to the large variety of electronic equipment being used with a high rotation rate by the electronic engineers.

5.9 Summary and conclusions

This chapter describes:

- The development of a novel interface to connect a GC to an ICP-MS and perform compound specific analysis of PBDEs

- The indoor dust sampling of a building of new construction followed by a sampling of the same environment after a period of population

- The use of a fast, inexpensive extraction technique that provides the means to semi-quantitatively analyse PBDEs in dust without the use of expensive solvents or internal standards

- The use of a traditional GC-HRMS technique to confirm the identity of the compounds detected with GC-ICP-MS

The statistical evaluation of PBDE congener signatures before and after population and between different rooms, considering their use and furniture.

A brief summary of the findings of this study is reported below:

- as a general comparison, the average concentration of PBDEs in the sampled rooms increased on average by ca. 30% after the population period, this increase had statistical significance for all congeners except BDE-209.

- BDE-209 and BDE-206 (deca-mix) characterised the dust signature for the first sampling campaign, showing that building material used in the new rooms contained deca-mix

- in the second campaign, BDE-47 and BDE-99 dominated the congener profile of most offices and meeting rooms: these two congeners are the main components of the two most common penta mixtures with respectively 38% w/w (BDE-47) and 49% w/w (BDE-99) for DE-71 and 43% w/w (BDE-47) and 45% w/w (BDE-99) for Bromkal 70-5DE (La

Guardia et al., 2006b) with their main use being in PU foam (Hale et al., 2002b). This foam is used to fill sponge chairs present in these rooms (Wilford et al., 2005).

- BDE-183 strongly characterised EE rooms: this congener is a marker for octa-mix (42% w/w in Bromkal 79-8 DE)

- When PBDE concentrations are factorised within each room, offices and meeting rooms showed similarities in the congener pattern in contrast to EE rooms which showed a different congener signature. The cause of this can be ascribed to the fact that both room types (MR and O) are similarly equipped with electric and electronic appliances, therefore the frequency with which certain PBDEs are found in dust is similar, as for the EE rooms showing a different profile, this can be ascribed to the substantially different use of these rooms, where engineers take apart, solder and store internal circuits, printed circuit boards and other electronic components.

6 Summary

Brominated Flame Retardants have been used extensively in a variety of consumers' goods that are subject to heating up during use or that contain or are made of flammable materials (chiefly electric and electronic equipment, furniture and upholstery). Among these, Polybrominated Diphenyl Ethers are one of the most widespread class of BFRs. After decades of use, concerns about their environmental impact were raised and over the first decade of the 21st century, two of the most used formulations (penta-mixture and octa-mixture) were banned in the EU and other jurisdictions. Moreover, the last standing commercial formulation (decaBDE) has been subject to restrictions since 2008. Since the enforcement of these restrictions and bans, PBDEs – for the most part – are no longer added intentionally to new goods. Nonetheless, they are still found in notable amounts- but not enough to provide flame retardancy- in polymers and polymeric fibres. This is likely attributable to recycling processes that supply reground waste plastic to goods manufacturers for them to mix in variable amounts with new polymers in order to produce new goods. If no control is applied on the quality of the polymer waste sourced to make new goods, with time and recycling generations following one another, these pollutants will be present in lower and lower amounts (diluted through mixing with new plastics) but also in wider and wider ranges of goods. Relative to the life cycle of many of these consumers' goods (cars, TV sets, computers, printers etc…), the regulation restricting the use of PBDEs are still recent and it is reasonable to assume the PBDEs contained in them survived 1 or 2 generations, so that an increase in the average concentration of unwanted PBDEs in waste plastic can be

expected. For this reason the European Commission's Restriction of Hazardous Substances (RoHS) and WEEE directives set low POP concentration limits (LPCLs) for WEEE at 0.1% for the most common BFRs, including PBDEs. If the WEEE plastics exceed the LPCLs, they cannot be recycled. These limits are however, difficult to enforce due to the sheer volume and vastly diverse provenance of waste items. In addition, socioeconomic arguments make the issue more complex: countries that perform sorting of waste material are characterised –to a large extent- by economies that- although quickly developing- have not had the time or the political stability to grow the necessary network of infrastructure and know-how that would allow the technological challenges required for controlled waste management to be overcome. Moreover, even in countries that have advanced technological means, the cost of the required chemical analysis are not covered by the value of the analysed item. For these reasons analytical techniques that enable evaluation of waste compliance with regulatory limits, accurately and repeatedly for high volumes of samples at relatively low cost and minimal to no use of consumables are highly desirable.

Given the above, the main objective of this study was to evaluate to what extent techniques that do not require lengthy sample preparations can provide valuable data (selective and sensitive enough for the purposes of the investigation) to reduce the flow of PBDE-contaminated waste into PBDE-free waste streams so that new goods can be manufactured without toxic substances polluting them and PBDE-containing articles can be isolated and suitably treated to be reclaimed.

Furthermore in view of the environment in which these techniques are most likely to be used, an additional liquid sampling method that analyses dust extracts in working environments using relatively small amounts of solvents and preparation time was developed: this was done to provide a suite of economically viable options for sorting plants not only to analyse the waste but also to monitor the working conditions of the employees working in them.

The achievements of this study are:

- a matrix matched calibration combined with a mathematical model that corrects for the effect of non-ideal sample thicknesses on the detected Br concentration was developed for **XRF handheld spectrometers**

- This calibration was then used to quantitatively measure with XRF Br in WEEE, Toys and FCAs as a metric of BFR content and the results validated against **LA-ICP-MS**. In each of the investigated consumers' categories, unintentionally added BFRs were found in a number of samples.

- The results obtained were then compared with semi-quantitative compound-specific data (obtained with **TD-GC-MS**) to investigate the relative proportions of different BFRs in each sample

- Toys and FCAs were also analysed with LA-ICP-MS to measure REEs (used to different extents in the production of EEE) and other typical inorganic fillers (Ca, Ti etc…)

- The REEs concentrations were combined with the TD-GC-MS data and with **FTIR** data (acquired to identify the polymer type of each sample) and summarized with PCA. The trends and relationships between certain REEs (used in a particular class of EEE) and certain BFRs gave an insight into how different waste streams contribute to the production of new goods.

- The results from this evaluation show that the ABS waste flow (chiefly laptops and copying/printing equipment) is the main contributor into the plastic material used to manufacture toys and FCAs.

- A **DIP-HRMS** method that reliably quantifies BDE-209 was developed and validated using ABS solid reference materials with Direct Insertion Probe (DIP) in combination with magnetic sector high resolution mass spectrometry (HRMS).

- This method was then used to analyse a set of toys and FCAs samples.

- The potential for using a cold plasma ionisation source (**DART** source) coupled to a high-resolution accurate-mass mass spectrometer (**Q Exactive Focus**) was explored: a method was developed to analyse BDE-209 in ABS and unequivocally identify it solely with accurate (meaning that the mass uncertainty between measured and theoretical is such that identification is unequivocal) mass determination.

- It was possible to detect BDE-209 in amounts as low as the LPCLs (0.1% w/w).

- A calibration curve was built using the nine reference materials spanning from 0 to 15% w/w of BDE-209: linearity was satisfactory on the [M-Br]$^-$ product ion.

- **GC-ICP-MS** was shown to provide reliable data for PBDEs in indoor dust

- The method was then applied to determine the concentrations of PBDEs in dust both before and after occupation and furnishing of a new office building. The results showed that furnishing and occupation significantly increased concentrations of Penta- and Octa-BDE congeners, while those of Deca-BDE remained steady indicating building materials to be the principal of this congener in the building tested;

- Results also showed substantial variation in the PBDE congener pattern depending on the room use and other parameters.

In summary, XRF proved to be the ideal technique for routine screening of plastic material used for recycling because it is fast, it can be applied in situ and – being able to accurately quantify Br- it is more likely to give false positive than false negative results for BFRs which is acceptable for this application.

DIP-HRMS or DART-HRAM showed potential for the compound specific analysis of those samples that present a Br concentration exceeding the estimated equivalent BFR concentration. It can be envisaged that those samples are sent to a laboratory for a rapid compound specific analysis that does not require sample preparation of the BFRs present, the results of which can

be communicated in a relatively short time. Figure 6-1 is a graphic representation of the cost (intended as a combination of hardware cost, consumables and labour) of each of the techniques explored in this thesis versus the quality/ depth of information these techniques can provide, Table 6-1 gives a summary of each technique's pro and contra, application range, target and limitations.
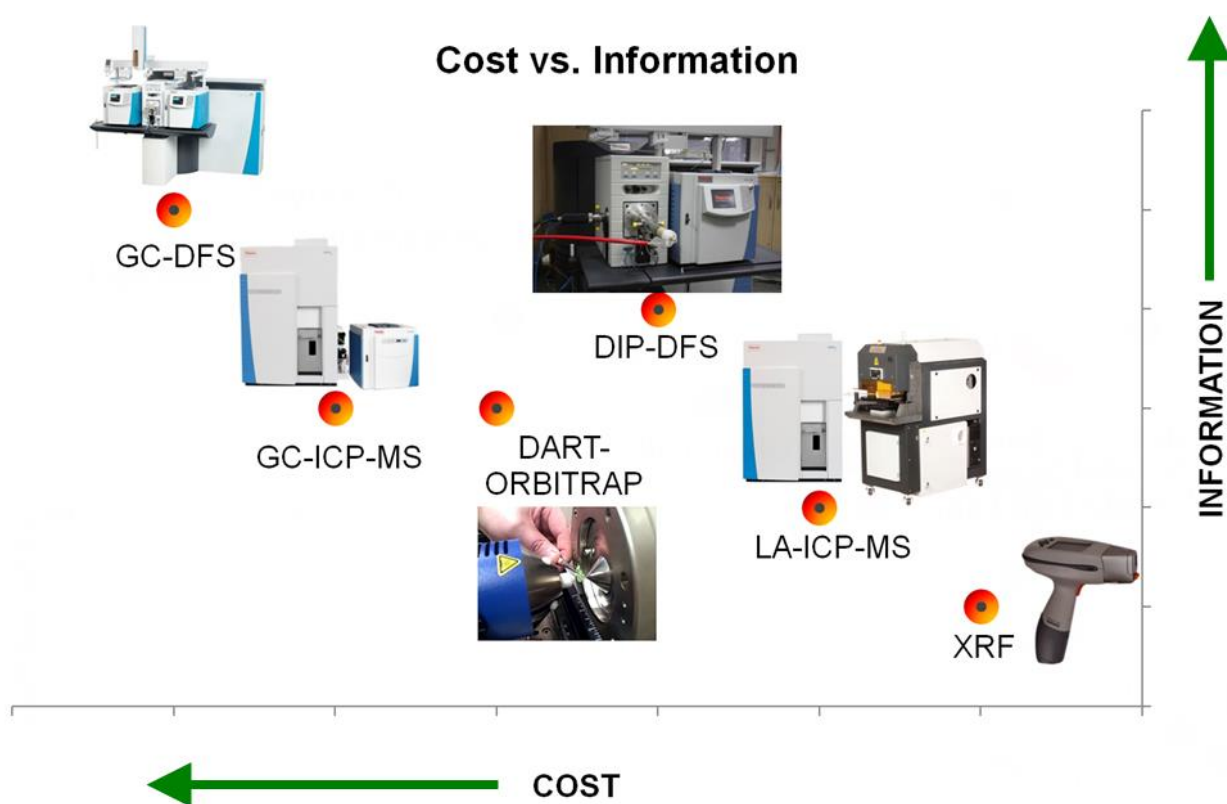
Figure 6-1 graphic comparison of analytical techniques information benefits against financial cost. Axes are in arbitrary units. Each technique was graded for hardware cost, sample preparation complexity, consumables expenses for the "cost" score and for BFRs identification accuracy, BFR quantification accuracy, sensitivity for the "information" axis.

Based on this overview it is desirable that solid sampling techniques (like DART-HRMS and DIP-HRMS) be studied more in depth, expanding their field of application to other BFRs and other matrices and developing easy to use calibration routines. These techniques are the most promising for their sensitivity and their compound-specific determination capabilities.

Table 6-1 Summary of *pro et contra* and application ranges of each technique explored in this study

	Target	Limitations	Sensitivity	Operation range
XRF	Br in solid samples	Doesn't provide compound specific information	0.0011% w/w Br	0.0011% - 12% w/w Br
LA-ICP-MS	Br in solid samples	Doesn't provide compound specific information. Requires cutting a small piece of sample	0.0004% w/w Br	0.0004% - 12% w/w Br
DART-HRAM-MS	PBDEs in solid samples	Requires SRM for compound specific quantification	In this study only used for compound identification	0.1%-15% w/w BDE209
DIP-HRmsMS	PBDEs in solid samples	Requires SRM for compound specific quantification; requires accurate (and time consuming) sample weighing.	0.112 mg kg-1 BDE209	0.112 mg kg-1- 2% w/w BDE209

| GC-ICP-MS | PBDEs in dust extracts | Requires sample preparation | Between 0.1 and 1.1 ppb for most common PBDEs | 0.1 and 102000 ppb for 12 most common PBDEs |
| GC-HRmsMS | PBDEs in dust extracts | Requires sample preparation and expensive equipment | In this study only used for compound identification | - |

References

2009. Governments unite to step-up reduction on global DDT reliance and add nine new chemicals under international treaty.

(EC), C. R. 2008. No 282/2008 of 27 March 2008 on recycled plastic materials and articles intended to come into contact with foods and amending Regulation (EC) No 2023/2006. *Off J Eur Union L. 86:9 and J, R, E.*

(UNEP)-CHEMICALS., U. N. E. P. 2006. Report of the Persistent Organic Pollutants Review Committee: Risk profile on commercial pentabromodiphenyl ether Geneva: United Nations Environment Programme.

(UNEP)-CHEMICALS., U. N. E. P. 2010. *Technical review of the implications of recycling commercial Penta and Octabromodiphenyl ethers. Stockholm Convention document for 6th POP Reviewing Committee meeting* Geneva. , UNEP/POPS/POPRC.6/2.

(UNEP)-CHEMICALS., U. N. E. P. 2017. Guidance for the inventory of polybrominated diphenyl ethers (PBDEs) listed under the Stockholm Convention on Persistent Organic Pollutants.

ABDALLAH, M. A.-E., IBARRA, C., NEELS, H., HARRAD, S. & COVACI, A. 2008. Comparative evaluation of liquid chromatography–mass spectrometry versus gas chromatography–mass spectrometry for the determination of hexabromocyclododecanes and their degradation products in indoor dust. *Journal of Chromatography A,* 1190**,** 333-341.

ABDALLAH, M. A. G. A.-E. 2010. *Investigating the sources and magnitude of human exposure to halogenated organic pollutants using advanced methods for environmental analysis.* University of Birmingham.

ADAMEC. 2017. *Recycling Elektro-Elektronikschrott* [Online]. Available: http://www.adamec.de/ [Accessed 18 September 2017].

ALAEE, M., ARIAS, P., SJODIN, A. AND BERGMAN, A. 2003. An overview of commercially used brominated flame retardants, their applications, their use patterns in different countries/regions and possible modes of release. *Environment International,* 29**,** 683-9.

ALLEN, J. G., MCCLEAN, M. D., STAPLETON, H. M. & WEBSTER, T. F. 2008a. Critical factors in assessing exposure to PBDEs via house dust. *Environment international,* 34**,** 1085-1091.

ALLEN, J. G., MCCLEAN, M. D., STAPLETON, H. M. & WEBSTER, T. F. 2008b. Linking PBDEs in house dust to consumer products using X-ray fluorescence. *Environmental science & technology,* 42**,** 4222-4228.

ALLEN, V., KALIVAS, J. H. & RODRIGUEZ, R. G. 1999. Post-consumer plastic identification using Raman spectroscopy. *Applied spectroscopy,* 53**,** 672-681.

ANNE WEGNER, C. S., STEPHANIE HANNING,CHRISTIAN MANS UND MARTIN KREYENSCHMIDT 2010. Brom in Polymeren mit ICP-MS analysieren. *In:* PLATTHAUS, M. (ed.). http://www.laborpraxis.vogel.de [accessed 26 July 2018].

ATSDR 2017. Toxicological Profile for Polybrominated Diphenyl Ethers (PBDEs).

AUSTIN, C., HARE, D., RAWLING, T., MCDONAGH, A. M. & DOBLE, P. 2010. Quantification method for elemental bio-imaging by LA-ICP-MS using metal spiked PMMA films. *Journal of Analytical Atomic Spectrometry,* 25**,** 722-725.

BABAYEMI, J., SINDIKU, O., OSIBANJO, O. & WEBER, R. 2015. Substance flow analysis of polybrominated diphenyl ethers in plastic from EEE/WEEE in Nigeria in the frame of Stockholm Convention as a basis for policy advice. *Environmental Science and Pollution Research,* 22**,** 14502-14514.

BAIGUINI, A., COLLETTA, S. & REBELLA, V. 2011. Materials and articles intended to come into contact with food: evaluation of the rapid alert system for food and feed (RASFF) 2008-2010. *Igiene e sanita pubblica,* 67**,** 293-305.

BAIRD, P., HERMAN, H., MORTIMORE, W. & STEVENS, G. 2010. A new rapid analysis method for fire retardants in polymers. *InterFlam, Interscience Communications.* University of Nottingham Nottingham, UK.

BALLESTEROS-GÓMEZ, A., DE BOER, J. & LEONARDS, P. E. 2013. Novel analytical methods for flame retardants and plasticizers based on gas chromatography, comprehensive two-dimensional gas chromatography, and direct probe coupled to atmospheric pressure chemical ionization-high resolution time-of-flight-mass spectrometry. *Analytical chemistry,* 85**,** 9572-9580.

BART, J. 2001. Direct solid sampling methods for gas chromatographic analysis of polymer/additive formulations. *Polymer testing,* 20**,** 729-740.

BATTERMAN, S., GODWIN, C., CHERNYAK, S., JIA, C. & CHARLES, S. 2010. Brominated flame retardants in offices in Michigan, USA. *Environment international,* 36**,** 548-556.

BECKHOFF, B., KANNGIEßER, B., LANGHOFF, N., WEDELL, R. & WOLFF, H. 2007. *Handbook of practical X-ray fluorescence analysis*, Springer Science & Business Media.

BFIP 2011. Study on waste related issues of newly listed POPs and candidate POPs. Beratungsgesellschaft fuer integrierte Problemloesungen.

BIRNBAUM, L. S. A. S., D. F. 2004. Brominated flame retardants: Cause for concern? *Environmental Health Perspectives,* 112**,** 9-17.

BOULESTEIX, A. L. 2005. A NOTE ON BETWEEN-GROUP PCA. *International Journal of Pure and Applied Mathematics,* 19**,** 359-366.

CHEN, S. J., MA, Y. J., WANG, J., CHEN, D., LUO, X. J. & MAI, B. X. 2009. Brominated flame retardants in children's toys: concentration, composition,and children's exposure and risk assessment. *Environ SciTechnol,* 43**,** 4200–4206.

CHEN, S. J., MA, Y. J., WANG, J., TIAN, M., LUO, X. J., CHEN, D. & MAI, B. X. 2010. Measurement and human exposure assessment of brominated flame retardants in household products from South China. *J Hazard Mater,* 176**,** 979–984.

CHRISTIANSSON, A., TECLECHIEL, D., ERIKSSON, J., BERGMAN, Å. & MARSH, G. 2006. Methods for synthesis of nonabromodiphenyl ethers and a chloro-nonabromodiphenyl ether. *Chemosphere,* 63**,** 562-569.

CODY, R. B., LARAMÉE, J. A. & DURST, H. D. 2005. Versatile new ion source for the analysis of materials in open air under ambient conditions. *Analytical chemistry,* 77**,** 2297-2302.

COMMISION, E. 1994. Environmental Health Criteria 162: Brominated Diphenyl Ethers. Geneva.

COMMISION, E. 2002. European Union Risk Assessment Report. Luxembourg: Office for Official Publications of the European Communities.

COMMISION, E. 2003. Risk Profile and Summary Risk Assessment Report for Octabromodiphenyl ether. Luxembourg: Office for Official Publications of the European Communities.

COMMISION, E. 2006. Commission Regulation (EC) No 1881/2006 of 19 December 2006 setting maximum levels for certain contaminants in foodstuff. 2006R1881-EN-01.09. 2014-014.001-1.

COMMISSION, E. 2009. Directive 2009/48/EC of the European Parliament and of the Council of 18 June 2009 on the safety of toys.

COMMISSION, E. 2015. COMMUNICATION FROM THE COMMISSION TO THE EUROPEAN PARLIAMENT, THE COUNCIL, THE EUROPEAN ECONOMIC AND SOCIAL COMMITTEE AND THE COMMITTEE OF THE REGIONS Closing the loop - An EU action plan for the Circular Economy.

CONVENTION, S. Governments unite to step-up reduction on global DDT reliance and add nine new chemicals under international treaty. COP4, 2009.

COVACI, A., VOORSPOELS, S. & DE BOER, J. 2003a. Determination of brominated flame retardants, with emphasis on polybrominated diphenyl ethers (PBDEs) in environmental and human samples--a review. *Environ Int,* 29**,** 735-56.

COVACI, A., VOORSPOELS, S. & DE BOER, J. 2003b. Determination of brominated flame retardants, with emphasis on polybrominated diphenyl ethers (PBDEs) in environmental and human samples—a review. *Environment International,* 29**,** 735-756.

COVACI, A., VOORSPOELS, S., RAMOS, L., NEELS, H. & BLUST, R. 2007a. Recent developments in the analysis of brominated flame retardants and brominated natural compounds. *J Chromatogr A,* 1153**,** 145-71.

COVACI, A., VOORSPOELS, S., RAMOS, L., NEELS, H. & BLUST, R. 2007b. Recent developments in the analysis of brominated flame retardants and brominated natural compounds. *Journal of chromatography A,* 1153**,** 145-171.

CUNHA, S., KALACHOVA, K., PULKRABOVA, J., FERNANDES, J., OLIVEIRA, M., ALVES, A. & HAJSLOVA, J. 2010. Polybrominated diphenyl ethers (PBDEs) contents in house and car dust of Portugal by pressurized liquid extraction (PLE) and gas chromatography–mass spectrometry (GC–MS). *Chemosphere,* 78**,** 1263-1271.

DANYUSHEVSKY, L., ROBINSON, P., GILBERT, S., NORMAN, M., LARGE, R., MCGOLDRICK, P. & SHELLEY, M. 2011. Routine quantitative multi-element analysis of sulphide minerals by laser ablation ICP-MS: Standard development and consideration of matrix effects. *Geochemistry: Exploration, Environment, Analysis,* 11**,** 51-60.

DARNERUD, P. O. 2003. Toxic effects of brominated flame retardants in man and in wildlife. *Environment International,* 31**,** 841-53.

DE LOS CONTAMINANTES, C. D. E. & PERSISTENTES, O. ÉTER DE OCTABROMODIFENILO COMERCIAL.

DE WIT, C. A., ALAEE, M. & MUIR, D. C. G. 2006. Levels and trends of brominated flame retardants in the Arctic. *Chemosphere,* 64**,** 209-33.

DIGANGI, J., STRAKOVA, J. & BELL, L. 2017. POPs Recycling Contaminates Children's Toys with Toxic Flame Retardants.

DIRTU, A. C., RAVINDRA, K., ROOSENS, L., VAN GRIEKEN, R., NEELS, H., BLUST, R. & COVACI, A. 2008. Fast analysis of decabrominated diphenyl ether using low-pressure gas chromatography–electron-capture negative ionization mass spectrometry. *Journal of Chromatography A,* 1186**,** 295-301.

DIWAKAR, P. K., HARILAL, S. S., LAHAYE, N. L., HASSANEIN, A. & KULKARNI, P. 2013. The influence of laser pulse duration and energy on ICP-MS signal intensity, elemental fractionation, and particle size distribution in NIR fs-LA-ICP-MS. *Journal of analytical atomic spectrometry,* 28**,** 1420-1429.

DONOHUE, D. & HARRISON, W. 1975. Radiofrequency cavity ion source in solids mass spectrometry. *Analytical Chemistry,* 47**,** 1528-1531.

ESWI, C. 2011. Study on waste related issues of newly listed POPs and candidate POPs. *Service request under the framework contract,* No ENV.G.4/FRA/2007/0066.

EVANS, E. H. & GIGLIO, J. J. 1993. Interferences in inductively coupled plasma mass spectrometry. A review. *Journal of Analytical Atomic Spectrometry,* 8**,** 1-18.

FROMME, H., KÖRNER, W., SHAHIN, N., WANNER, A., ALBRECHT, M., BOEHMER, S., PARLAR, H., MAYER, R., LIEBL, B. & BOLTE, G. 2009. Human exposure to polybrominated diphenyl ethers (PBDE), as evidenced by data from a duplicate diet study, indoor air, house dust, and biomonitoring in Germany. *Environment International,* 35**,** 1125-1135.

GABRIEL, K. R. 1971. The biplot graphic display of matrices with application to principal component analysis. *Biometrika,* 58**,** 453-467.

GALLEN, C., BANKS, A., BRANDSMA, S., BADUEL, C., THAI, P., EAGLESHAM, G., HEFFERNAN, A., LEONARDS, P., BAINTON, P. & MUELLER, J. F. 2014. Towards development of a rapid and effective non-destructive testing strategy to identify brominated flame retardants in the plastics of consumer products. *Sci Total Environ,* 491-492**,** 255-65.

GONZALEZ-GAGO, A., PRÖFROCK, D. & PRANGE, A. 2015. Comparison of GC–NCI MS, GC–ICP-MS, and GC–EI MS–MS for the determination of PBDEs in water samples according to the Water Framework Directive. *Analytical and bioanalytical chemistry,* 407**,** 8009-8018.

GONZALEZ, J., MAO, X., ROY, J., MAO, S. & RUSSO, R. 2002. Comparison of 193, 213 and 266 nm laser ablation ICP-MS. *Journal of Analytical Atomic Spectrometry,* 17**,** 1108-1113.

GOUIN, T., THOMAS, G. O., CHAEMFA, C., HARNER, T., MACKAY, D. & JONES, K. C. 2006. Concentrations of decabromodiphenyl ether in air from Southern Ontario: implications for particle-bound transport. *Chemosphere,* 64**,** 256-61.

GUIDELINE, I. H. T. 2005. Validation of analytical procedures: text and methodology. *Q2 (R1),* 1.

GUILLONG, M. & GÜNTHER, D. 2002. Effect of particle size distribution on ICP-induced elemental fractionation in laser ablation-inductively coupled plasma-mass spectrometry. *Journal of Analytical Atomic Spectrometry,* 17**,** 831-837.

GUILLONG, M., HORN, I. & GÜNTHER, D. 2003. A comparison of 266 nm, 213 nm and 193 nm produced from a single solid state Nd: YAG laser for laser ablation ICP-MS. *Journal of analytical atomic spectrometry,* 18**,** 1224-1230.

GUZZONATO, A., MEHLMANN, H., SCHLUETER, H.J. 2017a. *Heated Transfer Line*. US patent application US 20170184552.

GUZZONATO, A., PUYPE, F. & HARRAD, S. J. 2017b. Evidence of bad recycling practices: BFRs in children's toys and food-contact articles. *Environ Sci Process Impacts,* 19**,** 956-963.

HAARMAN, A. & GASSER, M. 2016. Managing hazardous additives in WEEE plastic from the Indian informal sector. *A study on applicable identification & separation methods. Sustainable Recycling Industries, Swiss Federal Laboratories for Materials Science and Technology, ISBN***,** 978-3.

HACALOGLU, J. 2012. Direct Insertion Probe Mass Spectrometry of Polymers. *In:* HAKKARAINEN, M. (ed.) *Mass Spectrometry of Polymers – New Techniques.* Berlin, Heidelberg: Springer Berlin Heidelberg.

HALE, R. C., KIM, S. L., HARVEY, E., LA GUARDIA, M. J., MAINOR, T. M., BUSH, E. O. & JACOBS, E. M. 2008. Antarctic research bases: Local sources of polybrominated diphenyl ether (PBDE) flame retardants. *Environmental Science & Technology,* 42**,** 1452-572.

HALE, R. C., LA GUARDIA, M. J., HARVEY, E. & MAINOR, T. M. 2002a. Potential role of fire retardant-treated polyurethane foam as a source of brominated diphenyl ethers to the U.S. environment. *Chemosphere,* 46**,** 729-35.

HALE, R. C., LA GUARDIA, M. J., HARVEY, E. & MAINOR, T. M. 2002b. Potential role of fire retardant-treated polyurethane foam as a source of brominated diphenyl ethers to the US environment. *Chemosphere,* 46**,** 729-35.

HAMMER, Ø., HARPER, D. & RYAN, P. 2001. Paleontological statistics software: Package for education and data analysis. *Palaeontologia Electronica*.

HARNER, T. & SHOEIB, M. 2002. Measurements of octanol– air partition coefficients (K OA) for polybrominated diphenyl ethers (PBDEs): Predicting partitioning in the environment. *Journal of Chemical & Engineering Data,* 47**,** 228-232.

HARRAD, S., IBARRA, C., ABDALLAH, M. A.-E., BOON, R., NEELS, H. & COVACI, A. 2008a. Concentrations of brominated flame retardants in dust from United Kingdom cars, homes, and offices: causes of variability and implications for human exposure. *Environment International,* 34**,** 1170-1175.

HARRAD, S., IBARRA, C., DIAMOND, M., MELYMUK, L., ROBSON, M., DOUWES, J., ROOSENS, L., DIRTU, A. C. & COVACI, A. 2008b. Polybrominated diphenyl ethers in domestic indoor dust from Canada, New Zealand, United Kingdom and United States. *Environment International,* 34**,** 232-238.

HARRAD, S., WIJESEKERA, R., HUNTER, S., HALLIWELL, C. & BAKER, R. 2004. Preliminary assessment of UK human dietary and inhalation exposure to polybrominated diphenyl ethers. *Environmental science & technology,* 38**,** 2345-2350.

HAYAKAWA, K., TAKATSUKI, H., WATANABE, I. & SAKAI, S.-I. 2004. Polybrominated diphenyl ethers (PBDEs), polybrominated dibenzo-p-dioxins/dibenzofurans (PBDD/Fs) and monobromo-polychlorinated dibenzo-p-dioxins/dibenzofurans (MoBPXDD/Fs) in the atmosphere and bulk deposition in Kyoto, Japan. *Chemosphere,* 57**,** 343-356.

HIRAI, Y. & SAKAI, S. 2007. Brominated Flame Retardants in Recycled Plastic Products. *BFR2007: 4th International Symposium on Brominated Flame Retardants*.

HITES, R. A. 2004. Polybrominated diphenyl ethers in the environment and in people: A metaanalysis of concentrations. *Environmental Science & Technology,* 38**,** 945-56.

HOFFMANN, V., KASIK, M., ROBINSON, P. K. & VENZAGO, C. 2005. Glow discharge mass spectrometry. *Analytical and bioanalytical chemistry,* 381**,** 173-188.

HOPEWELL, J., DVORAK, R. & KOSIOR, E. 2009. Plastics recycling: challenges and opportunities. *Philosophical Transactions of the Royal Society of London B: Biological Sciences,* 364**,** 2115-2126.

HOSAKA, A., WATANABE, C. & TSUGE, S. 2005. Rapid determination of decabromodiphenyl ether in polystyrene by thermal desorption-GC/MS. *Analytical sciences,* 21**,** 1145-1147.

IEC, I. E. C. 2008. Technical Committee 111 "Environmental standardization for electrical and electronic products and systems", Working Group #3 "Test methods of hazardous substances".

IONAS, A. C., DIRTU, A. C., ANTHONISSEN, T., NEELS, H. & COVACI, A. 2014. Downsides of the recycling process: Harmful organic chemicals in children's toys. *Environment international,* 65**,** 54-62.

IONAS, A. C., ULEVICUS, J., GÓMEZ, A. B., BRANDSMA, S. H., LEONARDS, P. E., VAN DE BOR, M. & COVACI, A. 2016. Children's exposure to polybrominated diphenyl ethers (PBDEs) through mouthing toys. *Environment international,* 87**,** 101-107.

İZGI, B. & KAYAR, M. 2015. Determination of bromine and tin compounds in plastics using laser ablation inductively coupled plasma mass spectrometry (LA-ICP-MS). *Talanta,* 139**,** 117-122.

JAKAB, E., UDDIN, M. A., BHASKAR, T. & SAKATA, Y. 2003. Thermal decomposition of flame-retarded high-impact polystyrene. *Journal of analytical and applied pyrolysis,* 68**,** 83-99.

JANA, H., LUKAS, V., JANA, P., JAN, P. & TOMAS, C. 2008. DART–TOFMS: a challenging approach in rapid monitoring of brominated flame retardants in environmental matrices. *Organohalogen Compounds,* 70**,** 000922.

JOHNSON, B. 2008. *Exposure to and bioaccumulation of brominated flame retardants in humans and marine wildlife: Comparison to patterns of chlorinated contaminants*, State University of New York at Albany.

JONES-OTAZO, H. A., CLARKE, J. P., DIAMOND, M. L., ARCHBOLD, J. A., FERGUSON, G., HARNER, T., RICHARDSON, G. M., RYAN, J. J. & WILFORD, B. 2005. Is house dust the missing exposure pathway for PBDEs? An analysis of the urban fate and human exposure to PBDEs. *Environmental science & technology,* 39**,** 5121-5130.

JUNG, J., BAE, S., LEE, L., SHIN, J. K., CHOI, J. & LEE, S. 2009. Rapid identification of brominated flame retardants by using direct exposure probe mass spectrometry. *Microchemical Journal,* 91**,** 140-146.

JUSTICE, E. C. O. April 1 2008. Exemption of DecaBDE from the prohibition on use. *European Court of Justice* [Online]. [Accessed European Court of Justice European Court of Justice].

KAJIWARA, N., NOMA, Y. & TAKIGAMI, H. 2011. Brominated and organophosphate flame retardants in selected consumer products on the Japanese market in 2008. *J Hazard Mater,* 192**,** 1250-9.

KALNICKY, D. J. & SINGHVI, R. 2001. Field portable XRF analysis of environmental samples. *Journal of hazardous materials,* 83**,** 93-122.

KARLSSON, M., JULANDER, A., VAN BAVEL, B. & HARDELL, L. 2007. Levels of brominated flame retardants in blood in relation to levels in household air and dust. *Environment International,* 33**,** 62-69.

KIKUCHI, S., KAWAUCHI, K., OOKI, S., KUROSAWA, M., HONJHO, H. & YAGISHITA, T. 2004. Non-destructive rapid analysis of brominated flame retardants in electrical and electronic equipment using Raman spectroscopy. *Analytical sciences,* 20**,** 1111-1112.

KOCH, J., FELDMANN, I., JAKUBOWSKI, N. & NIEMAX, K. 2002. Elemental composition of laser ablation aerosol particles deposited in the transport tube to an ICP. *Spectrochimica Acta Part B: Atomic Spectroscopy,* 57**,** 975-985.

KOSLER, J. 2008. Laser ablation sampling strategies for concentration and isotope ratio analyses by ICP-MS. *Laser ablation ICP-MS in the Earth sciences: current practices and outstanding issues.*

LA GUARDIA, M. J., HALE, R. C. & HARVEY, E. 2006a. Detailed polybrominated diphenyl ether (PBDE) congener composition of the widely used penta-, octa-, and deca-PBDE technical flame-retardant mixtures. *Environmental science & technology,* 40**,** 6247-6254.

LA GUARDIA, M. J., HALE, R. C. & HARVEY, E. 2006b. Detailed polybrominated diphenyl ethers (PBDE) congener composition of the widely used penta-, octa-, and deca-PBDE technical flame-retardant mixtures. *Environmental Science & Technology,* 40**,** 6247-54.

LAGALANTE, A. F., OSWALD, T. D. & CALVOSA, F. C. 2009. Polybrominated diphenyl ether (PBDE) levels in dust from previously owned automobiles at United States dealerships. *Environ Int,* 35**,** 539-44.

LLORCA-PORCEL, J., MARTÍNEZ-SÁNCHEZ, G., ALVAREZ, B., COBOLLO, M. & VALOR, I. 2006. Analysis of nine polybrominated diphenyl ethers in water samples by means of stir bar sorptive extraction-thermal desorption-gas chromatography–mass spectrometry. *Analytica Chimica Acta,* 569**,** 113-118.

LONGERICH, H. 1996. Laser ablation inductively coupled plasma mass spectrometric transient signal data acquisition and analyte concentration calculation. *J. Anal. At. Spectrom.,* 9**,** 899-904.

LUDA, M., BALABANOVICH, A. & CAMINO, G. 2002. Thermal decomposition of fire retardant brominated epoxy resins. *Journal of Analytical and Applied Pyrolysis,* 65**,** 25-40.

LUDA, M., BALABANOVICH, A., ZANETTI, M. & GUARATTO, D. 2007. Thermal decomposition of fire retardant brominated epoxy resins cured with different nitrogen containing hardeners. *Polymer degradation and stability,* 92**,** 1088-1100.

MANS, C., HANNING, S., SIMONS, C., WEGNER, A., JANBEN, A. & KREYENSCHMIDT, M. 2007. Development of suitable plastic standards for X-ray fluorescence analysis. *Spectrochimica Acta Part B: Atomic Spectroscopy,* 62**,** 116-122.

MANS, C., SIMONS, C., HANNING, S., JANßEN, A., ALBER, D., RADTKE, M., REINHOLZ, U., BÜHLER, A. & KREYENSCHMIDT, M. 2009. New polymeric candidate reference materials for XRF and LA-ICP-MS—development and preliminary characterization. *X-Ray Spectrometry,* 38**,** 52-57.

MARK, H. F. 2013. *In:* MARK, H. F. (ed.) *Encyclopedia of Polymer Science and Technology.* 4th ed. Pittsburgh: Wiley.

MARKOWICZ, A. A. & VAN GRIEKEN, R. E. 1993. *Handbook of X-ray Spectrometry: Methods and Techniques*, Marcel Dekker New York.

MARTINHO, G., PIRES, A., SARAIVA, L. & RIBEIRO, R. 2012. Composition of plastics from waste electrical and electronic equipment (WEEE) by direct sampling. *Waste Management,* 32**,** 1213-1217.

MCDONALD, T. A. 2002. A perspective on the potential health risks of PBDEs. *Chemosphere,* 46**,** 745-755.

MÖRCK, A., HAKK, H., ÖRN, U. & WEHLER, E. K. 2003. Decabromodiphenyl ether in the rat: absorption, distribution, metabolism, and excretion. *Drug metabolism and disposition,* 31**,** 900-907.

MUENHOR, D. & HARRAD, S. 2012. Within-room and within-building temporal and spatial variations in concentrations of polybrominated diphenyl ethers (PBDEs) in indoor dust. *Environment international,* 47**,** 23-27.

MUENHOR, D., HARRAD, S., ALI, N. & COVACI, A. 2010. Brominated flame retardants (BFRs) in air and dust from electronic waste storage facilities in Thailand. *Environ Int,* 36**,** 690-8.

NILSSON, N. H., COWI & VANDTEKNIK, T. I. K.-O. 2009. *Development and Use of Screening Methods to Determine Chromium (VI) and Brominated Flame Retardants in Electrical and Electronic Equipment*, Danish Environmental Protection Agency.

NIU, J., SHEN, Z., YANG, Z., LONG, X. & YU, G. 2006. Quantitative structure–property relationships on photodegradation of polybrominated diphenyl ethers. *Chemosphere,* 64**,** 658-665.

O'GRADY, A., DENNIS, A. C., DENVIR, D., MCGARVEY, J. J. & BELL, S. E. 2001. Quantitative Raman spectroscopy of highly fluorescent samples using pseudosecond derivatives and multivariate analysis. *Analytical chemistry,* 73**,** 2058-2065.

PEETERS, J. R., VANEGAS, P., DEVOLDERE, T., DEWULF, W. & DUFLOU, J. R. 2013. Product clustering for closed loop recycling of flame retardant plastics: A case study for flat screen TVs. *Re-engineering Manufacturing for Sustainability.* Springer.

PISONERO, J., COSTA, J. M., PEREIRO, R., BORDEL, N. & SANZ-MEDEL, A. 2004. Radiofrequency glow-discharge devices for direct solid analysis. *Analytical and bioanalytical chemistry,* 379**,** 17-29.

PITTS, J. J. 1972. Antimony- Halogen synergistic reactions in fire retardants(Antimony-halogen synergistic reactions in fire retardants, noting antimony oxychloride role). *Journal of Fire and Flammability,* 3**,** 51-84.

PÖHLEIN, M., LLOPIS, A. S., WOLF, M. & VAN ELDIK, R. 2005. Rapid identification of RoHS-relevant flame retardants from polymer housings by ultrasonic extraction and RP-HPLC/UV. *Journal of Chromatography A,* 1066**,** 111-117.

PRITCHARD, G. 2012. *Plastics additives: an AZ reference*, Springer Science & Business Media.

PUYPE, F., SAMSONEK, J., KNOOP, J., EGELKRAUT-HOLTUS, M. & ORTLIEB, M. 2015. Evidence of waste electrical and electronic equipment (WEEE) relevant substances in polymeric food-contact articles sold on the European market. *Food Additives & Contaminants: Part A,* 32**,** 410-426.

RAUERT, C. & HARRAD, S. 2015. Mass transfer of PBDEs from plastic TV casing to indoor dust via three migration pathways—A test chamber investigation. *Science of The Total Environment,* 536**,** 568-574.

RAUERT, C., KURIBARA, I., KATAOKA, T., WADA, T., KAJIWARA, N., SUZUKI, G., TAKIGAMI, H. & HARRAD, S. 2016. Direct contact between dust and HBCD-treated fabrics is an important pathway of source-to-dust transfer. *Sci Total Environ,* 545-546**,** 77-83.

REGULATION, E. 2014. No. 202/2014 of 3 March 2014 amending European Commission Regulation (EU) No. 10/2011 on plastic materials and articles intended to come into contact with food. *Official Journal of the European Union L,* 62.

RIESS, M., ERNST, T., POPP, R., MÜLLER, B., THOMA, H., VIERLE, O., WOLF, M. & VAN ELDIK, R. 2000. Analysis of flame retarded polymers and recycling materials. *Chemosphere,* 40**,** 937-941.

RUDEL, R. A., CAMANN, D. E., SPENGLER, J. D., KORN, L. R. & BRODY, J. G. 2003. Phthalates, alkylphenols, pesticides, polybrominated diphenyl ethers, and other endocrine-disrupting compounds in indoor air and dust. *Environmental science & technology,* 37**,** 4543-4553.

RUSSO, R. E., MAO, X. & MAO, S. S. 2002. Peer reviewed: The physics of laser ablation in microchemical analysis. ACS Publications.

SAKAI, S., WATANABE, J., HONDA, Y., TAKATSUKI, H., AOKI, I., FUTAMATSU, M. & SHIOZAKI, K. 2001. Combustion of brominated flame retardants and behavior of its byproducts. *Chemosphere,* 42**,** 519-31.

SAMSONEK, J. & PUYPE, F. 2013a. Occurrence of Bominated flame retardants in black thermo cups and selected kitchen utensils purchased on the European market. *Food Addit Contam Part A Chem Anal Control Expo Risk Assess,* 30**,** 1976–1986.

SAMSONEK, J. & PUYPE, F. 2013b. Occurrence of brominated flame retardants in black thermo cups and selected kitchen utensils purchased on the European market. *Food Additives & Contaminants: Part A,* 30**,** 1976-1986.

SÁNCHEZ-BRUNETE, C., MIGUEL, E. & TADEO, J. L. 2006. Determination of polybrominated diphenyl ethers in soil by ultrasonic assisted extraction and gas chromatography mass spectrometry. *Talanta,* 70**,** 1051-1056.

SCHLUMMER, M. 2011. Contributions to the Stockholm Convention guideline drafts. *Vienna, Austria,* 23**,** 2011.

SCHLUMMER, M., GRUBER, L., MÄURER, A., WOLZ, G. & VAN ELDIK, R. 2007. Characterisation of polymer fractions from waste electrical and electronic equipment (WEEE) and implications for waste management. *Chemosphere,* 67**,** 1866-1876.

SCHLUMMER, M. & MÄURER, A. 2006. Recycling of styrene polymers from shredded screen housings containing brominated flame retardants. *Journal of applied polymer science,* 102**,** 1262-1273.

SCHLUMMER, M., MÄURER, A., LEITNER, T. & SPRUZINA, W. 2006. Report: recycling of flame-retarded plastics from waste electric and electronic equipment (WEEE). *Waste management & research,* 24**,** 573-583.

SEIDEL, T., GOLLOCH, A., BEERWALD, H. & BÖHM, G. 1993. Sliding spark spectroscopy. *Fresenius' journal of analytical chemistry,* 347**,** 92-102.

SERAFETINIDES, A., MAKROPOULOU, M., SKORDOULIS, C. & KAR, A. 2001. Ultra-short pulsed laser ablation of polymers. *Applied surface science,* 180**,** 42-56.

SERÔDIO, P., CABRAL, M. S. & NOGUEIRA, J. 2007. Use of experimental design in the optimization of stir bar sorptive extraction for the determination of polybrominated diphenyl ethers in environmental matrices. *Journal of Chromatography A,* 1141**,** 259-270.

SHAW, P. J. 2009. *Multivariate statistics for the environmental sciences*, Wiley.

SINDIKU, O., BABAYEMI, J., OSIBANJO, O., SCHLUMMER, M., SCHLUEP, M. & WEBER, R. 2011. Screening e-waste plastic in Nigeria for brominated flame retardants using XRF—towards a methodology for assessing POPs PBDE in ewaste exports. *Organohalogen Compd,* 73**,** 785-788.

SJÖDIN, A., PÄPKE, O., MCGAHEE, E., FOCANT, J.-F., JONES, R. S., PLESS-MULLOLI, T., TOMS, L.-M. L., HERRMANN, T., MÜLLER, J. & NEEDHAM, L. L. 2008. Concentration of polybrominated diphenyl ethers (PBDEs) in household dust from various countries. *Chemosphere,* 73**,** S131-S136.

SOMMER, E. J. & RICH, J. T. 2001. Application of Raman spectroscopy to identification and sorting of post-consumer plastics for recycling. Google Patents.

STAPLETON, H. M., HARNER, T., SHOEIB, M., KELLER, J. M., SCHANTZ, M. M., LEIGH, S. D. & WISE, S. A. 2006. Determination of polybrominated diphenyl ethers in indoor dust standard reference materials. *Analytical and bioanalytical chemistry,* 384**,** 791-800.

STEHRER, T., HEITZ, J., PEDARNIG, J., HUBER, N., AESCHLIMANN, B., GÜNTHER, D., SCHERNDL, H., LINSMEYER, T., WOLFMEIR, H. & ARENHOLZ, E. 2010. LA-ICP-MS analysis of waste polymer materials. *Analytical and bioanalytical chemistry,* 398**,** 415-424.

STRINGER, R., LABUNSKA, I., SANTILLO, D., JOHNSTON, P., SIDDORN, J. & STEPHENSON, A. 2000. Concentrations of phthalate esters and identification of other additives in PVC children's toys. *Environmental Science and Pollution Research,* 7**,** 27-36.

SUNG, Y. & LIM, H. 2000. Double membrane desolvator for direct analysis of isopropyl alcohol in inductively coupled plasma atomic emission spectrometry (ICP-AES) and inductively coupled plasma mass spectrometry (ICP-MS). *Microchemical journal,* 64**,** 51-57.

SUZUKI, G., KIDA, A., SAKAI, S. & TAKIGAMI, H. 2009. Existence state of bromine as an indicator of the source of brominated flame retardants in indoor dust. *Environ Sci Technol,* 43**,** 1437-42.

TAKIGAMI, H., SUZUKI, G., HIRAI, Y. & SAKAI, S. 2008. Transfer of brominated flame retardants from components into dust inside television cabinets. *Chemosphere,* 73**,** 161-9.

TAKIGAMI, H., SUZUKI, G., HIRAI, Y. & SAKAI, S. 2009. Brominated flame retardants and other polyhalogenated compounds in indoor air and dust from two houses in Japan. *Chemosphere,* 76**,** 270-7.

TIEN, H., HEISE, S., SEGUÍ, X., CASAL, J., DARBRA, R. M., SUCIU, N., CAPRI, E., TREVISAN, M., SCHUHMACHER, M., NADAL, M. & ROVIRA, J. 2013. Tracking Global Flows of E-Waste Additives by Using Substance Flow Analysis, with a Case Study in China. *In:* BILITEWSKI, B., DARBRA, R. M. & BARCELÓ, D. (eds.) *Global Risk-Based Management of Chemical Additives II: Risk-Based Assessment and Management Strategies.* Berlin, Heidelberg: Springer Berlin Heidelberg.

TODOLí, J.-L. & MERMET, J.-M. 1998. Study of polymer ablation products obtained by ultraviolet laser ablation—inductively coupled plasma atomic emission spectrometry. *Spectrochimica Acta Part B: Atomic Spectroscopy,* 53**,** 1645-1656.

TOMS, L.-M. L., BARTKOW, M. E., SYMONS, R., PAEPKE, O. & MUELLER, J. F. 2009. Assessment of polybrominated diphenyl ethers (PBDEs) in samples collected from indoor environments in South East Queensland, Australia. *Chemosphere,* 76**,** 173-178.

TROITZSCH, J. H. 1990. *International plastics flammability handbook: Principles, regulations, testing and approval,* Münich, Germany, Hanser Publishers.

TSENG, L. H., LI, M. H., TSAI, S. S., LEE, C. W., PAN, M. H., YAO, W. J. & HSU, P. C. 2008. Developmental exposure to decabromodiphenyl ether (PBDE 209): effects on thyroid hormone and hepatic enzyme activity in male mouse offspring. *Chemosphere,* 70**,** 640-647.

UNEP-CHEMICALS. 2010. Guidance on best available techniques and best environmental practices for the recycling and disposal of articles containing polybrominated diphenyl ethers (PBDEs) listed under the Stockholm Convention on Persistent Organic Pollutants.

VANHOOF, C., HOLSCHBACH-BUSSIAN, K., BUSSIAN, B., CLEVEN, R. & FURTMANN, K. 2013. Applicability of portable XRF systems for screening waste loads on hazardous substances as incoming inspection at waste handling plants. *X-Ray Spectrometry,* 42**,** 224-231.

VÁZQUEZ, A. S., COSTA-FERNANDEZ, J. M., ENCINAR, J. R., PEREIRO, R. & SANZ-MEDEL, A. 2008. Bromine determination in polymers by inductively coupled plasma-mass spectrometry and its potential for fast first screening of brominated flame retardants in polymers and paintings. *Analytica chimica acta,* 623**,** 140-145.

VETTER, W., HAASE-ASCHOFF, P., ROSENFELDER, N., KOMAROVA, T. & MUELLER, J. F. 2009. Determination of halogenated natural products in passive samplers deployed along the Great Barrier Reef, Queensland/Australia. *Environmental science & technology,* 43**,** 6131-6137.

VILAPLANA, F., KARLSSON, P., RIBES-GREUS, A., IVARSSON, P. & KARLSSON, S. 2008. Analysis of brominated flame retardants in styrenic polymers: comparison of the extraction efficiency of ultrasonication, microwave-assisted extraction and pressurised liquid extraction. *Journal of Chromatography A,* 1196**,** 139-146.

VOJTA, S., BECANOVA, J., MELYMUK, L., KOMPRDOVA, K., KOHOUTEK, J., KUKUCKA, P. & KLANOVA, J. 2017. Screening for halogenated flame retardants in European consumer products, building materials and wastes. *Chemosphere,* 168**,** 457-466.

WÄGER, P., SCHLUEP, M. & MÜLLER, E. 2010. RoHS substances in mixed plastics from waste electrical and electronic equipment. *Final Report,* 17**,** 2010.

WATANABE, I. & SAKAI, S. 2003. Environmental release and behavior of brominated flame retardants. *Environment International,* 29**,** 665-82.

WEBER, R. & KUCH, B. 2003. Relevance of BFRs and thermal conditions on the formation pathways of brominated and brominated-chlorinated dibenzodioxins and dibenzofurans. *Environment International,* 29**,** 699-710.

WILFORD, B. H., SHOEIB, M., HARNER, T., ZHU, J. & JONES, K. C. 2005. Polybrominated diphenyl ethers in indoor dust in Ottawa, Canada: implications for sources and exposure. *Environmental science & technology,* 39**,** 7027-7035.

WILFORD, B. H., THOMAS, G. O., JONES, K. C., DAVISON, B. & HURST, D. K. 2008. Decabromodiphenyl ether (deca-BDE) commercial mixture components, and other PBDEs, in airborne particles at a UK site. *Environment International,* 34**,** 412-419.

WURL, O., POTTER, J. R., DURVILLE, C. & OBBARD, J. P. 2006. Polybrominated diphenyl ethers (PBDEs) over the open Indian Ocean. *Atmospheric Environment,* 40**,** 5558-5565.

XIE, Z., EBINGHAUS, R., LOHMANN, R., HEEMKEN, O., CABA, A. & PÜTTMANN, W. 2007. Trace determination of the flame retardant tetrabromobisphenol A in the atmosphere by gas chromatography–mass spectrometry. *Analytica chimica acta,* 584**,** 333-342.

ZHANG, M., BUEKENS, A. & LI, X. 2016. Brominated flame retardants and the formation of dioxins and furans in fires and combustion. *J Hazard Mater,* 304**,** 26-39.

ZHENG, X., FU, W., ALBIN, S., WISE, K., JAVEY, A. & COOPER, J. 2001. Self-referencing Raman probes for quantitative analysis. *Applied Spectroscopy,* 55**,** 382-388.

ZOTA, A. R., RUDEL, R. A., MORELLO-FROSCH, R. A. & BRODY, J. G. 2008. Elevated house dust and serum concentrations of PBDEs in California: unintended consequences of furniture flammability standards? *Environmental science & technology,* 42**,** 8158-8164.